



HAL
open science

Analyse multi-échelle des déformations différées dans les matériaux cimentaires sous dessiccation ou réaction sulfatique interne

Marie Malbois

► **To cite this version:**

Marie Malbois. Analyse multi-échelle des déformations différées dans les matériaux cimentaires sous dessiccation ou réaction sulfatique interne. Génie civil. Université Paris Saclay (COmUE), 2019. Français. NNT : 2019SACLN025 . tel-02328736

HAL Id: tel-02328736

<https://theses.hal.science/tel-02328736>

Submitted on 23 Oct 2019

HAL is a multi-disciplinary open access archive for the deposit and dissemination of scientific research documents, whether they are published or not. The documents may come from teaching and research institutions in France or abroad, or from public or private research centers.

L'archive ouverte pluridisciplinaire **HAL**, est destinée au dépôt et à la diffusion de documents scientifiques de niveau recherche, publiés ou non, émanant des établissements d'enseignement et de recherche français ou étrangers, des laboratoires publics ou privés.

Multi-scale analysis of delayed deformations in cement-based materials submitted to drying or delayed ettringite formation

Thèse de doctorat de l'Université Paris-Saclay
préparée à l'École normale supérieure de Cachan
(École normale supérieure de Cachan-Paris-Saclay)

École doctorale n°579 : sciences mécaniques et énergétiques,
matériaux et géosciences
Spécialité de doctorat : solides, structures et matériaux

Thèse présentée et soutenue sous réserve d'accord des rapporteurs à
l'École normale supérieure Paris-Saclay, le 12 juillet 2019, par

Mme Marie Malbois

Composition du Jury :

M. Xavier Brunetaud	Maitre de conférences (HDR), Université d'Orléans	Rapporteur
M. Joseph Absi	Professeur, Université de Limoges	Rapporteur
M. Jean-Baptiste Colliat	Professeur, École Polytechnique Universitaire de Lille	Président
Mme. Alexandra Bourdot	Maîtresse de conférences, École Normale Supérieure Paris-Saclay	Examinatrice
M. Farid Benboudjema	Professeur, École Normale Supérieure Paris-Saclay	Directeur de thèse
Mme. Aveline Darquennes	Professeure, INSA de Rennes	Co-Encadrante
Mme. Caroline De SA	Professeure agrégée, École Normale Supérieure Paris-Saclay	Co-Encadrante
M. Jean-Michel Torrenti	Professeur, École Nationale des Ponts et Chaussées	Co-Encadrant
M. Laurent Charpin	Ingénieur-Chercheur, EDF	Invité

Titre : Analyse multi-échelle des déformations différées dans les matériaux cimentaires sous dessiccation ou réaction sulfatique interne

Mots clés : Dessiccation, Réaction sulfatique interne, Déformations différées, Fissuration, granulats, échelle mesoscopique

Résumé : Aujourd'hui, la durée d'exploitation de certaines structures en béton est amenée à être prolongée, en parallèle, des structures présentent prématurément des signes d'endommagements dû parfois à une mauvaise prise en compte des conditions environnementales. Assurer la durabilité des structures, c'est également assurer leur exploitation de façon sécuritaire, économique et écologique. Notre objectif est dans un premier temps de comprendre les phénomènes et mécanismes en jeu, ainsi que leur potentiels couplages ; puis, dans un deuxième temps, de créer des modèles prédictifs fiables de ces comportements. Le travail présenté s'intéresse en particulier aux structures nucléaires, qui en plus d'avoir un enjeu majeur, présentent des risques vis-à-vis de la dessiccation et de pathologies thermo-activées comme la réaction sulfatique interne (RSI). Plus précisément, l'objectif de cette thèse est de comprendre la participation des granulats dans les mécanismes de dégradation du matériau sous ces deux sollicitations respectives, puis leur couplage. A cet effet, une approche expérimentale multi-échelle est menée. Elle s'intéresse à l'évolution des déformations différées ainsi que des propriétés mécaniques et de transfert de matériaux cimentaires soumis soit à la dessiccation, soit à la RSI. Dans les deux cas, les paramètres influents des granulats dans les mécanismes ont été mis en évidence et une étude paramétrique a été mis en place afin de dégager clairement l'influence de ces paramètres. Dans un premier temps, l'étude de la dessiccation est basée sur le suivi et la caractérisation de sept formulations modèles ; i.e. dont les squelettes granulaires ont été contrôlés et sélectionnés selon la taille et la fraction volumique des granulats dans le matériau ; sur 200 jours. Les essais ont mis en évidence l'influence de ces paramètres dans le phénomène d'incompatibilités de déformations entre pâte de ciment et granulats. En parallèle, l'étude expérimentale de la réaction sulfatique interne s'intéresse à caractériser l'influence de la nature minéralogique des granulats sur la formation et la progression de la pathologie. Nous nous intéressons à l'influence de ce paramètre sur la cinétique et le taux de la réaction, mais également sur l'évolution des propriétés du matériau, afin d'identifier tous les mécanismes physico-chimiques présents. Enfin, une dernière étude s'intéresse au couplage entre RSI et dessiccation. Ici, les paramètres granulats ont été fixés, et des échantillons réactifs vis-à-vis de la RSI ont été soumis à des cycles de séchage-imbibition.



Title: Multi-scale analysis of delayed deformations in cement-based materials submitted to drying or delayed ettringite formation

Keywords: Drying, Delayed ettringite formation, Delayed deformations, Cracking, aggregates, mesoscopic scale

Abstract: Today, the operating life of some concrete structures is likely to be extended, in parallel, structures show early signs of damage due sometimes to poor consideration of environmental conditions. Ensuring the sustainability of structures also means ensuring their safe, economical and ecological operation. Our objective is first to understand the phenomena and mechanisms at play, as well as their potential couplings; then, in a second step, to create reliable predictive models of these behaviours. The work presented is particularly interested in nuclear structures, which, in addition to having a major stake in our societies, present risks with regard to desiccation and thermo-activated pathologies such as the delayed ettringite formation (DEF). More precisely, the objective of this thesis is to understand the participation of aggregates in the degradation mechanisms of the material under these two respective stresses, and then their coupling. To this end, a multi-scale experimental approach is being conducted. It takes interest in the evolution of delayed deformations as well as the mechanical and transfer properties of cementitious materials subjected to either desiccation or DEF. In both cases, the influential parameters of the aggregates in the mechanisms were identified and a parametric study was carried out to clearly identify the influence of these parameters. First, the desiccation study is based on the monitoring and characterization of seven model formulations; i.e. granular skeletons were controlled and selected according to the size and volume fraction of the aggregates in the material; over 200 days. The tests revealed the influence of these parameters in the phenomenon of aggregate restraint. In parallel, the experimental study of DEF aims at characterizing the influence of the mineralogical nature of aggregates on the formation and progression of the pathology. We are interested in the influence of this parameter on the reaction kinetics and rate, but also on the evolution of the material properties, in order to identify all the physico-chemical mechanisms at stake. Finally, a final study is interested in the coupling between RSI and desiccation. Here, the aggregate parameters were set, and samples reactive to DEF were subjected to drying and soaking cycles.



Contents

I	Introduction: origin and role of aggregates in concrete mixes	7
1	Introduction on aggregates	9
1.1	Aggregates	9
1.1.1	Intrinsic characteristics of aggregates	10
1.1.2	Characteristics induced by extraction	11
1.2	Interface transition zone	12
1.2.1	Definitions	12
1.2.2	Impact of aggregate parameters on ITZ	13
II	Effects of aggregates and drying on model cementitious materials behaviour	19
2	State of the art : Drying phenomenon	21
2.1	Desiccation	22
2.1.1	Description of the water loss mechanisms	22
2.1.2	Impact of aggregates on drying	23
2.2	Shrinkage mechanisms	23
2.2.1	Description of the shrinkage mechanisms	24
2.2.2	Impact of aggregates on desiccation shrinkage	26
2.3	Cracking mechanisms	30
2.3.1	Macroscopic scale : hydric gradient	30
2.3.2	Mesoscopic scale : aggregate restraint	30
2.3.3	Nano- and micro-scopic scale : local effects	33
2.4	Creep deformations	33
2.4.1	Basic creep	34
2.4.2	Drying Creep	35
2.5	Influence drying on mechanical properties	37
2.6	Conclusions and definition of the experimental campaign conditions	39
3	Experimental campaign	41
3.1	Materials	41
3.2	Experimental procedure	43
3.2.1	Casting and conditioning	43
3.2.2	Observation of cracking patterns	44
3.2.3	Monitoring of drying	46
3.2.4	Assessment of mechanical properties	46
3.2.5	Assessment of transfer properties	48

4	Results and analysis	51
4.1	Cracking observations	51
4.1.1	Observation of superficial cracking	51
4.1.2	X-Ray micro-tomographic observations	54
4.2	Effects of aggregates on delayed behaviour induced by drying	61
4.2.1	Drying	61
4.2.2	Shrinkage	63
4.2.3	Comparison of experimental results with conventional homogenisation models	65
4.3	Effect of aggregates and drying on transfer and mechanical properties	69
4.3.1	Mechanical properties	69
4.3.2	Transfer properties	76
4.4	Conclusion	79
 III Effects of aggregates and preservation conditions on delayed ettringite formation		85
5	State of the art : Delayed Ettringite Formation	87
5.1	Ettringite, what is it ?	87
5.1.1	Definition	87
5.1.2	Types of ettringite	88
5.1.3	Ettringite stability	88
5.2	Focus on delayed ettringite	90
5.2.1	Formation mechanisms	90
5.2.2	Expansion mechanisms	90
5.3	Influential parameters of delayed ettringite formation	93
5.3.1	Thermal history	93
5.3.2	Concrete composition	95
5.3.3	Environmental conditions	99
5.4	Effect of DEF on concrete structures	102
5.4.1	Effect on mechanical properties	102
5.4.2	Effect on transfer properties	104
5.5	Conclusions and definition of the experimental campaign conditions	105
6	Experimental campaign	107
6.1	Materials	107
6.2	Experimental procedure	108
6.2.1	Casting, thermal treatment and conditioning	108
6.2.2	Monitoring of mass and expansion	111
6.2.3	Assessment of mechanical properties	112
7	Effect of aggregates mineralogical nature on DEF	115
7.1	Article presented in EDF conference "Dam Swelling Concrete"	115
7.2	Summary and conclusions	126
8	Effect of drying cycles on DEF in concrete	129
8.1	Article from Construction and Building Materials Journal	129
8.2	Conclusions	137

9	Conclusions and perspectives	143
A	Materials composition	145
A.1	Composition of cement : CEM II/A-LL 42,5 R	145
A.2	Composition of Boulonnais aggregates	146
B	Article de Projet d'Initiation à la Recherche de Matthieu Briat, Élève de Master 1 : <i>Experimental study on the effect of a viscosity modifying admixture on the delayed deformations and mechanical properties of cement-based materials.</i>	149
C	Article de Projet d'Initiation à la Recherche de Pierre Aymeric, Élève de Master 2 Recherche : <i>Étude du fluage du béton suivant les caractéristiques des granulats.</i>	165

Introduction

Context

In France, nuclear power accounts for 75% of electricity production. However, the future of this means of production is being questioned by:

- the ageing of nuclear power plants, which is the subject of the study presented,
- energy transition programmes promoted by public policies.

Two aspects need to be controlled: ensuring that the structure will be able to withstand the mechanical stresses exerted and ensuring that the transfer properties of deteriorated concrete guarantee that the rate of possible leakage of radioactive products into the environment is sufficiently low.

The evaluation of massive structures of this type is long and tedious. One way to accelerate these studies is to use predictive modelling that takes into account the entire thermal, hydric, chemical and mechanical history of the structure and by extension of the material. Many studies aim at developing these tools, and in particular the constitutive laws to be considered for a correct consideration of the physical phenomena present. ([Poyet 2003; Briffaut 2010; Hilaire 2014; Soleilhet 2018; Kchakech 2015; Alain Sellier and Buffo-Lacarrière 2009]) However, these phenomena tend to be coupled, more or less strongly and they are dependent on many parameters: factors inherent to the formulation, geometry, methods of implementation, surrounding environment...

Three categories of modelling types are commonly used for concrete with their share of advantages and disadvantages.

- Models using homogeneous meshes, which can be enhanced with multi-parametric behaviour laws. These models allow global studies of large structures but will have difficulty representing local effects;
- Homogenized models, which take into account the heterogeneous aspect of cementitious materials but which cannot consider potentially decisive internal cracking phenomena;
- Models using heterogeneous meshes, which are very interesting for the study of local phenomena, but their use is difficult on structures due to the huge amount of numerical computations needed.

In order to be able to correctly choose the appropriate type of modelling, let us return to the main focus of our study: the confinement structure of a nuclear power plant. This type of structure has very particular characteristics, which are likely to develop effects that compromise their durability. First of all, desiccation, inherent in all structures put into service, which leads to external and internal cracking. But also the pathologies inherent

in massive structures such as the formation of delayed ettringite (DEF or internal sulfatic reaction). Indeed, during the manufacture of structural elements, thermal heating can occur and thermo-activate unwanted chemical reactions. The consequence is a swelling of the material, and the structure, due to the precipitation of chemical species in the concrete voids.

Many studies have been carried out on these two effects, and have highlighted the influence of many parameters. We will take the example of Francois Soleilhet's thesis [Soleilhet 2018] who developed a model registration tool to determine the parameters of the model implemented by [Hilaire 2014]. The parameters inherent to the material are determined experimentally (porosity, mass loss, sorption-desorption curves). He concludes by comparing his experimental results with the consideration of different phenomena related to desiccation in his modelling: shrinkage, creep, capillary pressure. Two results, for compression and tensile test results, are shown in Figures 1a and 1a. It can be seen that although the modelling is close to the experimental curve, the fitting is not yet perfect, showing that some effects still may have been neglected. One of its proposals would be to take into account the phenomenon of aggregate restraint, a source of internal cracking.

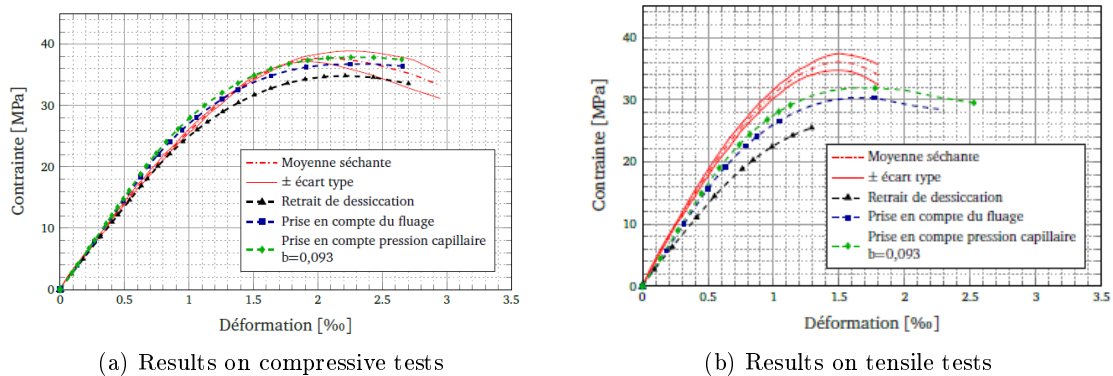


Figure 1 – Examples of different aggregates mineralogical nature

Since several years, authors have regularly address this issue of characterising and implementing this phenomenon. [Hon15; Bisschop 2002; Bisschop and J. G. v. Mier 2002; Lagier et al. 2011] Nonetheless, it mostly highlights that numerous characteristics, and the different mechanisms at stake, are yet to be decoupled and thoroughly understood. In parallel with this first example, we will note that aggregates are one of the formulation parameters that influence the formation of delayed ettringite in concrete. Indeed, Xavier Brunetaud ([Xavier Brunetaud 2005]) had already shown that the choice of aggregates, in particular with regard to mineralogical nature, had a significant impact on the amplitude and kinetics of the reaction and thus, the degradation rate of the material.

ANR MOSAIC

This work was financed by the French National Research Agency (ANR), as part of the *Mesoscopic Scale durability Investigations on Concrete* (M.O.S.A.I.C.) national project.

This project is a collaboration between four French laboratories all recognised for their expertise within the field of cement-based materials durability: LaMcube (Lille, France), LMT Cachan (Cachan, France), LMDC (Toulouse, France) and IFSTTAR (Marne-la-

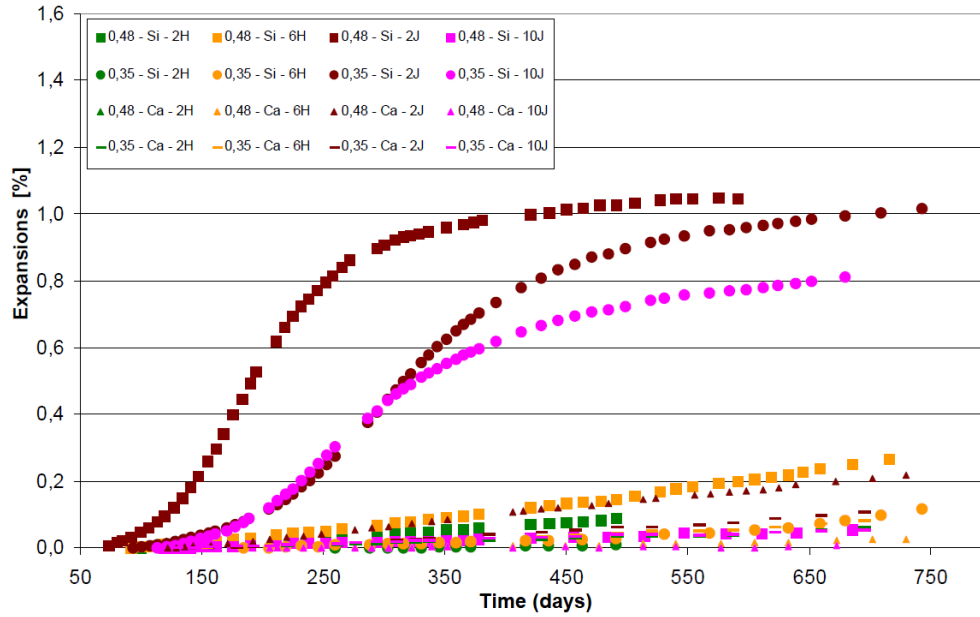


Figure 2 – Experimental results on several formulations where $w/c = 0.35$ or 0.48 , aggregates have a calcareous or siliceous nature, and thermal treatment varies from 2 hours to 10 days.

Vallée, France). This project aims at developing a predictive way of modelling the consequences of the effect of drying and delayed ettringite formation but also their coupling, at a mesoscopic scale.

On one hand, several teams are working on the set up of experimental methodologies based on studying the impact of aggregates under these two pathologies on "real" and "model" materials. To be more precise, some formulations are classic concrete mixes, while others have a controlled meso-scale morphology: it aims at easily uncoupling the effects of significant aggregate parameters on the global behaviour of the concrete by conducting parametric investigations. Aggregates can be "real" aggregates (with random geometry) or "model" aggregates (sphere or cubical inclusions). On the other, modelling studies are carried out to enrich the different models.

In these different studies, focuses are made on the characterisation of induced cracking phenomena, and on assessing the overall impact of aggregate parameters on the mechanical and transfer properties of deteriorated materials.



Figure 3 – Logo of the national research project MOSAIC

Manuscript outline

The proposed manuscript is aimed at studying the impact of aggregates on the degrading mechanisms induced by desiccation or delayed ettringite formation, and characterising their influence on the evolution of material properties.

In a first time, the aggregate parameters will be evaluated in an introductory section. They will allow us to identify the knowledge already acquired on the role of aggregates in the formulation process of cementitious materials, and on the behaviour of these materials when they are subjected to hydric, chemical and mechanical stresses.

In this context, we will see that the influential parameters are not the same depending on the pathology studied. Since several types of materials and mechanisms are studied, the manuscript will be structured around two parts: the study of desiccation, and the study of DEF. We will see that the influential parameters are not the same depending on the pathology studied.

In the first part, we will focus our attention on the state of the art of the hydro-mechanical behaviour of cementitious materials, with a specific focus on the role of aggregates. Once the various problematics have been presented, the experimental approach to the study of drying will be introduced, i.e. the choice of materials, tests and the global parametric procedure. The results of these different tests will be presented and analysed in a final chapter.

Then, in the second part, we will focus on the influence of aggregates on DEF. The two associated parametric studies will be presented in the form of articles from a publication in the *Construction and Building Materials* journal and the *Dam Swelling Concrete* congress proceedings.

Finally, a general conclusion will allow us to take an overview of the phenomena highlighted by these different studies, and to present the different perspectives opened by the work that has been carried out.

Bibliography

- Benkemoun, Nathan, Emmanuel Roubin, and Jean-Baptiste Colliat (Dec. 2017). “FE design for the numerical modelling of failure induced by differential straining in meso-scale concrete: Algorithmic implementation based on operator split method”. In: *Finite Elements in Analysis and Design* 137, pp. 11–25.
- Bisschop, Jan (2002). “Drying shrinkage microcracking in cement-based materials”. PhD thesis. Delft University of Technology.
- Bisschop, Jan and Jan G.M. van Mier (Sept. 2002). “Effect of aggregates on drying shrinkage microcracking in cement-based composites”. In: *Materials and Structures* 35, pp. 453–461.
- Briffaut, Matthieu (2010). “Étude de la fissuration au jeune âge des structures massives en béton : influence de la vitesse de refroidissement, des reprises de bétonnage et des armatures”. PhD thesis. École Normale Supérieure de Cachan.
- Hilaire, Adrien (2014). “Étude des déformations différées des bétons en compression et en traction, du jeune âge au long terme. Application aux enceintes de confinement”. PhD thesis. École Normale Supérieure de Cachan.
- Honorio de Faria, Tulio (2015). “Modelling Concrete Behaviour At Early-Age : Multiscale Analysis And Simulation Of A Massive Disposal Structure”. PhD thesis.
- Kchakech, Badreddine (2015). “Etude de l’influence de l’échauffement subi par un béton sur le risque d’expansions associées À la Réaction Sulfatique Interne”. PhD thesis. Université Paris-Est.
- Lagier, Fabien et al. (2011). “Numerical strategies for prediction of drying cracks in heterogeneous materials : comparison upon experimental results”. In: *Engineering Structures*.
- Poyet, S. (2003). “Etude de la dégradation des ouvrages en béton atteints par la réaction alcali-silice : Approche expérimentale et modélisation numérique multi-échelle des dégradations dans un environnement hydro-chemo-mécanique variable”. PhD thesis. Université de Marne-la-Vallée.
- Sellier, Alain and Laurie Buffo-Lacarrière (2009). “Vers une modélisation simple et unifiée du fluage propre, du retrait et du fluage en dessiccation du béton”. In: *European Journal of Environmental and Civil Engineering* 13(10), pp. 1161–1182.
- Soleilhet, Francois (2018). “Études expérimentales et numériques des matériaux cimentaires sous sollicitations hydro-mécaniques”. PhD thesis. Université Paris-Saclay - l’École Normale Supérieure de Paris-Saclay.

Part I

Introduction: origin and role of aggregates in concrete mixes

Chapter 1

Introduction on aggregates

Contents

1.1	Aggregates	9
1.1.1	Intrinsic characteristics of aggregates	10
1.1.2	Characteristics induced by extraction	11
1.2	Interface transition zone	12
1.2.1	Definitions	12
1.2.2	Impact of aggregate parameters on ITZ	13

1.1 Aggregates

This section is adapted from the book "Le grand livre des bétons" from Torrenti and D'Aiolo-Schwartzentruber. [Jean-Michel Torrenti and D'Aloia-Schwartzentruber 2014]

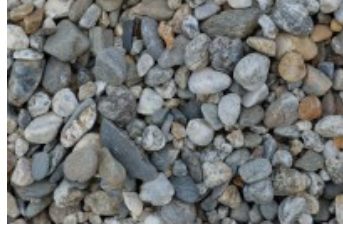
Aggregates used in construction and more precisely in the manufacture of cementitious materials can be of several types:

- **aggregates from massive rock quarries** These aggregates tends to be very resistant but with irregular geometries.
- **alluvial aggregates:** aggregates from marine extraction or from loose rock quarries. These aggregates will tend to be more regular and smooth, due to erosion and wind.
- **recycled or artificial aggregates:** they are obtained either by crushing demolition materials from buildings (concrete, gravel, stone...), or by using industrial by-products (furnace slag, foundry sand...)

Whatever the type of aggregates used, they present intrinsic characteristics or resulting from the processes used to obtain the aggregates. These different characteristics will be presented below, and the major influencing parameters of aggregates will be highlighted, then we will see how aggregates influence the formulation of cementitious materials, and therefore, the properties of these materials.



(a) Aggregates extracted from quarries



(b) Alluvial aggregates



(c) Recycled aggregates

Figure 1.1 – Examples of different aggregates (images found on www.beton-granulat.com and www.lafarge.fr)

1.1.1 Intrinsic characteristics of aggregates

- volume mass:** as for every material, real volume mass and apparent volume mass are among the basic parameters to know before any use. These characteristics are to be measured and known before starting any concrete formulation process. The assessment of this indicator actually lays on the assessment of the *aggregates mineralogical composition* and *porosity*.
- water absorption and adsorption:** the formulation of cementitious materials requires perfect control of the water supplied, which is necessary for the hydration reaction of cement. The slightest change in the water-cement ratio has important consequences on the mechanical and transfer properties of the material. This is why it is necessary to characterize the capacity of aggregates to absorb and adsorb water, in order not to consume so-called efficient water, essential for the optimal formulation of the material. These two characteristics are respectively greatly influenced by two inherent parameters of aggregates: *porosity* and *rugosity*. Indeed, if the porosity of the aggregate increases, it will tend to absorb and store more water in its porous network. At the same time, if the roughness of the material increases, the amount of water adsorbed to the surface of the aggregates increases.
- mechanical properties:** aggregates are found in large quantities in ordinary concrete (greater than or equal to 75% of the total volume). As they are the main contributors to the strength of cementitious materials, it is therefore important to characterize their mechanical properties to ensure optimal use. These properties are directly linked to the *mineralogical composition* of the rock from which aggregates were extracted.
- chemical properties:** the main objective of this characterisation is to ensure that their use is not suitable for concrete mixtures, in order to prevent the introduction of pollutants that could modify the curing process of concrete or affect the durability of the material. Here again, the chemical behaviour of aggregates in basic media depends on their chemical reactivity, and therefore *mineralogical composition* of the aggregates.

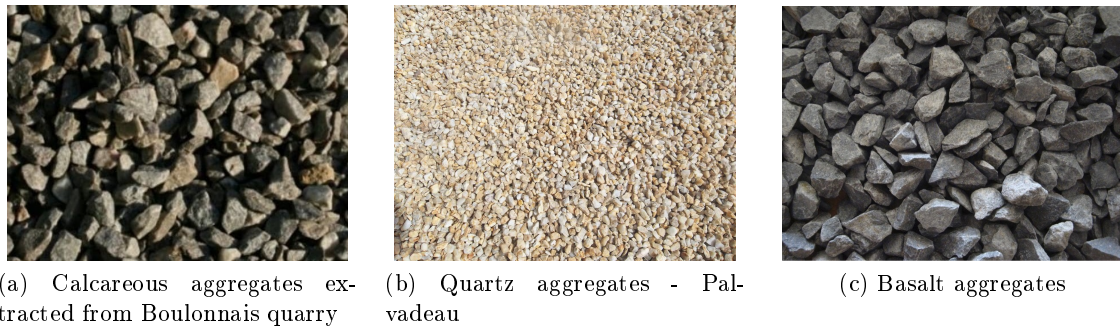


Figure 1.2 – Examples of different aggregates mineralogical nature

1.1.2 Characteristics induced by extraction

The origin and extraction of the products induce geometric characteristics, which can be controlled. These characteristics are:

- **granulometry:** This represents the dimensional distribution of the aggregates of the extracted quantity. This parameter is important for the formulation of concretes, allowing to optimize granular compaction in the mix. Indeed, improving compactness means to optimise the *volume of aggregate* into our sample. This allows, on the one hand, to increase the quantity of high-strength material in the concrete and, on the other hand, to reduce the voids in the concrete, thus optimizing the transmission of forces in the aggregates. This optimisation results in a considerable improvement in the mechanical properties of concrete.

The compactness is influenced by the *aggregates size* distribution and their *geometry*. The more smooth and spherical they are, the more the compactness will be optimised.

- **fineness module:** it is obtained by analysing the granulometric curves of aggregates extraction, allowing the characterisation of the ratio between fine and medium size aggregates in sand, and to classify them as fine sand or coarse sand. This sand characterisation is essential, as the modification of *size distribution* impacts compactness of aggregates and also the workability of fresh concrete. In addition, since the specific surface area of the aggregates, and therefore the interface between aggregates and cement paste, is proportionally opposite to the radius of the aggregates, control of the *size of the aggregates* is necessary in order to adjust the amount of binder in the concrete mix.
- **fineness quality:** The quality of fines in a sand corresponds to assessing the presence of clay fines in the sands that can alter the production and durability of concrete. They have a high water absorption and storage capacity, leading to a reduction in the amount of effective water required to hydrate the cement, and in the long term, to swell and stiffen the materials.
- **flatness:** this parameter is used to control the regularity and the *geometry of aggregates*, more specifically, it assesses the amount of flattened, or needle-shaped aggregates. The presence of these elongated inclusions hinders the optimization of the compactness of the granular mixture, and therefore tends to reduce mechanical properties, as mentioned just previously.

In this section, the main characteristics of aggregates have been presented and it has been brought out that it is necessary to control them in order to optimise the manufacture, durability and mechanical properties of cementitious materials. In addition, several parameters inherent to aggregates and their role in concrete were highlighted. These parameters are: porosity, rugosity, geometry and mineralogical nature of the aggregates and the volume distribution and size distribution of the aggregates in the mixture. However, one aspect was not studied here: the presence of aggregates, with their parameters and characteristics, disturbs the cement hydration process, and the curing one. It creates a Interface Transition Zone (also referred as ITZ), where the cement paste properties are altered. A focus is made on this specific zone in the next section.

1.2 Interface transition zone

1.2.1 Definitions

Some aggregate characteristics influence the setting of concrete, but more specifically, the presence of aggregates introduces local wall effects and modifies the nature and properties of the cement paste at the interface with the aggregates. This area is called the Interface Transition Zone (or ITZ). Its thickness varies according to the aggregate parameters but is generally less than or equal to $50\ \mu\text{m}$. There are several models of description of this ITZ, but it is the one of Diamond ([Sidney Diamond and Huang 2001]) that will be used here, in the case of ordinary concrete. Its representation of ITZ is presented Figure 1.3.

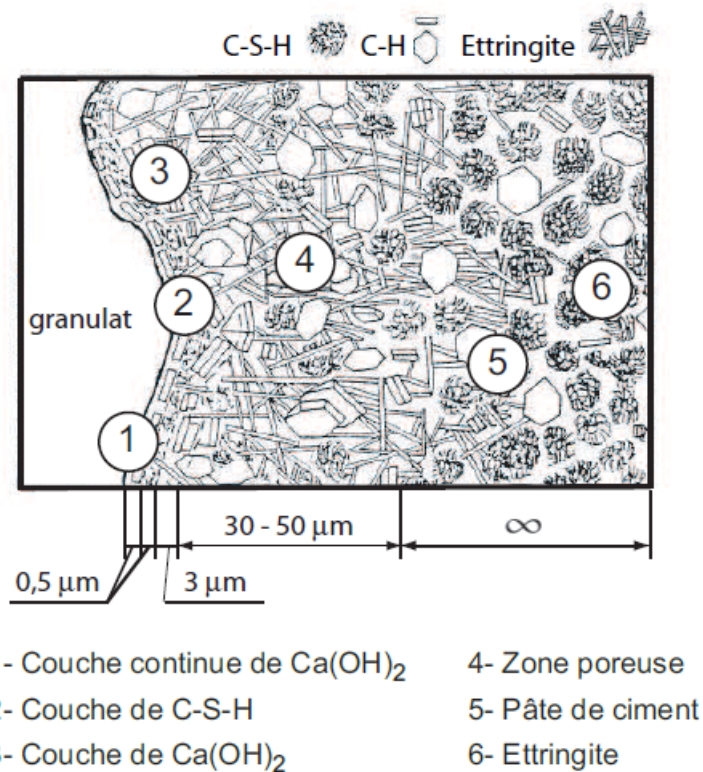


Figure 1.3 – Description of Diamond model for ITZ [Sidney Diamond and Huang 2001]

There are several areas of interest:

- a first layer, close to the aggregate surface, composed mainly of portlandite crystals oriented perpendicular to the aggregate;
- a second layer, composed of CSH sheets;
- an area with high porosity.

We will now present how the parameters identified above influence this interface transition zone, and by extension the macro-material behaviour and its properties.

1.2.2 Impact of aggregate parameters on ITZ

The parameters identified in the previous section are recalled:

- porosity;
- rugosity;
- geometry;
- mineralogical nature;
- volume distribution;
- size distribution.

As mentioned above, the porosity, rugosity and geometry of aggregates have a major influence on the amount of water absorbed and adsorbed by the aggregates. This implies that locally the water-cement ratio can be modified compared to the formulated cement paste, due to excessive water supply or consumption by the aggregates. This ratio is one of the key parameters in the formulation of concretes, and its modification results in a change in the material properties. For example, in a macroscopic case, if the global e/c ratio increases, the concrete will tend to be more porous (Figure 1.4), thus decreasing durability, while exhibiting a decrease in mechanical strength. These macroscopic effects are in fact generalized local effects. In the case of ITZ, these effects are concentrated around the aggregates, which can make this area a weakness point for concretes subjected to thermo-chemical-mechanical stresses (increase of diffusion, initialisation of cracks,...)

In parallel, several authors have shown that ITZ is highly dependent on the mineralogical nature of aggregates. Some inclusions, called reactive, have chemical exchanges with the cement paste (and in particular in basic environment) which can change; positively or negatively; the characteristics of this area. For example, the use of reactive siliceous aggregates causes a pathological chemical reaction called alkali-aggregate reaction, which is localized in ITZs, among other things. In addition, it has been shown that the use of non-reactive siliceous aggregates (quartz type) causes an acceleration and increase in the delayed formation of ettringite (DEF or internal sulfatic reaction) which is also very pathological for concrete. These same authors made comparisons with calcareous aggregates, and the concretes formulated with the latter showed better durability with regard to these pathologies.

Indeed, limestone aggregates seem to have a better chemical affinity with cement paste, and when set in ITZ, a reaction product called calcium aluminate is formed. These products will disrupt the orientation of portlandite, CSH and ettringite in the ITZ, which will give

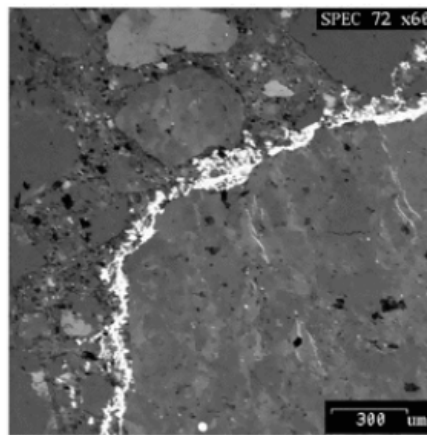
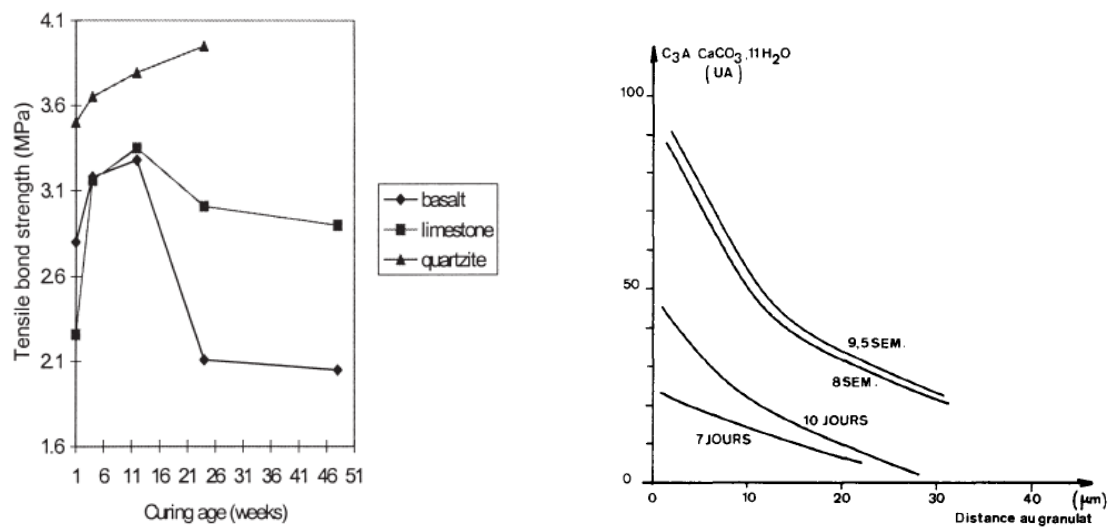


Figure 1.4 – Highlighting of ITZ porous zone using impregnation of concrete with Wood metal [Bentz and Garboczi 1991]

the local material a more limited porosity and an improvement in mechanical properties (due to a more resistant bond) under the stresses it might be subjected to.

In addition, the increase in rugosity will improve the adhesion of the cement paste to the aggregates. Smooth aggregates (such as alluvial aggregates or glass beads for example) will tend to show significant decohesions, even before the slightest stress is applied.



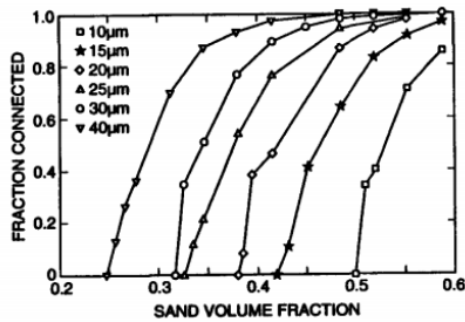
(a) Change in aggregate-cement paste tensile bond strength with curing age

(b) Evolution of hydrated carbo-aluminate in cement paste depending on the distance from the aggregate

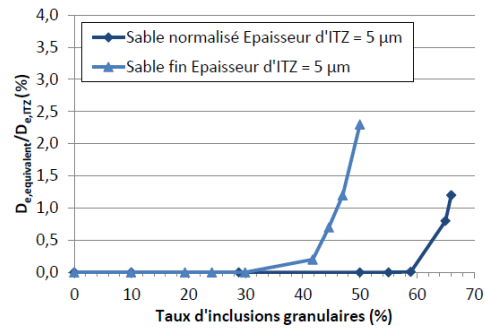
Figure 1.5 – Study of aggregates and ITZ parameters on inter-connexion of ITZ porosity

Moreover, this area is more likely to be present if the surface available to create the interface between aggregate and cement paste is large (larger contact area, larger amount of water adsorbed...). This surface is called the specific surface and is inversely proportional to the radius of the aggregates. The size of inclusions is therefore an important parameter of the ITZ, and this phenomenon will tend to be more pronounced for small aggregates (sand) than for coarse aggregates.

Last but not least, the last parameter studied is the volume fraction of aggregates in concrete (volume distribution). Increasing this parameter means an increase in the number of aggregates in the material, and the optimization of compactness, meaning that the aggregates will tend to approach each other in the material, or even touch each other. ITZs can overlap and create a percolation phenomenon. A closed porous network becomes connected and can lead to increased diffusion and permeability of the material, affecting its durability.



(a) Effects of ITZ size and of aggregate volume fraction on percolation phenomenon [Winslow et al. 1994]



(b) Effect of aggregates size (fine sand or coarse sand) and of aggregates volume fraction on the diffusion properties and ITZ inter-connexions [Bajja 2017]

Figure 1.6 – Study of aggregates and ITZ parameters on inter-connexion of ITZ porosity

In this section, we have defined an important effect of aggregates: the interface transition zone. It has been shown that the aggregate parameters identified above, respectively have a significant influence on the material and its local and global properties. The concomitance of these different parameters can therefore cause considerable disturbances to our initial formulation, creating areas of sensitivity in our material. In an unfavourable case of parameter combinations, the material may exhibit a measurable increase in diffusion and permeability, thus a decrease in durability, while becoming an area of crack location and progression, due to the decrease in mechanical strength.

Bibliography on aggregates

- Bajja, Zineb (2017). “Influence de la microstructure sur le transport diffusif des pâtes, mortiers et bétons á base de CEM I avec ajout de fumée de silice”. PhD thesis. Université Paris-Saclay, prepared at École Normale Supérieure de Paris-Saclay.
- Bentz, Dale P. and Edward J. Garboczi (1991). “Percolation of phases in a three-dimensional cement paste microstructural model”. In: *Cement and Concrete Research* 21.2, pp. 325–344. ISSN: 0008-8846.
- Diamond, Sidney and Jingdong Huang (Apr. 2001). “The ITZ in Concrete - A Different View Based on Image Analysis and SEM Observations”. In: *Cement and Concrete Composites* 23, pp. 179–188.
- Elsharief, Amir, Menashi D. Cohen, and Jan Olek (2005). “Influence of lightweight aggregate on the microstructure and durability of mortar”. In: *Cement and Concrete Research* 35.7, pp. 1368–1376. ISSN: 0008-8846.
- Head, Martin and Nick Buenfeld (Feb. 2006). “Measurement of Aggregate Interfacial Porosity in Complex, Multi-Phase Aggregate Concrete: Binary Mask Production Using Backscattered Electron, and Energy Dispersive X-Ray Images”. In: *Cement and Concrete Research* 36, pp. 337–345.
- M., Moranville-Regourd (1992). “Les bétons á Hautes Performances: caractérisation, durabilité, applications”. In: Presses de l’É.N.P.C. Chap. Microstructure des B.H.P.
- Ollivier, J.P., J.C. Maso, and B. Bourdette (1995). “Interfacial transition zone in concrete”. In: *Advanced Cement Based Materials* 2.1, pp. 30–38. ISSN: 1065-7355.
- Winslow, Douglas N. et al. (1994). “Percolation and pore structure in mortars and concrete”. In: *Cement and Concrete Research* 24.1, pp. 25–37.
- Wong, H.S. et al. (n.d.). “Influence of the interfacial transition zone and microcracking on the diffusivity, permeability and sorptivity of cement-based materials after drying”. In: *Magazine of Concrete Research* 61.8 (), pp. 571–589.

Part II

Effects of aggregates and drying on model cementitious materials behaviour

Chapter 2

State of the art : Drying phenomenon

Contents

2.1 Desiccation	22
2.1.1 Description of the water loss mechanisms	22
2.1.2 Impact of aggregates on drying	23
2.2 Shrinkage mechanisms	24
2.2.1 Description of the shrinkage mechanisms	24
2.2.2 Impact of aggregates on desiccation shrinkage	26
2.3 Cracking mechanisms	30
2.3.1 Macroscopic scale : hydric gradient	30
2.3.2 Mesoscopic scale : aggregate restraint	30
2.3.3 Nano- and micro-scopic scale : local effects	33
2.4 Creep deformations	33
2.4.1 Basic creep	34
2.4.2 Drying Creep	35
2.5 Influence drying on transfer and mechanical properties	37
2.5.1 Transfer properties	37
2.5.2 Mechanical properties	37
2.6 Conclusions and definition of the experimental campaign conditions	39

Ordinary concrete is composed with a quantity of water superior to the one needed for the cement hydration. Even if the porous network is not saturated, the internal relative humidity remains high and superior to the ambient relative humidity. As a consequence, an hydric disequilibrium appears between the core and the surface of the structure. In order to reach equilibrium, water migrates toward the exterior, this is the drying phenomenon.

Several phenomena are generated by this water loss : shrinkage, internal and surface cracking and evolution of the material properties. This chapter is organised around five parts :

- Origins and mechanisms of the desiccation;
- Shrinkage mechanisms induced by drying;

- Induced cracking;
- Participation of the creep phenomenon;
- Impact of drying on transfer and mechanical properties.

In each part, a focus is made on the impact of relevant aggregates parameters on the phenomena studied.

2.1 Desiccation

In concrete porous network, three phases coexist: the solid phase (represented by the cement paste matrix), the liquid phase (free and adsorbed water) and a gas phase (dry air and water vapour). The quantity of each phase depends both on the porous network (porosity, tortuosity, connectivity), but also on the environmental relative humidity in which the material evolves. Moreover, transfer mechanisms are complicated by the high concentrations of ions in the interstitial solutions or carbon dioxide in the gaseous phase.

2.1.1 Description of the water loss mechanisms

The water departure happens principally in the cement paste; except when aggregates present an important porosity; and is submitted to several mechanisms more or less coupled and displayed Figure 2.1. The importance of each process varies with the hydric conditions applied to the material [Baroghel-Bouny 1994].

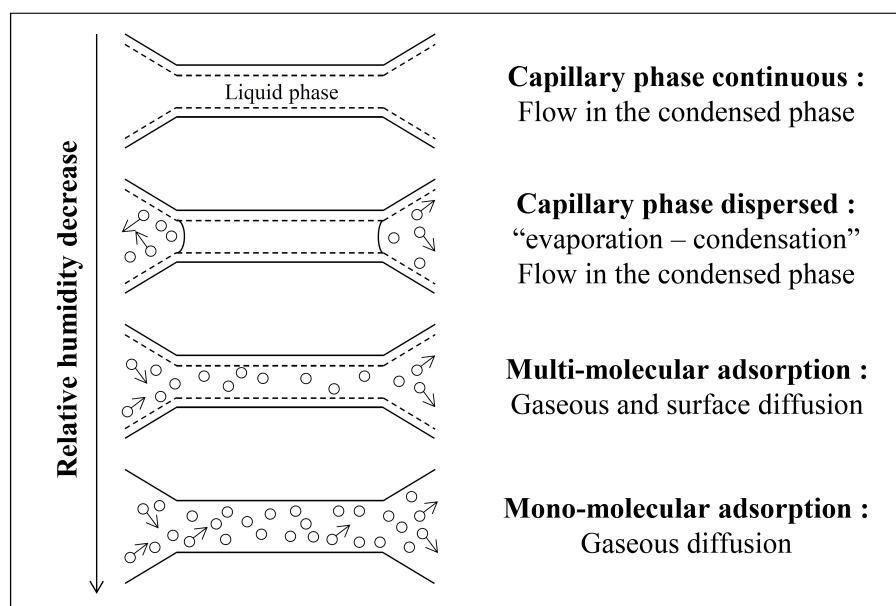


Figure 2.1 – Schematics of the water transfers depending on the environmental relative humidity [Baroghel-Bouny 1994]

High relative humidity When the material is saturated - e.g. at the removal of the forms from the structure - water continuously fills in the capillary network. As soon as the relative humidity decreases, a flow is set from the inside toward the outside of the material. Yet, the water is mainly found as a liquid phase and, as long as this phase is continuous, water movements in the material are mainly ruled by the liquid

pressures - almost equal to capillary pressures - which correspond to permeation of liquid water.

Medium relative humidity In that case, water as a liquid phase and a gaseous phase coexist. When the relative humidity drops, water leaves the macro-pores and evaporates. The continuity of the liquid phase is disrupted but can still be found in the fine porosity network. Water movement happens through an exchange with the gaseous phase via evaporation and condensation cycles, and is associated to a flow of condensed phase.

Low relative humidity Water is mainly in a gaseous phase and water transport is ruled by gaseous diffusion. But some adsorbed liquid water can be present in the pores, creating water films with a thickness of some molecules. As a consequence, an additive transport due to the migration of the water molecules can be observed, called surface diffusion. When relative humidity becomes very low, the adsorbed water disappears and transport is ruled only by gaseous diffusion.

This water loss leads to the appearance of gradients of water "concentration" (in gaseous and liquid forms) from the core to the surface of the material, generating strains and stresses gradients in the structure. These effects will be studied in the next sections.

2.1.2 Impact of aggregates on drying

Volume fraction It is mostly the cement paste that is able to lose water and consequently to undergo the drying phenomenon (under the hypothesis that the aggregates present a low porosity). Thus, if the aggregate volume fraction increases, the cement paste volume fraction decreases and so is drying. The Figure 2.2(a), from [Bisschop and J. G. v. Mier 2002] demonstrates this phenomenon. As seen in the introduction chapter, the increase of aggregate volume fraction can lead to two competing phenomena: the increase of the open porosity, that could result in the increase of water movements in the material and thus of drying; and the increase of tortuousness of the pores network, that could result in a decrease of the observed water loss.

However, in Figure 2.2(b) is displayed the mass loss of the different samples normed by the cement paste fraction and the increase of the volume of aggregates does not seem to impact the drying phenomenon. The most plausible explanation of this observation is that the amount of aggregates studied is too low to allow the interconnection of ITZs. Also the aggregates used in this study are glass spheres, the presence of ITZ in these conditions is very debatable.

Size When the aggregate size is modified, the characteristics (length, connectivity, tortuousness) of the pores network are changed which could lead to a modification of the water loss of the material. In the same paper of [Bisschop and J. G. v. Mier 2002], a study on the effect of inclusion (glass spheres) size on moisture loss is also made, Figure 2.3. It shows that inclusion size does not impact significantly the drying phenomenon.

2.2 Shrinkage mechanisms

Under desiccation, concrete suffers from an apparent deformation called drying shrinkage and directly linked to water loss. This phenomenon is dependent of the quantity

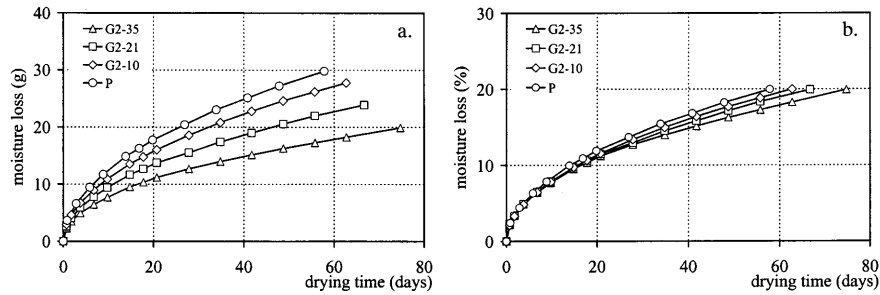


Figure 2.2 – a) Moisture loss of model materials presenting different aggregate volume fraction b) Moisture loss of the same materials normed by the cement paste volume fraction [Bisschop and J. G. v. Mier 2002] - *in the legends of the images, G:glass inclusions; 2:diameter of inclusions (2mm); 10, 21 and 35:amount of drying/water loss (in percent); P:cement paste.*

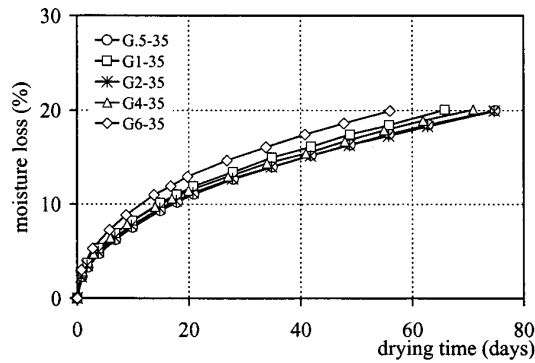


Figure 2.3 – a) Moisture loss of model materials presenting different sizes (0.5, 1, 2, 4 and 6 mm) of inclusions [Bisschop and J. G. v. Mier 2002] - *in the legends of the images, G:glass inclusions; 0.5,1,2,4,6 :diameter of inclusions (in mm); 35:amount of drying/water loss (in percent).*

of internal water, thus of environmental relative humidity [Baroghel-Bouny 1994; Neville 2000, among others]. It can be expressed as the global observed deformation reduced by the autogenous shrinkage deformation (also called endogenous shrinkage), measured on a specimen protected from desiccation.

2.2.1 Description of the shrinkage mechanisms

Endogenous shrinkage

During the hardening of Portland cements, one can observe volumic variations even without loading. The hydration of cement is accompanied by an increase in apparent volume at the same time as a contraction in absolute volume. Indeed, the volume of hydrates produced is less than the sum of the volume of reagents (water and cement). This contraction is commonly called Le Chatelier's contraction, chemical shrinkage or absolute volume decrease. Before hardening, this volume deformation of the cement paste is free, given the fluid behaviour of the material. However, during hardening, chemical shrinkage is gradually retained by the formation of the solid skeleton. From this point on, the apparent volume variation of the cement paste is negligible compared to that due to the Le Chatelier's contraction.

Moreover, the composition of the internal porosity is then dependent on the hydration reaction. During hardening, the porosity is almost saturated with liquid water. As the reaction progresses, this water is consumed for hydration of anhydrous cement and the water content of the capillary pores decreases. As a result, the internal relative humidity decreases and a capillary depression appears. The cementitious matrix is then loaded by capillary forces [Hua, Paul Acker, and Ehlacher 1995] and a contraction called self-desiccation shrinkage follows.

In general, autogenous shrinkage is the sum of chemical shrinkage before hardening and self-desiccation shrinkage. Therefore, the mechanical problem only considers the shrinkage of self-desiccation since its evolution begins with the solidification of the material.

However, for concrete with a high water/cement ratio; i.e. superior to 0.45; this deformation becomes negligible compared to the one due to temperature in the case of massive structures or to drying in the case of thin structures, as seen in [Granger 1996; Jensen and P. Hansen 2001; Briffaut 2010].

Desiccation shrinkage

Three main mechanisms have been identified to explain this phenomenon [Baron 1982; Baroghel-Bouny 1994].

Capillary pressure The decrease of relative humidity in the concrete due to drying leads to the decrease of the liquid water pressure, due to its vaporisation. The co-existence of water as a liquid and a gaseous phase leads to the formation of a meniscus at the liquid-gas interface, and the establishment of capillary stresses. It leads to the contraction of the rigid skeleton, corresponding to drying shrinkage.

Disjunction pressure The phenomenon of disjunction pressure was introduced by Powers in his model [Powers 1968], and was experimentally proved by an experiment led by [Beltzung and F.H. Wittmann 2005]. Two spheres made of quartz are put in contact one above the other in a dry environment. When relative humidity rise, water is adsorbed on the surface, the disjunction pressure rise and the two spheres pull away from each other. Similarly, a decrease of a relative humidity leads to a decrease of the thickness of adsorbed water in the zone of prevented adsorption, as a consequence, the disjunction pressure decrease. The rigid skeleton contracts, corresponding to drying shrinkage [F. H. Wittmann 1982; Baroghel-Bouny 1994].

Variation of the surface tension The surface tension depends on the quantity of adsorbed water. A decrease of relative humidity, generated by drying, tends to rise the surface tension. As a consequence the rigid skeleton contracts to equilibrate stresses [F. H. Wittmann 1982].

Combination of mechanisms It seems that these mechanisms occur as a combination, and at certain range of relative humidity loads as displayed Figure 2.4. Under 40%RH, the predominant shrinkage mechanism is the variation of surface tension. Between 30% and 50%RH, two mechanisms are competing : disjunction pressure and surface tension variation. Above 50%RH, the two mechanisms competing are : disjunction and capillary pressures.

	Relative humidity					
	0	20	40	60	80	100
Powers (1965)	←			Disjunction pressure		→
Ishai (1965)	←	Surface energy	→	←	Capillary pressure	→
Feldman & Sereda (1970)			←	Capillary pressure + Surface energy		→
Wittmann (1968)	←	Surface energy	→	←	Disjunction pressure	→

Figure 2.4 – Drying shrinkage mechanisms according Soroka [Soroka 1979]

2.2.2 Impact of aggregates on desiccation shrinkage

Volume fraction As it is mainly the cement paste that shrinks, increasing the volume of rigid aggregates in the material will consequently lead to the decrease of shrinkage. This phenomenon was fully studied, on an experimental point of view, by several authors, mainly [Carlson 1939] and [W. Hansen and Almudaiheem 1987] quoted in [Bisschop 2002], but also [Bissonnette; Pickett 1956; Lagier et al. 2011; Eguchi and Teranishi 2005]. In the last one, a comparison of several experimental works is made, the results are displayed Figures 2.5 and 2.6 where a proportional decrease of shrinkage can be observed.

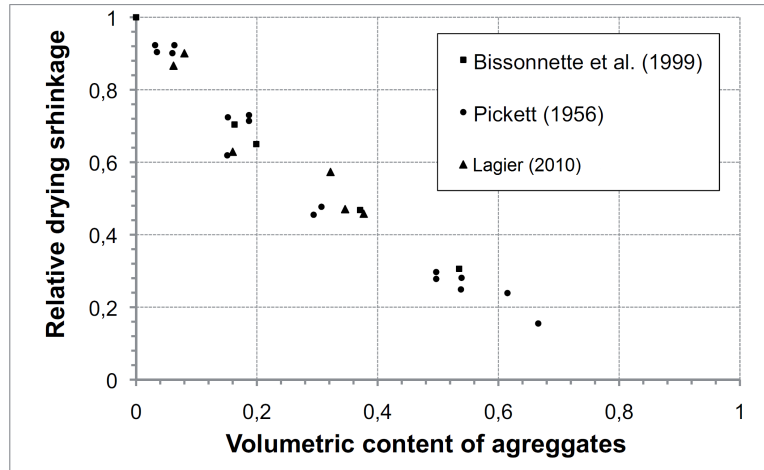
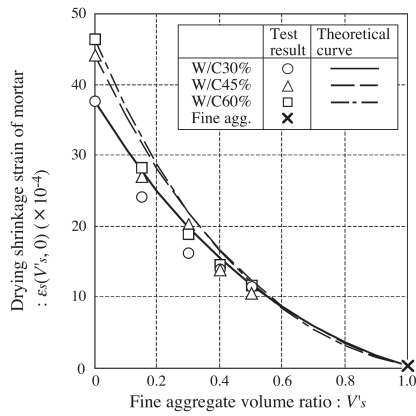
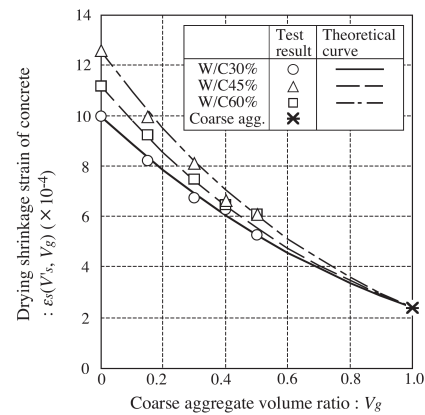


Figure 2.5 – Comparison of experimental results of drying shrinkage versus aggregates volume fraction. From [Lagier et al. 2011] with results also from [Pickett 1956] and [Bissonnette, Pierre, and Pigeon 1999]

Size The effect of aggregate size on shrinkage is not well studied in the literature. It was first studied by [Carlson 1939], quoted by [Bisschop 2002], who found out that aggregate size was not a significant parameter on shrinkage evolution. However, it seems that in the experiments reported the maximum aggregate size was changed, but at the same time the cement content was changed to maintain constant workability and water-cement ratio. The measured effect was a combination of maximum aggregate size and aggregate volume percentage, it is difficult to achieve a conclusion on the matter. A numerical study, conducted by [De Sa, Benboudjema, and Michou 2013], demonstrated a low influence of aggregate size on apparent drying shrinkage (Figure 2.7).



(a) Drying shrinkage strain as a function of fine aggregate volume fraction in mortar



(b) Drying shrinkage strain as a function of coarse aggregate volume fraction in concrete

Figure 2.6 – Relationship between drying shrinkage strain and aggregate volume ratio in mortar and concrete - drying period of 182 days [Eguchi and Teranishi 2005]

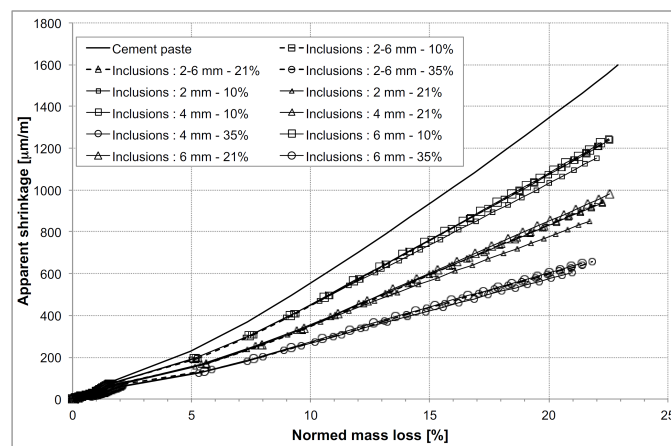
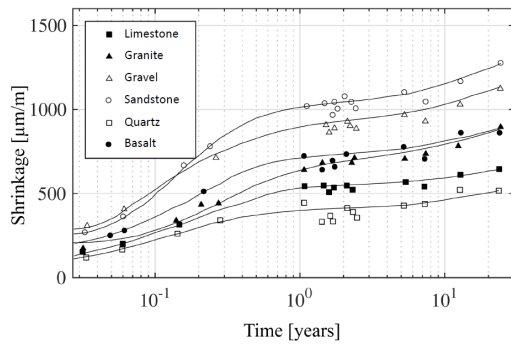
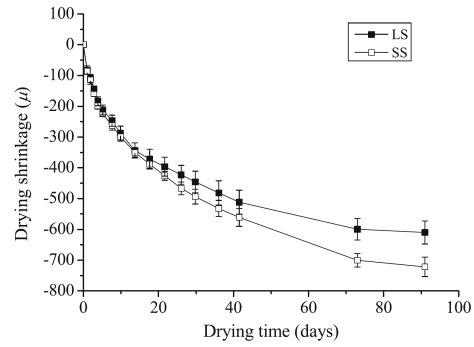


Figure 2.7 – Numerical study on the effect of aggregate size and volume fraction [De Sa, Benboudjema, and Michou 2013]

Mineralogical nature The mineralogical nature of aggregates has a important impact on the concrete shrinkage. [Neville 2000] demonstrated that, as seen in Figure 2.8a some types of dolerite, basalt and sedimentary rocks presented shrinkage whereas the common aggregates used in concrete as granite, quartz and limestone display a shrinkage that can be considered negligible. [Maruyama, Sasano, and Lin 2016] also took an interest in comparing two aggregate mineralogy, as displayed 2.8b . They observed that samples with sandstone aggregates tend to shrink more than the ones with limestone aggregates.



(a) Impact of aggregate mineralogy on shrinkage [Neville 2000]

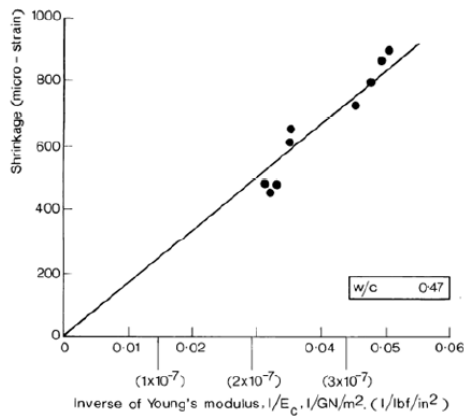


(b) Comparison of concrete shrinkages [Maruyama, Sasano, and Lin 2016] - *LS*: concrete with limestone aggregates and *SS*: concrete with sandstone aggregates

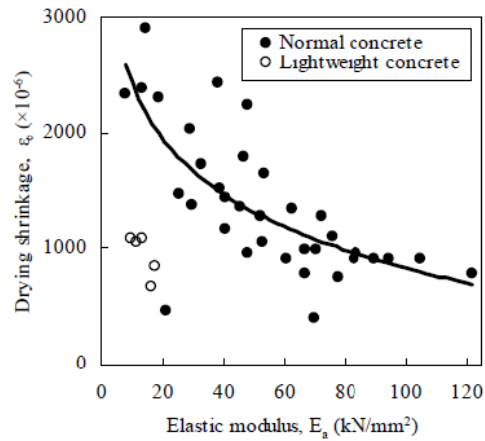
Figure 2.8 – Impact of aggregate mineralogy on shrinkage

Two parameters can be the origin of this observation : **Young Modulus** and **aggregate shrinkage**.

[Carlson 1939] showed the link between aggregate stiffness and shrinkage by placing highly elastic rubber particles instead of stiff aggregates. The concrete displayed a shrinkage as large as the one of plain cement paste. [T. Hansen and Nielsen 1965] also reached the same conclusion by using aggregates presenting the same magnitude of shrinkage as the matrix. Finally [Hobbs 1974] and [Fujiwara 2008] took an interest in this matter and showed that the concrete shrinkage increases with the decrease of aggregate stiffness, as shown Figure 2.9.



(a) Influence of aggregate stiffness on shrinkage [Hobbs 1974]

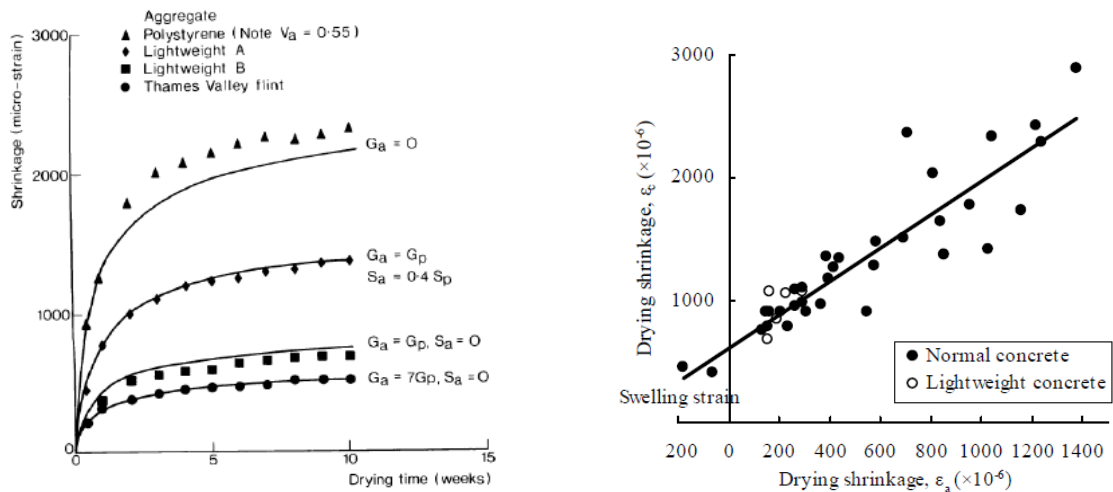


(b) Influence of aggregate Young Modulus on concrete shrinkage [Fujiwara 2008]

Figure 2.9 – Relationship between drying shrinkage and aggregate Young Modulus

However, they both concluded that the effect of stiffness variation remains weak compared to the one of aggregate volume fraction variation. They also highlighted

that aggregate shrinkage was significantly influential. Figure 2.10 demonstrates that, at a fixed stiffness, aggregates with different shrinkage characteristics influence the drying deformation of concrete : composition with shrinking aggregates has a higher total deformation than the one with inert aggregates. The ability of aggregates to shrink is mostly due to their porosity as shown in the study of [Cortas 2012] where he used aggregates with different porosity in the concrete mixes and observed the drying shrinkage. Results are displayed Figure 2.11. It shows that the compositions made with aggregates presenting the higher porosity (porous limestone - Beauvilliers (BV), and lightweight aggregates (GL)) tends to shrink more than the composition with compact quartz aggregates (Palvadeau (PL)). it also shows that the choice of aggregates is more influential than the change of water-cement ratio from 0.5 to 0.6.



(a) Influence of aggregate shrinkage on drying shrinkage [Hobbs 1974] (G: stiffness, S: shrinkage, a: aggregate, p: cement paste)

(b) Influence of aggregate shrinkage on drying shrinkage [Fujiwara 2008] (ε_a: aggregate shrinkage, ε_c: concrete shrinkage)

Figure 2.10 – Relationship between drying shrinkage and aggregate Young Modulus

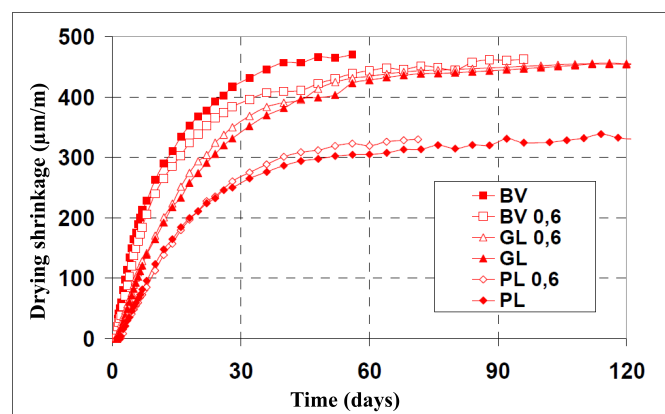


Figure 2.11 – Impact of aggregate porosity and W/C ratio on concrete drying shrinkage [Cortas 2012] - PL : Palvadeau aggregates, BV : Beauvilliers aggregates, GL : lightweight aggregates

To summarise, the major mechanisms of shrinkage were highlighted, and the impact of aggregates parameters studied. It reveals that aggregate volume fraction and aggregate mineralogy are two very influential parameters, while the size of the aggregates seems to have a more limited effect.

2.3 Cracking mechanisms

The desiccation shrinkage causes the appearance of a strain gradient between the core and the surface of the sample but also internal strains states that could lead to the initiation of structural and local degradations. Three mechanisms were identified occurring at three different scales.

2.3.1 Macroscopic scale : hydric gradient

The hydric gradient induced by drying of the material leads to a differential shrinkage : the shrinkage of the surface is most important. As a consequence, the skin of the sample is submitted to a tensile stress whereas the core to compressive stress. If the tensile stress become higher than the tensile strength of the material, a superficial micro-cracking appears ([Z. Bažant and F.H. Wittmann 1982; Paul Acker 1988; Paul Acker 1991; Neville 2000], among others). This mechanism is sketched in Figure 2.12. The cracks are perpendicular to the surface of the specimen and presents a range of width of $50 - 100\mu\text{m}$. As the stresses are relaxed, the tensile zone moves toward the core of the material, leading to the cracking progression [Benboudjema 2002].

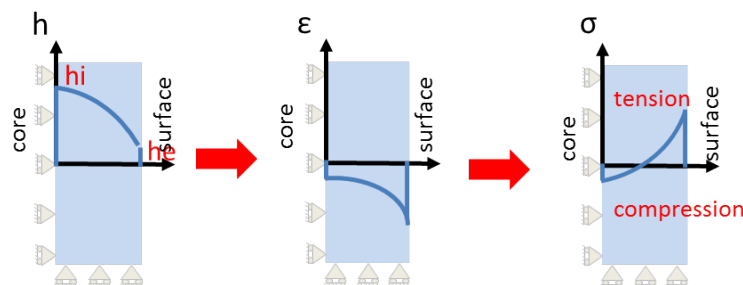


Figure 2.12 – Cracking mechanisms induced by the hydric gradient [De Sa 2007]

2.3.2 Mesoscopic scale : aggregate restraint

Mechanisms The concrete material is very heterogeneous. Aggregates usually display a low porosity and therefore remain inert face to the drying phenomenon, whereas the cement paste tends to contract, in particular for high water-cement ratio. The strains differential leads to the appearance of a tensile stress at the interface transitional zone, which could lead - if it becomes superior to the tensile strength - to the initiation of a radial and circumferential cracking around the aggregates. [Bisschop 2002; Bisschop, Pel, and J. G. M. v. Mier 2001; Bisschop and J. G. v. Mier 2002; Lagier et al. 2011] This mechanism is sketched in Figure 2.13.

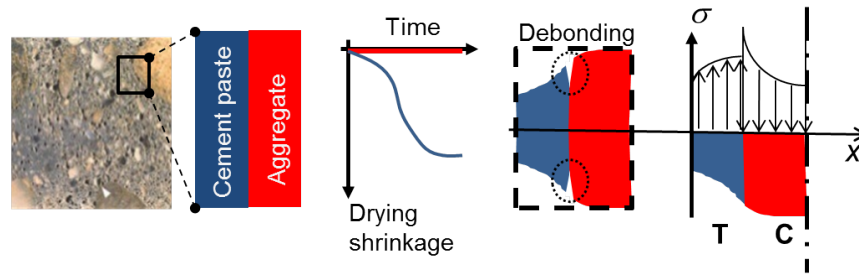


Figure 2.13 – Cracking mechanisms induced by the aggregate restraint [De Sa 2007]

The aggregate parameters are influential factors of this internal cracking. We are taking an interest in the major ones.

Impact of the aggregates

Volume fraction The decrease of shrinkage explained in Section 2.2.2 leads to the modification of internal stresses and strains gradients. Several authors took an interest in this phenomenon, such as [Lagier et al. 2011] or [Wong et al. 2009], but it is mostly Jan Bisschop who fully explored the effects of volume fraction on cracking induced by drying in several papers - among which [Bisschop 2002; Bisschop, Pel, and J. G. M. v. Mier 2001; Bisschop and J. G. v. Mier 2002] - as displayed Figure 2.14. His results show that the amount of micro-cracking is reduced by the increase of aggregates volume fraction.

Size The work of [Bisschop 2002; Lagier et al. 2011; Wong et al. 2009] showed that aggregates size plays an important role in the initiation and development of internal cracking. The restraint tends to become more important when the size of aggregates increases. Regarding Figure 2.15 from [Bisschop, Pel, and J. G. M. v. Mier 2001], a clear pattern is appearing : the increase of aggregate size leads to the increase of internal cracking, but more importantly, it shows that aggregates with a diameter inferior to 6mm induce a very limited amount of internal cracking. It seems that from a specific diameter (between 4 and 6mm) the internal stresses become high enough to induce cracking.

Mineralogical nature It was seen in Section 1.2.2 that the aggregate mineralogical nature of aggregates influences the shrinkage induced by desiccation, thus the induced strains and stresses gradients in the materials. These stresses are responsible for the cracking phenomenon. Changing the aggregates Young Modulus and porosity leads to a modification of cracking patterns.

[Bisschop 2002] took an interest in characterising the impact of aggregates Young Modulus on internal cracking. He used several type of aggregates : "soft" aggregates, having a Young Modulus lower than the one of glass spheres (close to the one of aggregates) and "stiff" aggregates, having a Young Modulus larger than the one of glass spheres. The results are displayed in Figure 2.16. It reveals that, unless $E_{agg} \ll E_{cp}$ as in the polystyrene case, the cracking patterns don't seem very affected by the change of aggregates types. However Bisschop specifies that he observed differences on the circumferential cracking, which is not presented in his results as

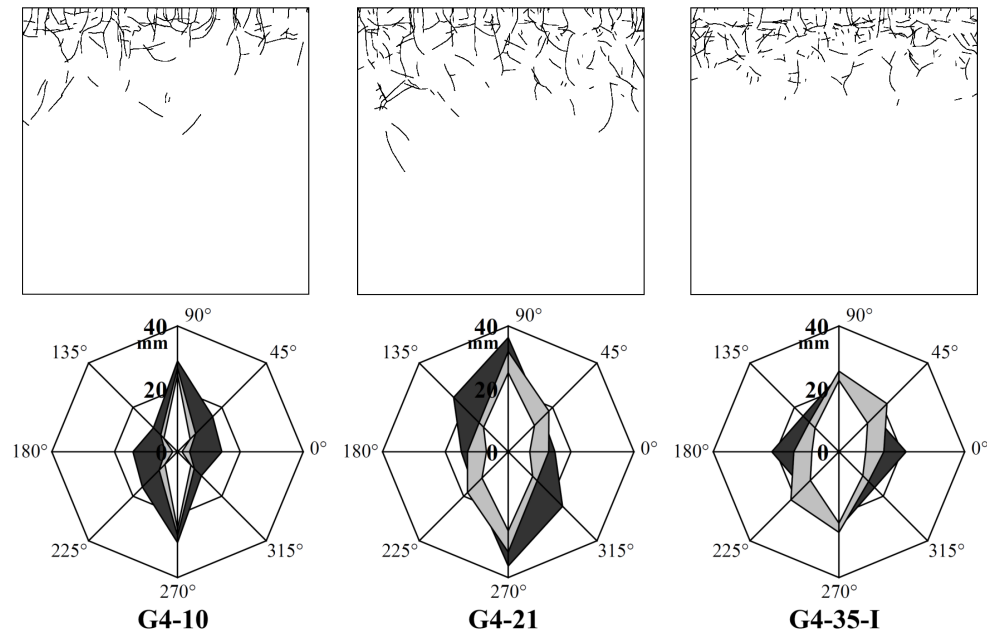


Figure 2.14 – Effect of aggregate volume percentage on drying shrinkage microcracking for composites with 10%, 21% and 35% of 4mm-spherical aggregates. Crack-maps are at 30% drying; radar-diagrams are for 10% (white), 20% (grey), and 30% (black) drying - adapted from [Bisschop 2002]

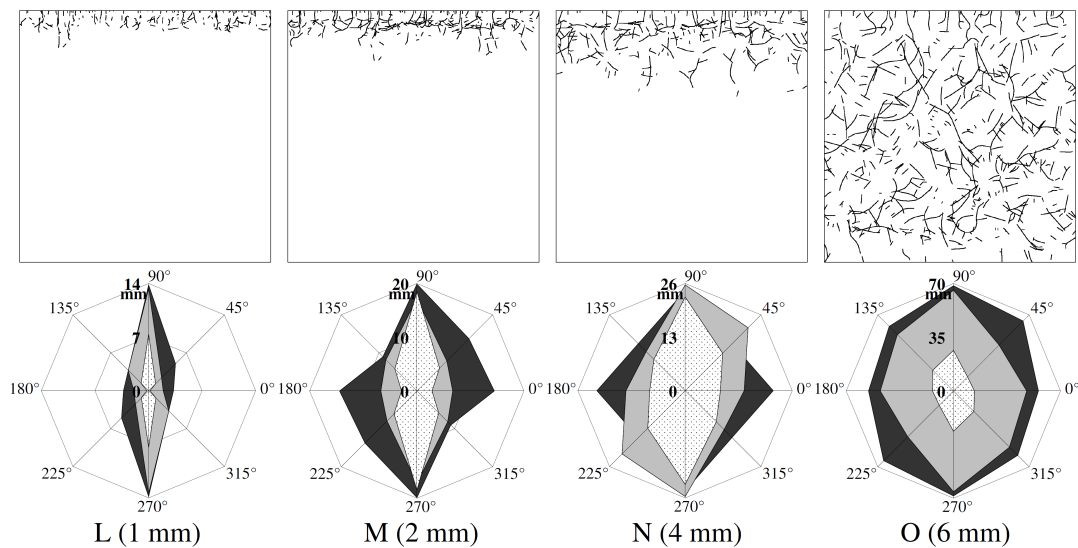


Figure 2.15 – Effect of sphere size on drying shrinkage microcracking. Crack-maps are at 30% drying; radar-diagrams are for 10% (white), 20% (grey), and 30% (black) drying [Bisschop, Pel, and J. G. M. v. Mier 2001].

the initial interface was hard to characterise, the opening and orientation of cracks. Finally he concluded that the impact of this parameters remains very limited as long as $E_{agg} \geq 4E_{cp}$.

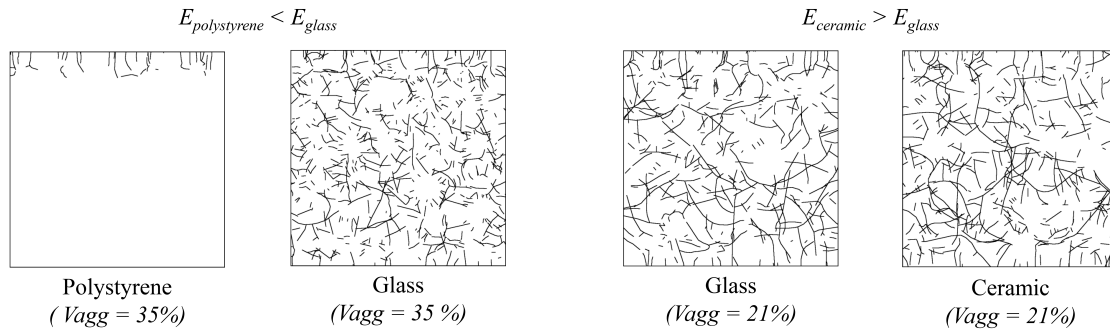


Figure 2.16 – Effect of sphere stiffness on drying shrinkage microcracking, at 30% drying and with spheres diameter of 6mm.[Bisschop, Pel, and J. G. M. v. Mier 2001].

2.3.3 Nano- and micro-scopic scale : local effects

The phenomenon of restraint described at the mesoscopic scale can be observed at a nanoscopic scale. Cement paste is mainly made of C-S-H, which tend to contract face to drying, and portlandite, which is invariant under drying. This leads to the same path of mechanisms and the possible appearance of radial and circumferential cracking around portlandite particles [Hearn 1999; Baroghel-Bouny 1994; Neville 2000]. Also, at microscopic scale, this phenomenon is observed between hydrated cement paste and anhydrous cement particles (Figure 2.17) and between the cement paste and fine aggregates.

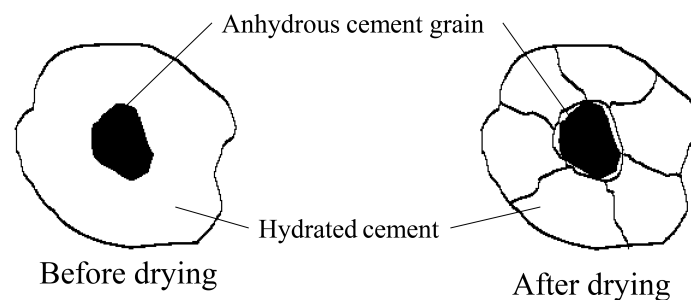


Figure 2.17 – Radial and circumferential cracking around an anhydrous cement grain [Hearn 1999]

In this section, one has seen the major role of aggregates in cracking mechanisms. They are at the origin of a developed internal cracking. All of the aggregates characteristics directly impact cracks initialisation and progression.

2.4 Creep deformations

Creep is the delayed deformation of concrete element under a constant loading. It is impossible to directly measure this deformation, but it can be obtained by subtracting the delayed deformation of a non-loaded concrete to the one of loaded one.

The creep deformation can be expressed as the sum of two deformations: one induced by basic creep, obtained under endogenous conditions, and an other one induced by desiccation

creep generated by the drying of the material. In this section we will see the mechanisms of those deformations, and the influence of aggregates parameters.

2.4.1 Basic creep

Basic creep mechanisms

Basic creep is the deformation measured on a loaded sample protected from external drying from which was subtracted the autogenous shrinkage deformation and the instantaneous elastic deformation. Two main mechanisms are to be considered to explain the concrete basic creep according [Ulm and Paul Acker 1998].

1. **On a short term** : creep is due - according [Ulm and Paul Acker 1998] and [F. H. Wittmann 1982] - to a diffusive mechanism of water in the capillary network, induced by macroscopic loading. Strains are transmitted at a microscopic scale, through the products of hydration which surround the capillary pores. This strain transfer induces a local thermodynamic disequilibrium between water molecules in a free adsorption state in this transition zone and the ones further in the network. To set back the equilibrium, water molecules migrate in the layers of adsorbed water toward capillary porosity, leading to the deformation of the rigid skeleton.

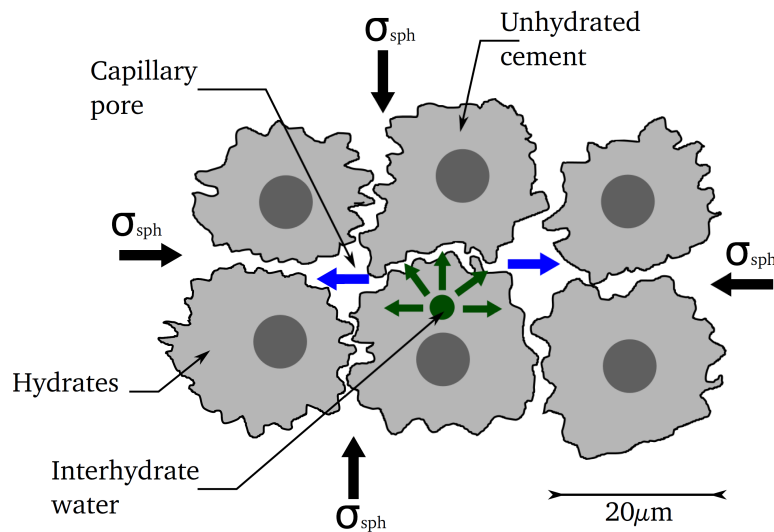


Figure 2.18 – Basic creep short-term mechanisms : migration of absorbed water ([Benboudjema 2002] adapted from [Ulm and Paul Acker 1998])

2. **On a long term** : creep is depending on the ageing of the material and it is mostly due to a mechanical mechanisms that finds its origin at a nanoscopic scale, in the C-S-H pores according [A. Bažant Z. H., Baweja, and Ulm 1997] and [Ulm and Paul Acker 1998] . In the zone of prevented adsorption developed during hydration, bounds between surfaces due to mutual attraction or atomic bonding to equilibrate disjunction pressure are put into tension during hydration. They become unstable and can break to create new bonds with adjacent atoms in less-tensed zones leading to the sliding of C-S-H sheets. The local shear strain is relaxed and is redistributed, leading to the creation of a new local tensed zone, leading to new bonds breaking.

This process successively exhaust the creep activated zones and lead to the ageing observed for the creep kinetics.

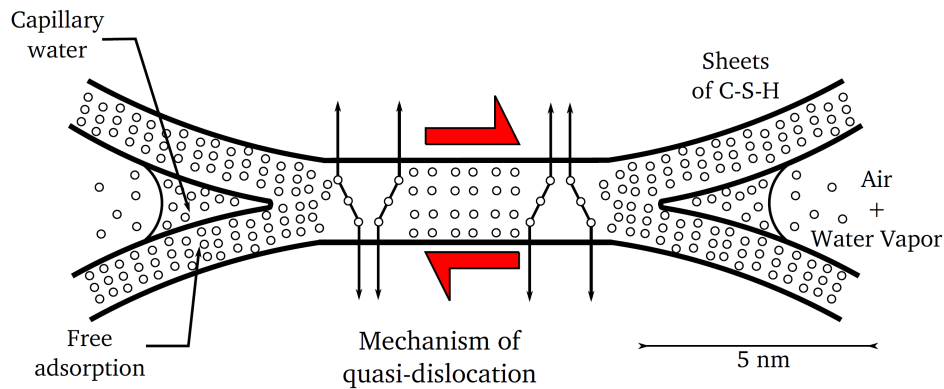


Figure 2.19 – Basic creep long-term mechanisms : sliding C-S-H sheets([Ulm and Paul Acker 1998])

Impact of aggregates on basic creep

The cement paste and the aggregates have different behaviours face to basic creep: cement paste tends to deform whereas aggregates are inert. Therefore, the aggregates restraint applied to the deforming cement paste generates local tensile strains in the cement paste and compressive strains in the aggregates, which could lead to internal microcracking localised in the interfacial transition zone. This phenomenon could be the reason why cracking was detected using an acoustic emission device on concrete samples submitted to basic creep tests [Rossi et al. 1993]. As it was showed in paragraph 2.3.2, aggregates parameters tends to have an impact on this internal cracking.

Volume fraction The basic creep deformation is mainly due to the deformation of cement paste, as aggregates tends to remain invariant. As a consequence, the amount of basic creep is directly dependent of the cement paste volume fraction in the material. [Domone 1974] and [Haroun 1968] highlighted this phenomenon, but also that evolutions of basic creep as functions of water-cement ratio or aggregates-cement ratio are different: the influence of the water in the concrete is more influential than the amount of aggregates.

Size The influence of aggregates size was not thoroughly studied. Nevertheless, in his PhD thesis [El-Baroudy 1940] showed that the use of coarse aggregates of an important diameter ($D=25.4$ mm) leads to more significant creep deformation than with coarse aggregates with a moderate diameter (9.5 mm). The same mechanisms than in Paragraph 2.3 are at stake here: the bigger are the aggregates, the higher the restraint of cement paste will be, leading to a more localised and opened cracking pattern.

2.4.2 Drying Creep

Drying creep mechanisms

In 1942, G. Pickett experimentally showed that uniformly dried specimens present less creep than saturated ones. However, when the specimen is simultaneously dried and

loaded, the creep deformation is higher than the one which was first dried and then loaded [Pickett 1942]. This paradoxical behaviour is called the "Pickett Effect". The additional deformation observed is defined as drying creep. The mechanisms at stake are still subjected to debate and are fully enumerated by [Hilaire 2014] and [Benboudjema 2002]. The first consensus reached is that all mechanisms can be sorted in two groups : structural and intrinsic drying creep.

1. **Structural drying creep** : The drying of the concrete leads to a non-uniform strains state within the material. The hydric gradient generated leads to important tensile stresses at the surface of the sample, which could lead to the local appearance of cracks. This cracking relaxes the stresses induced by drying and diminish the shrinkage amplitude. Moreover, if concrete is submitted to a compressive stress (as drying creep), the stress gradient in the concrete is lowered and most of the material is under compressive strains. As a consequence, the skin micro-cracking is significantly mitigated.
2. **Intrinsic drying creep** : This deformation was highlighted by an experiment led by [R. Day, Cuffaro, and Illston 1984] who showed that drying creep was observed on fine samples of cement paste, and consequently not submitted to hydric gradient. Among several mechanisms found in the literature, the one of [Z. Bažant and Chern 1985] seems to be the most commonly used. It supposes that the "stress-induced shrinkage" is due to two processes of water diffusion occurring at macro-scale and micro-scale. The diffusion in the micro-porosity of the concrete leads to a local flow of water molecule between free adsorption areas and capillary pores, accelerating the ruptures of bonds between C-S-H. This theory was then modified by [A. Bažant Z. H., Baweja, and Ulm 1997], putting forward that - similarly to the phenomenon describe in section 2.4.1 - the relaxation of these "micro-stresses" in the free adsorption areas leads to the drying creep deformations.

Several authors ([Z. Bažant and Y. Xi 1994; Granger 1996; Benboudjema 2002, among others]) studied the coupling of these mechanisms. They experimentally observed and numerically showed that the deformation induced by the structural mechanisms represent a small, but not negligible, part of the total drying creep deformation.

Impact of the aggregates

The influence of aggregates was not thoroughly studied.

According to [Alain Sellier and Buffo-Lacarrière 2009] drying creep is an increase of drying shrinkage due to a better transmission of the effects of capillary pressure decrease toward the rigid skeleton; this theory is close to the one of [Z. Bažant and Chern 1985]. The authors differ regarding the origins of the phenomenon, [Alain Sellier and Buffo-Lacarrière 2009] put forward that it is due to a micro-damaging (cf. Figure 2.20) generated by the phenomena of restraint occurring at meso-scale (deformations incompatibilities between aggregates and cement paste) and micro-scale (deformations incompatibilities between anhydrous cement grains and hydrated cement).

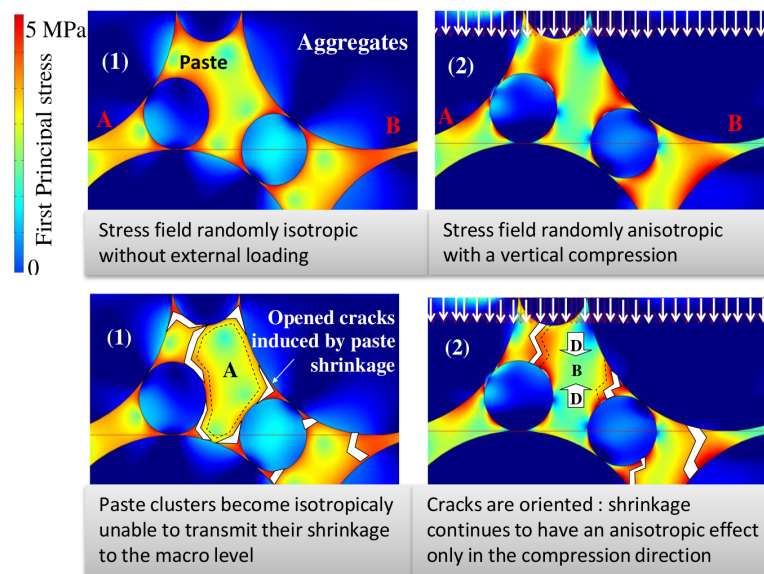


Figure 2.20 – Numerical study on the influence of aggregates on intrinsic drying creep ([Alain Sellier and Buffo-Lacarrière 2009])

2.5 Influence drying on mechanical properties

Compressive strength

Several authors observe that the strength of a dry specimen is generally higher than that of a saturated specimen (RH close to 100%). These authors differ with the evolution of the compressive strength between these two limits. [Neville 2000; Yurtdas 2003; Soleilhet 2018; Butcher 1958; Mills 1960; Pihlajavaara 1974; F. Wittmann 1968; Burlion, Bourgeois, and Shao 2005] observe alternating phases of increase and decrease in compressive strength as the RH varies (cf. Figure 2.21a). Whereas [Okajima, Ishikawa, and Ichise 1980; Popovics 1986; Mills 1960; Bartlett and J.G. 1994] only observe an augmentation, continuous or not, of the strength with RH decrease.

However some authors, among others [Jean-Michel Torrenti 1987], also observed a diminished strength when the material is dried compared to the one when the material is wet. Here again, the evolutions vary.

The increase trend is believed to be due to several concomitant phenomena leading to a stiffening of the material. On the one hand, water saturation reduces cohesion forces by increasing disjunction pressures and decreasing tensions. On the other hand, interstitial pressures increase. Finally hydric gradients tend to confine the core of the specimens. This latest behaviour induces a superficial micro-cracking. In parallel, a internal micro-cracking develops due to the aggregates restraint. Globally, there is a competition between the first phenomenon and the second one. The evolution of the compressive strength - that also depends on several other parameters (among others, the material nature, the components characteristics, of the testing conditions, etc.) leans one way or the other depending which phenomena are predominant.

Young's Modulus

The apparent elastic modulus determined with a compressive test seems to be negatively impacted by the desiccation. Most authors observe a global decrease in Young

Modulus with the decrease of relative humidity. In [Jean-Michel Torrenti 1987; Burlion, Bourgeois, and Shao 2005; Yurtdas et al. 2006] among others, between 100% and 40%RH, Young Modulus is constant and decreases between 40%RH and a dried state (0%RH). In [F. Wittmann 1968], for the same range of RH values, specimens display first a decrease of Young Modulus, and then an increase.

It seems this parameter is better able to describe the damaging suffered by the material, and is less perturbed by the parasite phenomena.

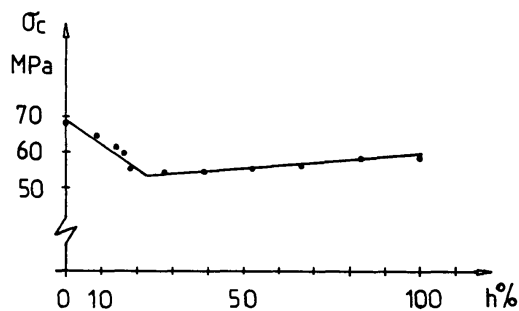
Flexural strength

The flexural strength is determined with three- or four-point flexural tests. This value gives us an indirect access to the tensile strength, as it is very difficult to determine it using direct methods.

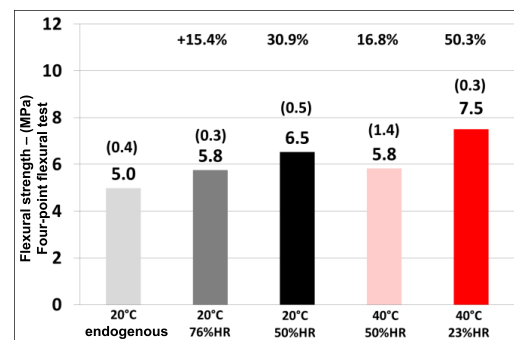
In general, the authors find that the flexural strength tends to increase with the decrease of relative humidity in the samples [Pihlajavaara 1974; Okajima, Ishikawa, and Ichise 1980; Soleilhet 2018; Bucher et al. 2017], cf. Figure 2.21b. Some report first a decrease of the strength then an increase; whereas several observe a progressive increase. Only two papers [Butcher 1958; Mills 1960] observe a general decrease, but they precise specific drying conditions (accelerated drying in an oven for example).

Several phenomena might be at stake here. First, when samples are subjected to drying, the superficial and internal cracking develops. Moreover, flexural tests apply a great amount of stress on the lower fibre of the samples; which is a very vulnerable area. The material is weakened by these damages; and therefore, has a lower bending strength. However, the stiffening of the material described in the paragraph above also occurs, causing an increase of the strength.

The different evolutions of flexural strength observed by the different authors is a consequence of the predominance of one phenomenon over the other. It is generally observed that the stiffening prevails for low relative humidity.



(a) Influence of drying on compressive strength [Pihlajavaara 1974], quoted in [Jean-Michel Torrenti 1987]



(b) Influence of drying on flexural strength [Bucher et al. 2017]

Figure 2.21 – Evolution of mechanical properties with drying

2.6 Conclusions and definition of the experimental campaign conditions

This chapter offered a summary of global knowledge on the effect of drying of concrete and cement-based materials. We took an interest in the delayed behaviour of concrete. The mechanisms of shrinkage and creep were described and influential parameters were highlighted. More specifically, and in the context of our study, the parameters related to aggregates were of particular interest to us. A summary table of the effect of the aggregates on the different aspect of the drying phenomenon is presented in Table 2.1.

	Aggregate parameters			
	Size	Volume fraction	Mineralogy Young Modulus	Porosity
Drying	-	++	-	++
Shrinkage	-	++	++	+
Cracking	++	+	++	+
Creep	-	++	++	-
Transfer properties	+	+	-	++
Mechanical properties	+	++	++	-

Table 2.1 – Summary table of the impacts of aggregates parameters - "-": *not impacted*, "+": *moderately impacted*, "++": *significantly impacted*

The study of the state of art brought out that the effect of mineralogy were well developed for concrete and mortar mixes. However, the impact of aggregates size and aggregates volume fraction were often studied on mortar mixes, and frequently with model inclusions (as glass spheres). This observation revealed the need to "think big" and to take an interest in the effects of coarse aggregates.

Our work aims at understanding the involvement of fine and coarse aggregates in the various physical phenomena at stake, in the material degradation mechanisms and in the evolution of materials properties under desiccation. In order to answer this problematic, an experimental study was realised and is presented hereunder. The state of the art enabled us to set up the specific parameters of this study.

Selection of materials

- The effect of aggregates on the concrete mix is well known and the impact of the mineralogy on desiccation has been fully studied. As a consequence, it was decided to set the mineralogy of the aggregates used in this study. The chosen aggregates are from the Boulonnais quarry. These aggregates were studied in [Makani 2011], and their petrographic nature is labelled as "hard compact Visean limestone". They present a Young Modulus of 80MPa - thus respecting the hypothesis of rigid inclusions ($E_{agg} > 4.E_{cp}$)- and a low porosity - thus are inert face to drying. Moreover, most of the papers presented were based on model materials with model aggregates (glass spheres for example) and the circumferential cracking was not studied due to poor interface conditions. In our study, we are using real inclusions to maintain the interface conditions, and observe the possible impact of the ITZ.
- As it was seen in the literature, the drying processes and mechanisms are very impacted by the formulation of the cement paste. To avoid disparities in results caused by different formulations, a concrete reference mix was set according previous studies

[Briffaut 2010; Hilaire 2014]. Thus, Calcia Airvault (CEM II/A-LL-42.5-R) cement is used, in water-cement ratio of 0.57. In addition, this condition allows to suppose autogenous shrinkage as negligible compared to desiccation shrinkage.

Selection of experimental conditions

- A parametric study is organised, and is taking an interest in aggregates size and aggregates volume fraction. To fully study the involvement of aggregates in the damaging mechanisms and more specifically to decoupled all phenomena, the reference concrete mix mentioned just above was decomposed in several cementitious materials. First cement paste and mortar corresponding to the material in the mix were studied, then they were used as matrix for the elaboration of morphologically controlled materials; i.e. model material were the part of the granular skeleton represented by coarse aggregates is selected, in our case in function of two parameters: size and volume fraction.
- Water departure in the sample is linked to the environmental conditions. In order to bring out the effects of the aggregates through our study, the hydric and thermal conditions were set to 30% RH and 25°C; and ensured by the use of a controlled room and a climatic enclosure. This relative humidity condition could seem very low at first, but the reference concrete mix studied is from the construction of Civaux nuclear plant where the concrete is submitted to this aggressive condition.
- The study of drying mechanisms highlighted that, if the samples are subjected too soon to desiccation a competition between cement hydration and drying appears. Thus, the test specimens all undergo a 28-day endogenous cure to ensure sufficient chemical stability.

Selection of tests to evaluate materials delayed deformations and properties

- In order to assess the evolution of the properties, each formulation is tested at two distinct moments of the procedure. First at the end of the autogenous cure, to fully characterise the materials, and at the end of the procedure on two types of samples: those kept in drying conditions and those kept in endogenous conditions throughout the campaign, used as control specimens. The evolution of mechanical properties is evaluated by subjecting all compositions to three-point flexural tests. Complementary compressive tests are carried out on selected materials. The evolution of transfer properties is followed by measuring the porosity accessible to water and performing chloride diffusion tests on selected materials. Gaz permeability was excluded because specimens must be dried before testing according to the French norm XP P 18-463, which would have introduced bias into our results.
- The work of [Lagier et al. 2011] allowed observations of cracking induced by aggregates restraint. He used thin plates of cement paste with cylinders representing the inclusions to limit hydric gradient. He observed the strains and stresses gradients induced using digital image correlation. The acquisition of a micro-tomograph by LMT gave us the opportunity to transpose this 2-D work in 3-D. Thus, a campaign on elementary samples was led to visualise the internal cracking and to attempt its characterisation using this non-destructive test coupled with digital volumes correlation.

Chapter 3

Experimental campaign

Contents

3.1	Materials	43
3.2	Experimental procedure	45
3.2.1	Casting and conditioning	45
3.2.2	Observation of cracking patterns	45
3.2.3	Monitoring of drying	48
3.2.4	Assessment of mechanical properties	48
3.2.5	Assessment of transfer properties	50

3.1 Materials

The different formulations studied come from the reference mix detailed Table 6.1, where the mass are indicated per m^3 of concrete, as well as the representative volume of each material in the concrete. This concrete formulation was made with CEM II/A-LL-42.5-R cement ; composition detailed in Annexe A.1 ; on a 0.57 water-cement ratio, and calcareous Boulonnais aggregates ; composition detailed in Annexe A.2.

	Concrete composition	Representative volume
Materials	kg/m^3	%
Cement	350	11,3
Water	201	20,1
Sand (0/4)	858	32
Gravel(4/12.5)	945	35,3
W/C ratio	0,57	

Table 3.1 – Concrete composition

Our objective is to experimentally determine quantitatively the influence of aggregates on the concrete delayed behavior and mechanical properties.

The two aggregate-related parameters chosen for this study are:

- **Aggregate size:** aggregates diameters between 0 and 4 mm, 6.3 and 8 mm and 10 and 12.5mm.

- **Aggregate volume fraction:** aggregates represent 0%, 30% and 50% of the total volume

The study is consequently based on different compositions where the granular skeleton is controlled, referred afterwards as "morphologically controlled materials" or "model materials" and represented in Figure 3.1.

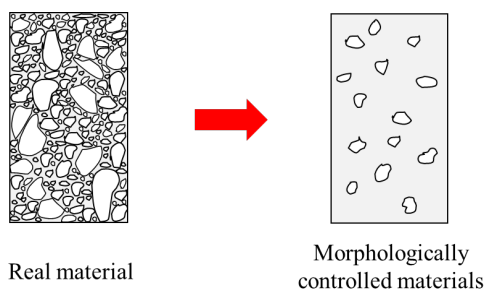


Figure 3.1 – Morphologically controlled materials

Seven compositions were selected and are indicated Table 3.2:

Composition	Aggregates size	Aggregates	Cement Paste
	mm	Volume Fraction	Volume Fraction
		%	%
Cement Paste		0	100
Mortar	0-4 mm	32	68
Model concrete 1	6.3-8 mm	30	70
Model concrete 2	6.3-8 mm	50	50
Model concrete 3	10-12.5 mm	30	70
Model concrete 4	10-12.5 mm	50	50
Model concrete 5	0-4 mm	32	38
	6.3-8 mm	30	

Table 3.2 – Formulations studied

The original particle size distribution is altered and in order to prevent aggregates and cement paste segregation, the use of viscosity modifying admixture is necessary. An optimisation campaign led to a mass dosage of 1,6% of cement mass of Sika Stabilizer 400 (Figure 3.2).

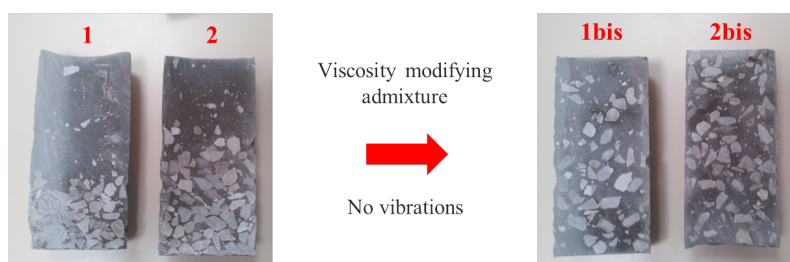


Figure 3.2 – Optimisation of viscosity modifying admixture dosage

3.2 Experimental procedure

The experimental procedure followed in this study is summarised in the schematic display in Figure 6.1. Protocols are then detailed.

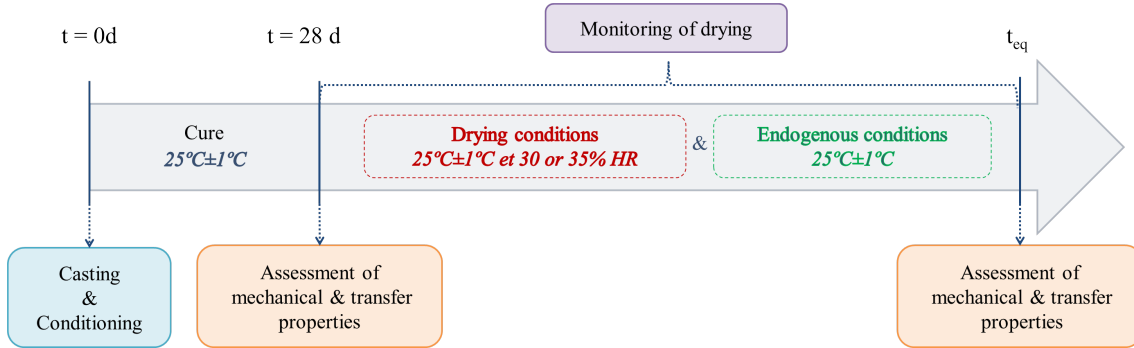


Figure 3.3 – Experimental procedure

3.2.1 Casting and conditioning

Samples are cast using either a 3-litres mortar mixer; for formulations without coarse aggregates; or a 30-litres concrete mixer; for formulations with coarse aggregates. Specimens are removed from the molds after 24 hours. They are then packed with one layer of plastic foil and two layers of aluminium foil to undergo a 28-days endogenous cure in a room maintained at $25 \pm 1^{\circ}\text{C}$. Samples are then divided in three categories :

- the ones tested to characterise the material at the end of the endogenous cure;
- the ones kept in endogenous cure throughout the procedure and then tested;
- the ones unwrapped and put in drying conditions ($25 \pm 1^{\circ}\text{C}$ temperature and $30 \pm 5\%$ relative humidity) throughout the procedure and then tested. To ensure unilateral drying, samples receive two layers of aluminium foil on their top and bottom.

In order to be representative and to limit side effects, the size of model concrete specimens is set to be minimum five times the diameter of the largest aggregates studied (12.5 mm). Cement paste and mortar formulations were studied on samples with smaller sizes to avoid segregation. Dimensions of specimens for each tests are indicated Table 3.3.

Test	Samples dimensions (mm)	
	Cement paste Mortar	Model concretes
Drying monitoring	40*40*160	70*70*280
Flexural test	40*40*160	70*70*280
Compressive test	-	70*160
Porosity	70*160	70*160
Chloride diffusion	110*110	110*220
External cracks observation	40*40*160	70*70*280
Internal cracks observation	25*15	25*15

Table 3.3 – Dimensions of the samples used in the different tests performed

As the size of samples is different the drying kinetics are different. An equivalent time of study is introduced (t_{eq} in Figure 6.1) expressed as a function of time and of the radius of the samples (r) : $t_{eq} = \frac{t}{r^2}$. The radius of samples is determined according the schematic Figure 3.4. The experimental procedure is followed until the equivalent time is met; corresponding to 66 days for cement paste and mortar samples ($r = 2$ cm), and 200 days for model concretes ($r = 3.5$ cm).

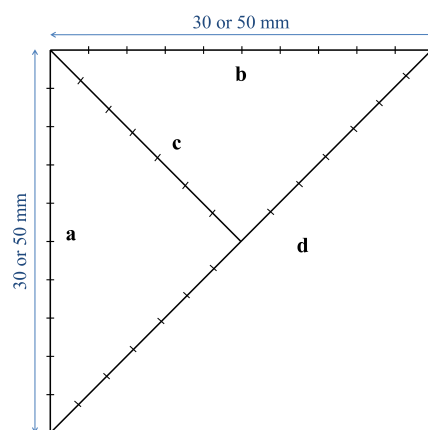


Figure 3.4 – Radius of prismatic samples

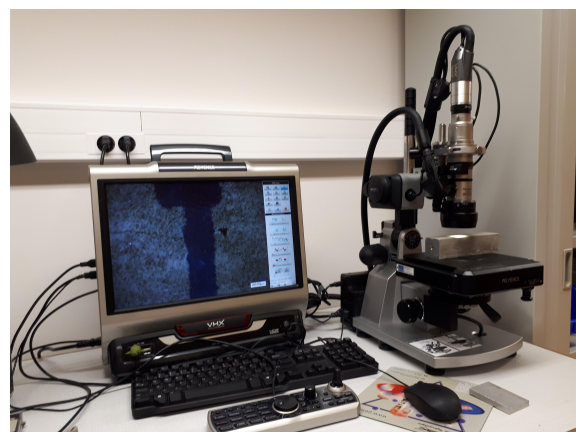
3.2.2 Observation of cracking patterns

Observation of superficial cracking

Superficial cracks are observed on the samples used to monitor drying. The visual referential represented in Figure 3.5a is drawn on one side of the sample, then the specimen is placed under the numerical microscope, as shown in the Figure 3.5b. The optical lens is moved along the lines of the referential. Every time a crack is encountered, several measures of width are made using a parameter of the microscope. Once the measurements are over, the cracks density is expressed for each line by dividing the number of cracks by the dimension of the line. The average cracks density and width are then expressed by combining the results of the four lines. The smallest and largest widths are also highlighted to assess if the range of cracks widths is affected by the aggregates parameters.



(a) Visual reference drawn on samples to assess cracks density and width



(b) Numerical microscope used to control superficial cracking

Figure 3.5 – Observation of superficial cracks

Observation of internal cracking

A campaign was led on small representative samples to visualise and quantify the internal micro-cracking induced by aggregates restraint using a X-ray microtomographe and a scanning electron microscope. Samples are cylinders with a diameter of 2.5cm and a hight of 1.5cm. Four formulations were observed:

- Cement paste,
- Mortar - 32% of 0 – 4 mm sand,
- Cement paste and one 12.5mm aggregate,
- Mortar (32% of 0 – 4mm sand) and one 12mm aggregate.

Samples are cast using plastic moulds. After 24 hours, the moulds are removed and samples undergo a 28-days endogenous cure. Samples are then put on the microtomographe rotary platform and will only be removed at the end of the procedure. They are scanned four times :

- Scan 1 : Samples are wrapped with plastic foil to prevent drying, in order to obtain a reference scan. Plastic foil is removed at the end of the scan and the drying phenomenon begin.
- Scan 2 : After 2 hours of drying.
- Scan 3 : After 9 hours of drying.
- Scan 4 : After 24 hours of drying.

The 2-D absorption projections obtained are reconstructed using the tomographe software to produce a 3-D map of the X-ray absorption of the sample (Figure 3.6).

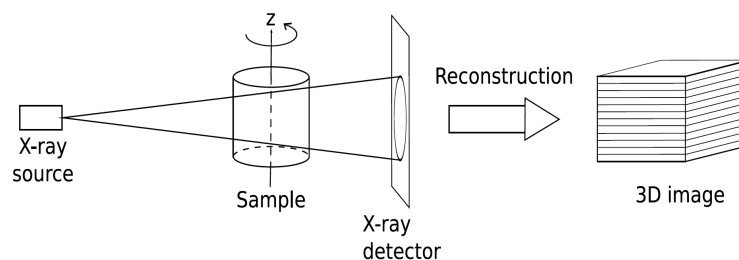


Figure 3.6 – Functioning principle of X-ray tomography

Scan conditions and characteristics are :

- Tomograph internal temperature : 30°C
- Tomograph internal relative humidity : 50%
- Number of projections acquired for each position of the samples : 15
- Final resolution : 17 μm

The 3-D maps are treated using Digital Volume Correlation (DVC), which is the 3-D extension of the Digital Image Correlation (DIC). The procedure is fully detailed in [Bouterf 2014]. It calculates the difference between a deformed configuration and the reference samples, and produce a residual that highlights the zones presenting a discontinuity of the displacement field, i.e. cracks.

In a second time, the samples are impregnated with resin, sawed, polished and observed in a scanning electron microscope to assess the cracks openings.

3.2.3 Monitoring of drying

Drying evolution of each composition is assessed by the monitoring of mass loss and shrinkage on six prismatic specimens equipped with two embedded brass pins on the top and bottom faces. Dimensions are indicated in Table 3.3. Mass is measured on a scale with a precision of 0.01 gram, and express as a percentage of mass loss via the Formula 6.1.

$$W = 100 \times \frac{W_i - W_0}{W_0} \quad (3.1)$$

In Formula 6.1,

- W_i is the measured mass at any time [g];
- W_0 is the initial mass, measured after unwrapping [g];
- W is the percentage of mass loss [%].

Shrinkage is measured on the device displayed Figure 3.7. The prisms are positioned and aligned thanks to the pins between a fixed support and a comparator with a precision of 0.002 mm.

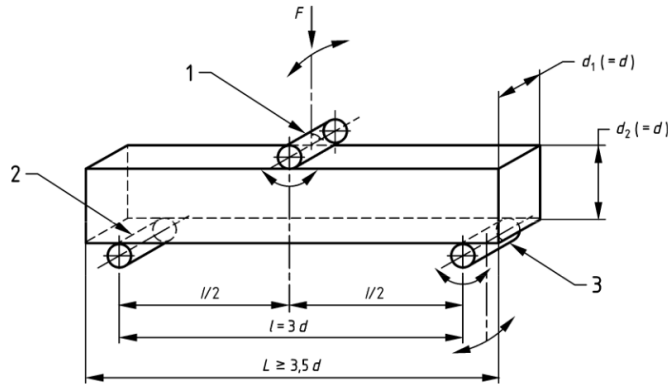


Figure 3.7 – Shrinkage monitoring

3.2.4 Assessment of mechanical properties

Three-points-flexural testing

Three-points-flexural tests are performed for each composition and each conditioning, according to the French norm NF-EN-12390-5 (Figure 3.8a), on three prims and are charge operated at a 0,5mm/s speed. Endogenous samples are unwrapped 10 minutes before being



(a) Schematic of three-points-flexural testing - 1. loading roller; 2 & 3. support rollers



(b) Picture Three-points-flexural testing with apparatus

Figure 3.8 – Three-points-flexural testing

tested. An apparatus was set up to ensure that no punching phenomenon appears, and also to measure the sample exact maximum deformation Figure 3.8b.

We are then able to determine the flexural resistance of each sample using the Formula 6.5.

$$f_{cf} = \frac{F_{max} \cdot l \cdot d}{8 \cdot I} \quad (3.2)$$

In Equation 6.5 and Figure 3.8a ,

- f_{cf} is the flexural strength [MPa];
- F_{max} is the maximum load [N];
- l is the distance between the support loaders [mm];
- I is inertia of the cross section [mm].

Uni-axial compressive testing

Compressive tests are performed for only three compositions, on cylindrical specimens with surfacing sulphur. The compositions tested are :

- $V_{agg} = 30\%$, $\phi = 10 - 12.5\text{mm}$
- $V_{agg} = 50\%$, $\phi = 6.3 - 8\text{mm}$
- $V_{agg} = 50\%$, $\phi = 10 - 12.5\text{mm}$

Endogenous samples are unwrapped 24 hours before being tested, to apply surfacing. In order to determine Young Modulus, samples are first equipped with an extensometric cage (J2P) composed of three LVDT sensors on three guide lines spaced with 120° , as display on Figure 6.5 and submitted to three loading-unloading cycles.

Then, after the removal of the apparatus, they are tested according to the French norm NF-EN-12390-3, until rupture. We are able to determine the compressive strength using the Formula 6.7:

$$f_c = \frac{F_{max}}{S} \quad (3.3)$$

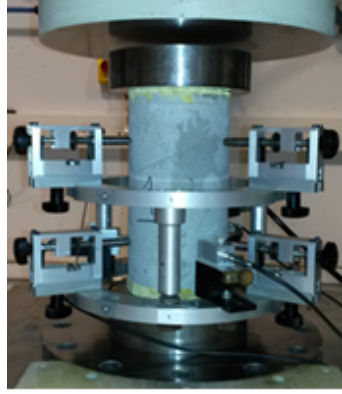


Figure 3.9 – Compressive testing

In Equation 6.7,

- f_c is the compressive strength [MPa];
- F_{max} is the maximum load [N];
- S is the area of the cross section [mm²].

3.2.5 Assessment of transfer properties

Porosity

Porosity measurement protocol is based on the French norm NF P 18-459, and performed on three compositions : cement Paste, mortar and one model concrete ($\phi_{agg} = 6.3 - 8 \text{ mm} - V_{agg} 30\%$). Cylindrical samples (Table 3.3) are cut into slices of either 1 cm thickness in the case of cement paste and mortar, or 3 cm for the model concrete. As the dried material is very friable, all samples were first coated with fibreglass and epoxy resin to ensure an easy sawing. After soaking in a vacuum desiccator during 48 hours, samples are weighed using a hydrostatic scale (W_{soak}) and a classical scale (W_{wet}). The slices are then put in an oven set to 40°C and 20% RH and daily weighed until the mass variation in 24 hours is inferior to 0.05% (W_{dry})- Figure 3.10.

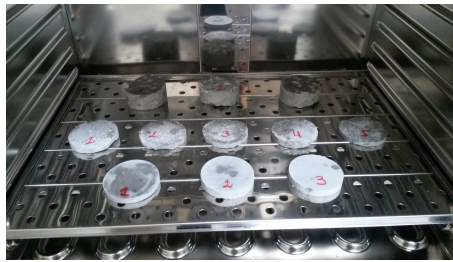


Figure 3.10 – Drying of porosity samples

Porosity is determined using the Formula 3.4 :

$$\phi = \frac{W_{wet} - W_{dry}}{W_{wet} - W_{soak}} \quad (3.4)$$

In formula 3.4:

- ϕ is the porosity [%];

- W_i are the masses measured and described in the previous paragraph [g].

Chloride diffusion

Chloride diffusion measurement protocol is based on the French norm NF P 18-463, and performed on three compositions : cement Paste, mortar and one model concrete ($\phi_{agg} = 6.3 - 8 \text{ mm} - V_{agg} 30\%$). Cylindrical samples (Table 3.3) are cut into slices with a thickness of 3 cm, as defined in the norm. As the dried material is very friable, all samples were first coated with fibreglass and epoxy resin to ensure an easy sawing. Samples are soaked with NaOH (0.5 mol/L) in a vacuum desiccator during 48 hours, then are placed in the testing cells represented in Figure 3.11a. To avoid any possible leak, silicon is put on all the joints, and needs to dry for at least 12 hours. Cells are then filled on one part with NaCl (0.7 mol/L) and on the other part with NaOH (0.7 mol/L). Finally the cells are connected to the testing apparatus displayed in Figure 3.11b, set to 10 Volts and 6 hours of testing.

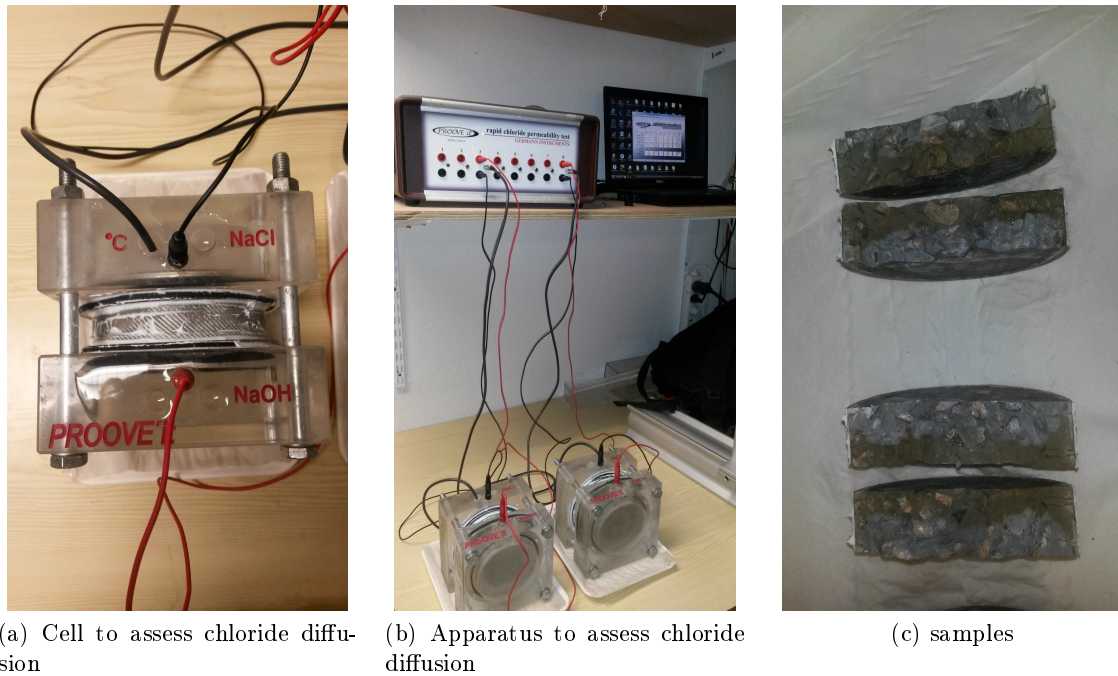


Figure 3.11 – Three-points-flexural testing

Once the test is over, cells are disassembled and samples are broken in two parts. The two faces exposed are then sprayed with AgNO_3 (silver nitrate). This solution reacts with the chloride ions and produce a white component when exposed to light, whereas it becomes black in the absence of chloride ions. Example of samples after testing are presented Figure 3.11c. The penetration front can be measured and the apparent diffusion coefficient can be calculated using Equation 3.5.

$$D_{app} = \frac{RTL}{zFU} \cdot \frac{x_d - \alpha x_d^{0.5}}{t} \quad (3.5)$$

In formula 3.5:

- L is the thickness of the sample, $L = 0.03 \text{ m}$;

- R is the perfect gas constant, $R = 8.31 \text{ J/mol.K}$;
- T is the temperature, $T = \text{K}$;
- z is the valence of the chloride ion, $z = 1$;
- F is the Faraday constant $F = 9.64 \times 10^4 \text{ J/mol.V}$;
- U is the mean potential difference between the faces of the sample, $U = 10\text{V}$;
- x_d is the mean measure of the penetration front [m];
- t is the duration of the tests, $t = 6\text{h}$ so $t = 21600 \text{ s}$;
- $\alpha = 2\left(\frac{RTL}{zFU}\right)^{0.5} \text{erfc}^{-1}\left(1 - \frac{2c_d}{c_0}\right)$;
- c_d is the chloride concentration for which the colorimetric test changes color ($c_d = 0.07\text{mol/L}$);
- c_0 is the initial chloride concentration in the solution $c_0 = 0.7 \text{ mol/L}$.

Chapter 4

Results and analysis

Contents

4.1 Cracking observations	53
4.1.1 Observation of superficial cracking	53
4.1.2 X-Ray micro-tomographic observations	56
4.2 Effects of aggregates on delayed behaviour induced by drying	64
4.2.1 Drying	64
4.2.2 Shrinkage	66
4.2.3 Comparison of experimental results with conventional homogeni- sation models	68
4.3 Effect of aggregates and drying on transfer and mechanical properties	72
4.3.1 Mechanical properties	72
4.3.2 Transfer properties	79
4.4 Conclusion	82

4.1 Cracking observations

As seen in the state of the art, cracking is inherent of the desiccation of cementitious materials (Section 2.3). Two experimental techniques were used to assess the involvement of aggregates in the different damage mechanisms. First, a numerical microscope was used to observe superficial cracks. Then a study of internal cracking was led using a X-ray micro-tomograph.

4.1.1 Observation of superficial cracking

The external cracking patterns were observed using a numerical microscope, as describe in Section 3.2.2. Results are gathered in Table 4.1. It displays the number of cracks per centimetres (also refereed as cracks linear density), the range of cracks opening and the mean opening of the cracks.

When taking an interest in the cracks density, it can be seen that the results are very variable. To see more clearly the trends, the values are presented in the form of a histogram, Figure 4.1, sorted by aggregate volume fractions.

Several observations can be made :

		Density (nb/cm)	Width (μm)		
			<i>mini</i>	<i>med</i>	<i>max</i>
Cement paste		1.32	8.1	27.4	71.4
V_{agg} = 30%	0-4	0.66	8.3	20.4	55.7
	6.3-8	1.66	11.3	37.3	91.2
	10-12.5	1.16	6.8	50.3	124.3
V_{agg} = 50%	6.3-8	2.69	6.7	35.2	82.9
	10-12.5	1.63	8.3	42.2	176.4
V_{agg} = 62%	0-4 and 6.3-8	-	-	-	-

Table 4.1 – Results of the microscopic observations : crack density and cracks range of width for each formulation

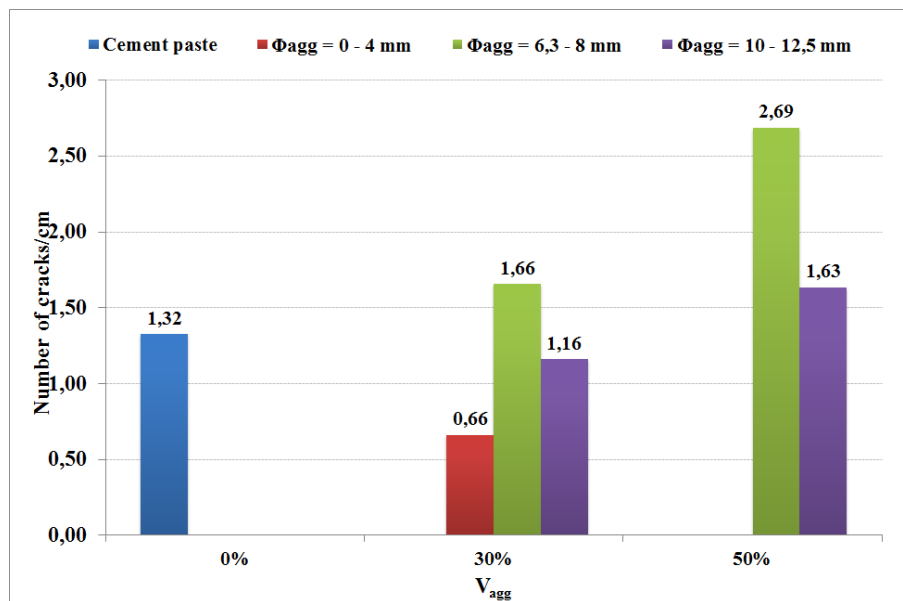


Figure 4.1 – Distribution of cracks density, sorted by aggregate volume fraction

- The cement paste, even if it doesn't contain aggregates, presents a quite significant cracks density. As there is no restraint induced internally by inclusions, this cracking pattern is attributed to the important hydric gradient in the material that generates tension on the surface of the sample and induces cracking;
- Compared to the cement paste, mortar displays a lower density cracks. The introduction of small inclusions reduces the quantity of cement paste in the material, thus reducing global deformation of the material. However, it is important to notice that these inclusions do not generate additional cracking, and even, seem to reduce the hydric gradient effects;
- When comparing the formulations with 30% of aggregates, mortar has the lowest crack density. Then, when focusing on formulation with coarse aggregates, the cracking is more important when 6.3 – 8mm aggregates are used rather than 10 – 12.5mm aggregates. The same observation can be made when taking an interest in the composition with 50% of aggregates: samples made with the formulation with 6.3 – 8mm

aggregates is the most cracked formulation. On one hand, the increase of coarse aggregates size tends to decrease cracks density, but on the other one, a equivalent phenomenon is noticeable with the introduction of very fine aggregates.

- Formulations with 50% of aggregates display more cracks than the ones with 30%, underlining an effect of aggregates volume.

Now, if we focus on the mean opening of cracks sorted by aggregate volume fraction, Figure 4.2, different trends can be discerned.

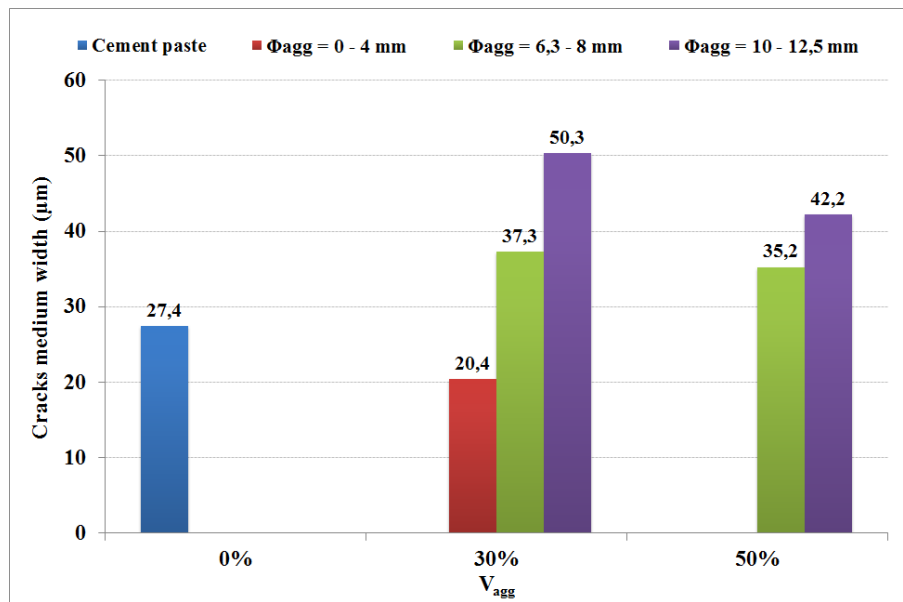


Figure 4.2 – Distribution of cracks mean width, sorted by aggregate volume fraction

- At a fixed volume fraction of aggregates (30% or 50%), the mean opening of cracks increases (respectively from $20.4\mu\text{m}$ to $50.3\mu\text{m}$ and from $35.2\mu\text{m}$ to $42.2\mu\text{m}$) with the increase of aggregate size.
- Cement paste displays a cracks mean opening slightly superior to the one of mortar.
- At a fixed size of aggregate, the increase of aggregates volume fraction leads to a slight decrease of the mean opening.

To complete these last results before completely analysing them, the distribution of maximal and minimal openings were expressed in Figures 4.3a and 4.3b.

One can see that globally the minimal crack opening is the same for all formulations ($8.3 \pm 3\mu\text{m}$). However, the trend of maximal cracks opening is quite different, as it increases significantly with the increase of aggregates volume fraction. Also, introducing small inclusions (0 – 4mm) leads to a reduced cracks range opening.

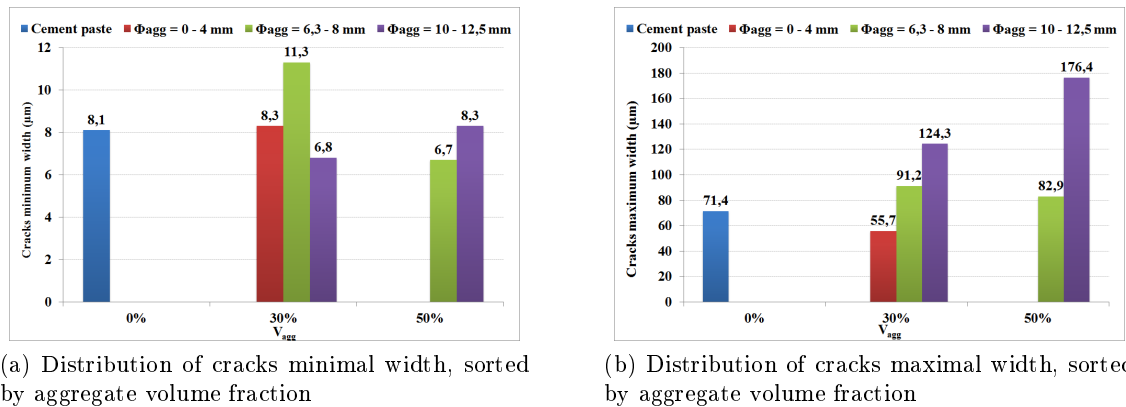


Figure 4.3 – Minimal and maximal crack opening observed with a numerical microscope

All of these observations led us to identify several cracking patterns, linked to the aggregates parameters. First, it seems that the increase of aggregate volume leads to a decrease of cracks density and mean opening, but also a larger range of cracks width and the presence of large cracks. Then, the increase of aggregates size leads to a decrease of the number of cracks but an increase of cracks opening. In other words, the increase of aggregate size and volume fraction leads to a more localised and more opened cracking phenomenon. Finally, the introduction of fine aggregates ($\Phi \leq 4$ mm) leads to decrease of the cracking induced by the hydric gradient, but also the density and width of cracks induced by both the hydric gradient and the aggregate restraint. These results are conform with previous observations made in the state of the art, in Figure 2.15. However, it is important to highlight that usually, superficial cracking is associated as an effect of hydric gradients but not of aggregates restraint but it is clear that both phenomena are linked, and influence the cracking mechanisms.

In order to confirm these first external observations and assess the mechanisms at stake here, a tomographic and SEB campaign was led on small representative enough samples while being submitted to drying.

4.1.2 X-Ray micro-tomographic observations

Protocols followed for this study are detailed in Section 3.2.3. Small samples were chosen in order to limit the hydric gradient phenomenon as much as possible, and to enhance the resolution of 2D projections and thus 3D reconstruction of the samples.

First, we will compare chosen 2D projections of X-ray absorption levels of each sample, then the cracks will be observed using SEB microscopy, and finally, we will present the preliminary DVC study.

Four formulations were studied here : cement paste, mortar, cement paste with one aggregate, and mortar with one aggregate.

Study of 2D projections of x-ray absorption levels of the different samples

Figure 4.4 presents slides of absorption levels of the different samples each time from the last scan performed (around 24h of drying). In Figure 4.4 a)cement paste, b)cement

paste and sand (mortar), c) cement paste and one coarse aggregate and d) mortar and one coarse aggregates.

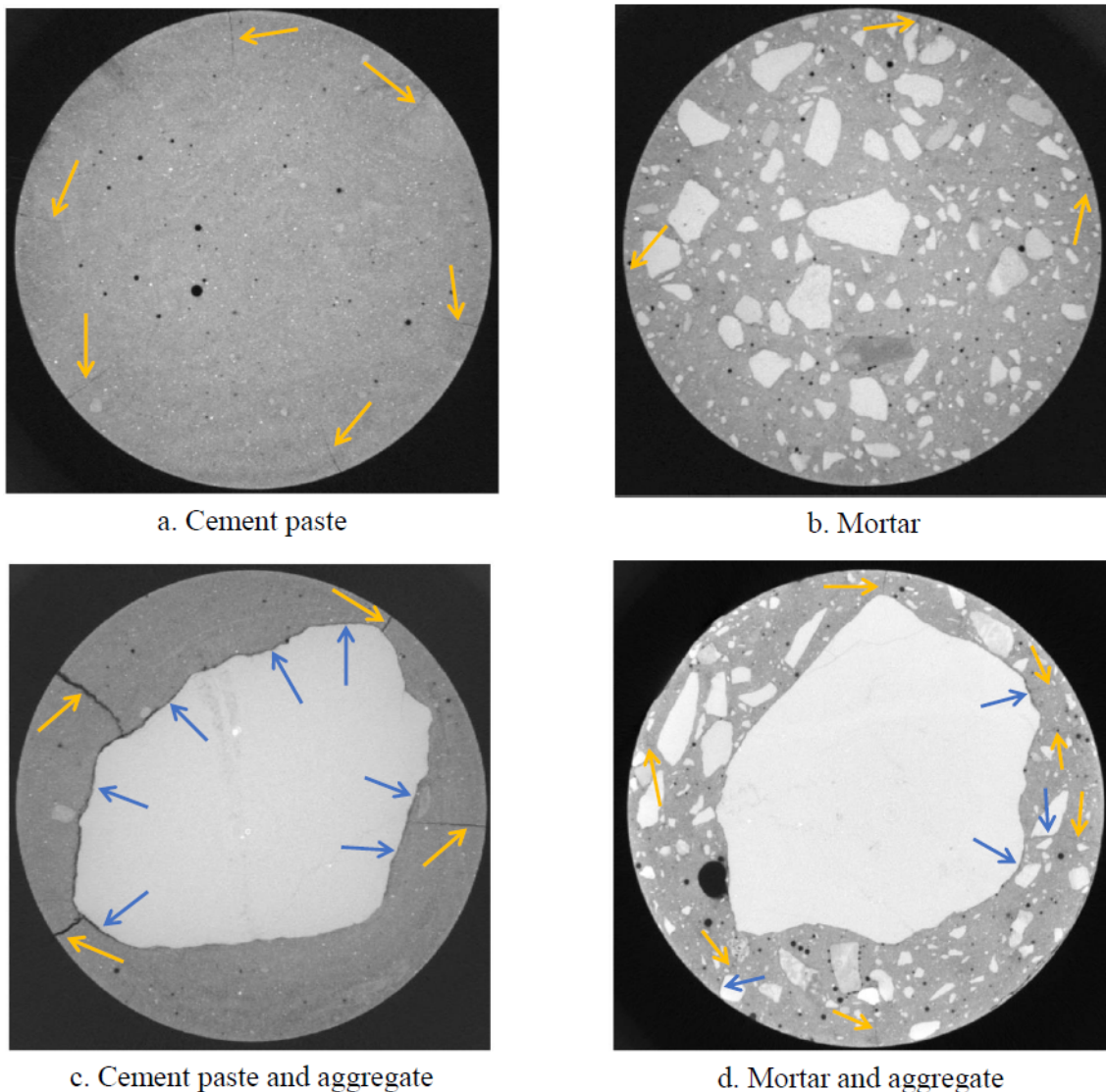


Figure 4.4 – 2-D projection of the X-Ray absorptions of the different samples studied after 24h of drying at 50%RH

Several observations can be made:

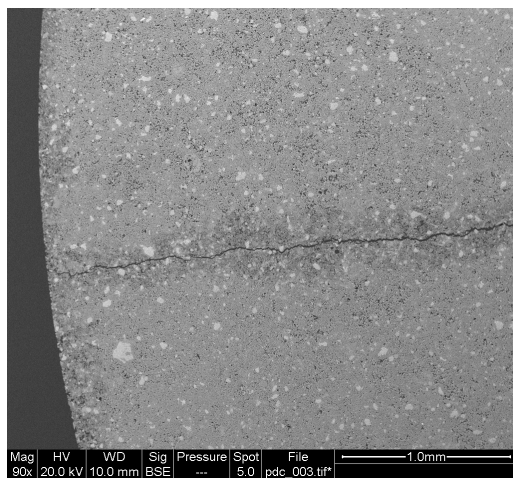
- In all samples, cracks initiate at the surface of the sample (showed by the yellow arrows in Figure 4.4), on the surface, towards the sample core, perpendicular to the surface. These are characteristic of cracking mechanisms due to the water gradient in the material. The small sample size did not completely avoid this phenomenon as hoped, but a compromise had to be made: the samples had to be small enough to obtain maximum image resolution, while remaining representative of the cementitious materials studied.
- Comparing respectively images a) and b) and images c) and d), it can be observed that cracks are harder to observe, i.e. with a smaller width, and are more distributed in samples with a mortar matrix (Samples b) and d)). The introduction of small

aggregates, as it was observed in the superficial microscopic study, induces these changes.

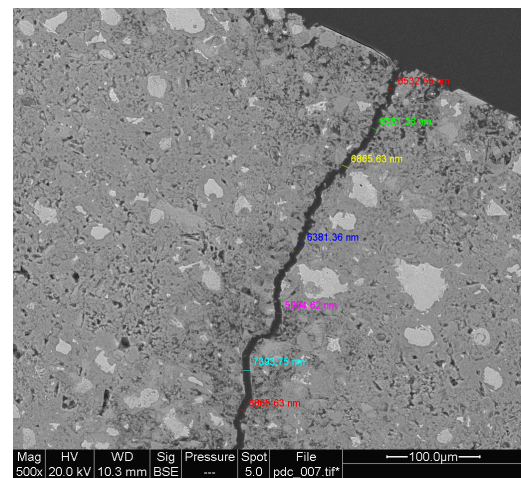
- By comparing image a) to image c) and, image b) and d), it can be seen that the introduction of coarse inclusion changes the cracks pattern. It creates more localised and more opened cracks. More particularly, it induces a debonding phenomenon between the cement paste and the aggregates (shown with the blue arrows in the images). Here again these results are corroborating previous observations. By focusing on image d), it can be seen that this debonding phenomenon exists also with the introduction of small aggregates, and is more complicated to observe due to the very small width of the cracks, but also it highlights an effect of the aggregates mentioned in the state of the art: the ITZ is a singular zone of the concrete material, that tends to present a mechanical strength reduced, enabling and favouring the progression of cracks in this zone.

Observations of three samples using SEB microscopy

Samples were put in epoxy resin, and studied under a scanning electron microscope, using IFSTTAR (Marne-la-Vallée, France) facilities. Unfortunately, a lap of time had passed between the end of the tomographic observations and the samples preparation. Nevertheless, these observations give us access to a number of interesting informations on the samples. Only three samples were studied : cement paste (Figure 4.5), mortar (Figure 4.6) and cement paste with one coarse aggregate (Figure 4.7)



(a) Image of a crack in the cement paste sample

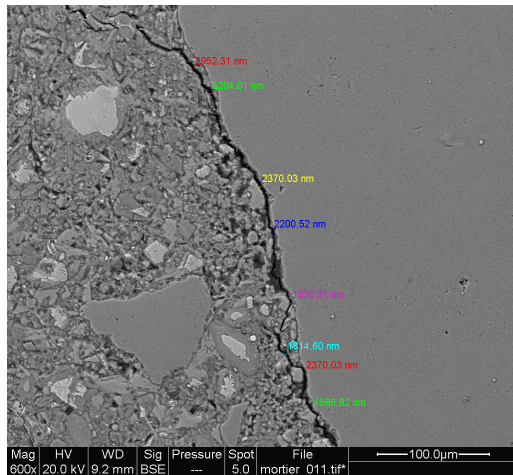


(b) Image and measures of a crack in the cement paste sample

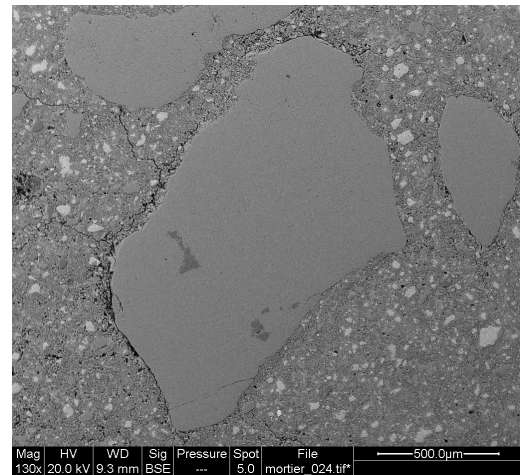
Figure 4.5 – Observations of the cement paste sample cracking pattern using a scanning electron microscope and measures of cracks openings

Several observations can be made :

- Figure 4.5, shows perpendicular cracks with an opening of a few micrometres in the cement paste
- Figure 4.6, shows that the cracks initiates at the surface and are stopped by small aggregates actually round the aggregates through the ITZ, creating a local debonding

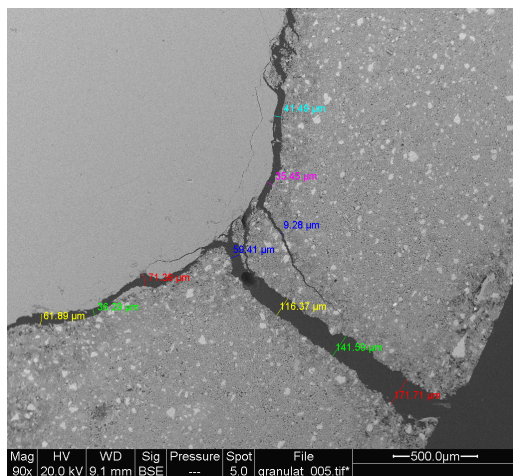


(a) Image and measures of a crack in the mortar sample

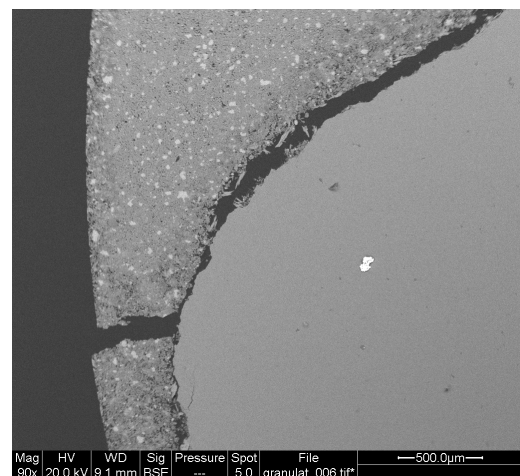


(b) Image of a crack in the mortar sample

Figure 4.6 – Observations of the mortar sample cracking pattern using a scanning electron microscope and measures of cracks opening



(a) Image and measures of a crack in the sample with cement paste and one aggregate



(b) Image of a crack in the sample with cement paste and one aggregate

Figure 4.7 – Observations of the cement paste and one aggregate sample cracking pattern using a scanning electron microscope and measures of cracks openings

phenomenon, and progress creating radial cracks between aggregates. They present width of around one micrometer.

- Figure 4.7, shows that the introduction of one coarse aggregate induces very large cracks (around 100 micrometres) and in this case, the debonding phenomenon is significant, and cement paste seems to have been torn from the surface of the aggregates.

The addition of inclusions limits the propagation of cracks but the size of the inclusions (small or large) influences the dimensions of the developing cracks, as well as the localisation of the cracks. This corresponds to the observations made previously, and in the bibliography: the presence of a transition zone with modified mechanical properties that will influence the progression of cracks in the material.

Preliminary DVC study

In Figures 4.8, 4.9, 4.10 and 4.11 shows DVC results on the four samples. For each figure, on the first row are presented one slide of the reference scan (0h of drying), and the same slide of the final scan (24h of drying), corrected (Fig. 4.8) or not (Fig. 4.9-11) by the displacement gradient. On the second row, DVC residual images are displayed (the result of the final scan reconstruction, corrected by the displacement field identified, and subtracted with the reference scan reconstruction) and one displacement field.

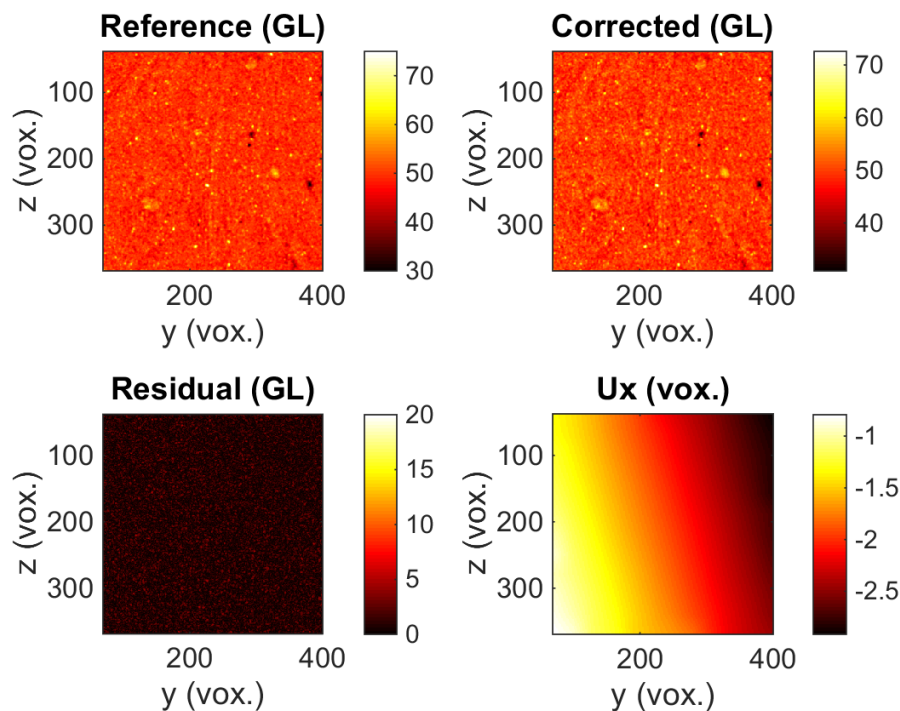


Figure 4.8 – Results of the DVC analysis, slide $z = 240$

The DVC residual images allows the detection of cracks, it particularly visible for the sample with one aggregate in a cement paste matrix. If we correlate these observations with the respective displacement fields, one can see that the gradients are perturbed in the area containing the cracks. However, we were not able to quantify the cracks opening using this technique. Usually, the use of displacement fields should gives us access to the cracks characteristics. However, in our case, the best voxel resolution that could be reached is 17 micrometres. This means that most of the cracks we are trying to study have a smaller size than the voxel, as seen in the SEB observations. The DVC study can not gives us access to a reliable assessment of the cracks characteristics.

Nevertheless, one sample presents cracks that are important enough to be studied

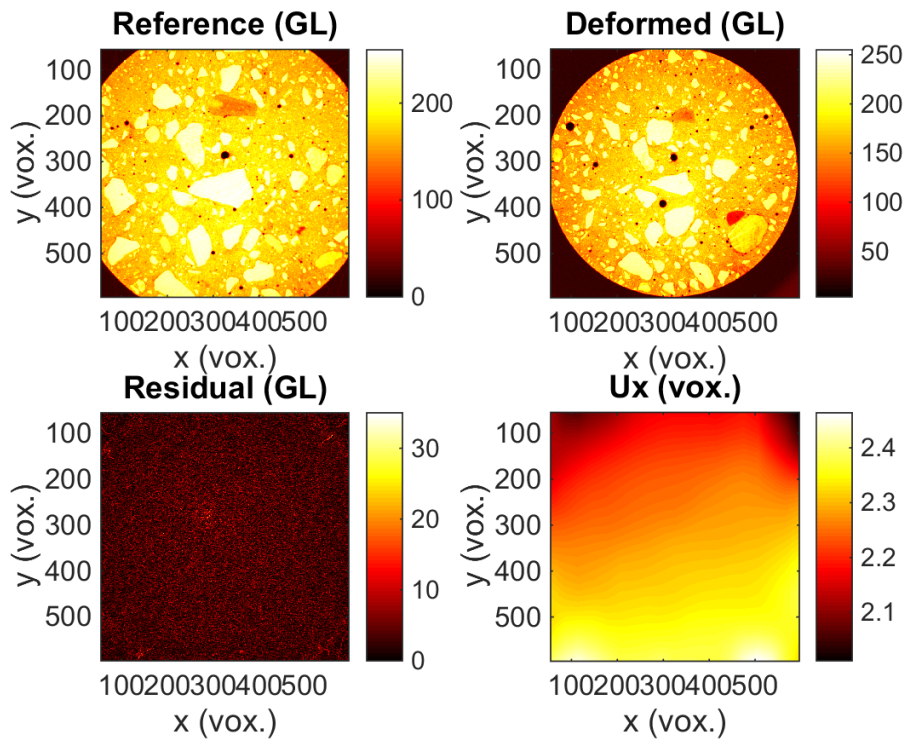


Figure 4.9 – Results of the DVC analysis, slide $z = 180$

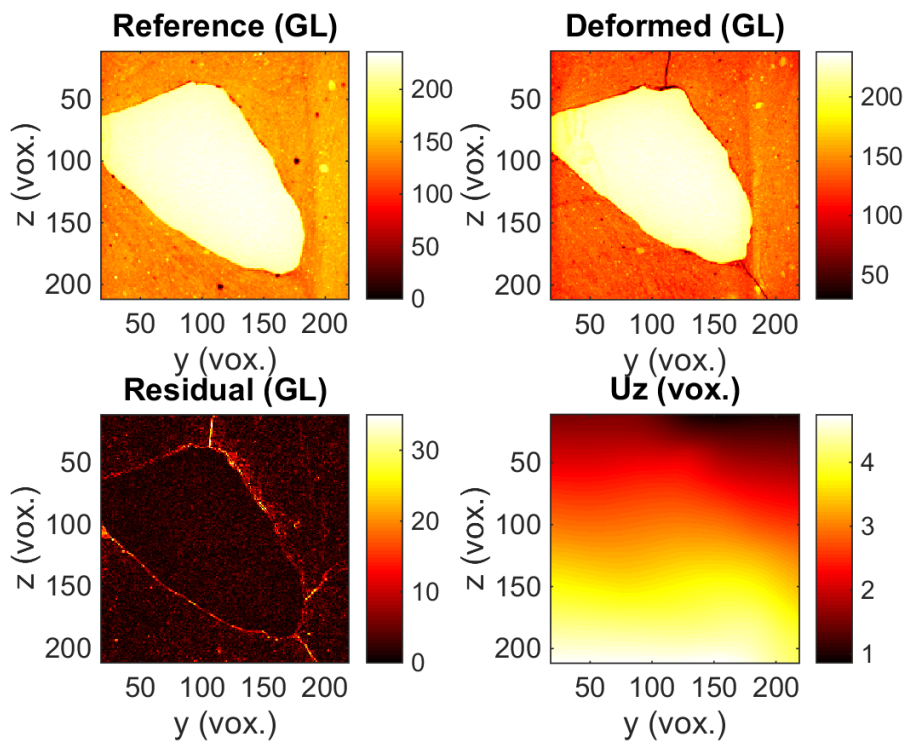


Figure 4.10 – Results of the DVC analysis, slide $z = 180$

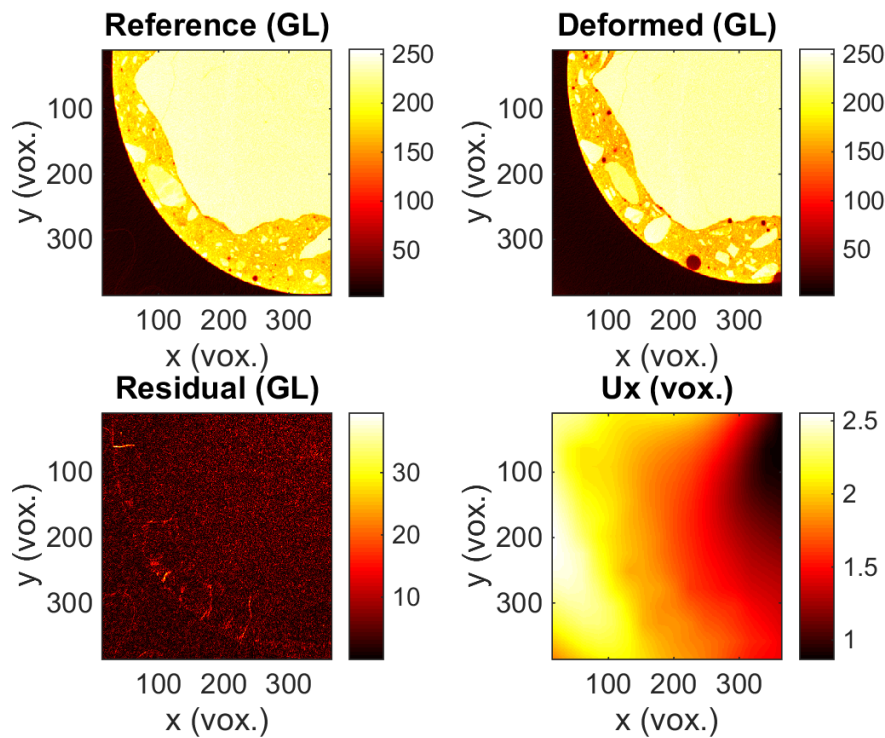


Figure 4.11 – Results of the DVC analysis, slide $z = 200$

using this technique : cement paste and one aggregate. As displayed in Figure 4.12, 3D reconstructions of reference and deformed scans, and the residual volume could be generated, using Paraview software. Using Paraview parameters, we were able to isolate the aggregate in the reference reconstruction and superposition with the residual volume allows us a clear visualisation of the debonding phenomenon and of the cracks patterns.

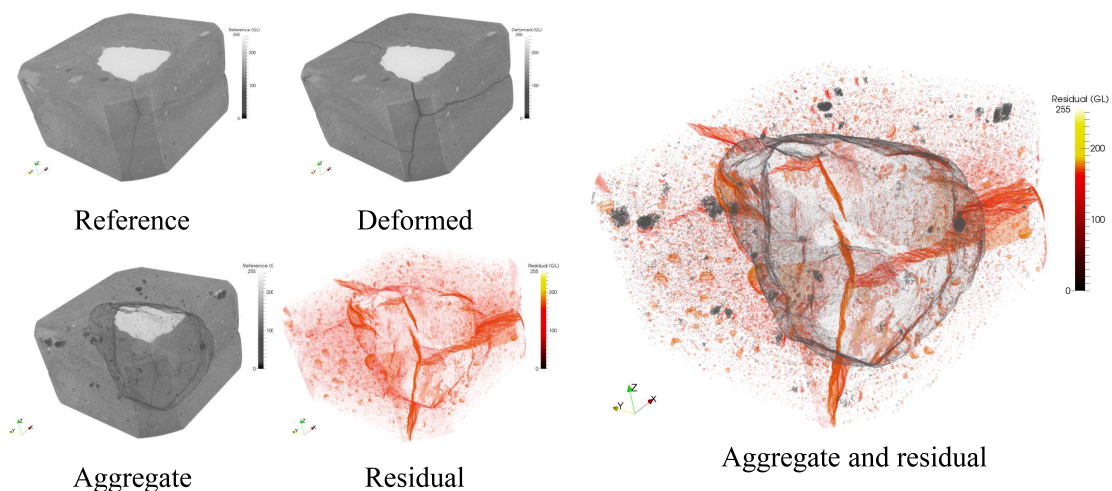


Figure 4.12 – 3-D reconstruction of the different tomographic observations. On the left, the 3-D reconstruction of the reference and deformed scans, the placement of the aggregate in the sample and the residual. On the right, a superposition of the aggregate and the residual.

4.2 Effects of aggregates on delayed behaviour induced by drying

4.2.1 Drying

Figure 4.13 displays the mass loss of the different formulations expressed as a function of the root of equivalent time, defined in Section 3.2.1. As a reminder, $t_{eq} = \frac{t}{R_m^2}$ where t is the time and R_m is the mean radius of the samples.

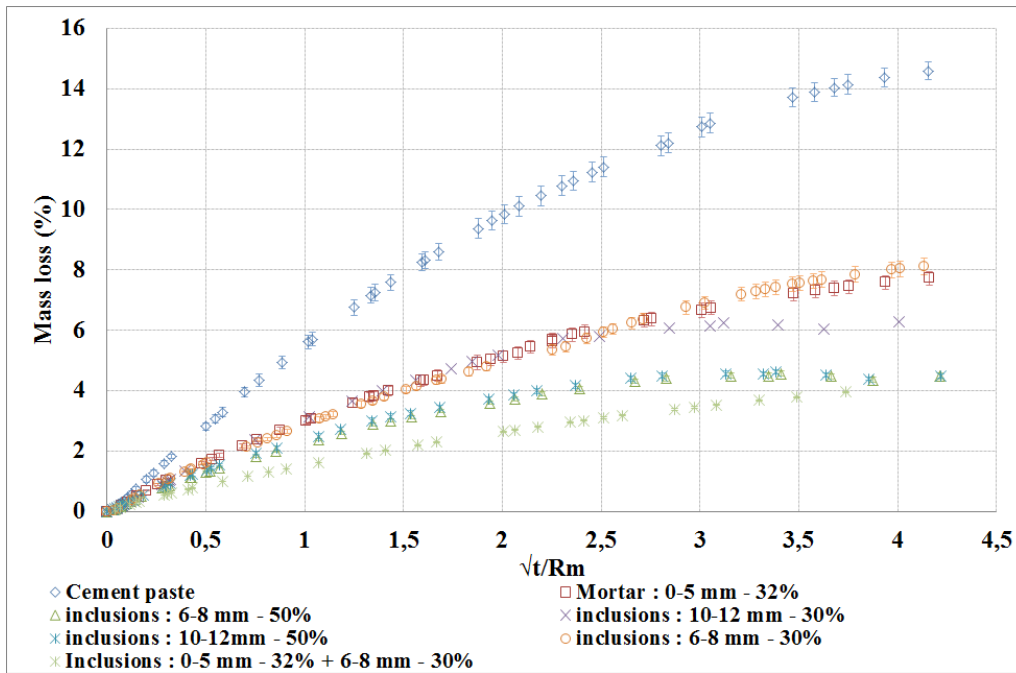


Figure 4.13 – Mass loss evolution of different compositions with time under drying conditions

It can be observed that:

- The more aggregates there are in the formulations, the less the amount of mass loss is. This result was expected as it can be seen in Section 2.2.2, as the departure of water mainly occurs in the cement paste;
- Also, if we take an interest at the compositions with the same amount of aggregates the curves nearly superimpose them-selves, thus the aggregates size doesn't seem to be an influential parameter (cf curves "inclusions:6-8mm/10-12mm - 30%/50%").
- However, three formulations are to be analysed with caution. The formulations "cement paste + 30% of 10 – 12.5mm aggregates" (curve with blue stars) , "cement paste + 50% of 10 – 12.5mm aggregates" (curve with green triangle) and "cement paste + 50% of 6.3 – 8mm aggregates" (curve with purple crosses) were preserved in a controlled room, which underwent a incident that raised the relative humidity to 50% (cf. Figure 4.14). This explains why at $t_{eq} = 2,5s^{0.5}.m^{-1}$ the curve with purple crosses, diverges from the others. The same occurs with the curves with blue stars and green triangles, but as they were studied in parallel, the phenomenon is not as clear as before. The curves were cut at this point for the following study of mass loss.

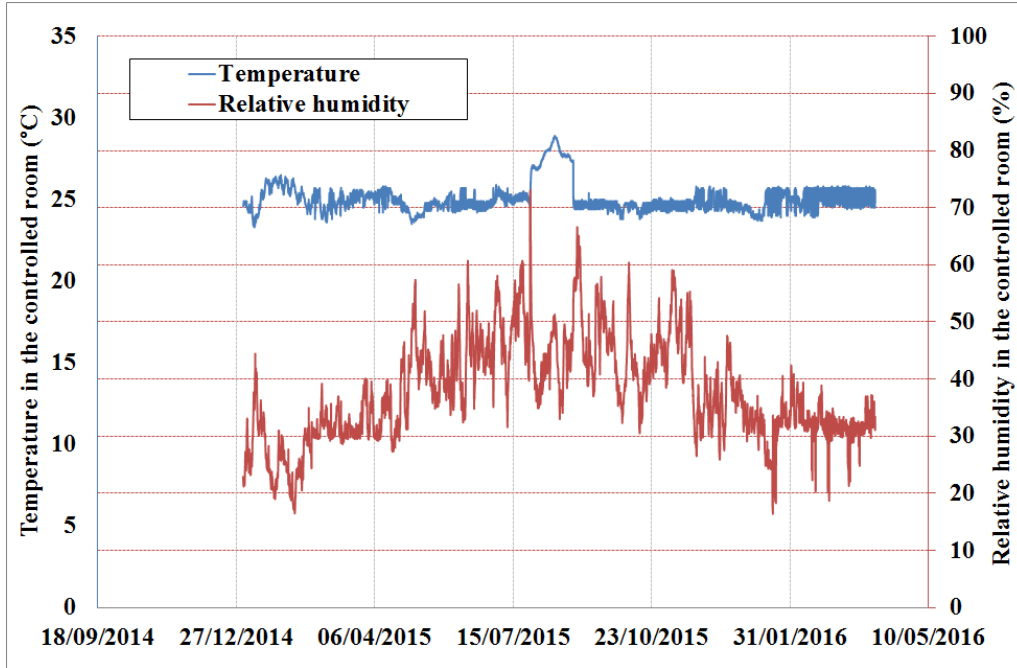


Figure 4.14 – Evolution of hygrometry and temperature in the controlled room

As we noted just above, the mass loss depends principally on the quantity of cement paste, and in order to ease the comparisons, the measures were normalised to express the mass loss for an equivalent amount of matrix according the formula 4.1.

$$W_n = \frac{1}{f_{cp}} \cdot \frac{\rho_{sp}}{\rho_w} \cdot W \quad (4.1)$$

In formula 4.1 :

- W_n is the normed water loss [%],
- f_{cp} is the cement paste volume fraction [.] ,
- ρ_{sp} is the specimens volume mass [$\text{kg} \cdot \text{m}^{-3}$],
- ρ_w is the water volume mass [$\text{kg} \cdot \text{m}^{-3}$],
- W is the measured water loss [%].

The results are expressed Figure 4.15.

All compositions tend to have the same behaviour and present the same range of mass loss.

These results highlight that aggregate volume fraction is an influential parameter on the drying of cementitious, but mostly due to the fact that the water movements mainly occur in the cement paste and that aggregates remain inert face to drying as they present a low porosity. Moreover; once the mass losses normed to the same amount of cement paste; it was demonstrated that neither aggregate size nor volume fraction affect water movements and that the cracking phenomenon is not important enough to alter the water transport.

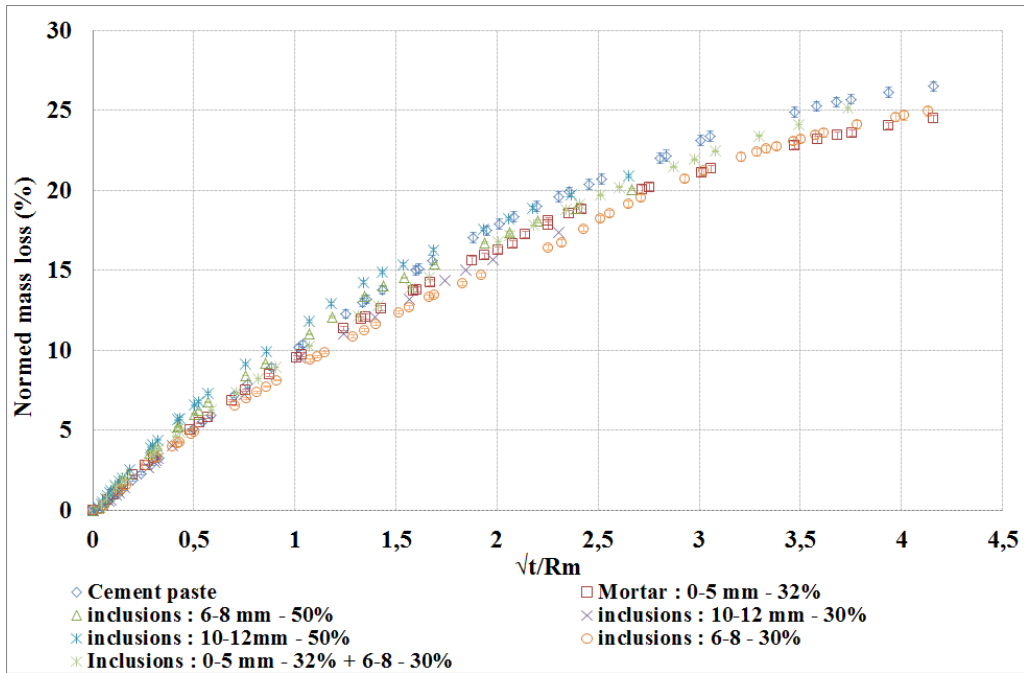


Figure 4.15 – Normed mass loss evolution of different compositions with time under drying conditions

4.2.2 Shrinkage

The evolution of apparent shrinkage of the different compositions during time, expressed as the equivalent time, is displayed on Figure 4.16 and expressed as a function of normed mass loss in Figure 4.17.

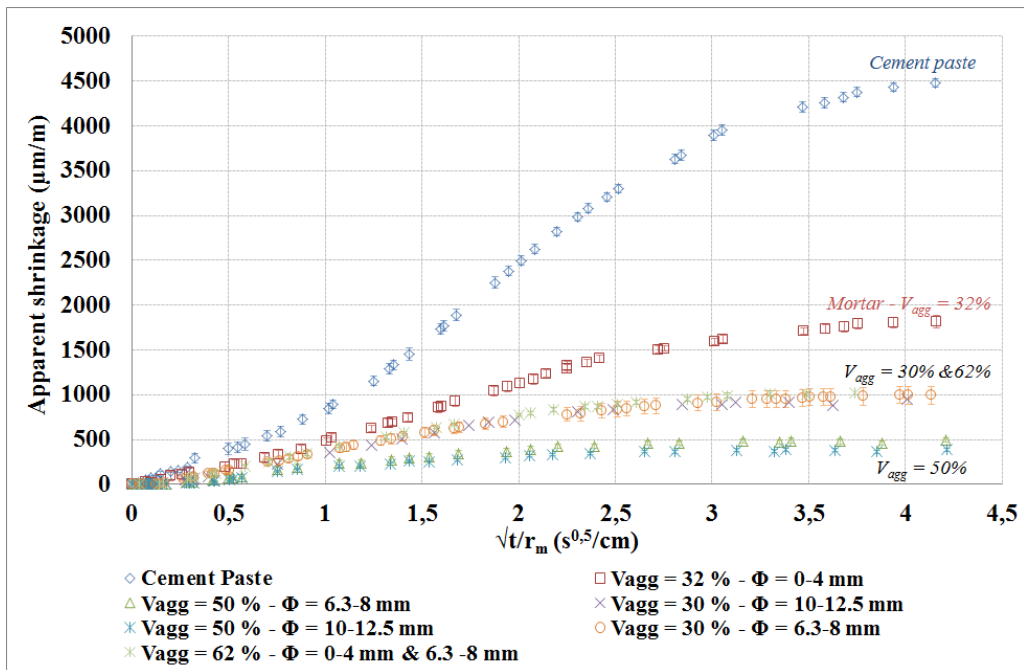


Figure 4.16 – Apparent shrinkage evolution of different compositions with time under drying conditions

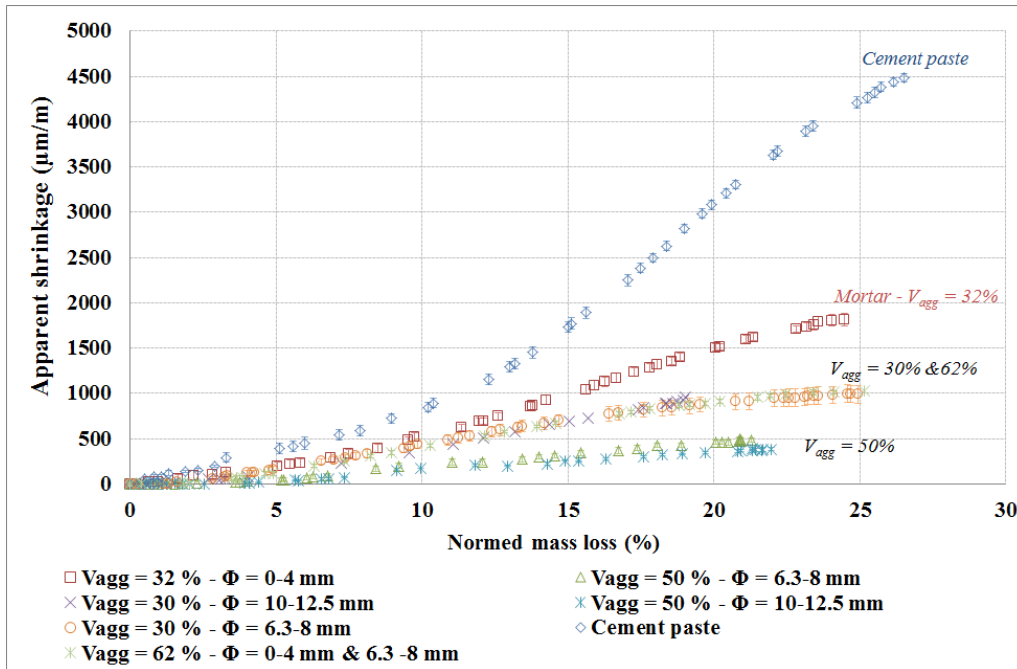


Figure 4.17

Several observations can be made :

- Apparent shrinkage decrease with the increase of the volume fraction of aggregates, highlighting the important role of this parameter. But, as it was described in the state of the art, it is mostly the cement paste that shrinks, so it is normal to observe this trend.
- At fixed volume fraction of aggregates, the formulations with 10–12.5mm aggregates tend to display an apparent shrinkage less important than the ones with 0–4mm or 6.3–8mm aggregates. This phenomenon is particularly present in the case of mortar (which contains 32% of sand), compared to the other formulations with 30% of aggregates. This observation underlines the effect of aggregates size.
- Finally, the formulation with a mortar matrix and 30% of 6.3–8mm aggregates displays a behaviour almost contradictory to the other ones : it seems that changing a cement paste matrix to a mortar one has a very little impact on the shrinking phenomenon, and it is mostly governed by the presence of coarse aggregates; which is not an expected behaviour, if not aberrant.

Several conclusions can be expressed from these observations. First, volume fraction of aggregates is an important parameter, as it modifies greatly the amplitude of shrinkage. Moreover, it was observed that when the size of aggregates increases, the amount total deformation decreases. It is certainly due to the restraint exercised by the aggregates on the cement paste, that increases with the aggregates size. Besides, based on the results of the cracking observations, the introduction of sand tends to decrease the restraint and the cracking phenomenon within the material. As a consequence, the fact that mortar has a shrinkage amplitude more important than other formulations with 30% of aggregates makes sense. Last but not least, it explains the behaviour of the formulation with 62% of aggregates. Indeed, the introduction of sand led to a decrease of the restraint exercised by the bigger aggregates, and allowed a bigger deformation of the cement paste. It is believed that it is a coincidence that the curve superimposes the other ones.

4.2.3 Comparison of experimental results with conventional homogenisation models

In order to fully understand the behaviours at stake here and to confirm the hypothesis of parameters influence described before, deformation values of each compositions were compared to conventional homogenisation models. The different models are:

- the serial (4.2) and parallel (4.3) models to set the superior and inferior limits;
- the Hashin's bisphere model (4.4);
- the trisphere models developed by Xi and Jennings and adapted from Christensen (4.8) and Le Roy, under different hypotheses of calculus (4.6 and 4.7).

Serial model

$$\varepsilon_{serial} = f_{cp}\varepsilon_{cp} \quad (4.2)$$

Parallel model

$$\varepsilon_{parallel} = \frac{f_{cp}E_{cp}}{f_{agg}E_{agg} + f_{cp}E_{cp}}\varepsilon_{cp} \quad (4.3)$$

Hashin's bisphere model [Hashin 1983]

$$\varepsilon_{Hashin} = \frac{(E_{cp} + E_{agg})f_{cp}}{(1 + f_{agg})E_{agg} + E_{cp}f_{cp}}\varepsilon_{cp} \quad (4.4)$$

Le Roy's model [Robert Le Roy 1995]

First, the variable g^* needs to be defined. It is the maximal compactness, calculated with Caquot's empirical formula below; where d is the diameter of the smallest aggregate and D the maximal one :

$$g^* = 1 - 0.47\left(\frac{d}{D}\right)^{1/5} \quad (4.5)$$

$$\varepsilon_{Leroy} = \frac{\left(1 + \frac{E_{cp}}{E_{agg}}\right)\left(1 - \frac{f_{agg}}{g^*}\right) + \frac{4\frac{E_{cp}}{E_{agg}}(1 - g^*)\frac{f_{agg}}{g^*}}{g^* + \frac{E_{cp}}{E_{agg}}(2 - g^*)}}{1 + \frac{f_{agg}}{g^*} + \frac{E_{cp}}{E_{agg}}\left(1 - \frac{f_{agg}}{g^*}\right)}\varepsilon_{cp} \quad (4.6)$$

Le Roy's model with the hypothesis of rigid inclusions ($E_{agg} \geq 4E_{cp}$) [Robert Le Roy 1995]

$$\varepsilon_{Leroy-rigid} = \frac{1 - \frac{f_{agg}}{g^*}}{1 + \frac{f_{agg}}{g^*}} \varepsilon_{cp} \quad (4.7)$$

Table 4.2 shows the value of Leroy's coefficients for our range of aggregates sizes and volumes.

Leroy's coefficients						
f_{agg}	0.3		0.32	0.5		0.62
d-D (mm)	6.3-8	10-12.5	0.063-4	6.3-8	10-12.5	0.063-8
C_L	0.425	0.424	0.485	0.200	0.199	0.194
C_{L-rigid}	0.296	0.295	0.426	0.049	0.048	0.140

Table 4.2

Christensen's model - Xi-Jennings's model [Christensen and Lo 1979; Christensen 1979; Yunping Xi and Jennings 1997]

For a question of simplification, Poisson coefficients were chosen equal: $\nu_{cp} = \nu_{agg} = 0.2$

$$\varepsilon_{Christensen} = 1 - \frac{f_{agg} \frac{E_{agg}(1 - 2\nu_{cp})}{E_{cp}(1 - 2\nu_{agg})}}{1 + \left(\frac{E_{agg}(1 - 2\nu_{cp})}{E_{cp}(1 - 2\nu_{agg})} - 1 \right) \frac{3 - 4f_{agg} \frac{3(1 - 2\nu_{cp})}{2(1 + \nu_{cp})}}{3 + 4f_{agg} \frac{3(1 - 2\nu_{cp})}{2(1 + \nu_{cp})}}} \varepsilon_{cp} \quad (4.8)$$

In formulas 4.2, 4.3, 4.4, 4.6, 4.7 and 4.8:

- ε_{cp} is the deformation of the cement paste;
- f_{cp} is the volume fraction of cement paste;
- E_{cp} is the Young Modulus of the cement paste;
- f_{agg} is the volume fraction of aggregates - $f_{agg} = 1 - f_{cp}$;
- E_{agg} is the Young Modulus of aggregates;
- g^* is the theoretical maximal compactness;
- d is the diameter of the smallest aggregate;
- D is the diameter of the biggest aggregate;
- ν_{cp} is the Poisson coefficient of the cement paste;
- ν_{agg} is the Poisson coefficient of aggregates.

Figure 4.18 shows the different models adapted for the parameters of our study expressed as function of aggregate volume fraction. Several experimental results from our study and from the bibliography were added. It should be noted that the latest are mostly based on mortar compositions.

Several observations can be made :

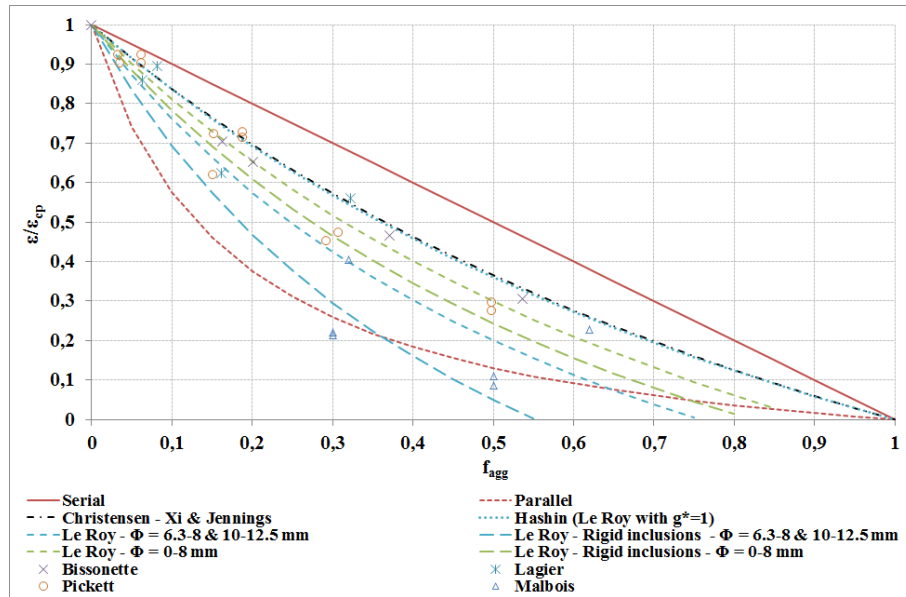


Figure 4.18 – Comparisons of shrinkage experimental results [Bissonnette; Pickett 1956; Lagier et al. 2011] to several analytical models

- Xi-Jennings model coincides with the Hashin model with our hypotheses;
- The introduction of Leroy's parameter g^* in his models (with and without the rigid inclusion hypothesis) leads to a shift of the curves and to be adapted to only a reduced range of aggregate fractions;
- Most of the experimental results are in between the models limits (serial and parallel models). However, four of our results - the ones of model concretes with a cement paste matrix - are under the parallel model, thus out of the limits. These are also the four formulations displaying important cracking. However, the models used here only assures the elastic behaviour of our composite materials and do not take into account the cracking phenomenon.
- Two of our results, the ones composed with sand, tend to have a behaviour that can be represented by one of the analytical models. This is probably due to the introduction of sand that diminished the strains and thus the cracking phenomenon. They were drawn in Figures 4.19 and 4.20 as function of equivalent time and compared to the different models (based on the cement paste deformations obtained in our study).

One can see that the experimental results can respectively be described quite correctly by one model, but not the same one: mortar is described best by Leroy's model with the hypothesis of rigid inclusions, whereas model concrete seems closer (at the end of the curve) to Christensen's model. Here again the presence of a cracking phenomenon, even reduced in comparison with the other formulations, can be the source of these differences.

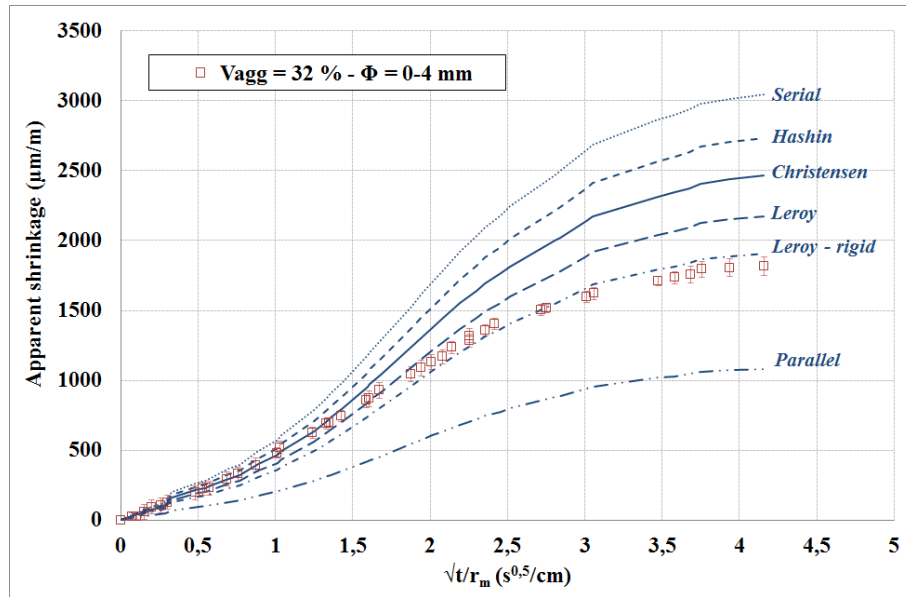


Figure 4.19 – Comparison between the experimental shrinkage of mortar and the different analytical models as a function of time - Mortar: Vagg = 32%; $\phi=0-4\text{mm}$

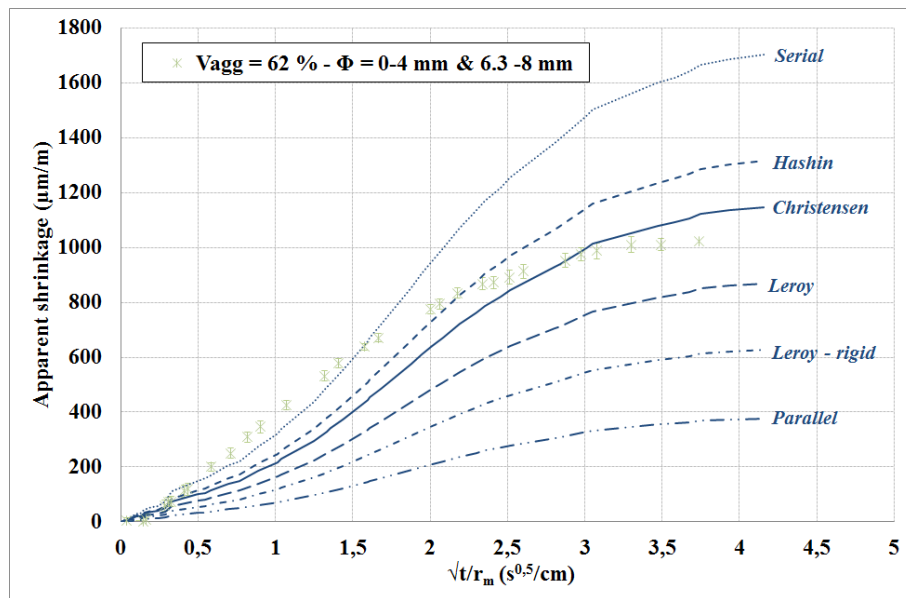


Figure 4.20 – Comparison between the experimental shrinkage of mortar-based material and the different analytical models as a function of time - Model material: Vagg = 62%; $\phi = 0 - 4$ and $6.3 - 8\text{mm}$

In this part, the results obtained from the shrinkage monitoring were compared to experimental works of different authors of the literature, and to several analytical models, that take into account several parameters of the aggregates in their formulas. Our study brought out that these models are only valid for composition presenting a low, or a very low, internal cracking phenomenon. Indeed, one of the major hypothesis of these models is that the materials evolve in a pure elastic behaviour. However, the presence of cracks is a sign that the elastic domain was locally out-reached. However, for formulations that respect the low cracking phenomenon, these models could be relevant. Yet, the focus was made with two compositions of our study (with a mortar based matrix), and we saw that the evolution of shrinkage could be approximated, but with different models. This prevents us to conclude on the validity of these models so far.

4.3 Effect of aggregates and drying on transfer and mechanical properties

4.3.1 Mechanical properties

Evolution of flexural strength

Flexural strength values are obtained according the procedure described in Section 3.2.4. Results are gathered in Table 4.3. It shows the values of the characterisation phase after the endogenous cure, and the ones at the end of the monitoring in drying and endogenous conditions.

	Flexural strength (MPa)							
	28 days Characterisation		$t_{eq-final}$ Drying		$t_{eq-final}$ Endogenous		Variation	
	Value	Standard Deviation	Value	Standard Deviation	Value	Standard Deviation	%	
Cement paste	3.14	0.21	1.98	0.29	3.55	0.23	- 32.5	
Mortar	6.23	0.92	6.53	0.26	6.6	0.09	- 1.01	
Vagg = 30%	6.3-8	4.16	0.66	2.79	0.13	4.91	0.92	- 43.2
	10-12.5	6.6	1.08	3.33	0.22	5.08	0.31	- 34.5
Vagg = 50%	6.3-8	3.6	0.46	2.1	0.04	4.8	1.19	- 56.6
	10-12.5	6.17	0.32	2.30	0.21	5.10	0.59	- 54.8
Vagg = 62%	0-4 & 6.3-8	6.66	0.41	7.91	0.46	7.41	0.28	+ 6.8

Table 4.3 – Evolution of flexural strength

Also, percentage of variation between the drying and the autogenous samples (age : $t_{eq-final}$) were calculated according formula 4.9:

$$V_{f_{cf}} = 100 \times \frac{f_{cfendo} - f_{cfdry}}{f_{cfendo}} \quad (4.9)$$

In formula 4.9:

- $V_{f_{cf}}$ is the variation in [%],
- $f_{cfendo/dry}$ is the flexural strength value of the specimens that were kept in endogenous or drying conditions in [MPa].

This variation calculus allows the identification of the effects of drying on the materials studied, and of the possible influence of aggregates : the variation of rates could indicate a different state of damage of the materials induced by the restraint of the cement paste by the aggregates when submitted to drying. All formulations, except the last one, display a decrease of flexural strength with drying. However the loss is very fluctuating from a composition to an other : from -1% to -57% . The particular formulation, composed with mortar and coarse aggregates (6.3 – 8mm), shows a 6.8% increase of flexural strength with drying.

In order to identify a pattern, the losses of performances were sorted by aggregate volume fractions in the histogram in Figure 4.21.

Several observations can be made :

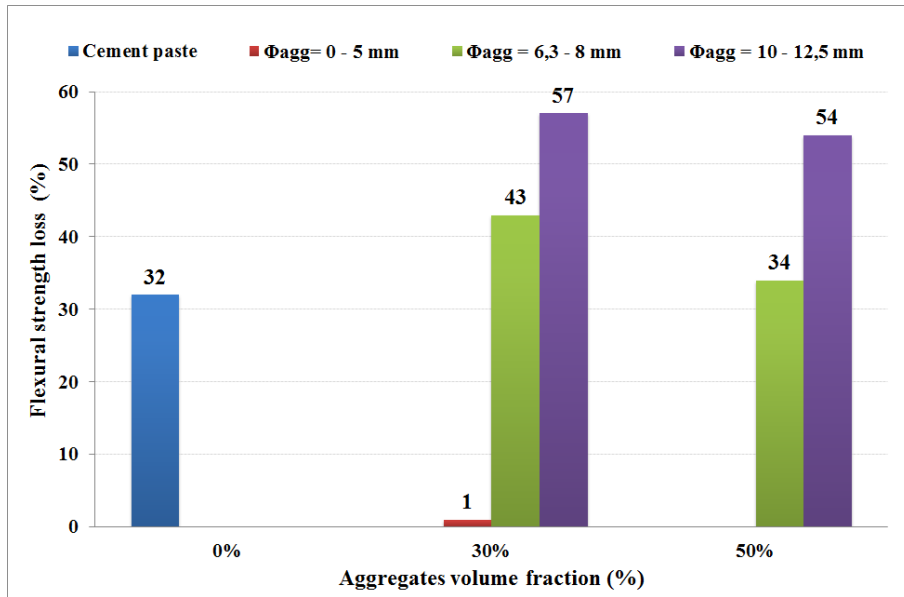


Figure 4.21 – Comparison between dried and endogenous specimens - Decrease of flexural strength

- Formulations with 10–12.5mm aggregates tend to show a decrease of flexural strength more important than the ones with 6.3–8mm aggregates. This observation is consistent with the ones made in Section 4.2.2 : the increase of the size of coarse aggregates tends to induce higher restraint stresses in the material and, as a consequence, the damage level is more important.
- Formulations with 30% of aggregates show slightly higher decrease levels than the ones with 50% of aggregates. Increasing the volume fraction of aggregates leads to a redistribution of the stresses in the material, generating a damaging less important.
- Cement paste displays a 32% decrease of flexural strength, this damaging is exclusively due to the effects of the hydric gradient in the material, due to the lack of aggregates.
- Cement paste displays a 32% loss of strength opposed to 1% for the mortar. It seems that the introduction of small inclusions ($\phi \leq 4\text{mm}$) leads to a decrease of the effects of hydric gradients and to a more resistant material.
- Also, the formulation with 30% of 6.3 – 8mm aggregates displays a loss of 43% whereas the same formulation with a mortar matrix shows an increase of almost 7% of strength. The introduction of small inclusions ($\phi \leq 4\text{mm}$) leads to observe an increase of flexural strength with drying. These observations are consistent with those highlighted in Section 4.2.2, and could be attributed to capillary pressure effects as observations made in the state of the art.

To summarise what was enumerated just above, it can be seen that aggregate size and aggregate volume fraction play an important role in the evolution of flexural strength with drying. Indeed, we have seen that the increase of coarse aggregates size leads to a local and open cracking pattern, creating a preferential path for the mechanically induced crack and resulting in an important reduction of the flexural strength. However, the introduction of fine aggregates leads to a global distribution of the cracks, with small openings that introduce new mechanisms: there are no preferential path for the mechanically induced crack and the capillary effects tends to pre-stress the material, which tends to display a higher flexural strength than the witness samples prevented from drying. Also, aggregate volume fraction seems to also have an impact. As a matter of fact, when the volume of aggregates is low, cracks will tend to developed throughout the material to connect the different inclusions and thus, leading to a material with a reduced flexural strength. Increasing the volume of aggregates positions inclusions closer to each other (at fixed diameter), and thus limits the amount of damage of the material.

Equivalent cross sections From the previous results, it is possible to assess the quantity of undamaged material in the dried specimens. Based on Formulas 4.10 and 4.11, equivalent geometries are calculated, and are presented Table 4.4 and Figures 4.22 and 4.23.

$$f_{cf} = \frac{F_{max} \cdot L \cdot d}{8 \cdot I} = \frac{3 \cdot F_{max} \cdot L}{2 \cdot d^3} \quad (4.10)$$

$$f_{cf_{endo}} = \frac{F_{max_{dry}} \cdot L \cdot d}{8 \cdot I} = \frac{3 \cdot F_{max_{dry}} \cdot L}{2 \cdot d_{eq}^3} \Rightarrow d_{eq}^3 = \left(\frac{3 \cdot F_{max_{dry}} \cdot L}{2 \cdot f_{cf_{endo}}} \right)^{-\frac{1}{3}} \quad (4.11)$$

In formulas 4.10 and 4.11:

- $f_{cf_{endo}}$ is the mean flexural strength of the specimens tested at t_{eq} and kept in endogenous conditions [$\mu.m/m$],
- $F_{max_{dry}}$ is the mean rupture load of specimens kept in drying conditions and tested at t_{eq} [mm],
- L is the distance between the support rolls [mm],
- I is the inertia of the specimens [mm],
- d is the length of the side of the charged square section [mm],
- d_{eq} is the equivalent value of the side of the charged square section [mm].

In Table 4.4 are indicated the initial geometries and sections (labelled d_{ini} and S_{ini}), and the equivalent geometries calculated (labelled d_{eq} and S_{eq}). The quantity of undamaged material is indicated in the last column and is obtained by the formula : $U_{eq} = 100 \times \frac{S_{eq}}{S_{ini}}$, and is expressed in [%]. A comparison of these percentages is presented in Figure 4.22.

		d_{ini} [N]	d_{eq} [mm]	S_{ini} [mm ²]	S_{eq} [mm ²]	Undamaged material [%]
Cement paste		40	33.2	1600	1105	69.1
Vagg = 30%	Mortar	40	39.9	1600	1592.8	99.5
	6.3-8	70	57.9	4900	3357.1	68.5
	10-12.5	70	60.8	4900	3695.1	75.4
Vagg = 50%	6.3-8	70	53	4900	2886.5	58.9
	10-12.5	70	53.7	4900	2810.2	57.4
Vagg = 62%	0-4 & 6.3-8	70	71.6	4900	5120.7	104.5

Table 4.4 – Equivalent geometries and sections

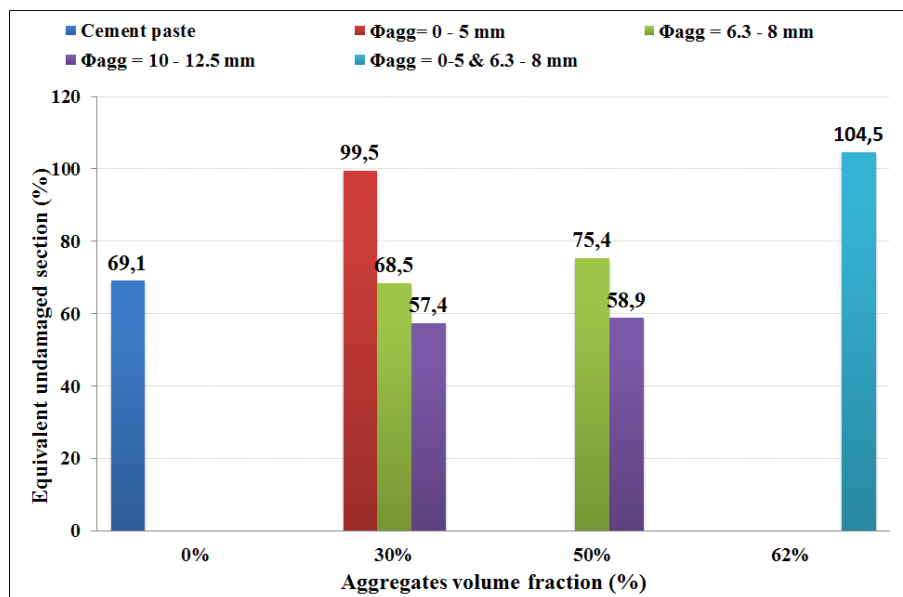


Figure 4.22 – Comparison between equivalent undamaged sections

The trends observed are consistent with the ones of the flexural tests : the amount of damage is more important when the aggregate size increases and when the aggregate volume fraction decreases. However it shows slightly different percentages. Must of all, it provides a practical understanding and viewing of the impacts of aggregates and drying on the material. The Figure 4.23 allows a viewing of the equivalent sections compared to the initial ones.

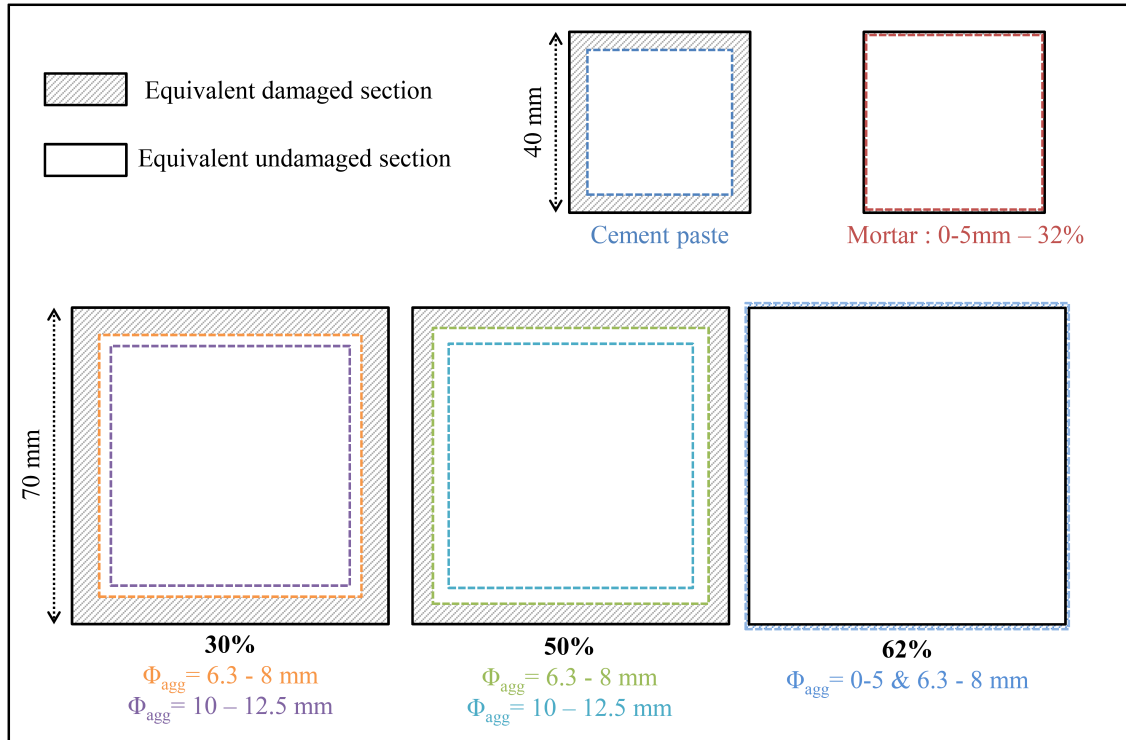


Figure 4.23 – Comparison between equivalent undamaged sections calculated for all the specimens tested according to the flexural strengths obtained after drying

Evolution of Young Modulus coefficient

Young Modulus coefficient is calculated from the uni-axial compressive tests as describe in Section 6.2.3. Only three formulations were tested, with the following parameters:

- $V_{agg} = 30\%$, $\phi = 10 - 12.5\text{mm}$
- $V_{agg} = 50\%$, $\phi = 6.3 - 8\text{mm}$
- $V_{agg} = 50\%$, $\phi = 10 - 12.5\text{mm}$

Results are gathered in Table 4.5. It shows the values of the characterisation phase at 28 days, and the ones at the end of the monitoring. Also, it indicates the percentage of variation between the drying and the autogenous samples (age : t_{eq}) calculated according the formula 4.12.

$$V_E = 100 \times \frac{E_{endo} - E_{dry}}{E_{endo}} \quad (4.12)$$

In Formula 4.12,

- V_E is the variation in %,
- $E_{endo/dry}$ is the Young Modulus coefficients of the specimens that were kept in endogenous or drying conditions in GPa.

The first observation that can be made is that drying has altered the behaviour of the material under a compressive load, and all formulations present an important decrease of

		Young Modulus (GPa)						V_E %
		28 days		$t_{eq-final}$		$t_{eq-final}$		
		Characterisation		Drying conditions		Autogenous conditions		
		Value	Standard Deviation	Value	Standard Deviation	Value	Standard Deviation	
Vagg = 30%	10-12.5	18.6	0.5	9.3	0.5	20.3	0.5	- 54
	6.3-8	24.5	5.9	13.3	1.4	23.5	1.9	- 43
Vagg = 50%	10-12.5	24.8	0.4	10.9	0.9	22.2	1.2	- 51

Table 4.5 – Evolution of Young Modulus

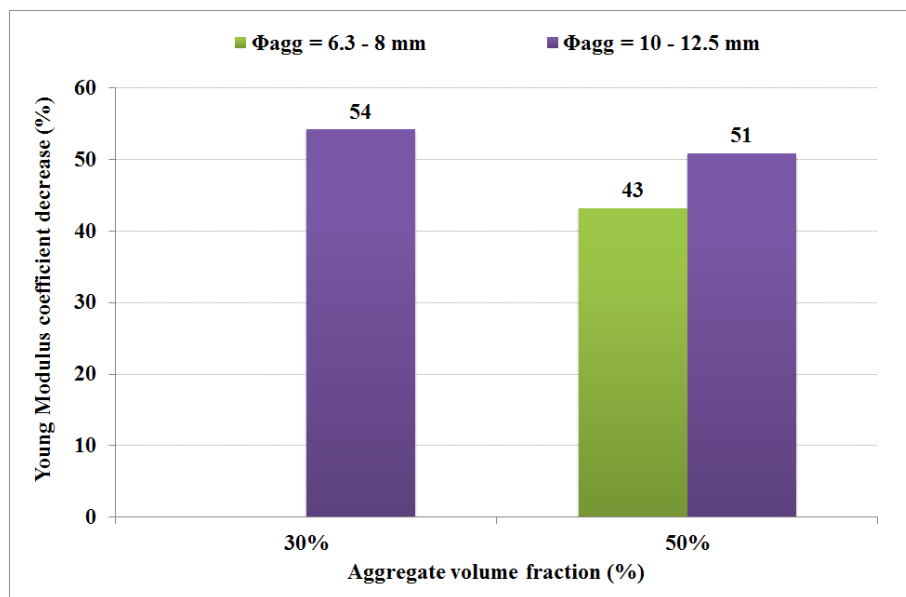


Figure 4.24 – Comparison between dried and endogenous specimens - Decrease of Young Modulus

Young Modulus coefficient with drying. The variations were sorted by aggregates volume fractions in the histogram Figure 4.24.

As observed in the study of flexural strength, aggregates size and volume fraction have an influence on the variation of Young Modulus:

- Specimens with 10 – 12.5mm aggregates tends to present a more important decrease of the static elastic modulus than the ones with 6.3 – 8mm aggregates. Even if the comparison can be made only with a volume of 50% of aggregates, it confirms the tendency observed in previously in Sections 4.1 and 4.2, that the increase of the diameters of inclusions leads to the increase of internal damages induced by drying.
- Increasing the volume represented by aggregates leads to a decrease of Young Modulus loss. As observed previously, increasing the number of inclusions generates a decrease of the internal damage due to the fact that aggregates will be closer the inter-granular cracking will be less localised and through the material.

Even if the comparison is made on fewer formulations, it confirms the tendency observed in previously in Sections 4.1 and 4.2, that the increase of the diameters of inclusions and the decrease of aggregates volume fraction lead to the increase of internal damages induced by drying.

Evolution of compressive strength

Compressive strength is calculated from the uni-axial compressive tests as describe in Section 6.2.3. We remind that only three formulations were tested. Results are gathered in Table 4.6. It shows the values of the characterisation phase at 28 days, and the ones at the end of the monitoring. Also, it indicates the percentage of variation between the drying and the autogenous samples (age : t_{eq}) calculated according the Formula 4.13:

$$V_{f_c} = 100 \times \frac{f_{cendo} - f_{cdry}}{f_{cendo}} \quad (4.13)$$

In Formula 4.13:

- V_{f_c} is the variation in %,
- $f_{cendo/dry}$ is the compressive strength of the specimens that were kept in endogenous or drying conditions in MPa.

		Compressive strength (MPa)						V_{f_c} %
		28 days		$t_{eq-final}$		$t_{eq-final}$		
		Characterisation		Drying conditions		Autogenous		
		Value	Standard Deviation	Value	Standard Deviation	Value	Standard Deviation	
Vagg = 30%	10-12.5	21.0	2.1	13.3	1.8	24.6	1.0	-46
	6.3-8	21.5	1.3	14.4	1.0	25.7	2.2	-44
Vagg = 50%	10-12.5	18.84	0.6	11.9	1.0	20.5	1.5	-42

Table 4.6 – Evolution of Compressive Strength

Once again, all formulations present an important decrease of property with drying. The variations of compressive strength were sorted by aggregates volume fractions in the histogram Figure 4.25.

Two observations can be made :

- As observed previously, the increase of aggregates volume fraction decreases the variation of properties, meaning that the material tends to be less damaged by drying.
- The increase of aggregates diameter generates a decrease of compressive strength variation. This means that, contrary to the previous observations, the increase of aggregate diameter induces a reduction of the internal damages. However these results can be explained by the fact that applying a compressive load to fractured material will first close up a part of the cracks that will transmit the loading.

The comparison of compressive strength evolution was made on only three formulations and presented a slightly different observation than the study of drying, flexural strength and Young Modulus. But it was shown that these differences could be explained and do not affect our previous conclusions.

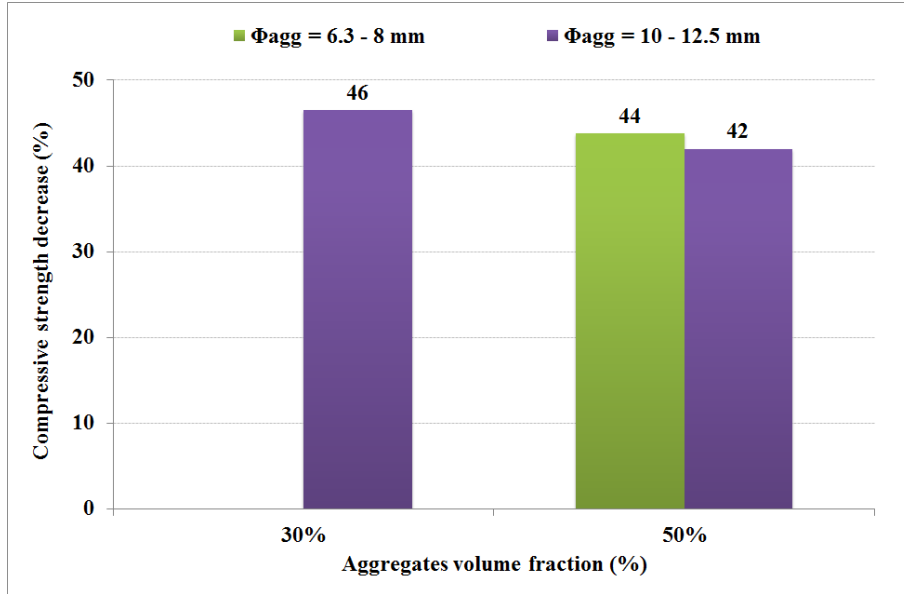


Figure 4.25 – Comparison between dried and endogenous specimens - Decrease of compressive strength

4.3.2 Transfer properties

In order to complete mechanical evolution but also to properly study the durability of the materials, two tests were conducted to assess the transfer properties: porosity accessible to water and chloride diffusion.

However, those experiments were made only on three compositions :

- Cement paste;
- Mortar;
- Cement paste and 30% of 6.3 – 8mm aggregates.

This choice of samples allows us to observe the effect of aggregate size by using aggregates of 0 – 4mm and 6.3 – 8mm. The aim is also to characterise the cement paste and to see if the introduction of aggregates would modify the porosity network. Moreover, the aggregates selected would interact differently with the cement paste and lead to different ITZs according to the state of the art; thus this could also influence the transfer properties.

However, these samples present different quantities of aggregates, therefore of cement paste. Since water transport occurs mainly in cement paste, it was important to compare equivalent quantities. Thus, the results displayed for the mortar and model concrete were normalised by the volume fraction of cement paste present in the mixture according to the Formula 4.14.

$$X_n = f_{cp} \cdot X \quad (4.14)$$

In Formula 4.14:

- X is the porosity or diffusion as measured on the samples
- X_n is porosity or diffusion, normed by volume fraction of cement paste
- f_{cp} is the cement paste volume fraction

Evolution of the porosity

The porosity accessible by water was determined using the protocol detailed in Section 3.2.5. The results are gathered in Table 4.7.

		Porosity (%)					
		28 days Characterisation		$t_{eq-final}$ Drying		$t_{eq-final}$ Autogenous	
		Value	Standard Deviation	Value	Standard Deviation	Value	Standard Deviation
Vagg = 30%	Cement paste	39.5	0.53	35.3	0.76	33.9	0.31
	Mortar	36.9	1.32	34.2	0.97	33.4	0.45
	6.3-8	41.1	0.75	34.4	2.63	35.1	2.01

Table 4.7 – Porosity normed by the cement paste fraction

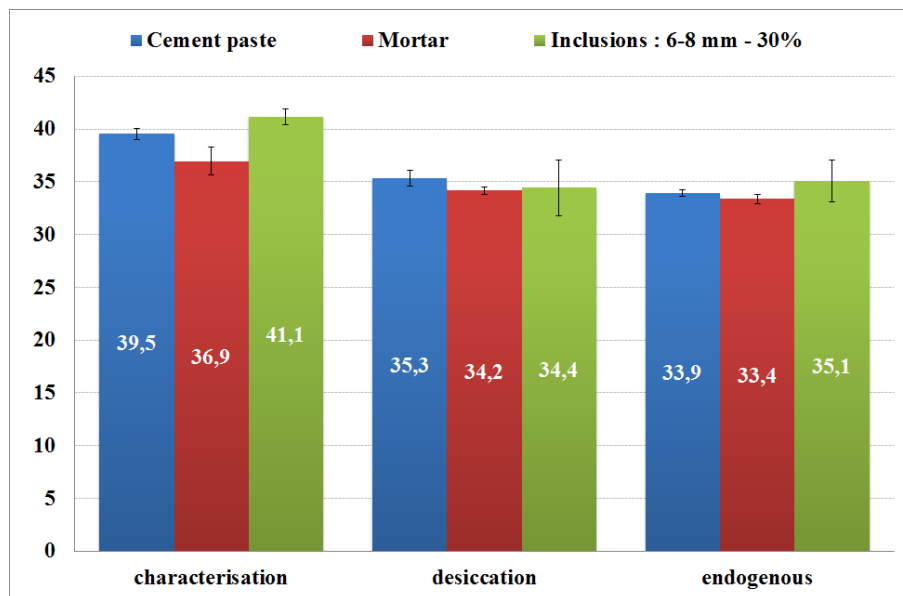


Figure 4.26 – Evolution of porosity accessible to water, normed by cement paste volume fraction

Several observations can be made :

- Values at the end of endogenous cure (characterisation values on Figure 4.26) are higher than the ones at the end of the endogenous procedure (endogenous values on Figure 4.26). The first explanation is that the cement hydration is not complete at the end of the 28 days of cure and continues throughout the procedure, leading to a decrease of the porosity. The second explanation could be that for the tests at the end of the procedure, in order to ensure the cohesion of the slices, the specimens were coated with epoxy resin reinforced with glass fibres, resulting in a filling of a part of the porosity that was accessible before.
- Cement paste and mortar display a slight increase of porosity between endogenous and dried state at the end of the procedure. However the variation is very limited and knowing that this procedure has a high range of uncertainty of measurement,

this variation can hardly be interpreted as an effect induced by internal or superficial cracking due to drying.

- Model concrete displays a slight decrease of porosity, but for the same reasons than for the two other formulations, the variation is not significant enough to reach a conclusion concerning the evolution of porosity in the material.

Desiccation and the presence of aggregates seem to have no significant impact on the porosity accessible to water of the materials. This means that the internal cracking induced by aggregate restraint - which presence was demonstrated in the studies of evolutions of shrinkage and mechanical properties - is not opened enough to modify the porosity and the water transport. This observation is consistent with the observations made in Figure 4.15. Indeed, water loss did not suffer from a change of kinetics due to the initialisation and development of cracking.

Evolution of the chloride diffusion

The coefficients of diffusion of chloride ions in samples were determined according to the protocol detailed in Section 3.2.5. Results are presented Table 4.8.

Chloride diffusion coefficient ($10^{-11} \text{ m}^2 \cdot \text{s}^{-1}$)						
28 days			$t_{eq-final}$		$t_{eq-final}$	
Characterisation			Drying		Autogenous	
	Value	Standard deviation	Value	Standard deviation	Value	Standard deviation
Cement paste	1,38	0,29	2,10	0,79	0,33	0,15
Vagg = 30% Mortar	1,70	0,12	2,21	0,53	0,44	0,36
6.3-8	1,73	0,18	2,71	0,79	1,21	0,02

Table 4.8 – Diffusion coefficient normed by the cement paste fraction

Several observations can be made:

- The characterisation values are higher than the ones at the end of the endogenous procedure. As seen in the study of porosity, cement hydration is not complete at the end of the endogenous cure and continues throughout the procedure, leading to a decrease of porosity, thus of chloride diffusion.
- All formulations display an increase between the endogenous average results and dried ones. They also present an increase between characterisation average results and dried ones. It can be assumed that these increases are symptomatic of the cracking phenomenon occurring during drying. Indeed, chloride ions are more able to diffuse in dried samples, due to an increase of the porosity network generated by the internal cracking.
- When comparing formulations with aggregates, one can see that mortar seems to suffer from a total increase (+240%) more important than concrete (+123%). At first, this result could seem contradictory with the conclusions made in the previous paragraphs. Indeed, as we saw that model concrete formulations with a cement paste matrix are concerned by a open and localised internal cracking, we were expecting

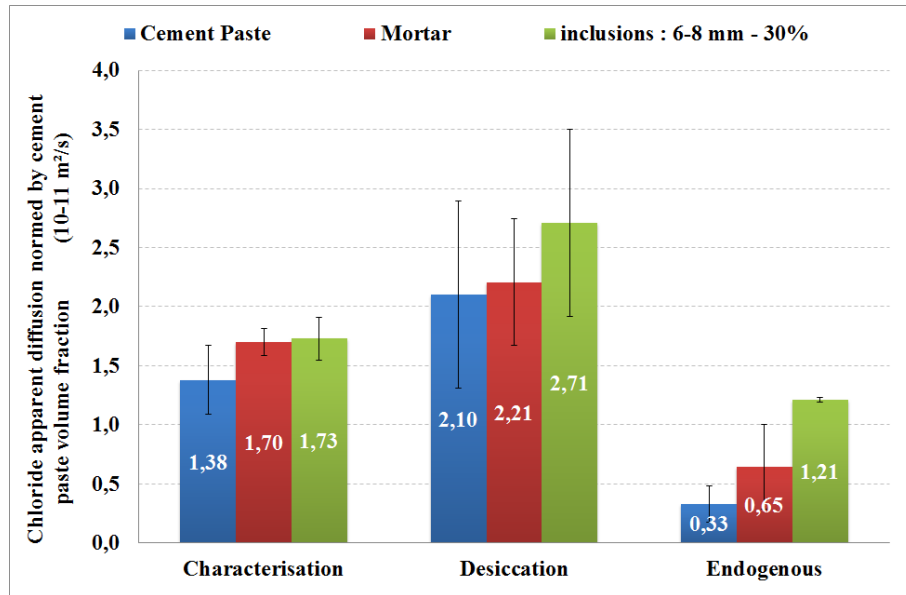


Figure 4.27 – Evolution of chloride diffusion with drying

to observe a more important diffusion. However, in the case of mortar, cracking is more fine but also more spread in the material, that could lead to a more global interconnection of ITZs and thus increasing the porous network and the diffusion of chloride.

- Nearly all results display a very important standard deviation. First, this could be due to the fact that these results have been determined on a limited number of samples and that, if an outlier value is present, it is difficult to identify and therefore taken into account. Moreover, this experiment has a high range of uncertainty of measurements. Unfortunately, given that the order of magnitude of these results remain unchanged by the procedure, the variation observed here are not significant enough to conclude to an effective modification of the porosity network by drying. They could just be due to the variability of the material.

Desiccation and the presence of aggregates seem to have an impact on chloride diffusion, however not significant enough to conclude to a clear pattern. The conclusions drawn from the porosity assessments are valid here again: internal cracking induced by aggregate restraint is present but not opened enough to modify water transports. These results are consistent with the observations gathered from other authors in the state of the art. Indeed, they also concluded that the effect of drying were limited when observed via chloride diffusion.

4.4 Conclusion

The experimental study presented in this chapter concerns the drying of morphologically controlled materials to evaluate the impact of aggregates parameters (size and volume fraction) on the delayed behaviour of these cementitious materials. Seven formulations were tested from cement paste to a model material that approximates ordinary concrete. The parametric study lied on two aggregate parameters :

- **Aggregate volume fraction:** aggregates represent 0, 30, 50 or 62% of the total volume of the samples;
- **Aggregate size:** aggregates diameters is included in these ranges : 0-4 mm, 6.3-8 mm and 10-12.5 mm.

The analysis of all the results of mass loss, deformations, changes in the properties of the materials and cracking observations makes it possible to formulate several concluding remarks.

- The observation of samples using a microscope and a X-ray microtomograph revealed that the restraint exerted by the aggregates led to very different surface and internal cracking patterns. The increase of the diameter of coarse aggregates lead to a localisation of the cracks and an opening more important. However, the introduction of fine aggregates (sand, $\phi \geq 4mm$) induce a dwindling of cracks opening and a wider distribution of the cracks, meaning that the restraint levels in the material are greatly reduced.
- The comparison of the mass losses of the samples showed that aggregates volume fraction is an influential parameter of the mass variations. However, it was demonstrated that the amount of mass loss is directly linked to the volume fraction of cement paste, and; once the mass losses normed; that the water transport in not modified by the aggregate parameters.
- The observations made for mass variations were verified when porosity and chloride diffusion were assessed. Indeed, the presence of a cracking phenomenon is not contested, but the cracks developed in any of the materials studied is not open enough and/or don't lead to an interconnection of the porosity sufficient enough to significantly modify the water movements in the materials.
- The comparison of samples shrinkage highlighted that the volume fraction of aggregates is an important parameter as it modifies greatly the amplitude of shrinkage. Moreover, it was observed that the restraint exercised by coarse aggregates ($\phi \leq 4mm$) on the cement paste; that increases with the aggregates size; also have an impact on the amount of total shrinkage. However, the introduction of fine aggregates (sand, $\phi \geq 4mm$) tends to decrease the restraint; and thus the cracking phenomenon; within the material, leading to a shrinkage more important than the formulations with a cement matrix. The two parameters therefore have a significant impact, but the impact of the size of the aggregates is subject to the presence of a threshold that reverses its effects, whereas the volume fraction of the aggregates is influential in all cases.
- The same effects were observed when taking an interest in the mechanical properties. On one hand, the introduction of a number (thus, a volume) of aggregates too low leads to a opened and developed cracking pattern. The increasing of aggregates volume allows us to better control and limit the cracks development and progression. On the other hand, the presence of the threshold in aggregate diameters around 4mm is confirmed. Indeed, the modification of the size of coarse aggregates impacts the mechanical response; but it is when fine aggregates are used that a new phenomena appear that tends to improve the mechanical behaviour of the materials: the capillary effect. The cracking is more fine and when water leaves the porosity (including cracks) due to desiccation, a suction effect appears that pre-stresses the samples.

Bibliography on drying

- Abbas, A. (1998). “Écoulement gazeux dans les bétons partiellement saturés : application à la mesure de perméabilité”. PhD thesis. Université de Toulouse - INSA de Toulouse.
- Abbas, A., M. Carcasses, and Olliver J.-P. (1999). “Gas permeability of concrete in relation to its degree of saturation”. In: *Materials and Structures* 32, pp. 3–8.
- Acker, Paul (1988). “Comportement mécanique du béton : apport de l’approche physico-chimique”. PhD thesis. École Nationale des Ponts et Chaussées.
- (1991). “Retraits et fissurations du béton : Causes, mécanismes, modèles”. In: *AFPC*.
- Acker, Paul, M. Mamillan, and B. Miao (1990). “Drying and shrinkage of concrete: the case of massive parts”. In: *Serviceability and Durability of Construction Materials. ASCE*. Ed. by B.A. Eds, pp. 1072–1081.
- Baroghel-Bouny, Véronique. (1994). “Caractérisation des pâtes de ciment et des bétons. Méthodes, analyse, interprétation”. PhD thesis. École Nationale des Ponts et Chaussées.
- Baron, J. (1982). *Le béton hydraulique : connaissance et pratique*. Les retraits de la pâte de ciment.
- El-Baroudy, H.F. (1940). “The strength, shrinkage, and creep of concrete as affecting the design of re-inforced concrete structures containing liquids”. PhD thesis. University of London (Battersea Polytechnic).
- Bartlett, F.M. and MacGregor; J.G. (1994). “Effect of moisture condition on concrete core strengths”. In: *Materials Journal* 91(3), pp. 227–236.
- Bažant Z.P. and Huggaard, A.B., S. Baweja, and Franz-Joseph Ulm (1997). “Microprestress-solidification theory for concrete creep. I: Aging and drying effects”. In: *Journal of Engineering Mechanics* 123(11), pp. 1188–1194.
- Bažant, Z.P. and J. Chern (1985). “Concrete creep at variable humidity : constitutive law and mechanism”. In: *Material and Structures* 18(1), pp. 1–20.
- Bažant, Z.P. and F.H. Wittmann (1982). *Creep and Shrinkage in Concrete Structures*.
- Bažant, Z.P. and Y. Xi (1994). “Drying creep of concrete : constitutive model and new experiments separating its mechanisms”. In: *Materials and Structures* 27, pp. 3–14.
- Beltzung, F. and F.H. Wittmann (2005). “Role of disjoining pressure in cement based materials”. In: *Rencontres AUGCIBPSA, Chambéry, France* 35(12), pp. 2364–2370.
- Benboudjema, Farid (2002). “Modélisation des déformations différées du béton sous sollicitations biaxiales. Application aux enceintes de confinement de bâtiments réacteurs des centrales nucléaires”. PhD thesis. Université de Marne-La-Vallée.
- Bisschop, Jan, Leo Pel, and Jan G. M. van Mier (2001). “Effect of aggregate size and paste volume on drying shrinkage microcracking in cement-based composites”. In: *Creep, Shrinkage and Durability Mechanics of Concrete and other Quasi-Brittle Materials, Proc. of CONCREEP-6 at MIT*. Ed. by Z.P. In Bažant, F. Ulm, and F.H. Eds Wittmann. Boston, USA.

- Bissonnette, Benoit, Pascale Pierre, and Michel Pigeon (1999). "Influence of key parameters on drying shrinkage of cementitious materials". In: *Cement and Concrete Research* 29(10), pp. 1655–1662.
- Bouterf, Amine (2014). "Comportement mécanique de la plaque de plâtre étudié par tomographie et essais mécaniques in-situ". PhD thesis. ENS Cachan.
- Bucher, R. et al. (2017). "Impact of aggregate properties on the development of shrinkage-induced cracking in concrete under restraint conditions". In: *In Proceedings - CFM17*.
- Burlion, Nicolas, Francois Bourgeois, and J.-F. Shao (2005). "Effects of desiccation on mechanical behaviour of concrete". In: *Cement and concrete composites* 27(3), pp. 367–379.
- Burlion, Nicolas, Frederic Skoczylas, and Thierry Dubois (2003). "Induced anisotropic permeability due to drying of concrete". In: *Cement and Concrete Research* 33, pp. 679–689.
- Butcher, W. (1958). "The effect of air drying before test : 28-day strength of concrete". In: *Constructional Review*, pp. 31–32.
- Cabrera, J.G. and Lynsdale C.J. (1988). "A new gas permeameter for measuring the permeability of mortar and concrete". In: *Magazine of Concrete Research* 40(144), pp. 177–182.
- Carlson, R.W. (1939). "Drying shrinkage of concrete as affected by many factors". In: *In proc. of the American society for testing materials* Part 2, 38, pp. 419–437.
- Christensen, R.M. (1979). *Mechanics of Composite Materials*.
- Christensen, R.M. and K.H. Lo (1979). "Solutions for effective shear properties in three phase sphere and cylinder models". In: *d. Mech. Phys. Solids* 27, pp. 315–330.
- Cortas, Rachid (2012). "Nouvelle approche expérimentale pour la maîtrise de la fissuration du béton jeune : influence de la nature et de la saturation des granulats". PhD thesis. École Centrale de Nantes et Université Libre de Bruxelles.
- Day, R., P. Cuffaro, and J. Illston (1984). "The effect of rate of drying on the drying creep of hardened cement paste". In: *Cement and Concrete Research* 14(3), pp. 329–338.
- De Sa, Caroline (2007). "Etude hydro-mecanique et thermo-mecanique du beton". PhD thesis. ENS Cachan.
- De Sa, Caroline, Farid Benboudjema, and Alexandre Michou (2013). "Delayed strains of cementitious materials-impact of heterogeneities and creep on cracking induced by drying". In: *Mechanics and Physics of Creep, Shrinkage, and Durability of Concrete : A Tribute to Zdenek P. Bazant : Proc. of CONCREEP-9 at Cambridge, Massachusetts, USA*.
- Domone, P.L. (1974). "Uniaxial tensile creep and failure of concrete". In: *Magazine of Concrete Research* 26(88), pp. 144–152.
- Eguchi, Kiyoshi and Kohji Teranishi (2005). "Prediction equation of drying shrinkage of concrete based on composite model". In: *Cement and Concrete Research*.
- El Sawda, Christina et al. (2019). "Multiscale heterogeneous numerical simulation of asphalt mixture". In: *Material Design & Processing Communications*, e42.
- Fujiwara, Tadashi (2008). "Effect of aggregate on drying shrinkage of concrete". In: *Journal of Advanced Concrete Technology* 6, pp. 31–44.
- Granger, L. (1996). "Comportement différé du béton dans les enceintes de centrales nucléaires. Analyse et modélisation". PhD thesis. Ecole Nationale des Ponts et Chaussées.
- Hansen, T.C. and K.E.C. Nielsen (1965). "Influence of aggregate properties on concrete shrinkage". In: *Journal of ACI* 62(7), pp. 783–794.
- Hansen, W. and A. Almudaiheem (1987). "Ultimate drying shrinkage of concrete - influence of major parameters". In: *ACI Materials Journal* 84(3), pp. 217–223.

- Haroun, Walid A. (1968). "Uniaxial Tensile Creep and Failure of Concrete". PhD thesis. University of London.
- Hashin, Z. (1983). "Analysis of composite materials". In: *J. of Applied Mechanics* 50, pp. 481–505.
- Hearn, N. (1999). "Effect of Shrinkage and Load-Induced Cracking on Water Permeability of Concrete". In: *ACI Materials Journal* 96(2), pp. 234–241.
- Hobbs, D.W. (1974). "Influence of aggregates restraint on the shrinkage of concrete". In: *ACI Journal* 30, pp. 445–450.
- Hua, C., Paul Acker, and A. Ehrlacher (1995). "Analyses and models of the autogenous shrinkage of hardening cement paste : I. Modelling at macroscopic scale". In: *Cement and Concrete Research* 25(7), pp. 1457–1468.
- Hubert, F.-X. (2004). "Contribution À l'étude du comportement mécanique des ouvrages en béton avec prise en compte des effets de la dessiccation". PhD thesis. Université Lille 1.
- Jensen, O.M. and P.F. Hansen (2001). "Autogenous deformation and RH-change in perspective". In: *Cement and Concrete Research* 31(12), pp. 1859–1865.
- Larive, Catherine (1997). "Apports combinés de l'expérimentation et de la modélisation à la compréhension de l'alcali-réaction et de ses effets mécaniques". PhD thesis. Ecole Nationale des Ponts et Chaussées.
- Le Roy, Robert (1995). "Déformations instantanées et différées des bétons à hautes performances". PhD thesis. École Nationale des Ponts et Chaussées.
- Lydon, F.D. (1995). "Effect of coarse aggregate and water/cement ratio on intrinsic permeability of concrete subjected to drying". In: *Cement and Concrete Research* 25(8), pp. 1737–1746.
- Makani, Abdelkadir (2011). "Influence de la nature minéralogique des granulats sur le comportement mécanique différé des bétons". PhD thesis. Université de Toulouse - INSA de Toulouse.
- Maruyama, Ipppei, Hiroshi Sasano, and Mao Lin (2016). "Impact of aggregate properties on the development of shrinkage-induced cracking in concrete under restraint conditions". In: *Cement and Concrete Research* 85, pp. 82–101.
- Mills, R.H. (1960). "Strength-maturity relationship for concrete which is allowed to dry". In: *In RILEM international symposium on concrete and reinforced concrete in hot countries, Haifa*.
- Montlous-Bonnaire, J.P., J. Verdier, and B. Perrin (2004). "Prediction of the relative permeability to gas flow of cement-based materials". In: *Cement and Concrete Research* 34, pp. 737–744.
- Neville, A. (2000). *Propriétés des bétons*.
- Okajima, T., T. Ishikawa, and K. Ichise (1980). "Moisture effect on the mechanical properties of cement mortar". In: *Transactions of the Japan Concrete Institute* 2, pp. 125–132.
- Picandet, V. (2002). "Influence d'un endommagement mécanique sur la perméabilité et sur la diffusivité hydrique des bétons". PhD thesis. Université de Nantes.
- Pickett, Gerald (1942). "The effect of change in moisture-content on the creep of concrete under a sustained load". In: *ACI Journal Proceedings* 38.
- (1956). "Effect of aggregate on shrinkage of concrete and a hypothesis concerning shrinkage". In: *Journal of ACI* 27(5), pp. 581–590.
- Pihlajavaara, S. (1974). "A review of some of the main results of a research on the ageing phenomena of concrete : Effect of moisture conditions on strength, shrinkage and creep of mature concrete". In: *Cement and Concrete Research* 4(5), pp. 761–771.

- Popovics, S. (1986). "Effect of curing method and final moisture condition on compressive strength of concrete". In: *In Journal Proceedings* 83, pp. 650–657.
- Powers, T.C. (1968). "The thermodynamics of volume change and creep". In: *Materials and Structures* 1, pp. 487–507.
- Rossi, Pierre et al. (1993). "Utilisation de la technique d'auscultation par émission acoustique pour étudier le fluage propre du béton". In: *Bulletin des Laboratoires des Ponts et Chaussées* 186, pp. 88–92.
- Rougelot, Thomas (2008). "Étude expérimentale multi-échelles des couplages hydriques, mécaniques et chimiques dans les matériaux cimentaires". PhD thesis. Université des Sciences et Technologies de Lille.
- Samaha, H.R. and K.C. Hover (1992). "Influence of microcracking on the mass transport properties of concrete". In: *ACI Materials Journal* 89(4), pp. 416–424.
- Samouh, H., E. Roziere, and A. Loukili (2012). "Interpretation des mesures du retrait de dessiccation des bétons autoplaçants (In French)". In: *Cement and Concrete Research*.
- Sanjuan, M.A. and R. Munoz-Martialay (1996). "Oven-drying as a preconditioning method for air permeability test on concrete". In: *Materials Letters* 27(4-5), pp. 263–268.
- Soroka, Itzhak (1979). *Portland Cement Paste and Concrete*. Macmillan Education UK.
- Torrenti, Jean-Michel (1987). "Comportement multiaxial du béton : aspects expérimentaux et modélisation". PhD thesis. Ecole Nationale des Ponts et Chaussées.
- Ulm, Franz-Joseph and Paul Acker (1998). "Le point sur le fluage et la recouvrance des bétons." In: *Bulletin des Laboratoires des Ponts et Chaussées* Spécial XX, pp. 73–82.
- Ulm, Franz-Joseph, Fabrice Le Maou, and Claude Boulay (1999). "Creep and shrinkage coupling: new review of some evidence". In: *Revue Française de Génie Civil* 3, pp. 21–37.
- Wittmann, F. (1968). "Surface tension shrinkage and strength of hardened cement paste". In: *Materials and Structures* 1(6), pp. 547–552.
- Wittmann, Folker H (1982). *Creep and Shrinkage in concrete Structures*. Creep and shrinkage mechanisms. Wiley-Interscience.
- Wong, H.S. et al. (2009). "Influence of the interfacial transition zone and microcracking on the diffusivity, permeability and sorptivity of cement-based materials after drying". In: *Magazine of Concrete Research* 61(8), pp. 571–589.
- Xi, Yunping and Hamlin.M. Jennings (1997). "Shrinkage of cement paste and concrete modelled by a multiscale effective homogeneous theory". In: *Materials and Structures* 30, pp. 329–339.
- Yurtdas, Ismail (2003). "Couplage comportement mécanique et dessiccation des matériaux matrices cimentaires : étude expérimentale sur mortier". PhD thesis. Université des sciences et des technologies de Lille et l'École Centrale de Lille.
- Yurtdas, Ismail et al. (2006). "Influences of water by cement ratio on mechanical properties of mortars submitted to drying". In: *Cement and Concrete Research* 36(7), pp. 1286–1293.

Part III

Effects of aggregates and preservation conditions on delayed ettringite formation

Chapter 5

State of the art : Delayed Ettringite Formation

Contents

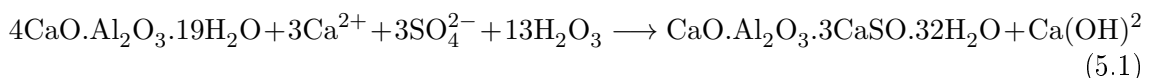
5.1 Ettringite, what is it ?	91
5.1.1 Definition	91
5.1.2 Types of ettringite	92
5.1.3 Ettringite stability	92
5.2 Focus on delayed ettringite	93
5.2.1 Formation mechanisms	93
5.2.2 Expansion mechanisms	94
5.3 Influential parameters of delayed ettringite formation	96
5.3.1 Thermal history	96
5.3.2 Concrete composition	98
5.3.3 Environmental conditions	103
5.4 Effect of DEF on concrete structures	105
5.4.1 Effect on mechanical properties	105
5.4.2 Effect on transfer properties	106
5.5 Conclusions and definition of the experimental campaign conditions	107

The Delayed Ettringite Formation (or DEF) is an endogenous pathology that affects certain concrete structures. This pathology is caused by the late precipitation of ettringite, a normal product of cement hydration, under several conditions that will be detailed in this chapter.

5.1 Ettringite, what is it ?

5.1.1 Definition

Ettringite, or calcium trisulfoaluminate, is a white mineral crystal that can be found in concrete. Its formation is due to the reaction of sulfates with calcium aluminates and water, according this chemical reaction :



Three types of ettringite can be found in concrete, simultaneously or not. Their types depend on the time of formation in the life of the concrete and on the formation mechanisms. Moreover, they are not all at the origin of an expansion phenomenon.

5.1.2 Types of ettringite

Primary or premature ettringite Its formation occurs during cement hydration and is the result of the reaction between gypsum with tricalcium aluminates. It precipitates in the interstitial solution in the form of needles. It participates in the setting and hardening of the concrete and contributes to the cohesion of the cement paste at a young age. The maximum amount of primary ettringite is generally formed after 24 hours.

Secondary or late ettringite it corresponds to an ettringite which crystallizes in hardened concrete, due to water circulation in concrete (dissolution/recrystallisation phenomenon) and external or internal sulphate sources. In the first case, it is formed by dissolution then recrystallisation of the pre-existing ettringite, in the form of needles, in the free spaces of the concrete (pores, cracks, ITZ) and generally does not have an expansive character. However secondary ettringite formation following an external or internal supply of sulphates is likely to generate internal swellings mainly attributed to crystallization pressures. This pathological ettringite crystallizes in a massive and compressed form.

Delayed ettringite This ettringite differs from the secondary ettringite essentially by the origin of the sulphate ions necessary for its formation. It results from a set of concomitant conditions, and complex processes following an increase in temperature at a young age (such as in massive structures). Indeed, in case of important production of heat during cement hydration or due to the thermal treatment underwent by pre-cast parts, primary ettringite is not stable and is either prevented from forming or is dissolved in the interstitial water and in the inter-sheet porosity of the C-S-H, becoming an internal source of sulphate ions. Subsequently, after cooling of the hardened concrete, and in a humid environment, ettringite crystals can form in the voids of the concrete, and are likely to cause swelling pressures leading to expansion. Delayed ettringite can be found in its three forms: needles, massive or compressed.

Figure 5.1 shows the different forms of ettringite in concrete: in fonction of the available space for the formation of ettringite, and also the amount crystallised, it can be found as shaped in needles (3) or compressed, sometimes similar to a gel.

5.1.3 Ettringite stability

It is difficult to fully study the the chemical system involved in the hydration of a Portland klinker cement, thus model environments are often studied to evaluate the thermodynamic stability of ettringite. We are taking a particular interest in the system developed by [Damidot and Glasser 1993] and [Loic Divet 2001]: $\text{CaO-Al}_2\text{O}_3\text{-CaSO}_4\text{-H}_2\text{O}$. Divet used a graphical representation to show the stability range of this system and influential parameters of this stability: temperature, alkaline concentration and CO_2 dissolution. Figure 5.2 corresponds to a simplified diagram of $\text{CaO-Al}_2\text{O}_3\text{-CaSO}_4\text{-H}_2\text{O}$ stability evolution at 25, 50 and 80°.

In Figure 5.2a, it can be seen that ettringite is a stable mineral for a large range of sulphate concentrations in cement paste at room temperature (25°C). However, at 50°C,

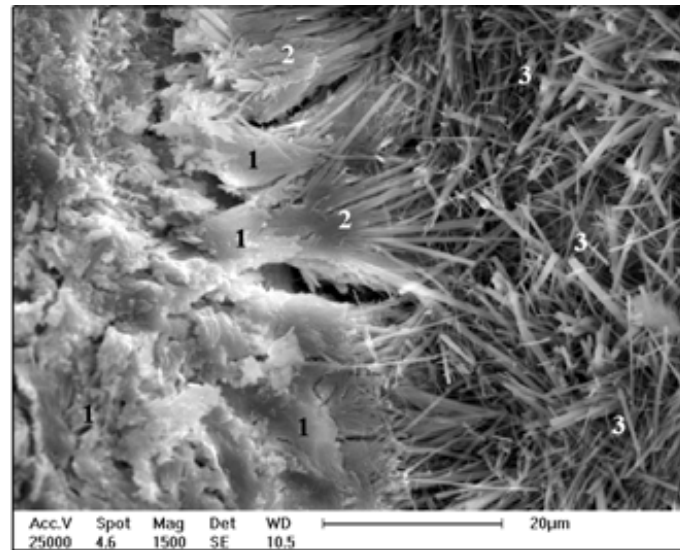


Figure 5.1 – Different kind of ettringite observations: 1 corresponds to compressed ettringite, 3 to free ettringite shaped in the form of needles, 2 is a intermediary state. [Loïc Divet 2001]

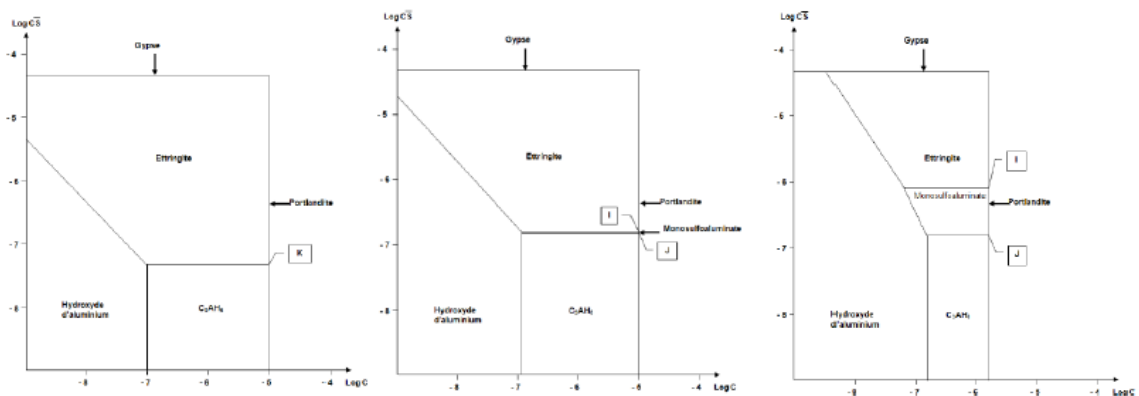


Figure 5.2 – Ettringite stability at 25, 50 and 80°C [Loïc Divet 2001]

portlandite solubility diminution leads to the appearance of mono-supho-aluminate of hydrated calcium as a stable phase. The increase of temperature to 80°C causes the extension of the mono-supho-aluminate of hydrated calcium stability domain.

Several types of ettringites can be encountered when studying concrete, however they don't have the same formation and progression mechanisms, and most particularly, they are not all associated with material damages. A focus will be made now on the latest type of ettringite: delayed ettringite. Its formation mechanisms will be detailed, along with the parameters influencing its development and the degradations mechanisms of concrete associated.

5.2 Focus on delayed ettringite

5.2.1 Formation mechanisms

There are two types of "sulfatic" attacks of the concrete: the one where the chemical reaction is supplied with external source of sulphate ions, which leads to a degradation of the material from the external face toward the core of the samples; the second one is based on the same chemical reactions but they are completely independent from external inflows of products, especially sulphates ions. This latest pathology, known as delayed ettringite formation or DEF, affects all the material, regardless of its location in the sample. [Loic Divet 2001] This pathology was encountered in massive or pre-cast concrete structure elements in which the temperature during cement hardening can reach 65°C or above. More over several studies have shown that concrete composition has a great impact on DEF and that some kinds of formulas, due to the composition of cement or to the mineral composition of aggregates, kept in humid environments present degradations comparable to the one of ASR, i.e. swelling and macroscopic cracking. This is due to the stability, or more precisely the instability, of ettringite crystals generated by the increase of temperature mentioned in Section 5.1.3. It was seen that above 60°C, ettringite decomposes and SO₄²⁻ ions, among others, are dissolved in CSH interstitial water. When concrete cools back down to room temperature and in presence of very high relative humidity, an expansive ettringite forms in the hardened cement paste and generates swellings and cracking.

It is important to highlight that those phenomena and chemical reactions takes to several years to emerge, and usually, once a structure is diagnosed with this pathology, the only possible action is the slowing down of the damaging. That is why it is essential to fully understand all the mechanisms at stakes here, and the different threshold values that needed to be respected to avoid the formation of delayed ettringite. This is what we are going to focus on in the next sections of the bibliographic study.

5.2.2 Expansion mechanisms

Microscopic scale

Water adsorption by colloidal ettringite This theory was presented by [P. Mehta 1973]. It supposes that, in presence of portlandite, colloidal ettringite is formed. As it is negatively charged and its molecules have an important specific surface, polarised water molecule are attracted and surround the colloidal particules, which could lead to rapid expansions.

Electric double layers phenomenon This theory is based on the repulsion phenomenon generated by the electric double layer was put forward by Li et al. [Li, Le Bescop, and Moranville 1996]. Colloidal ettringite, negatively charged, fixes alkaline ions (Na⁺, K⁺). Due to leaching, alkaline ions are released to exterior environment and their concentrations in the colloidal ettringite drop. This reduction favours electrostatics repulsion forces over Van-Der-Walls forces, and as a consequence, the distance between ettringite particles increases which leads to a global expansion.

Mesosopic scale

Uniform expansion of cement paste This theory was presented by Scrivner et al 1993 and [H. F. W. Taylor, Famy, and Scrivener 2001] and then [Famy 1999]. It supposes that when concrete is exposed to a heating cure, a big quantity of mono-sulpho-aluminate of

hydrated calcium is concentrated in CSH. Moreover, as presented by Barabrulo [Remi Barabrulo 2002], CSH sheets tend to absorb sulphate and aluminate ions. As a consequence, at the end of the heating process, CSH present a high concentration of SO_3 and Al_2O_3 . After cooling, and with a sufficient water supply, sulphate ions are freed in interstitial water and trigger ettringite crystallisation. However, CSH are the majority hydrates in the cementitious matrix, and have a homogeneous distribution, which leads to a homogeneous expansion of the cement paste, generating cracks in the cement paste and in the ITZs. This theory has been highly criticised, particularly by Diamond [S. Diamond 2004], who deplores the lack of consideration of the effect of aggregates and their mineralogy in the degradation mechanism.

Expansion in ITZs In 1999, Yang and al [Yang et al. 1999]. are the first to take an interest in the impact of the aggregate mineralogical nature on DEF, and they observed different amount of degradation in ITZ if the concrete is made with siliceous or calcareous aggregates. Based on these results, Diamond link the type of aggregates to the triggering of significant swellings. This theory supposes that ettringite crystallises in the large voids of the concrete (cracks, large porosity) and the growth of the crystal could generate pressures which could lead to swellings. The use of Portland cements and the presence of C3A in sufficient quantities, once in contact with sulphates, produce an extreme saturation leading to the rapid crystallisation of ettringite. The crystallisation pressure is could be important enough to initialise cracks.

Several authors believe that these two latest mechanisms of expansion are not necessarily incompatible.

Macroscopic scale : mechanisms as seen by Brunetaud [Xavier Brunetaud 2005]

In his thesis, Brunetaud [Xavier Brunetaud 2005] put forward a scenario on the global mechanism of DEF degradation. It combines two main mechanisms presented above (i.e. mesoscopic scale mechanisms). Four distinct phases describe the progression of phenomena until concrete macroscopic degradation, a diagram for his thesis is presented in Figure 5.3 and is detailed afterwards.

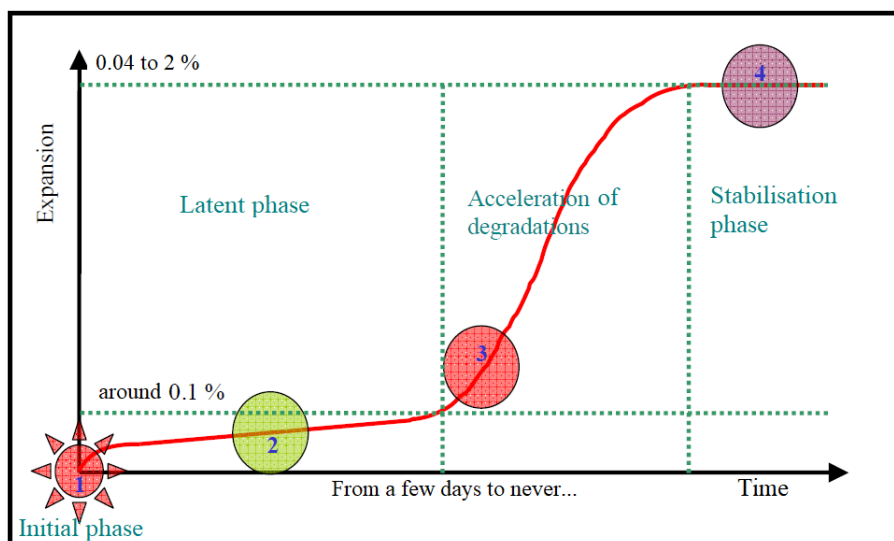


Figure 5.3 – Expansion mechanisms as put forward by Brunetaud [Xavier Brunetaud 2005]

Initial phase: Initially, this phase corresponds to the duration during which ettringite is thermodynamically unstable. The ions dissolve in interstitial solution, or integrated in the C-S-H, or can also participate in the formation of hydrated calcium monosulfoaluminate. The length of this initial phase depends essentially on the alkali content and the thermal history, as developed in Section 5.3. The phase stops at the end of the heating treatment.

Latent phase: The latent phase starts as soon as the material returns to room temperature. It is an incubation period of the DEF. At first sight, nothing seems to happen as the swelling is very weak and no major modification of the modulus of elasticity and the density of the material is observed. Nevertheless, a slight slow swelling can be noticed and is mostly attributed to the mechanisms of homogeneous swelling of the cement paste. Brunetaud estimates that ettringite could be located in the C-S-H of capillary porosity as Taylor proposes ([Xavier Brunetaud 2005; H. F. W. Taylor, Famy, and Scrivener 2001]). Cracking in the ITZs marks the end of the latency period and results in a first drop in the dynamic modulus.

Acceleration of degradations phase: Once incubation is complete, material degradation can occur as the first cracks in the ITZs have altered the distribution of stress. The ettringite can then form in the created voids. The ettringite formed homogeneously in the paste passes back into solution in order to migrate towards zones more favourable to their precipitation: the new free porosity in particular the interface paste/granulates. This phenomenon is known as Ostwald ripening. The author concludes that the ettringite which develops at the paste/aggregates interfaces is the source of the acceleration of the degradations and thus of the concrete damage.

Stabilisation phase: The deceleration of the swelling introduces the last phase called the stabilization phase. This phase occurs either because the material finally manages to resist swelling, or because the C-S-H have completely emptied their sulphate ion reserve. However, the expansion continues to progress slowly so the Ostwald ripening continues without the addition of C-S-H ions.

Brunetaud concludes and synthesizes the degradation mechanism he proposes as follows: the significant expansions of the materials affected by RSI are due to the localized crystalline pressure of ettringite, itself being the consequence of a prior uniform expansion of the cement paste [Xavier Brunetaud 2005].

In this section, the formation and progression mechanisms of DEF were presented. It pointed out that this pathology can be found only if a particular set of parameters and conditions are met: a overheating of the concrete, the concrete composition and very humid environment. On the matter of expansion mechanisms, previous results from the literature show that DEF interfere with mechanisms at different scales: microscopic, mesoscopic and macroscopic. The progression is described in four phases, as Brunetaud presented it: initial, latent, acceleration of degradation and stabilisation. The duration of the different phases depends on concrete used.

5.3 Influential parameters of delayed ettringite formation

5.3.1 Thermal history

Heating cure at young age

As it was mentioned before, the thermal history underwent by a concrete sample is a determining factor to DEF. As a matter of fact, most of the structures that have been diagnosed with internal sulfatic reaction are massive structures or precast parts of concrete structures. The initial heating temperature is a necessary condition for the development of delayed ettringite in concrete. Cement hydration is an exothermic reaction that can lead to a significant rise in temperature in the case of massive concrete structure parts. Indeed, the release of heat due to the hydration reaction combined with unfavourable geometry of the part to evacuate the heat leads to prolonged heating of the material. In the case of precast concrete samples, a heating treatment is performed to ensure a certain strength to the material at early age, in order to remove quickly the casting moulds. Several studies have been conducted to know the influence of the thermal cure on the DEF. The heat treatment is characterised by two key parameters :

Temperature level: it is the maximum temperature reached during the heating treatment. In general, the rise in maximum temperature leads to faster kinetics and more important final rates [R. Martin et al. 2012]. Bagdadi ([Bagdadi 2008]) has led an experimental campaign, displayed Figure 5.4 where he compared the expansions of concrete submitted to different heating treatment. Many studies have focused on finding a threshold cure temperature at which a risk of DEF is expected. The hydration of a cementitious material at a temperature above 70°C could be the cause of DEF according to some authors [Odler and Chen 1995] [Fu 1996] [C. Lawrence 1999] [Yang et al. 1999]. However, studies show swelling of DEF in concrete at a cure temperature value around 65°C [Xavier Brunetaud 2005] and even 60°C [Sahu and Thaulow 2004]. Finally, the authors conclude that the DEF may appear for temperatures below 70°C under certain favourable conditions (high contents alkali, sulphate and C3S cement, high cement fineness, concrete with a high cement content and low E/C ratio). However, it was shown that this threshold temperature is dependent on the duration of the heating phase [A. Pavoine, X. Brunetaud, and L. Divet 2012].

Heating time: it is the time during which the maximum temperature is maintained. Several findings available in the literature highlight the important impact of the duration of heating on the DEF, among others [Xavier Brunetaud 2005; Bagdadi 2008; Kchakech 2015; Fu, Ding, and J. Beaudoin 1997; R. Barbarulo et al. 2005]. They all agree that at first, an increase of heating time tends to increase kinetics and intensity of DEF expansion. However, in second time, they observed a pessimum effect : there is a threshold value of temperature beyond which the swelling decreases ([Xavier Brunetaud 2005]). The work of Brunetaud ([Xavier Brunetaud 2005]), shows that a concrete can have strong swellings for a temperature rise of 85C during 48 hours while no swelling is observed for a 2 hours cure at 80C and 10 days at 85C. The warm-up time therefore has an influence on the DEF training process. Similarly during this work, Barbarulo ([R. Barbarulo et al. 2005]) concludes, without being able to explain the phenomenon, that expansion can be delayed or removed by a long cure at high temperature during hydration. [Bagdadi 2008] showed in Figure 5.4, with a heating cure set to 80°C, that a 3-days cure led to higher final expansion rates than for a 1-day cure, or a 5-days one. He also highlighted cure duration also impact the

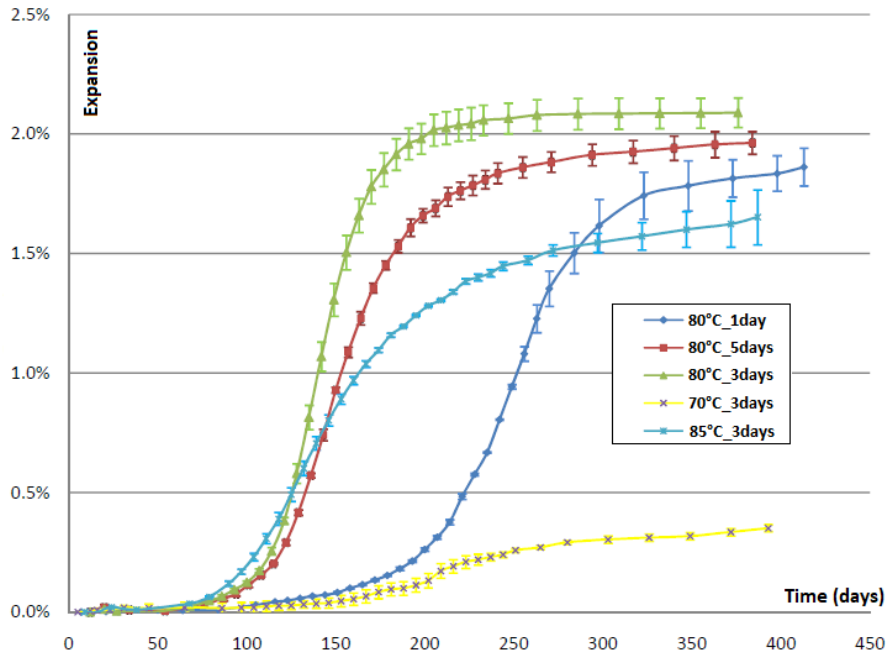


Figure 5.4 – Effect of temperature level on DEF expansions. [Bagdadi 2008]

reaction kinetics as the 1-day cure shows a delay compared to the two other curves. Based on these observations Kchakech ([Kchakech 2015]), set up a global campaign with durations between 1 and 14 days, expansion curves are displayed Figure 5.5. He also tested these heating times and different types of cement, and converged with the other authors : there is not one threshold temperature but rather a specific threshold temperature for each study depending on cement composition and the chosen cure maximum temperature.

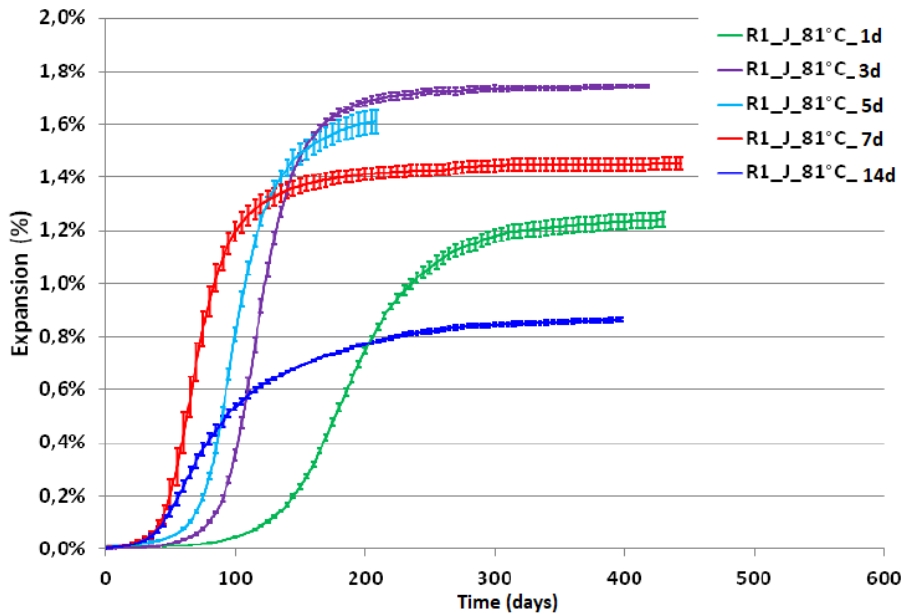


Figure 5.5 – Influence of the thermal cure duration on expansions induced by DEF.[Kchakech 2015]

Delayed or second heating cure

[Remi Barbarulo 2002; R.-P. Martin 2010; Xavier Brunetaud 2005; Kchakech 2015] have shown through their work that expansions due to DEF could be triggered in concrete by a second heating cure or by a delayed one. However, these expansions have different effect on the delayed behaviour of the material. First they tend to present a final expansion rate inferior to the one measured after a first early heating, or to the equivalent heating applied at young age, as observed by Barbarulo (Figure 5.7, [Remi Barbarulo 2002]) and more recently, by Kchakech [Kchakech 2015], as displayed Figure 5.6.

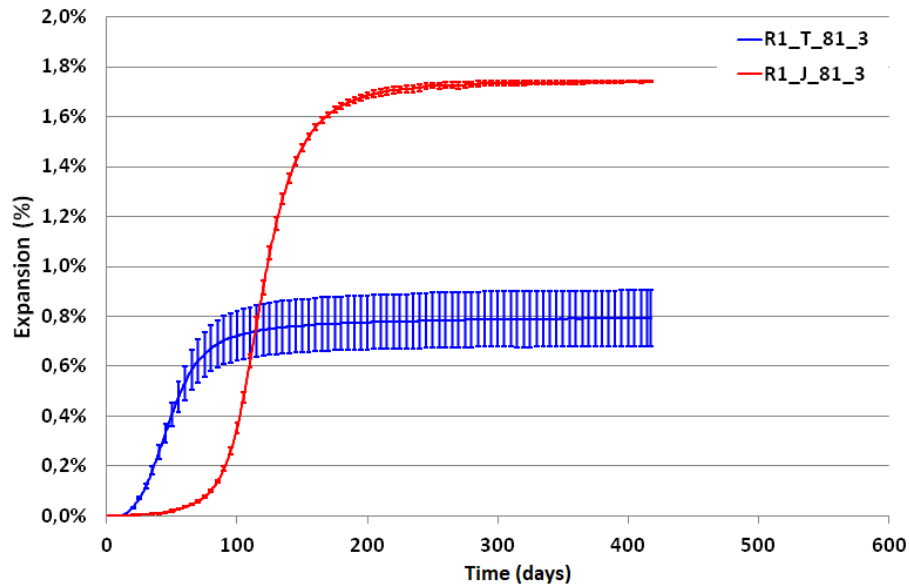


Figure 5.6 – Comparison between expansion generated in the same concrete by heating treatment at young age (in red) and the one generated by delayed heating cure (in blue), at 81C during 3 days.[Kchakech 2015]

Then, in the case of delayed heating, whether there was a first heating cure or not, the latency phase tend to be very reduced or even not existing.

5.3.2 Concrete composition

Cement composition

Aluminate and sulphate concentrations The swellings caused by the delayed formation of ettringite are strongly related to the content of sulphates and aluminates in cement. Some authors link the assessment of concrete's expansion potential to the $\text{SO}_3/\text{Al}_2\text{O}_3$ ratio of cement. Day ([R.L. Day 1992]) shows that under certain heat treatments and exposure conditions, a $\text{SO}_3/\text{Al}_2\text{O}_3$ ratio greater than 0.7 can lead to delayed ettringite formation. This is confirmed by Zhang([Zhang, J. Olek, and S. Diamond 2002]) who showed using the results of studies by [Fu, Ding, and J. Beaudoin 1997] and [Famy 1999], that the critical threshold of the $\text{SO}_3/\text{Al}_2\text{O}_3$ ratio is 0.8 and that the expansion achieved seems to pass through a maximum for a value of this ratio equal to 1.1%. Other authors use the ratio $(\text{SO}_3)_2/\text{Al}_2\text{O}_3$ to determine the amplitude of expansion. According to Heinz et al ([Heinz, Kalde, et al. 1999]), cements with a ratio $(\text{SO}_3)_2/\text{Al}_2\text{O}_3$ of less than 2 are not subject to delayed ettringite formation, taking into account the amount of alumina contained only in tricalcium aluminate. On the other hand, Odler and Chen ([Odler and Chen 1995]) find

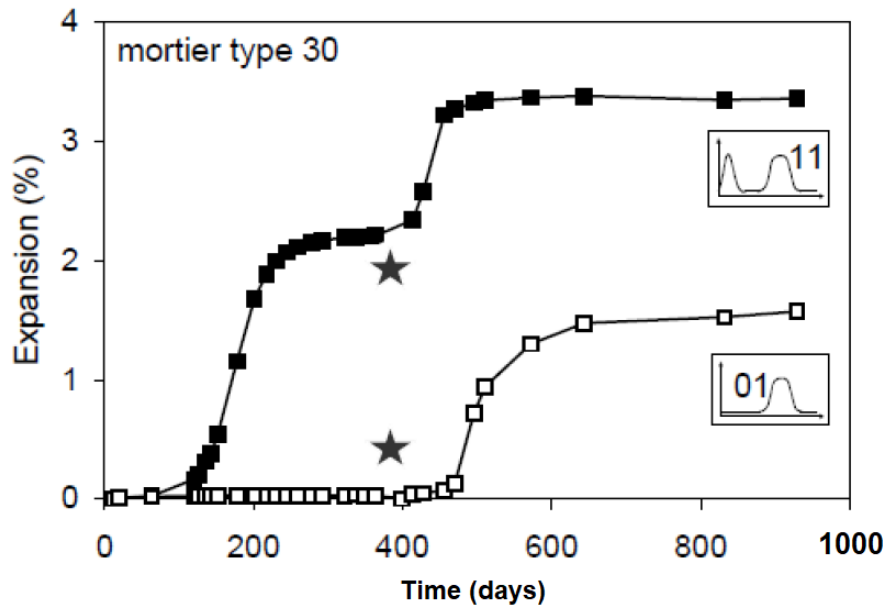


Figure 5.7 – Expansion of a mortar submitted to different kind of thermal treatment (indicated next to each curves) - Delayed treatment conditions: 85C during one month ([Remi Barbarulo 2002])

that these ratios do not have a significant impact on the expansion of the material, and they essentially find an increase in swelling in relation to the increase in concentrations of both aluminates and cement sulfates. Indeed, they consider that most of the expansion cases observed concern cements rich in C3A (above 10%) and SO₃ (above 3%). Finally, Leklou ([Leklou 2008]) shows that C3A content does not seem to be a limiting factor and that DEF can, under certain conditions, develop in cements with a low C3A content.

Alkaline concentration Alkaline agents (mainly Na⁺ and K⁺) have a very important role in the development of swelling due to DEF ([M.C., K.L., and S. 1995]). Their contents considerably modify the pH of the interstitial solution, thus influencing the stability of ettringite, as seen in Figure 5.2. This effect is accentuated by the rise in temperature. They can come either from cement (main source), additives or adjuvants, or even from certain reactive aggregates. Their presence is expressed by the equivalent alkaline mass content :

$$\text{Na}_2\text{O}_{\text{eq}} = \text{Na}_2\text{O} + 0.658\text{K}_2\text{O}. \quad (5.2)$$

The use of cements containing high alkaline contents, combined with the effect of temperature, leads to a delay in the formation of primary ettringite and an increase in its solubility (According to several authors[[Heinz, Kalde, et al. 1999], [Hime and Marusin 1999],[Loic Divet 2001]). The increase in final expansion values with alkali content was also confirmed by Kelham's work ([Kelham 1996]) on cement paste to which he adds KOH and K₂SO₄, and by Escadeillas' work ([Escadeillas et al. 2007]) on Na₂SO₄-doped mortar samples. The assumed mechanism is that during cement hydration, the presence of alkalis promotes the absorption process of sulphate ions by C-S-H [Loic Divet 2001].

According to Brunetaud ([Xavier Brunetaud 2005]), alkalis act in the same way as the temperature or duration of the heating, but in a less abrupt way. The addition of KOH

to the mixing water is of less importance than a rise in the heating temperature from 65 to 85°C for example, but is still capable of triggering a very significant reaction. Therefore, these parameters seem to be essential in the development of delayed ettringitis and in the intensity of swelling. However, there are no critical levels of alkalis, sulphates and aluminates that are perfectly established and validated.

In addition, some studies have found a link between DEF and alkali leaching, and have shown that the more favourable the conditions are for rapid alkali leaching, the earlier expansions start.

Mineral additions Several investigations were carried out on the influence of mineral additions on the delayed formation of ettringite through the years. Four types of additions were studied : fly ash, blast furnace slag, silica fume and metakaolin. Based on the work of [Kelham 1996],[C. Lawrence 1999; Ramlochan et al. 2003] and [Santos Silva et al. 2006], show a decrease or even a suppression of swelling when adding the various additions

It appears that the replacement rate (% by mass) at which the reduction in expansion is effective is:

- for fly ash, the rate depends on its composition,
- 8-10% for metakaolin,
- 25-40% for blast furnace slag,
- 8-10% for silica fume,

These additions often have the effect of reducing the porosity of the cement paste, thus limiting the possibilities of ionic exchanges favourable to the precipitation of ettringite. In addition, the addition of mineral additions leads to a decrease in the alkalinity of the concrete pore solution due to the pozzolanic reaction and a reduction in the portlandite content.

Cement finesse Several studies have shown a relationship between the specific surface area of the cement and the delayed formation of ettringite [Kelham 1996], [Heinz, Kalde, et al. 1999] and [Fu, Ding, and J. Beaudoin 1997]. They show that DEF-induced expansions would increase with the reactivity of the binder. According to Tosun ([Tosun 2006]), it is due to a modification of cement hydration kinetics. Also, this may be related to the rise in temperature during hydration of a powder whose reactivity is increased by finer grinding [Alexandre Pavoine 2003].

Aggregates parameters

Mineralogical nature Several authors have noted that the mineralogical nature of the aggregates used in the concrete mix impacts significantly the delayed ettringite formation. They all seem to agree that using siliceous aggregates (as quartz, among others) leads to important DEF phenomenon, with significant formation kinetics and final rate of expansion. Most of the other mineralogy induce slower and less important swellings, as seen in Figure 5.8. The comparison is often made with calcareous aggregates, which use tends to slowdown the reaction. The differences of behaviour is usually attributed to the different nature of ITZ in the material. Indeed, as detailed in the introduction chapter, calcareous aggregates tend to chemically react with cement paste, whereas siliceous aggregates do not. In addition to the formation of carbo-aluminates in the ITZ that reorganises the different

hydrates and tends to decrease the nano-porosity of the ITZ as describe in Section 1.2.2, it consumes aluminates needed in the chemical reaction that produces delayed ettringite.

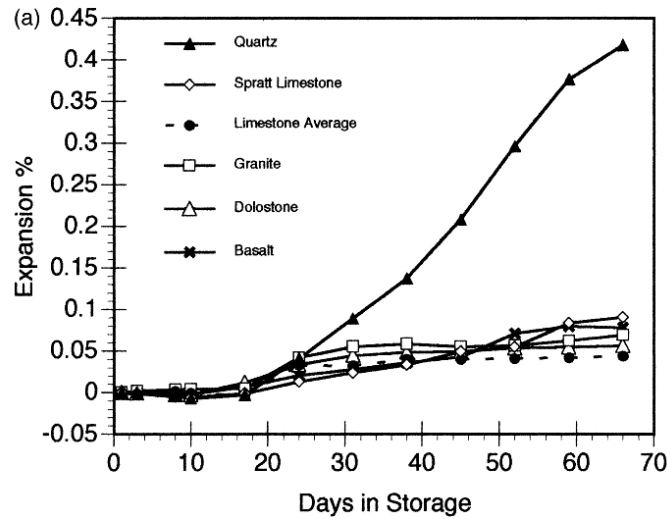


Figure 5.8 – Effect of aggregate mineralogical nature on expansion induced by DEF.

In his work, Brunetaud ([Xavier Brunetaud 2005]) also observed that the heat treatment might modify the ITZ quality, due among other things to the different dilatation coefficient of the aggregates, and he concluded that a mechanical bound between calcareous aggregates and cement paste exists, but it is not the case with siliceous aggregates. This argument could reinforce the previous observations. Indeed, the reorganisation of the ITZ due to the formation of carbo-aluminates could lead to an ITZ with better mechanical properties, which is also compatible with the reduced porosity. Finally, this difference of ITZ quality can be influential on the progression of DEF, as it will more able to endure the pressure exerted by the delayed ettringite.

Aggregate size and volume Several studies have shown that the particle size used also plays an important role in the development of swelling. The results of [Grattan-Bellew, J. J. Beaudoin, and Vallee 1998] show that mortar swelling is all the faster when the average aggregate size is small. Furthermore, these authors suggest a correlation between the specific surface of the aggregates and the expansion speed of the mortars. The expansion is proportional to the surface area of the aggregate (Figure I.12). They also note an increasing trend in the amount of ettringite detected by DRX as aggregate size decreases. Work by [Fu, Ding, and J. Beaudoin 1997] shows greater swelling when finer particles are used. On the contrary, the results of [Heinz, Kalde, et al. 1999] show that the use of very fine aggregates can lead to the suppression of swelling. These authors observe a decrease in latency time with increasing aggregate size. The most recent work on the subject was led by Al Shamaa, who showed that aggregates diameter and their substitution rates have an impact on DEF-induced expansion kinetics and amplitude. He observed the absence of significant swellings in materials formulated with small average diameter of inclusions ($20\mu\text{m}$ - $45\mu\text{m}$), whereas for larger average diameters ($510\mu\text{m}$ - $2800\mu\text{m}$) the expansions are relatively important as seen in Figure 5.9. Moreover, for the same volume rate of inclusions, the higher the average aggregate size, the faster and larger the swelling.

The effects of aggregate size are attributed by the authors to the fact that granular distribution influences material porosity in terms of size, distribution and connection. This then has an influence on the ionic exchanges necessary to meet the reagents on the one

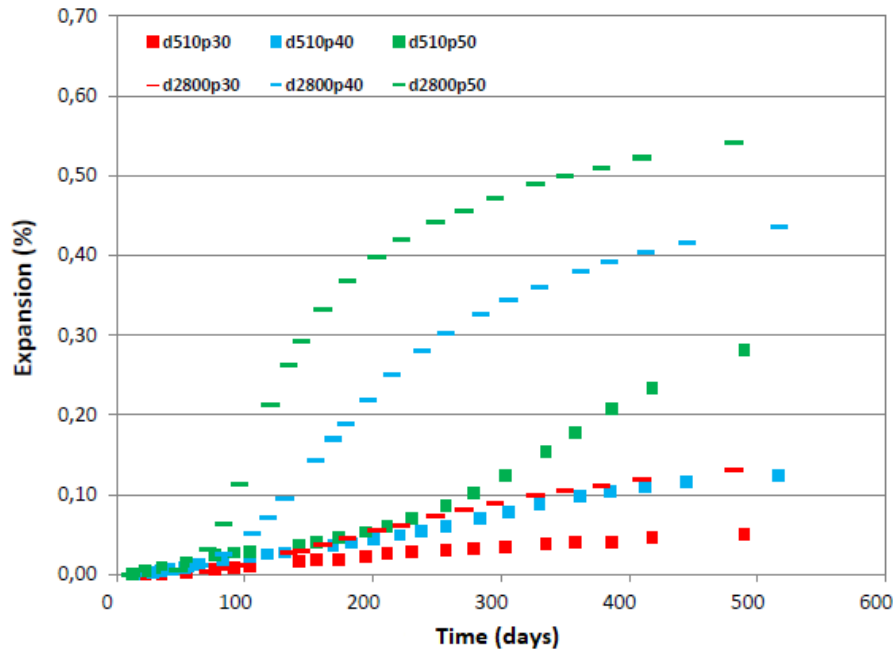


Figure 5.9 – Effect of aggregate size and volume fraction on expansion induced by DEF. *d*: diameter - *p*: volume fraction ("proportion" in French) [Mohamad Al Shamaa 2012]

hand, and on the possibility of developing crystallization pressures on the other hand, by allowing the growth of ettringite in confined spaces. According to [Heinz, Kalde, et al. 1999], an increase in aggregate size can promote the connection of porosity and thus facilitate ionic exchanges and reduce latency times. According to Fu et al. ([Fu, Ding, and J. Beaudoin 1997]); [Grattan-Bellew, J. J. Beaudoin, and Vallee 1998], reducing pore size by using finer aggregates can lead to increased swelling by promoting the appearance of higher crystallization pressures.

Water-cement ratio

Durability of concrete materials is directly linked to the water-cement ratio of the composition. The decrease of water-cement ratio induces an improvement of mechanical properties, but also a decrease of transfer properties, more especially of material porosity. This latest phenomenon leads to an important slowdown of DEF induced expansions as transfer are limited. However it also leads to an increase of the final expansion rate. Indeed, once the DEF has started, the swellings are locally more important as there is less or no voids in the concrete to play the role of expansion tank. The more DEF progresses, the more these local expansions become a global one ([Xavier Brunetaud 2005; Leklou 2008; Petrov 2003]). [Xavier Brunetaud 2005] showed the effect of water-cement ration on expansions, as presented in Figure 5.10.

5.3.3 Environmental conditions

Temperature

Preservation temperature has a significant impact on DEF. Several authors have studied the impact of this parameter and have reached the following conclusions:

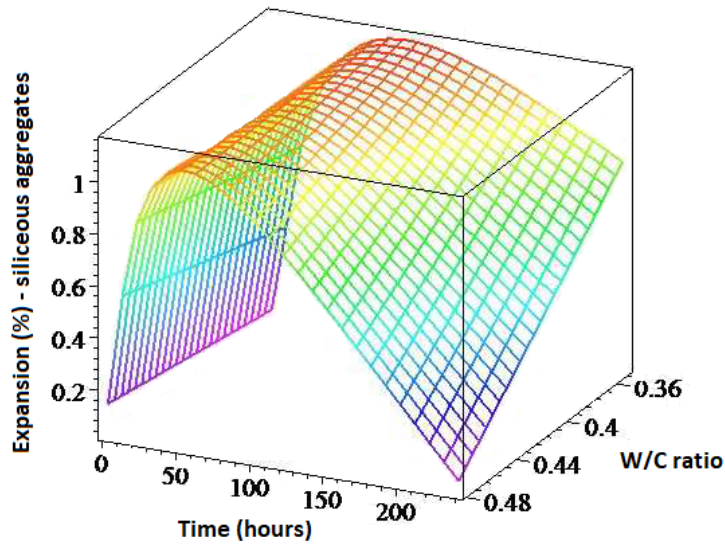


Figure 5.10 – Effect of water-cement ratio on DEF expansion [Xavier Brunetaud 2005]

- storing samples in water at 20-23°C is more favourable than to DEF evolution than in water at 38°C. [Famy et al. 2001; Alexandre Pavoine 2003]
- a preservation in a water at 40°C, or above, tends to accelerate DEF initialisation but do not change the final rates of expansion [Leklou 2008; Alexandre Pavoine 2003; Petrov 2003]

These latest affirmations were studied by [Leklou 2008], and presented in Figure 5.11. The last observation was at the origin of thermal cycles as describe in the French Norm [LCPC 66] to accelerate the formation of ettringite in the concrete and thus, allowing a visualisation of DEF consequences on the material in laboratory more quickly.

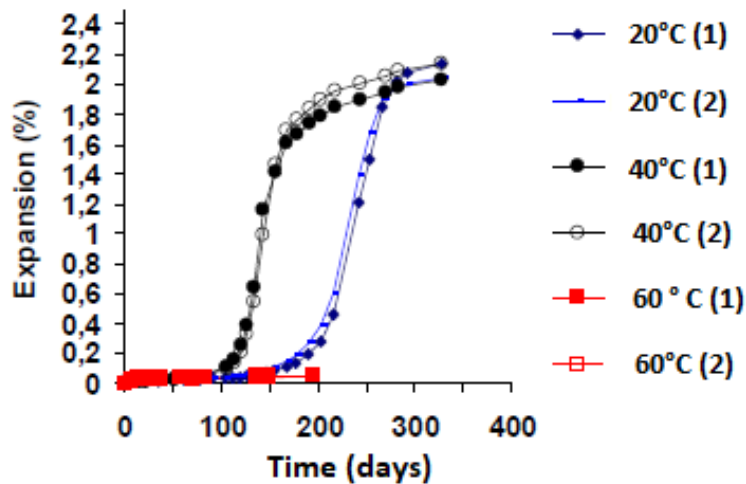


Figure 5.11 – Effect of temperature on DEF expansion [Leklou 2008]

Relative humidity

Relative humidity plays a significant role in the development of delayed ettringite, water can even be considered a key parameter because crucial roles in the ettringite formation process. First, water is a reagent necessary for the reaction as 32 moles of water are consumed to form 1 mole of ettringite. Then, water enable transfers of ionic species to ettringite crystallization sites while participating in alkali leaching which plays on the thermodynamic balance of ettringite. [Famy 1999] have shown through their experiments that alkali leaching accelerates the initialisation of the reaction, thus reducing the latent phase. They observed swellings of samples put in water and others in alkaline solution, and noticed a very important expansion on the first type of specimens, whereas the second one display expansion, but with a delay. Experiments by Thomas [Thomas et al. 2008] confirm this result: a mortar with a high alkali content and treated at 80C swells in distilled water and not in a NaOH solution. According to the author, the presence of alkalis prevents the formation of ettringite during storage. Indeed sulphates are mostly in C-S-H or participate in the formation of monosulfoaluminate and some ions are in the interstitial solution. When the concrete is stored in water, the pH gradually drops due to alkali leaching to a pH around 9-10, which favours the ettringite precipitation and triggers swelling. Finally, water is the most favourable reaction environment for DEF. Studies on the effect of water content have focused on finding a relative humidity threshold below which swelling would be inhibited. Heinz and Ludwig were the first to publish on this phenomenon and showed that no expansion was observed below 90% relative humidity after 780 days [Heinz and Ludwig 1987] but, when put back at 100% relative humidity development of expansions were observed after one year. [Graf 2007] have looked for the threshold value of relative humidity by storing samples in different humid environments from 75% to 100%, and concluded that below 92% RH, DEF is prevented. More recently, Al Shamaa [Mohamad Al Shamaa 2012] has observed a threshold of 98%R H on a similar campaign as shown in Figure 5.12. Below this relative humidity, no significant expansion was observed after 470 days of exposure. He has also proven the possibility of swelling during late humidification.[Mohamad Al Shamaa 2012; Bouzabata et al. 2012] Last but not least, according to [H. F. W. Taylor, Famy, and Scrivener 2001], samples stored in water swell faster than those stored at 100% relative humidity.

These studies emphasize that water is essential for the development of delayed ettringite, and its absence slows or even stops the chemical formation of ettringite and therefore, potential damage to structures, by preventing alkali leaching and also by creating a lack of reagent.

This section is a summary of the various influential parameters of the DEF. Three categories of parameters have been identified: those depending on the thermal history of the concrete, those related to the composition of the concrete and finally those related to environmental conditions. Our main interest is to characterise the effect of aggregates on the development of the pathology. The influential aggregate parameters are: mineralogical nature, size and volume present in the material. Aggregates do not participate in the chemical reaction leading to the appearance of delayed ettringite. On the other hand, they can play an important role in the kinetics and amplitude of the reaction.

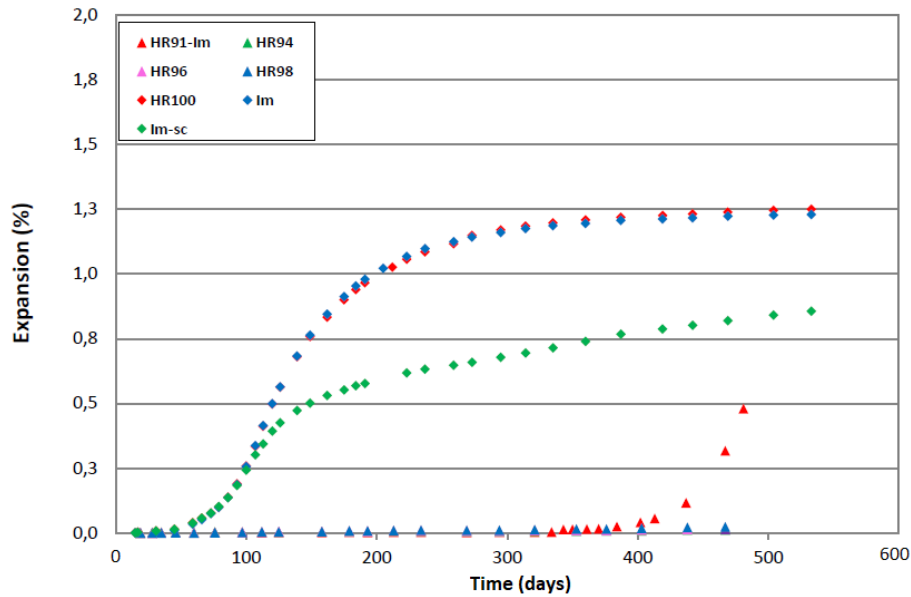


Figure 5.12 – Effect of environmental relative humidity on expansion rates [Mohamad Al Shamaa 2012]

5.4 Effect of DEF on concrete structures

5.4.1 Effect on mechanical properties

At the structural level, there are manifestations of the progression of the pathology. As we have seen previously in detail on the formation mechanisms of delayed ettringite, this results in the development of expansions leading to significant structural degradation. It is manifested by the development of a network of multi-directional cracks, located in parts of structures exposed to high humidity. An example of cracks patterns induced by DEF is presented Figure 5.13.



Figure 5.13 – Example of bridge pier presenting cracks induced by delayed ettringite formation - [Godart and L. Divet 2013]

The presence of cracks is synonymous with changes in the transfer and mechanical properties of the material. It is important to establish a characterisation of materials with DEF in order to ensure the stability of the structures and to choose the means to prevent their damage.

In particular, we would like to mention three authors who have taken an interest in this

issue. In 2003, Pavoine observed a 75% drop in compressive strength on concrete specimens with up to 1.6% expansion. Then in 2005, Brunetaud ([Xavier Brunetaud 2005]) tried to experimentally establish a relationship between the loss of compressive strength and the expansion of concrete. He concludes that for concretes with low expansion caused by DEF, there is no significant decrease in compressive strength compared to healthy control specimens. In 2012, Al Shamaa ([Mohamad Al Shamaa 2012]) does not reach the same conclusions. Indeed, he conducted several characterisation tests with several swelling milestones on the specimens. There are several conclusions that we detail below that will be supported by Figure 5.14 :

- The mechanical performance of the concrete studied suffers strong degradation despite slow kinetics, and limited expansion (less than 0.3%)
- Compressive strength and Young's modulus follow about the same evolution, i.e. a significant drop in their values to 400 days of study, then a recovery that can bring some indicators back to their initial value (in particular compressive strength). This may explain why Brunetaud observed a very limited loss at the end of expansion for concretes with low expansions.
- The dynamic module also undergoes variations of the same type but much more limited.
- the 400-day date corresponds to the end of the rapid expansion phase and the slowing down of the curve to enter the stabilization phase of the DEF.

In conclusion, the formation of delayed ettringite causes a significant drop in mechanical performance, but the mechanisms involved are not completely controlled.

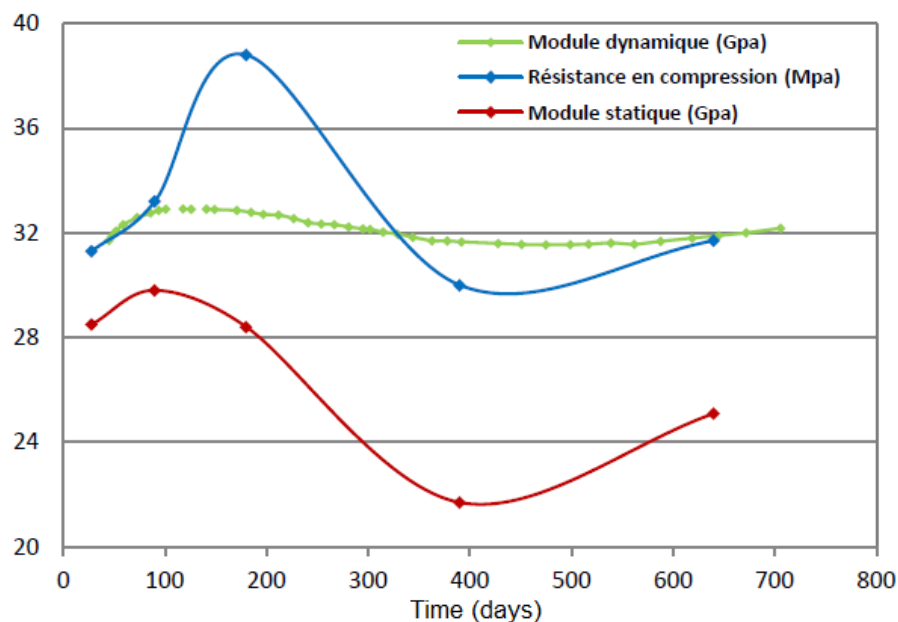
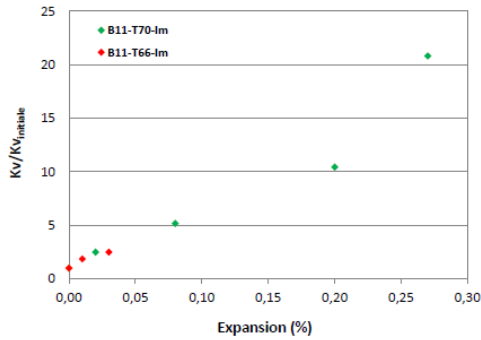


Figure 5.14 – Effects of the progression of delayed ettringite formation in concrete on its mechanical properties. Results of the assessments of compression strength (in blue), Young Modulus (in red) and dynamic modulus (in green) are presented through time. [Mohamad Al Shamaa 2012]

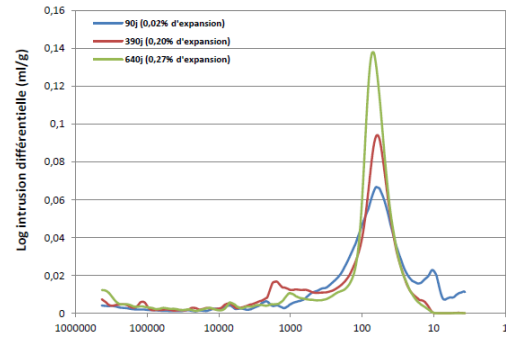
5.4.2 Effect on transfer properties

Al Shamaa ([Mohamad Al Shamaa 2012]) also undertook an evaluation of the evolution of the transfer properties with the progression of the DEF and therefore of the expansion. He was interested in several parameters: intrinsic permeability, apparent permeability, Klinkenberg effect, water accessible porosity, mercury porosity and pore distribution.

These results and conclusions are presented below, and are accompanied by the Figures 5.15a and 5.15b from his work.



(a) Evolution of intrinsic permeability with expansion from [Mohamad Al Shamaa 2012]



(b) Evolution of pores distribution with the progression of DEF, [Mohamad Al Shamaa 2012]

Figure 5.15 – Assessment of transfer properties in concrete submitted to DEF

The results show a significant increase in the intrinsic permeability of the material (x20), for apparent permeability (an order of magnitude) and for the Klinkenberg effect (x2). Al shamaa therefore concludes that the connected network is increasing as a result of the appearance of microcracking that could facilitate transfers. In addition, he shows that the pore diameter decreases, which he attributes to the precipitation of ettringite in the concrete voids, reducing the pore diameters.

On the other hand, when he looks at the porosity accessible to water and mercury, he sees that these parameters are stable despite the expansion observations. Delayed ettringite does generate the appearance of a connected porous network, but at the same time, the latter gradually fills up, making the evolution of porosity stable.

Finally, the work presented here is essential, but it remains comparative since the permeability measurements seem to be close to the observation limits of the apparatus used (CEMBUREAU). In addition, the test protocols are those of the norms NF P 18-459 and NF P 18-453, which use drying periods at high temperatures as conditioning of the specimens for the tests. Knowing that ettringite is not stable above 60C, these heat treatments may have altered the results. Since the protocols were applied to all the tests, it is nevertheless possible to attribute the variations as an effect of the DEF.

5.5 Conclusions and definition of the experimental campaign conditions

This chapter provided an overall look on the delayed ettringite formation: its initialisation, its progression mechanisms and its consequences on structures. We were able to identify several influential parameters, among them the mineralogical nature of the aggregates.

Our work aims at understanding the involvement of aggregates mineralogy in the material degradation mechanisms and in the evolution of materials properties under DEF. In order to answer this problematic, an experimental study was realised and is presented hereunder. The state of the art enabled us to set up the specific parameters of this study.

Selection of materials

- The effect of aggregates on the concrete submitted to DEF has been studied. However, authors mainly have focused their attention on the kinetics and magnitude of expansions, and not on the complete assessment on the evolution of material properties. Thanks to their work, we were able to fix the mineralogy of aggregates needed to bring out significant variations of mechanisms.

Two types of aggregates were chosen : on one hand, the aggregates of the first campaign were selected, these **aggregates are from the Boulonnais quarry**. These aggregates petrographic nature is labelled as "hard compact Visean limestone". They present a Young Modulus of 80MPa. On the other, siliceous aggregates were selected, with the condition that they needed to not be reactive in basic environments, and thus be inert toward the ASR. **Aggregates from the Palvadeau quarry** were chosen. Their petrographic nature is labelled as "quartz" and they present a Young Modulus of 70 – 80MPa.

- As our problematics are centered on the effect of aggregates, the cement chosen is the same than in the study of aggregates restraint and drying, presented in Part 2. CEM II/A-LL-42:5-R cement is used, in water-cement ratio of 0.57. Moreover, it corresponds to the cement used by [Mohamad Al Shamaa 2012] in one of his study, meaning that we are sure that DEF will occur and also that we have reference results to compare our own results.

Selection of experimental conditions

- In order to observe the development of DEF within the time of the thesis, it was decided to put the samples in the best conditions possible to favour the progression of the pathology. The samples are submitted to a thermal treatment of 80C during 3 days that increases the DEF kinetics.
- Moreover, samples are conditioned in water through the campaign, in order to create a stable and very humid environment (100%RH).
- As it was seen in the literature on delayed ettringite formation, this pathology is associated with an important cracking phenomenon. In all the experimental work carried out so far, the authors focus on determining the influential parameters and the mechanisms of only the DEF. However, in the reality, structures can be submitted to hydric variations (for example a dam with an adjustable level of water stocked), that could generate a desiccation phenomenon and generate surface and internal

cracks. In our study, we are taking an interest in this coupling by following samples submitted to drying and soaking cycles through the campaign. These samples are made with same components than the reference mix, with calcareous aggregates, to easy the interpretation of results.

Selection of tests to evaluate materials delayed deformations and properties

- In accordance with the different authors of the literature, to follow the evolution of DEF, three parameters are monitored through out the duration of the campaign: expansion rate, mass variation and dynamic modulus.
- In order to assess the evolution of the properties, each type of samples is tested at three distinct moments of the procedure. First at the end of the thermal treatment, to characterise the influence of this cure on properties, at the inflexion point of the expansion curve and after reaching the stabilisation phase, based on the observations of expansions. The evolution of mechanical properties is evaluated by subjecting all compositions to three-point flexural tests and to compressive tests. The evolution of transfer properties is followed by measuring the porosity accessible to water. For each type of tests, and for the first and last characterisation, witness samples, that were not subjected to thermal treatment and were stored in the exact same conditions, are also tested in order to compare the results to a sane material.

Chapter 6

Experimental campaign

Contents

6.1	Materials	109
6.2	Experimental procedure	110
6.2.1	Casting, thermal treatment and conditioning	110
6.2.2	Monitoring of mass and expansion	113
6.2.3	Assessment of mechanical properties	114

Two studies will be presented in this part, based on the variation of one parameter each time.

1. aggregates mineralogical nature;
2. conditioning conditions.

First materials for the concrete compositions is presented, then the experimental procedure and the different protocols are detailed.

6.1 Materials

The formulation studied is the reference mix detailed in the previous part, and detailed in Table 6.1. Weights are indicated for 1 m³ of concrete, as well as the representative volume of each material in the concrete.

	Concrete composition	Representative volume
Materials	kg/m³	%
Cement	350	11,3
Water	201	20,1
Sand (0/4)	858	32
Gravel(4/12.5)	945	35,3
Viscosity modifying admixture	6,3	0,6
W/C ratio	0,57	

Table 6.1 – Concrete composition

This concrete formulation was made with CEM II/A-LL-42.5-R cement, also refereed as Airvault cement ; which composition is detailed in section A.1 ; on a 0.57 water-cement

ratio. A viscosity modifying admixture, Sika Stabilizer 400 is added with a dosage of 1,6% of cement mass. The use of this admixture is necessary so the composition is similar with the other study of the ANR project that focuses, among others things, on model materials with a limited number of aggregates. This dosage was determined with an optimisation procedure.

As mentioned previously, two kind of aggregates are used :

- **Calcareous aggregates:** The aggregates selected are the same than in Section 3.1, i.e. "visean" limestone from the Boulonnais quarry (France).
- **Siliceous aggregates:** The selection of siliceous aggregates was proceeded with caution. These aggregates from the Palvadeau quarry (France) are made of quartz, but are classified as not reactive face to the alkali reaction.

6.2 Experimental procedure

The experimental procedure followed in this study is summarised in the schematic display in Figure 6.1. Protocols are then detailed.

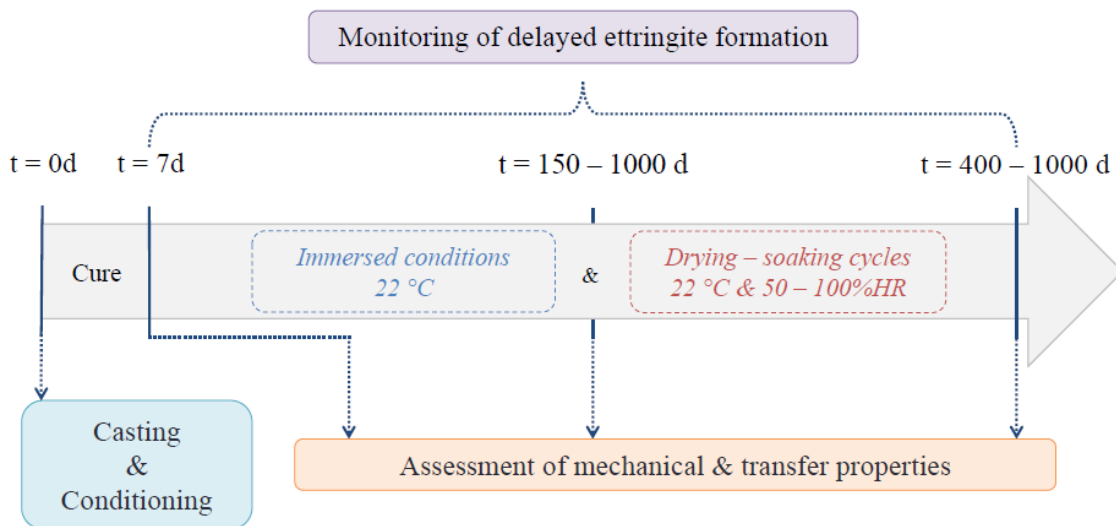


Figure 6.1 – Experimental procedure

6.2.1 Casting, thermal treatment and conditioning

Samples are casted using a 80-litres concrete mixer, each batch is limited to 55-litres. Fabrications were organised to cast a maximum of specimens that will be submitted to the same type of testing from the same batch.

Thermal treatment

The heating treatment is necessary to mimic the one of susceptible to happen in a massive structure. This treatment is realised in a climatic chamber. Samples are put directly after casting, with lids, are placed in the chamber. Also, a crystallizer filled with distilled water added to ease the chamber to reach the hydric instructions of 98%RH. The thermal treatment is represented in Figure 6.2 and can be decomposed in four phases :

- **Phase 1:** pre-treatment - 2 hours at 20°C;
- **Phase 2:** temperature rises from 20°C to 80°C in 24 hours (around 2.5°C per hour);
- **Phase 3:** continuous temperature - 80°C during 72 hours;
- **Phase 4:** temperature decreases back to 20°C in 72 hours (around 0.83°C per hour).

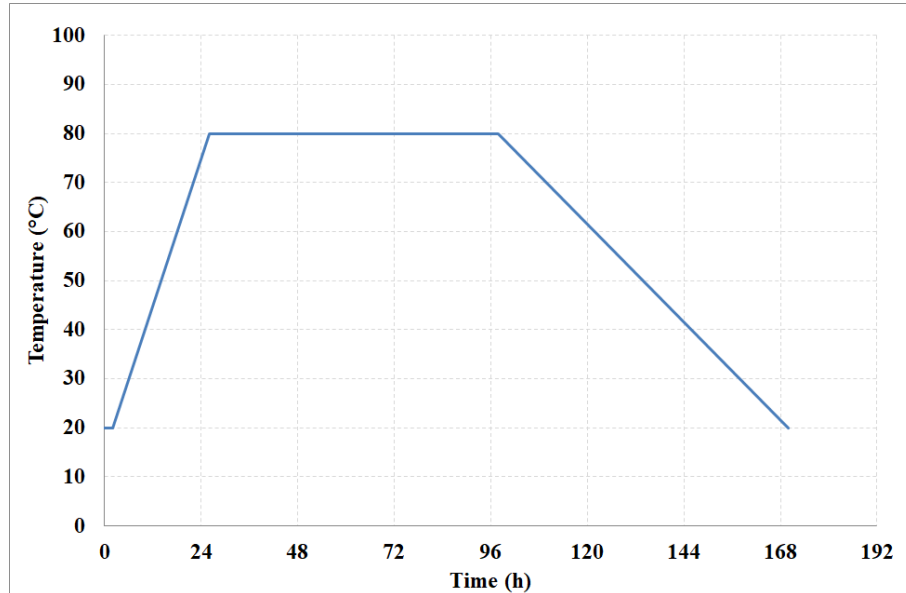


Figure 6.2 – Evolution of the instruction temperature of the thermal treatment submitted to the samples

After the heating treatment, moulds are removed from the specimens, which are put in their respective conditionings. All formulations are not submitted to drying and soaking cycles as described in the LCPC norm 66. Indeed, these cycles are designed to accelerate the delayed ettringite formation, however, only the heating treatment is mandatory to trigger the pathology, and even if we need to observe DEF rapidly, submitting the samples to the cycles could introduce damaging or variability in the material behaviour.

Conditionning

Several sizes of samples need to be conditioned, in order to carry out the tests planned, and it has been seen in the literature that DEF require a very humid environment. As a consequence, several boxes able to contain the samples and water were selected, however, two conditions have to be met:

1. the containers have to be hermetic in order to minimise the carbonation phenomenon;
2. the containers may contain more than one sample, but the amount of surrounding water have to be controlled to not cause a leaching of the specimens too important. Moreover, the water is never replaced during the campaign, but some containers required to be filled up due to vaporisation.

Samples destined to the monitoring are in individual cylindrical containers, whereas other type of samples were stored in boxes, by batch of 6 samples.

It was explained previously that one parameter studied in this study is the environmental conditions, more specifically, the impact of drying cycles on the DEF. Thus, the formulation with calcareous aggregates was made twice, and one the second one was submitted to drying and soaking cycles, detailed in Table 6.2.

Cycle	Soaking time	Drying time
<i>n</i> ^o	(<i>days</i>)	(<i>days</i>)
1	9	14
2	22	20
3	7	7
4	10	12
5	20	12
6	35	9
7	22	22
8	10	7
9	23	19
10	16	7
11	34	10
12	19	21
13	13	22
14	12	7
15	37	22
16	13	21
17	13	17
18	38	23
19	41	24
20	14	17
21	30	20
22	38	38
23	42	24

Table 6.2 – Cycles

6.2.2 Monitoring of mass and expansion

Delayed ettringite formation evolution of each type of samples is assessed by the monitoring of mass and volume variations. Mass is measured on a scale with a precision of 0.01 gram, and express as a percentage of mass variation via the Formula 6.1.

$$\Delta W(t) = 100 \cdot \frac{W(t) - W_0}{W_0} \quad (6.1)$$

In Formula 6.1,

- W_i is the measured mass at any time [g];
- W_0 is the initial mass [g];
- W is the percentage of mass variation [%].

Expansion is monitored on three cylinder specimens equipped with three series of two pins with 10 cm spaces and glued using an epoxy resin. The generatrices are equidistant of 120 degrees according to the circumference of the samples. It is the variation of the distance between plots - measured with an extensometer - which makes it possible to evaluate the expansion of the samples. Figure 6.3 represents a sketch of the principle of this measurement, based on the LCPC method 66, and Formula 6.2 allows us to express the variation of volume.

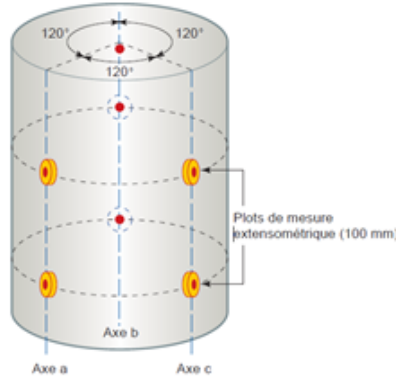


Figure 6.3 – Sketch of the samples monitored for DEF

$$\Delta \varepsilon(t) = \frac{\sum_{i=a}^c 100 \cdot \frac{d_i(t) - d_{i0}}{d_{th}}}{3} \quad (6.2)$$

In Formula 6.2,

- i is the generatrix a, b or c, where the measure is taken
- d_i is the measured distance between the pins of the generatrix i at any time [μm];
- d_{i0} is the initial distance between the pins of the generatrix i [μm];
- d_i is the theoretical distance between the pins of the generatrices [μm];
- $\Delta \varepsilon(t)$ is the percentage of volume variation at any time [%].

6.2.3 Assessment of mechanical properties

Monitoring of dynamic elastic modulus

Monitoring the evolution of the dynamic module is a non-destructive method based on the measurement of the resonance frequency of a wave propagating longitudinally in the test tube. It allows access to the dynamic modulus of elasticity, which reflects the stiffness of the material. The principle of this measurement consists in applying a pulse by the impact of a hammer to the center of one of the two bases of the cylindrical concrete test tube, so as to excite it in its longitudinal mode. The signal is collected by an piezoelectric captor located in the center of the opposite base. The specimen is positioned on a perfectly absorbent support to limit interferences likely to modify oscillations. The prototype software called "FRD" collects the signal and provides a frequency spectrum of oscillations. The frequency is defined by the first resonance mode. This frequency is related to the geometry and to the mechanical characteristics of the specimen by the relation 6.3.

For this study, every type of samples in the different conditioning are monitored on the same samples used for mass and volume variations, i.e. three 11*22 cylinders. Please note that some samples might have been sawn to insure that the bottom and top faces were parallel, and to prevent bad contacts with captors.

$$f_{longi}(t) = \frac{1}{2L} \cdot \sqrt{\frac{E_{dyn}(t)}{\rho(t)}} \quad (6.3)$$

- f_{longi} is longitudinal resonance frequency [s^{-1}];
- L is the height of the sample [m];
- E_{dyn} is the dynamic modulus of longitudinal deformations [Pa];
- ρ is the volumetric mass of the concrete sample [kg/m^3].

Three-points-flexural testing

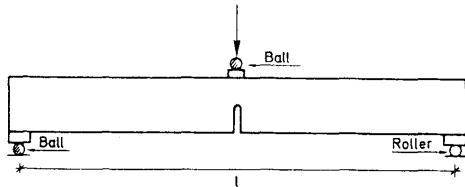
For each milestone and formulation, two 6x10x40 specimens, notched on the half height, are tested in three-point bending. They are equipped with four LVDT sensors: two following the maximal transversal deformation on either side of the sample, and two following the crack opening. We will then be able to exploit the results to assess cracking energy, flexural strength and Young Modulus. These tests are carried out according to the recommendations of the european norm RILEM 85.

The cracking energy is calculated by the formula:

$$G_f = \frac{W_0 + mg\delta_0}{A_{lig}} \quad (6.4)$$

In Formula 6.4,

- W_0 is the area under the load-displacement curve [N/m];
- $m = m_1 + m_2$ where m_1 is the weight of the beam between the supports, and m_2 is the weight of the equipment of the beam unattached to the press and presented on Figure 6.4b[kg];
- g is the acceleration due to gravity, for the calculus we take $g = 9.81$ [m/s^2];



(a) Schematic of three-points-flexural testing - 1. loading roller; 2 & 3. support rollers



(b) Picture Three-points-flexural testing with apparatus

Figure 6.4 – Three-points-flexural testing

- δ_0 is the maximal displacement at the final failure of the beam [m];
- A_{lig} is the area of the ligament. $A_{lig} = b \cdot \frac{h}{2} = 0,06 * 0,05$ [m²]

We are then able to determine the flexural strength of each sample using the Formula 6.5.

$$\sigma_{cf} = \frac{F_{max} \cdot l \cdot d}{8 \cdot I} \quad (6.5)$$

In Equation 6.5 and Figure 3.8a ,

- f_{cf} is the flexural strength [MPa];
- F_{max} is the maximum load [N];
- l is the distance between the support loaders [mm];
- I is inertia of the cross section [mm⁴].

Finally, the Young Modulus is determined by the Formula :

$$E_{flex} = \frac{K \cdot L^3}{48I} \quad (6.6)$$

Where,

- E_{flex} is the Young Modulus determined with the bending test [Pa];
- L is the length of the beam between the support loaders [m];
- I is the beam inertia, in our case $I = \frac{b \cdot h^3}{12} = \frac{0.06 \cdot 0.05^3}{12}$ [m⁴];
- K is the beam rigidity, and is determined on the load-displacement curve : it is the guide coefficient of the curve in the elastic domain [N/m].

Uni-axial compressive testing

Each formulation will be tested in compression at the different deadlines, on three 11*22 test tubes. After surfacing, the specimens are tested in compression, they are equipped with an extensome cage comprising three LVDT sensors for monitoring longitudinal deformations and two others for monitoring transverse deformations. The samples are cyclically loaded between 10% and 30% of the compressive breaking load, in order to remain in the elastic range. The use of the load-formation curves allows us to determine the Young's modulus and the Poisson's coefficient of the materials. The captors are then removed and the specimen is loaded until rupture, giving us access to compressive strength.

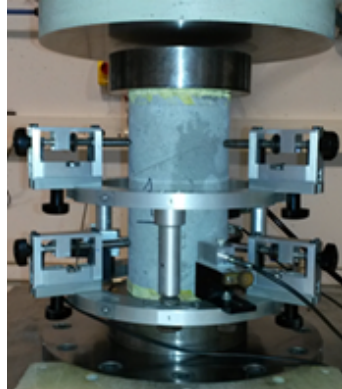


Figure 6.5 – Compressive testing

Then, after the removal of the apparatus, they are tested according to the French norm NF-EN-12390-3, until rupture. We are able to determine the compressive strength using the formula 6.7

$$f_c = \frac{F_{max}}{S} \quad (6.7)$$

In Equation 6.7,

- f_c is the compressive strength [MPa];
- F_{max} is the maximum load [N];
- S is the area of the cross section [mm²].

Young Modulus is determined by exploiting the compressive stress - longitudinal deformation curve. It is the guide coefficient of the curve in the elastic domain. As three cycles were made during the test and three samples are tested for each material, the Young Modulus expressed in the results table will be the average value of the nine values.

The Poisson coefficient is determined by exploiting the transversal deformation - longitudinal deformation curve and is the guide coefficient of the curve in the elastic domain.

Chapter 7

Effect of aggregates mineralogical nature on DEF

The results of this campaign are presented in the form of an article. This one comes from the Proceedings of the EDF conference "Dam Swelling Concrete" which took place in Chambéry in June 2017, and where our work was presented. It presents the monitoring of two compositions: a concrete made with limestone aggregates and a concrete made with siliceous aggregates. In addition, the results of the mechanical characterisations are also presented, at the progress of this moment.

7.1 Article presented in EDF conference "Dam Swelling Concrete"

Experimental study on effects of aggregates mineralogical composition and of preservation conditions on DEF in concrete.

M. Malbois*^{&***}, L. Divet**, S. Lavaud**, J.M. Torrenti**

*LMT - Cachan
ENS Cachan
61, avenue du Président Wilson,
94235 Cachan Cedex,
France
malbois@lmt.ens-cachan.fr

**IFSTTAR
14-20, Boulevard Newton,
Cité Descartes, Champs-sur-Marne,
F-77447 Marne la Vallée Cedex 2,
France
marie.malbois@ifsttar.fr
loic.divet@ifsttar.fr
stephane.lavaud@ifsttar.fr
jean-michel.torrenti@ifsttar.fr

ABSTRACT. DEF in concrete is likely to develop in massive civil engineering structures with major securities issues. DEF could lead to swelling and cracking which may impact in a significant manner mass transfer and mechanical properties. The on-going parametrical experimental campaign presented in this paper aims at quantifying the impact of aggregates chemical composition and of preservation conditions on DEF. Two concrete compositions are made, composed with calcareous or siliceous aggregates. The samples are then continuously preserved in water, or subjected to immersion and drying cycles. All compositions are monitored and tested at several deadlines to determine the evolution of mechanical (compressive and flexural tests). First results highlight the significant influence of aggregates composition on the formation kinetics, and also reveal that exposing samples to drying tends to slow DEF.

KEYWORDS: DEF, aggregates composition, drying cycles.

1. Introduction

Delayed ettringite formation in concrete can have a significant impact on the long term behaviour of massive concrete structure. Ettringite is a crystal characterised in 1970 by Moore and Taylor (Moore *et al.*, 1970) and its formation controls the concrete hardening but also the material workability at young age. Under a particular set of conditions, ettringite formation could be delayed and could lead degradations of the material. The swelling induced by the development of delayed ettringite generates internal and external cracking and so affect the durability of the concrete structures. Finally, the economic impact of DEF is significant due to the maintenance and repairing, or even destruction fees.

It is unanimously admitted that DEF develops only under peculiar conditions:

- Heat treatment (>65°C) during the concrete hardening, due to the cement hydration process or to thermic treatments undergone by pre-casted concrete parts. (Kchakech, 2012) took an interest in defining the impact of the length and the temperature of the thermic treatment on the DEF.

- Humid environment: DEF only develops in concrete in contact with water (Al Shamaa, 2012) (Heinz *et al.*, 1989) (Odler *et al.*, 1995) due to the departure of alkalines and the pH drop.

- Cement composition: (Pavoine, 2012) studied the impact of sulphates, aluminates and alkalis proportions and also the cement fineness on DEF.

- Aggregates mineralogical nature: (Monteiro *et al.*, 1986) (Grattan-Bellew *et al.*, 1998) (Brunetaud, 2005) demonstrated that sand or aggregates petrographic nature can impact the DEF, in terms of kinetics but also amplitude.

The presented study takes an interest in quantifying the effects of aggregates nature and also of the environmental conditions by submitting samples to soaking and drying cycles.

2. Experimental procedure

2.1. Materials

The concrete formulation used in this study is detailed Table 1.

Materials	Composition
Cement	350 kg
Water	201 kg
Sand (0-5 mm)	858 kg
Aggregates (5-12.5mm)	945 kg
Viscosity modifying admixture	5,6 kg
W/C	0,57
A/S	1,10
Density	2354 kg/m ³

Table 1 - Concrete composition

The Portland cement CEMII/A L with 6% of calcareous additions (42.5 MPa) is used with a 0.57 water-cement ratio. The aggregates are either calcareous (Boulonnais aggregates) or siliceous (Palvadeau aggregates).

2.2. Procedure

2.2.1. Thermic treatment

In order to simulate the heating induced by cement hydration in massive concrete structures, samples undergo a thermic treatment detailed in Figure 1, according to the LCPC N°66 method, with a 98% relative humidity. After treatment, samples are immersed in water ($20^{\circ}\text{C} \pm 3^{\circ}\text{C}$). Samples from the first study will be continuously kept under water, whereas samples from the second study will undergo soaking and drying cycles.

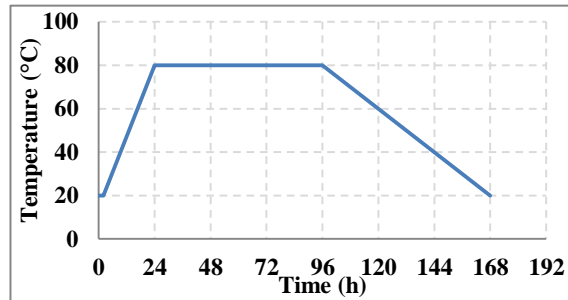


Figure 1 - Heating treatment

2.2.1. Protocols

Two types of testings are performed in this study. The first one is the monitoring throughout the procedure of three 11*22 cm cylindrical samples for:

- Mass variation
- swelling, following the n°66 LCPC method
- Dynamic Young Modulus, following the method detailed in (Brunetaud, 05) and (Al Shamaa, 12) with the “FDR” prototype.

The second type is mechanical testing at several deadlines, chosen to fit singular points of the expansion curves:

- 7 days, characterisation of healthy materials
- A few months to a few years, reorientation of the expansion curves
- From one to several years, stabilisation the expansion curves

The tests performed are:

- Compressive tests: three 11*22 cm cylindrical samples tested following the French norm (NF EN 12390, 2003), assessing the resistance strength and Young Modulus
- three-points bending tests: two 6*10*40 cm notched prismatic samples, with a 3cm notch depth, tested following the (RILEM 95 method) to determine the flexural strength and fracture energy.

3. Effect of aggregates mineralogical composition on DEF

3.1. Effects on expansion

In his thesis, (Brunetaud, 05) identify a four phases degrading phenomenon of samples undergoing DEF: initiation phase, latent phase (swelling under 0.1%), acceleration phase (swelling between 0.1 and 2%) and a stabilisation phase.

The evolution of mean expansions is presented Figure 2. The curve for the samples made with siliceous aggregates displays the complete profile of DEF induced expansion and is stabilised after one year with a maximum relative swelling of 0.959%; while the curve for the samples made with calcareous aggregates only just left the latent phase and is in the beginning of the swelling phase. The use of siliceous aggregates induces an important increase of the kinetic of delayed ettringite formation in this concrete.

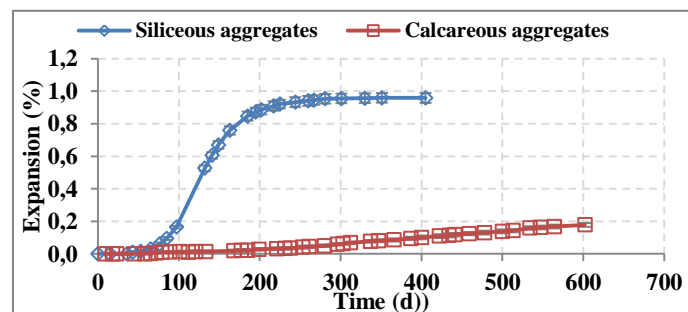


Figure 2 - Swelling of concrete samples with siliceous or calcareous aggregates

3.2. Effects on mechanical properties

3.2.1. Effect of the thermic treatment on mechanical properties

Both formulations are tested seven days after casting, on treated and not treated samples to determine the impact of the thermic treatment on the material. Results of compressive and three points bending tests are gathered in Table 2.

First, when taking an interest in the Young Modulus and compressive strength, the two formulations display a decrease, but it is more significant in the case of siliceous aggregates. Then, it can be noticed that the formulations have an opposite behaviour on the cracking energy results. Indeed, the “siliceous” samples undergo a cracking energy decrease of almost 15% after heating, whereas the “calcareous” samples cracking energy increase of more than 30%. These observations could be due to the nature of the interfacial transition zones and their evolution under heating.

		No treatment		With treatment		
		Value	Ecart type	Valeur	Ecart type	
Rc (MPa)	Siliceous	33.3	0.9	23.5	0.9	- 29.5 %
	Calcareous	36.9	1.1	29.5	0.5	- 20.1 %
E (GPa)	Siliceous	36.9	0.13	31.4	0.75	- 14.8 %
	Calcareous	36.0	0.14	33.2	0.30	- 7.7 %
Gf (N/m)	Siliceous	133.3	9.6	113.9	6.5	- 14.7 %
	Calcareous	73.4	2.5	96.9	7.4	+ 32 %

Table 2 - Effects of thermic treatment on mechanical properties

3.2.2. Effects of the aggregate composition on dynamic Modulus evolution

As the expansion, Dynamic Modulus has several evolution phases (Brunetaud, 05): a latent phase; a significant decrease of the Modulus, corresponding to the material stiffness loss due to the initialisation of cracking induced by the formation of delayed ettringite and an increase of the Modulus, corresponding to stiffness recovering due to filling of the voids by the ettringite.

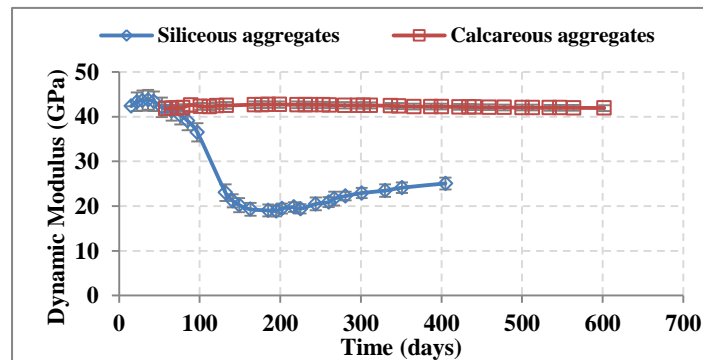


Figure 3- Dynamic Young Modulus evolution of concrete samples with siliceous or calcareous aggregates

On Figure 3, it can be observed that after one year, the samples with siliceous aggregates are at an advanced stage in the last phase, whereas the samples with calcareous aggregates are still in the dormant phase.

3.2.3. Discussion

The mineralogical nature of aggregates has a significant impact on the development of the pathology. The phenomenon is certainly induced by the different interaction between cement paste and aggregates. As a matter of fact, the roughness of siliceous or calcareous aggregates is different, leading to different adsorbed water on their surfaces, which could influence the transition zone properties and the quality of the interface. But also, siliceous aggregates are chemically inert during cement hydration, whereas calcareous aggregates have a better chemical affinity, and they react with the cement paste and form a hydrate which may strengthen the ITZ and decrease its porosity. Moreover, the decrease of mechanical properties after the heating cure could perhaps reveal that in case of siliceous aggregates, that the ITZ is fragile and the cure induces a first damage on the samples. In that case, the delayed ettringite could freely crystallise in the ITZ porosity and the cracks induced by the heating treatment. The samples with calcareous aggregates seem to offer less favourable conditions to the development of delayed ettringite, corresponding with a delayed appearance of DEF, and a slower evolution.

We will now take an interest in the evolution of the mechanical properties with the formation of delayed ettringite in samples made with siliceous inclusions.

4. Impact of DEF on mechanical properties

4.1 Evolution of mechanical properties

The formation of delayed ettringite in concrete structure leads to superficial and internal cracking, which could jeopardise the durability of structure and so its stability and the users security due to the alteration of mechanical properties. We will now see in which extend the DEF in samples composed with siliceous aggregates modifies the mechanical behaviours.

Results from compressive and bending tests at the three deadlines mentioned previously are gathered in Table 3.

	7 days		5 months		1 year	
	Value		Value		Value	
Rc (MPa)	23,5	0,9	12,3	0,2	12,5	0,1
E (GPa)	31,4	0,75	7,8	0,18	10,2	0,28
Gf (N/m)	113,9	13,0	100,5	14,0	97,8	3,3

Table 3 - Impact of DEF on mechanical properties

These results highlight the decrease of performance as soon as the expansion of samples begins for all indicators. However the decrease rates are the same for each factor:

- Compressive strength: -50%
- Static Young Modulus: -70%
- Dynamic Young Modulus: -45%
- Cracking Energy: -15%

The recovering of the Young Modulus or compressive strength noticed at in the final testing; but also leads to a more limited decrease; is certainly due to phenomenon described before: the delayed ettringite fills the voids of the concrete and brings stiffness to the material.

4.2 Viewing of the ettringite

To verify the causes of the damages and confirm the development of DEF, samples were controlled by the use of X-ray micro-tomography at every deadline and observed with a scanning electron microscope. The images in Figure 4 are slides from the micro-tomography scans made at the mechanics laboratory of Lille (LML).

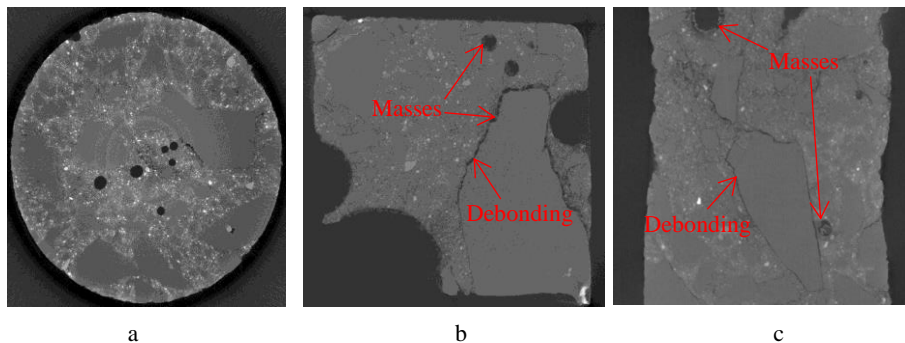


Figure 4 - Tomographic monitoring of samples with siliceous aggregates.
Mean diameter: 6mm, voxel size : 4 μ m
a.7 days, b. 5 months, c. 1 year

Image 4a is the reference image, scanned at the beginning of the study. The sample scanned after five months (Image 4b) shows an important porosity in which it can be noticed the formation of masses and also an important debonding phenomenon at the cement paste-aggregates interfaces. The cracks and porosity is progressively filled by the masses, as observed in the scan after one year (Image 4c).

In order to determine the nature of these masses, the sample scanned after a year was observed with a scanning electron microscope in the laboratory IFSTTAR. Figure 5 display the observations. Image 5a; obtained on a polish surface; indicate the presence of typical delayed ettringite formation as the form of a vein of compressed ettringite in an ITZ. Figure 5b, obtained on a fresh surface, presents two

vacuoles with ettringite masses, and also an aggregate covered with compressed ettringite. The spectrums obtained with the Energy Dispersive X-Ray Spectroscopy of the microscope confirm that the observed species is ettringite.

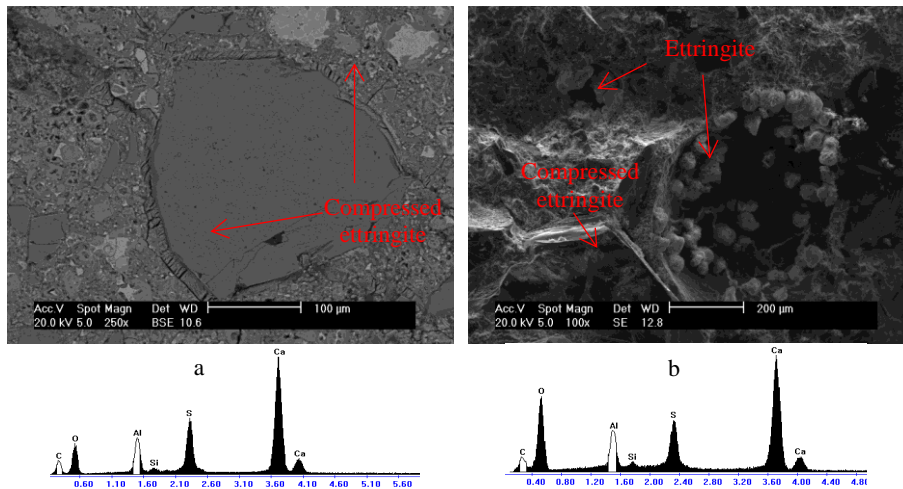


Figure 5 – Observations of samples with a scanning electron microscope
a. Vein of compressed ettringite at the aggregate-cement paste interface,
b. Void with free ettringite formation and aggregate covered with compressed ettringite.

5. Effect of soaking - drying cycles on DEF

A second set of samples with calcareous aggregates was casted and submitted to thermic treatment, and is submitted to drying ($20 \pm 3^\circ\text{C} - 50\% \text{RH}$ during 14 days) and soaking ($20 \pm 3^\circ\text{C}$ during 7 days) cycles. These preservation conditions represent a more realistic environment of some structures which are not in constant contact with water. The swelling monitoring of this new study is compared Figure 6 to the one of the composition previously studied and kept continuously in water. It seems that the cycles restrict the delayed ettringite formation in the material.

The curves presented Figure 7 highlight that the cycles slow down the formation, and do not prevent it. In other words, in the long term, the expansion will reach the same range than the one of immersed samples.

This delay could be due to the fact that thirty-two water molecules are needed to the crystallisation of ettringite ($3\text{CaO} \cdot \text{Al}_2\text{O}_3 \cdot 3\text{CaSO}_4 \cdot 32\text{H}_2\text{O}$) and during drying periods, the lack of water prevents its formation. Also, it could reveal the necessity of water as a reaction medium for DEF.

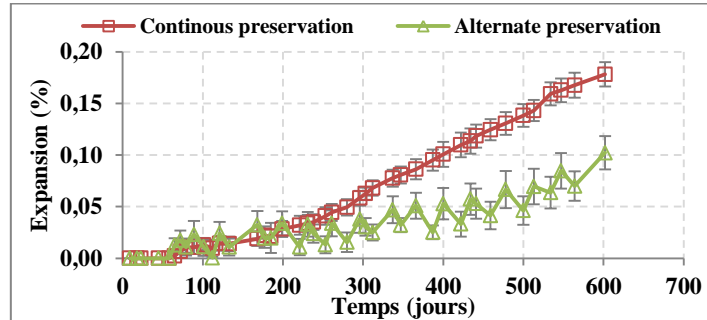


Figure 6 - Impact of drying cycles on the swelling of concrete samples

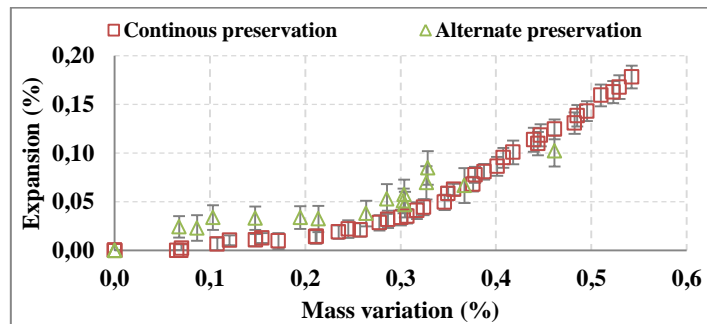


Figure 7 - Impact of drying cycles on DEF amplitude

5. Conclusion

1) The use of siliceous aggregates in heat-treated concrete leads to rapid and significant damaging due to DEF of the material; whereas the use calcareous aggregates in concrete leads to slow manifestation of DEF damaging.

We make the hypothesis that the main reason of these different behaviours could lay in the nature of aggregates-cement paste interfaces. The porosity and the mechanical behaviour of the ITZ are linked to the adsorbed water on the aggregate surfaces which is very dependant of aggregates nature. Also, calcareous aggregates have a better affinity with cement paste and leads to the formation of a hydrate which strengthen the ITZ. Moreover the decrease of mechanical properties of concrete made with siliceous indicates a pre-damage of the material, which could offer additional voids in which the delayed ettringite can easily crystallise.

2) Exposure to drying cycles tends to slow down the formation of delayed ettringite, indicating that water act as a reagent in the DEF but also as a reaction medium.

Acknowledgements

This research was achieved in the framework of the French research Project ANR MOSAIC. The authors would like to extend their appreciation and gratitude for the financial support provided by the French National Research Agency.

6. Bibliography/References

- Al Shamaa M., “Etude sur le risque de développement d’une réaction sulfatique interne et de ses conséquences dans les bétons de structure des ouvrages nucléaires”, Thesis, Université Paris-Est, France, 2012 (in French).
- Brunetaud X., “ Étude de l’influence de différents paramètres et de leurs interactions sur la cinétique et l’amplitude de la réaction sulfatique interne au béton”, Thesis, École Centrale des Arts et Manufactures « École Centrale Paris », France, 2005 (in French).
- Grattan-Bellew P.-E., Beaudoin J.-J., Vallee V.-G., “Effect of aggregate particle size and composition on expansion of mortar bars due to delayed ettringite formation”. *Cement and Concrete Research*, Vol. 28, n°8, 1998, p. 1147-1156.
- Heinz D., Ludwig U., Rüdiger I. (1989), Delayed ettringite formation in heat treated mortars and concretes, *Concrete Precasting Plant and Technology*, Vol. 11, 1989, p. 56-61.
- Kchakech B. (2015), “Etude de l’influence de l’échauffement subi par un béton sur le risque d’expansions associées à la Réaction Sulfatique Interne”, thèse de doctorat, Université Paris – Est, France, 2015 (In French).
- Méthode d'essai des lpc n°66, “Réactivité d’un béton vis-à-vis d’une réaction sulfatique interne. Essai de performance, techniques et méthodes des laboratoires des ponts et chaussées”, LCPC, 2007.
- Monteiro P.J.M. & Mehta P.K., “The transition zone between aggregate and type K expansive cement”, *Cement and Concrete Research*, Vol. 16, 1986, p. 111-114.
- NF EN 12390-3, “Essai pour béton durci – résistance à la compression des éprouvettes”, 2003.
- Moore A.E., Taylor H.F.W. (1970), Crystal Structure of Ettringite, *Acta Crystallographica*, 26(4), 1970, p. 386- 393.
- Odler I., Chen Y., “Effect of cement composition on the expansion of heat-cured cement pastes”, *Cement and Concrete Research*, 25(4), 1995, p. 853-862.
- Pavoine A., Brunetaud X., Divet L., “The impact of cement parameters on Delayed Ettringite Formation”, *Cement and Concrete Composites*, 34, 2012, p. 521-528.
- RILEM 95, “Determination of the fracture energy of mortar and concrete by means of three-point bend tests on notched beams”

7.2 Summary and conclusions

This article presents the effects of the mineralogical nature of aggregates on the development of DEF. A summary of the main results is presented in Table 7.1. These results express variations in the parameters of interest with respect to a healthy material (i.e. not having undergone heat treatment, nor the development of delayed ettringite). Only expansion and dynamic modulus results are expressed in relation to the initial state of the materials.

	Siliceous aggregates	Calcareous aggregates
Expansion rate	1 %	0,23 %
Stabilisation time	300 days	800 days
Dynamic modulus	- 55 %	- 2 %
Compressive strength	- 72 %	- 22 %
Flexural strength	- 37 %	- 12 %
Young Modulus (via compressive tests)	- 76 %	- 22 %
Young Modulus (via flexural tests)	- 6 %	- 33 %
Cracking energy	- 47 %	- 21 %

Table 7.1 – Summary of the evolution of the mechanical properties of materials with DEF. Percentages express the loss of properties compared to an equivalent healthy material.

As seen in the literature, specimens made with siliceous aggregates have higher expansion rates and much faster kinetics than when using calcareous aggregates. In addition, both batches of specimens have reduced mechanical performance. However, the batch manufactured from siliceous aggregates shows an overall and significant drop in properties, while the batch manufactured with calcareous aggregates has a much more moderate decrease.

Based on the study of the bibliography, several mechanisms are proposed to explain this difference in behaviour:

- **ITZ characteristics:** On one hand, siliceous aggregates, and more precisely quartz, tend to present a low rugosity and a limited chemical affinity with cement paste. Whereas calcareous aggregates have a good chemical affinity, resulting in a . As a result, ITZ present different compositions that influences their characteristics and more precisely, the transition zones between quartz aggregates and cement paste are considered weak;
- **Coefficient of thermal expansion of aggregates:** When submitted to heat, as during the heat treatment in the procedure, cement paste tends to shrink ($\alpha_{T_{cp}} = 10 - 30 \mu m.m^{-1}.K^{-1}$), whereas aggregates expand. However, depending on their mineralogical nature, the aggregates do not show the same behaviour with regard to thermal stresses. Indeed, calcareous aggregates display a coefficient of thermal expansion of $3 \mu m.m^{-1}.K^{-1}$, whereas it reaches $10 \mu m.m^{-1}.K^{-1}$ for siliceous aggregates between 20 and 100°C;
- **DEF mechanisms:** Delayed ettringite crystallise in concrete voids. Its progression induces crystallisation pressures, especially in ITZ due to the higher porosity rates, that could damage locally the material.

Being aware of these mechanisms and their particularities according to the mineralogical nature of the aggregates, it is possible to propose a pattern of evolution of the DEF in concrete:

Concrete with siliceous aggregates: During the manufacture of concrete, ITZ is created, and it will tend to have very high porosity and low mechanical performance. The specimens are then heat-treated, which results in high stresses due to the incompatibilities of deformation of the aggregates and cement paste. If these stresses are too great, and given the nature of ITZ, the material can crack at ITZ. This provides a large amount of voids in the concrete, facilitating the formation of delayed ettringite. The latter can rapidly develop and generate significant crystallisation pressures in the material, creating cracking again which allows the rapid progression of ettringite. Finally, siliceous aggregates may contain alkalis, which may cause a larger local leaching, which could accelerate the initialisation of the DEF. There is therefore significant damage to the material followed by a gradual recovery of the properties, corresponding to the filling of the voids by ettringite.

Concrete with calcareous aggregates: In this case, ITZ has lower porosity and good mechanical characteristics due to the good chemical affinity of the aggregates and cement paste, which consumes a portion of the aluminate ions to create carboaluminates, reducing the number available for the DEF reaction. In addition, during heat treatment the aggregates have a lower coefficient of thermal expansion than siliceous aggregates, so stresses are generated in the ITZ due to incompatibility of deformation but cracking may remain limited due to the good mechanical performance of the ITZ. Delayed ettringite therefore has few voids to crystallise in, and the material is more resistant to crystallisation pressures. This slows down the initialization and progress of the DEF. Concrete therefore has a more limited and slowly developing damage, allowing simultaneous filling of concrete voids.

Chapter 8

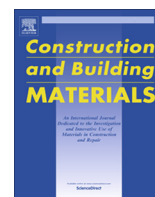
Effect of drying cycles on DEF in concrete

8.1 Article from Construction and Building Materials Journal



Contents lists available at ScienceDirect

Construction and Building Materials

journal homepage: www.elsevier.com/locate/conbuildmat

On DEF expansion modelling in concrete structures under variable hydric conditions

M. Malbois^a, B. Nedjar^{b,*}, S. Lavaud^b, C. Rospars^b, L. Divet^b, J.-M. Torrenti^b^a *Laboratoire de Mécanique et Technologie – ENS Cachan 61, Avenue du Président Wilson, 94235 Cachan Cedex, France*^b *Université Paris-Est, IFSTTAR/MAST 14-20, Boulevard Newton, Cité Descartes, 77447 Marne-la-Vallée Cedex 2, France*

HIGHLIGHTS

- Delayed Ettringite Formation is modelled under variable hydric conditions.
- The time of exposure to water is accounted for through the notion of effective time.
- Each material point has its own humidity history.
- The effective time is then an internal field variable.
- This notion is embedded within a classical form of evolution equations.

ARTICLE INFO

Article history:

Received 10 June 2018

Received in revised form 19 February 2019

Accepted 21 February 2019

Available online 28 February 2019

Keywords:

DEF pathology modelling

Variable humidity

Effective time concept

ABSTRACT

Delayed Ettringite Formation (DEF) in concrete is likely to develop in massive civil engineering structures such as bridges, nuclear plants, and dams with major security issues. In many cases, DEF pathology can lead to swelling and cracking which may significantly impact mass transfer and mechanical properties. It is then of major importance to build predictive tools for engineering conceptions and expertises. In this contribution, the chemical swelling evolution is integrated within the overall constitutive law of concrete that, besides, can experience other phenomena such like damage, plasticity, and long term creep, not all considered here. On another hand, as DEF is activated by environmental humidity above a certain threshold, we introduce the notion of effective time that takes into account the cumulative exposition above this threshold. Hence, a special care is taken with regards to the chemical irreversibility, together with the humidity-drying cycles. Computations are used to calibrate various sets of model parameters with the help of results from the literature, on the one hand, and from an experimental campaign where a calcareous aggregates-based concrete is studied, on the other hand. We show the efficiency of the developed numerical tool through a series of numerical examples.

© 2019 Elsevier Ltd. All rights reserved.

1. Introduction

Delayed ettringite formation (DEF) in concrete can have significant impact on the long term behaviour of massive concrete structures. The swelling induced by the development of this pathology generates cracking and so can in general affect the mechanical properties, the transfer properties, for instance see [1,2], and the durability of the concrete structures, for instance [3]. It is then of major importance to build numerical tools that can simulate this

expanding kinematics and its consequences on the structural serviceability. Ettringite formation is delayed under a particular set of conditions, that have been unequally thoroughly studied: cement compositions ([4–7] among others), aggregate mineralogical nature ([8–11], among others), curing ([12,13,7]) or environmental humidity. Few authors have focused on the study the influence of the ambient humidity of the material. Water has a significant role in the delayed ettringite formation. It has been noticed that the concrete structures with DEF pathology were in an environment with a high ambient relative humidity (submerged parts, inflows of water, or exposition to high humidity). Water seems to be both a reaction agent and environment, as ettringite crystallisation requires 32 molecules of water ([14]), but it also allows the transport of other agents that influence the formation of DEF ([15]). Indeed, it boosts the leaching of alkalines out of the

* Corresponding author.

E-mail addresses: malbois@lmt.ens-cachan.fr (M. Malbois), boumediene.nedjar@ifsttar.fr (B. Nedjar), stephane.lavaud@ifsttar.fr (S. Lavaud), clauderospars@ifsttar.fr (C. Rospars), loic.divet@ifsttar.fr (L. Divet), jean-michel.torrenti@ifsttar.fr (J.-M. Torrenti).

interstitial water in the material, leading to a decrease of pH which favours the formation of ettringite. It is nowadays unanimously accepted that the DEF rate and amplitude is increased by the increase of saturated water, thus environmental humidity, e.g. see for example [16,15,17–19]. For instance in [17,19], the authors have even demonstrated experimentally this impact by putting reactive mortar and concrete in different controlled environments from 75%RH to 100%RH. Based on macroscopic observations, they identified a RH threshold of about 92% to initiate DEF.

From the mathematical point of view, extensive research has been conducted to model expansions caused by DEF, see for example [18,13,20,21, among others] where expansions range around 0.25% to 1.3%, even, up to 3% [22], and further developments are nowadays still ongoing. The models are mostly based on phenomenological approaches formulated in terms of internal variables. The expansion is in general characterized by two important ingredients:

- (i) An amplitude that depends on the temperature history at early age due to hydration and/or on heating conditions if a curing process is employed such as for pre-casting;
- (ii) A kinetics that depends on the time, more precisely on the cumulated time, of exposure in contact with water.

Of interest in this work is the introduction of a new notion; the concept of *effective* time, that we denote throughout by \tilde{t} , and that is controlled by the amount of water (humidity) during time and, consequently, that influences the kinetics of expansion, i.e. the above ingredient (ii). This extends the applicability of the existing expansion models not only for cases of full saturation, but for varying environmental conditions as well. Among others, the effective time depends on a threshold below which the swelling process stops, and above which swelling strongly depends on humidity as well as on temperature. Within the continuum, the effective time is an internal field variable since each material point \mathbf{x} has its own humidity history during the real time t ; $\tilde{t} \equiv \tilde{t}(\mathbf{x}, t)$.

An outline of the remainder of this paper is as follows: we first recall the basic constitutive equations together with the kinematical assumption we adopt in this work. The notion of effective time is then motivated and detailed with a focus on the most relevant points involved by the present formulation. Finally, we present a set of numerical simulations to illustrate the effectiveness of the proposed framework that compare satisfactorily against experimental data from an experimental campaign and from results in the literature.

2. Swelling kinematics

The kinematical choice is as usual based on an additive split of the *total* strain tensor $\boldsymbol{\varepsilon}$ into an elastic part $\boldsymbol{\varepsilon}^e$ and complementary parts, each one corresponding to a phenomenon. To be as clear as possible, let us consider the simplest choice,

$$\boldsymbol{\varepsilon} = \boldsymbol{\varepsilon}^e + \boldsymbol{\varepsilon}_{th} + \boldsymbol{\varepsilon}_{hyd} + \boldsymbol{\varepsilon}_\chi, \quad (1)$$

where $\boldsymbol{\varepsilon}_{th}$ and $\boldsymbol{\varepsilon}_{hyd}$ are respectively the thermal and hydric dilations, and $\boldsymbol{\varepsilon}_\chi$ the chemical expansion tensor, in our case due to DEF. We can use the classical relations for the formers as:

$$\boldsymbol{\varepsilon}_{th} = \alpha(T - T_0)\mathbf{1}, \quad \boldsymbol{\varepsilon}_{hyd} = \varpi(S_r - S_{r0})\mathbf{1}, \quad (2)$$

where T is the temperature, S_r is the saturation, α and ϖ are respectively the thermal and hydric dilatation coefficients, assumed constant for simplicity, and $\mathbf{1}$ is the second-order identity tensor. Here T_0 and S_{r0} are the initial temperature and the initial saturation, respectively. Notice that a form based on the relative humidity can equivalently be used instead of the saturation-based form (2)₂. In

future contributions, inelastic deformations through a plastic strain $\boldsymbol{\varepsilon}^p$ together with creep through a viscoelastic strain $\boldsymbol{\varepsilon}^v$ will be appended to the decomposition (1) in a classical fashion, i.e. $\boldsymbol{\varepsilon} \equiv \boldsymbol{\varepsilon}^e + \boldsymbol{\varepsilon}_{th} + \boldsymbol{\varepsilon}_{hyd} + \boldsymbol{\varepsilon}_\chi + \boldsymbol{\varepsilon}^p + \boldsymbol{\varepsilon}^v$, see for example [23,24] for similar couplings.

Now if we consider a purely volumetric chemical expansion, we write:

$$\boldsymbol{\varepsilon}_\chi = \varepsilon_\chi \mathbf{1}, \quad (3)$$

where the scalar functional $\varepsilon_\chi \equiv \varepsilon_\chi(S_r, T, t \dots)$ is the so-called free chemical expansion, the expression of which depends on the humidity, the temperature, and of course on the time as well.

In fully saturated conditions ($S_r = 1$ all the time), one has the nowadays well known expression used for both of DEF and Alkali-Aggregate Reaction (AAR) expansions phenomena, see for example [10,25,18, among others]:

$$\varepsilon_\chi = \varepsilon_\infty^0 \frac{1 - e^{-\frac{t}{\tau_c}}}{1 + e^{-\frac{t-\tau_l}{\tau_c}}} \left(1 - \frac{\phi}{t + \delta}\right), \quad (4)$$

where,

- ε_∞^0 is the potential chemical strain that constitutes the amplitude of expansion, i.e. ingredient (i) in the Introduction Section,
- τ_c and τ_l are respectively the characteristic and latent times that characterize the kinetics of expansion,
- and ϕ and δ are parameters that control the long term kinetics. They are such that $\delta > \phi$. Eq. (4) reduces to Larive's law [26] when ϕ is set to zero.

For the case of a DEF analysis, ε_∞^0 depends on the thermal history at *early-age*. To fix the ideas the following definition can be used for its modelling, see for instance [25,27]:

$$\varepsilon_\infty^0 = \bar{\alpha} \int_0^{t_m} \begin{cases} 0 \, dt, & \text{if } T \leq T_{def} \\ e^{\left[-\frac{E_a^{def}}{R} \frac{1}{T - T_{def}}\right]} \, dt, & \text{if } T > T_{def} \end{cases} \quad (5)$$

where the constant $\bar{\alpha}$ is a material parameter, T_{def} is the threshold of temperature above which DEF can be generated (about 65 °C), E_a^{def} is the activation energy relative to DEF expansion, and t_m is the maturation time (few days to few weeks depending on the size of the considered structure).

Now to take into account the influences of both of the thermal and hydric conditions, relation (4) must be adapted. To be exhaustive, let us assume the following choices that not all will be considered in this step of the developments due to the lack of experimental results.

2.1. Variable thermal conditions

It has been shown experimentally that the ambient temperature has an influence on the kinetics of expansion. Among other choices, we can consider that the two characteristic times be thermo-activated with the forms

$$\tau_l = \bar{\tau}_l e^{\left[\frac{U_l}{R} \left(\frac{1}{T} - \frac{1}{\bar{T}}\right)\right]}, \quad \tau_c = \bar{\tau}_c e^{\left[\frac{U_c}{R} \left(\frac{1}{T} - \frac{1}{\bar{T}}\right)\right]}, \quad (6)$$

as suggested in [26,28] for AAR. Here $\bar{\tau}_l$ and $\bar{\tau}_c$ are reference characteristic times for a reference temperature \bar{T} , and U_l and U_c are activation energies. Notice that, even possible, the amplitude ε_∞^0 is not affected by temperature in our DEF case.

2.2. Variable hydric conditions

Experimental evidences have also shown that the expansion stops below a certain threshold of humidity, see for example [19]. The relation (4) must then be adapted to take into account this strong dependency. In terms of saturation, denoting the threshold below which the expansion reaction stops by \bar{S}_r , we can formally write:

$$\begin{cases} \dot{\varepsilon}_\chi = 0, & \text{if } S_r \leq \bar{S}_r, \\ \dot{\varepsilon}_\chi > 0, & \text{if } S_r > \bar{S}_r, \\ \text{and } \varepsilon_\chi \text{ is given by (4),} & \text{if } S_r = 1. \end{cases} \quad (7)$$

Now for $\bar{S}_r < S_r < 1$, we need to establish a *continuous* link between the extreme situations (7)₁ and (7)₃. We introduce for this an *effective* time that we denote by \tilde{t} and such that,

$$\dot{\tilde{t}} \equiv \dot{\tilde{t}}(S_r, t, \dots) \in [0, 1]. \quad (8)$$

A possible choice would be:

$$\dot{\tilde{t}} = \left(\frac{\langle S_r - \bar{S}_r \rangle_+}{1 - \bar{S}_r} \right)^{\bar{m}} \Rightarrow \tilde{t} = \int_0^t \left(\frac{\langle S_r - \bar{S}_r \rangle_+}{1 - \bar{S}_r} \right)^{\bar{m}} dt, \quad (9)$$

where the Macauley bracket $\langle \cdot \rangle_+$ denotes the positive part function, and the exponent parameter most probably depends on the saturation, i.e.

$$\bar{m} \equiv \bar{m}(S_r). \quad (10)$$

Hence, by replacing the real time t by the effective time \tilde{t} into the expression (4), we obtain a free expansion law that covers the requirements (7) for variable humidity.

3. Constitutive equations and mechanical balance

The kinematic decomposition, Eq. (1), must now be embedded into a constitutive relation. At this point, the simplest choice is to consider an elastic relation for the reversible behaviour:

$$\sigma = \mathbf{C} : \varepsilon^e, \quad (11)$$

where σ is the stress tensor and the elastic part of the strain tensor ε^e is the one that has been used in the decomposition (1). \mathbf{C} is the fourth-order elasticity tensor that can in turn be affected by chemical damage as

$$\mathbf{C} = (1 - d_\chi) \mathbf{C}_0, \quad (12)$$

where \mathbf{C}_0 is the elastic modulus for the undamaged concrete (Hooke's law) and d_χ is a damage variable in the sense of continuum damage mechanics, see for example [24,29]. Intuitively, it can be driven by the chemical expansion itself, then explicitly given as a function of the quantity ε_χ , for instance, the following form as adopted in [25]:

$$d_\chi = 1 - e^{\left[-\omega \langle \varepsilon_\chi - \varepsilon_{\text{trs}} \rangle_+ \right]}, \quad (13)$$

where ε_{trs} is the strain-like chemical damage threshold below which no damage occurs, and $\omega \geq 0$ a convenient parameter, i.e. no chemical damage takes place if we take $\omega = 0$.

With (11) we have a minimalist modelling framework with the simplest possible resolution procedure. The mechanical balance is linear since the thermal and hydric fields are a priori known at every time step, i.e. assuming a weak coupling between the thermo-hydric diffusion and the mechanical equilibrium. Let us notice however that when inelastic strains (plasticity) will be taken into account together with creep and mechanical damage, the problem clearly becomes nonlinear. Furthermore, the thermal and hydric parts of the modelling are left out of the scope of this paper. Nevertheless, let us stress that for the hydric part at least, care must be taken when solving for the saturation field. Indeed, on the one hand, the hydric diffusion is not constant and, on the other hand, concrete materials are characterized by typical hysteretic sorption-desorption responses that strongly influence the soaking-drying kinetics, to mention a few. Developments on this topic are still in progress.

At the actual time t_{n+1} for instance, the weak form of the mechanical balance at hand is given by:

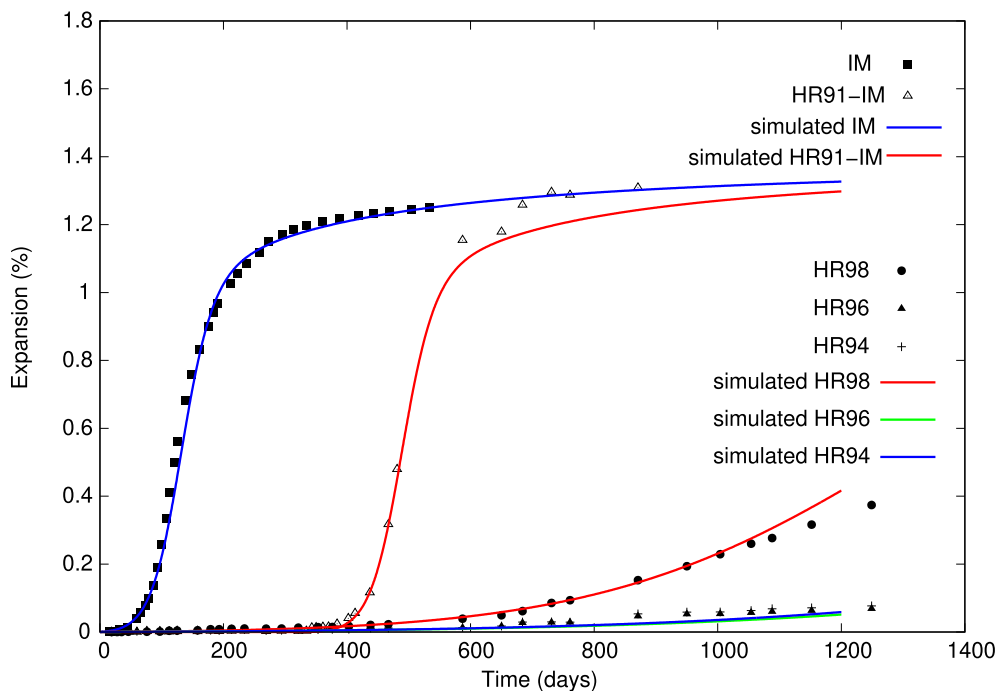


Fig. 1. Expansions of all concrete specimens. Experimental results from (Al Shamaa & al., 2015). Superposition with the results of the numerical simulations.

$$\int_B \nabla^s \delta \mathbf{u} : \mathbf{C}_{n+1} : \nabla^s \mathbf{u}_{n+1} dV = G_{n+1}^{\text{ext}}(\delta \mathbf{u}) + \int_B \nabla^s \delta \mathbf{u} : \mathbf{C}_{n+1} : (\boldsymbol{\varepsilon}_{\text{th}_{n+1}} + \boldsymbol{\varepsilon}_{\text{hyd}_{n+1}} + \boldsymbol{\varepsilon}_{\gamma_{n+1}}) dV, \quad (14)$$

which must hold for any displacement variation $\delta \mathbf{u}$, and where $\nabla^s(\cdot)$ is the symmetric gradient operator. Here G_{n+1}^{ext} is a short hand notation for the virtual work of the external loads embedding both of the volumetric forces in the body B and traction forces on part of its boundary $\partial_t B \subset \partial B$ applied at time t_{n+1} .

Eq. (14) is to be solved for the actual displacement field \mathbf{u}_{n+1} . However, care must be taken in evaluating the chemical strain $\boldsymbol{\varepsilon}_{\gamma_{n+1}}$ on the right hand-side of (14). Indeed, this latter is computed with the effective time \tilde{t}_{n+1} that must in turn be updated locally at each time step as:

$$\tilde{t}_{n+1} = \tilde{t}_n + \left(\frac{\langle S_{r_{n+1}} - \bar{S}_r \rangle_+}{1 - \bar{S}_r} \right)^{\bar{m}_{n+1}} \Delta t, \quad (15)$$

where $\Delta t = t_{n+1} - t_n$ is the real time increment, and the exponent parameter \bar{m}_{n+1} is evaluated with $S_{r_{n+1}}$, i.e. $\bar{m}_{n+1} \equiv \bar{m}(S_{r_{n+1}})$ in the form (10). Consequently, the effective time is treated as an internal field variable; $\tilde{t} \equiv \tilde{t}(\mathbf{x}, t)$.

4. Simulations of the influence of the relative humidity on DEF expansions

In this section we present simulations with regards to experimental tests given in [19] on the study of the influence of relative humidity on expansion associated with DEF in concrete. A set of 11×22 cm cylindrical samples made with a siliceous-based aggregate concrete were heat-treated at early age so as to potentially trigger DEF expansion, and then separated in different groups, each group submitted to a controlled constant relative humidity RH, see [19] for details:

- Samples that have been stored at 94%, 96%, 98% and 100% RH, respectively denoted by RH94, RH96, RH98 and RH100.;
- Samples that have been immersed continuously, denoted by IM;
- Samples that have been stored at 91% RH and then immersed in water at the age of 334 days, denoted by RH91-IM.

The experimental results are shown in Fig. 1 where interesting observations are to be pointed out:

- Expansions under continuous immersion and RH100 (not shown here) are almost identical;
- With a relative humidity of 91%, the saturation is under the threshold \bar{S}_r ;
- Above the saturation threshold, the expansion is very sensitive to the ambient humidity, i.e. from 94 to 100% RH.

Table 1

Material parameters with the expansion law (4) for the siliceous concrete of Fig. 1.

Definition	Identified values
Expansion amplitude ε_{∞}^0	1.4%
Latent time τ_l	128 days
Characteristic time τ_c	25 days
Parameter ϕ	68 days
Parameter δ	100 days

Table 2

Concrete composition.

Materials	Composition
Cement	350 kg
Water	210 kg
Sand (0–5 mm)	858 kg
Aggregates (5–12.5 mm)	945 kg
Viscosity modifying admixture	6.6 kg
W/C	0.57
A/S	1.1
Density	2354 kg/m ³

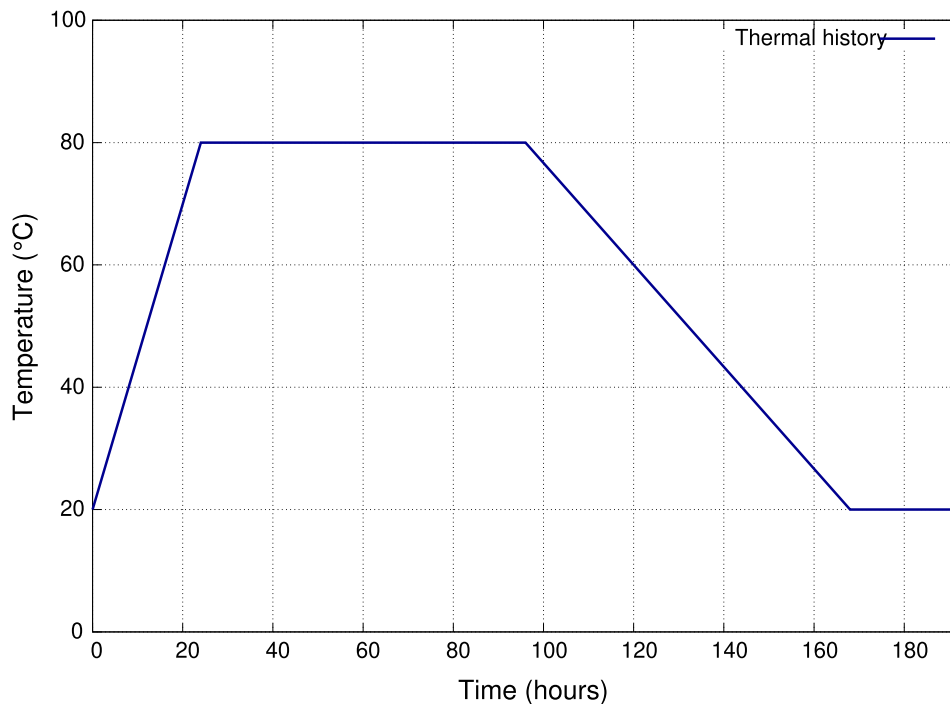


Fig. 2. Heating treatment of the 11×22 cm cylindrical samples during first hours after curing.

From the point of view of the modelling, the curve obtained at saturation $S_r = 1$ that corresponds to the case of RH100 or IM, is used to identify the parameters of the free-expansion law (4). They are summarized in Table 1 where the asymptotic parameters ϕ and δ are used for a better description of the long term expansion kinetics.

Now for the effective time, the property $(7)_2$ is active in this example, so the expression (9) must be used. We take $\bar{S}_r = 0.93$ for the saturation threshold, and the exponent parameter \bar{m} has the form (10) chosen here as a quadratic function given by,

$$\bar{m}(S_r) = 1 + 42.5(S_r - \bar{S}_r) + 1750(S_r - \bar{S}_r)^2. \tag{16}$$

With this set of parameters at hand, we show in Fig. 1 the numerical results predicted by the model for the different exposures to humidity. One can notice that the model is able to represent the experimental behaviour.

5. DEF expansions under cyclic soaking-drying cycles

An experimental campaign has been performed in this work as well. Concrete samples were designed for their known expansive behaviour when heat-treated and immersed in water after casting. The concrete formulation used is detailed in Table 2; A Portland cement CEMII/A L with 6% of calcareous additions (42.5MPa) is used with a 0.57 water-cement ratio. Calcareous aggregates were used (Boulonnais aggregates).

Now to simulate the heating induced by cement hydration in massive structures, the samples undergo a thermic treatment as shown in Fig. 2: the temperature was maintained at 20 °C for 2 h, then increased from 20 °C to 80 °C in 24 h, then maintained at 80 °C for three days, and then decreased from 80 °C to 20 °C in three days. After this treatment, half of the samples were immersed in water at 20 °C; the other half undergo soaking and drying cycles. In all cases, 11 × 22 cm cylindrical samples have been used, and are monitored following the LCPC method n°66.

Table 3

Material parameters with the expansion law (4) for the calcareous-based concrete.

Definition	Identified values
Expansion amplitude ϵ_∞^0	0.23%
Latent time τ_l	423.5 days
Characteristic time τ_c	135.48 days
Parameter ϕ	0
Parameter δ	0

Table 4

Soaking-drying cycles for the calcareous-based concrete samples.

Cycle n°	Soaking time (days)	Drying time (days)
1	9	14
2	22	20
3	7	7
4	10	12
5	20	12
6	35	9
7	22	22
8	10	7
9	23	19
10	16	7
11	34	10
12	19	21
13	13	22
14	12	7
15	37	22
16	13	21
17	13	17
18	38	23
19	41	24
20	14	17
21	30	20
22	38	38
23	42	24

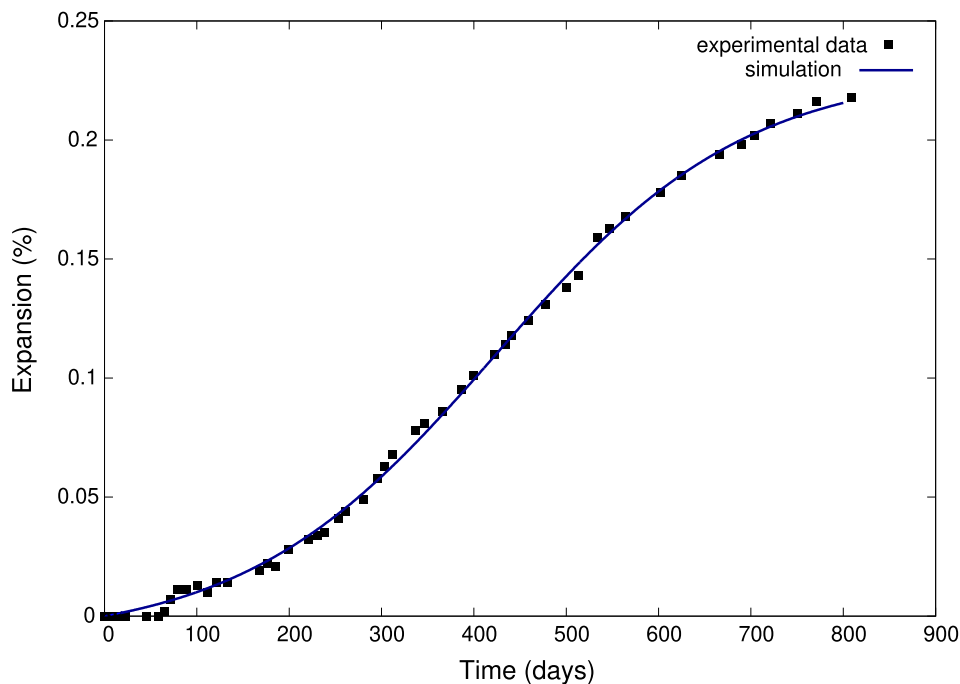


Fig. 3. Swelling of concrete samples with calcareous aggregates. Experimental data and numerical simulation.

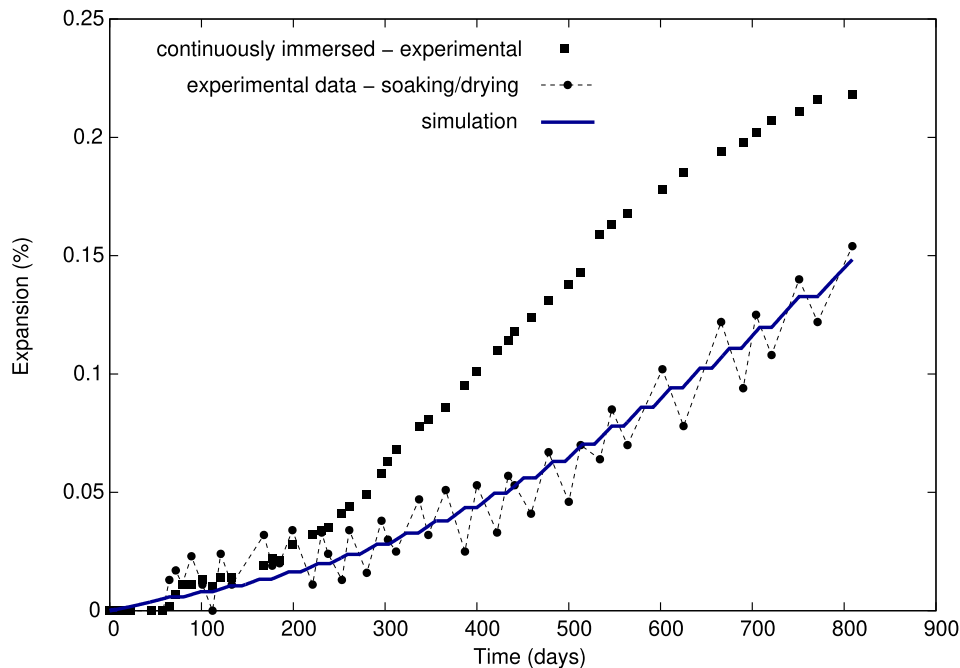


Fig. 4. Impact of drying cycles on the swelling of concrete samples with calcareous aggregates. Experimental data and numerical simulation.

5.1. Simulations for the immersed samples

The experimental evolution of the mean expansions for the samples is presented in Fig. 3, in square-dots-points. The phase of accelerated degradation is finishing and the stabilisation phase is taking place (about 0.23% maximum expansion).

Curve fitting with the free-expansion law (4) gives the parameters summarized in Table 3 where Larive's law is sufficient, i.e. with $\phi = 0$.

With these values, the simulated expansion is superposed in Fig. 3 where a good agreement is to be noticed. As the samples are immersed during the whole time, uniform saturation $S_r = 1$ is taken and, consequently, the effective time is identical to the real time.

5.2. Simulations of the effect of soaking-drying cycles on DEF

A second set of samples with the above calcareous aggregates was submitted to cycles of drying (at 50% of relative humidity and 23 °C) alternated with soaking (at 23 °C) to represent a more realistic environment of some structures which are not permanently in contact with water. The cycles are recorded in Table 4.

The swelling monitoring of this new study is plotted in Fig. 4 (the dashed line with circle dots), and compared to the previous experimental curve of Fig. 3 with the samples kept continuously immersed in water (square-dots-points curve). One can notice that the drying cycles restrict the delayed ettringite formation in the material and have an important impact on the expansion kinetics.

From the modelling point of view, this falls within the scope of the properties (7)₁ for drying, and (7)₃ for soaking. For the material parameters of the expansion law (4), we use the ones of Table 3. And for the effective time (9), we fix the saturation threshold to $\bar{S}_r = 0.95$. Here the computation is independent of the exponent parameter \bar{m} since:

$$\hat{t} = \begin{cases} 1 & \text{for soaking, with } S_r = 1, \\ 0 & \text{for drying, since } S_r \ll \bar{S}_r. \end{cases} \quad (17)$$

In the numerical computation, uniform saturation $S_r = 1$ is taken during the first 72 days, then cycles of drying for 13 days at

$S_r = 0.48$ followed by soaking for 19 days at $S_r = 1$ are prescribed. In total, the sample is immersed 514 days and dried 295 days.

The simulated expansion is superposed in Fig. 4 where good agreement is again observed. Notice further that the expansion after 809 days of alternate soaking/drying cycles is almost the same as the 514 days' expansion in continuous immersion conditions.

6. Conclusions

In this study, we have presented and numerically tested an efficient tool for the modelling of the influence of relative humidity on the development of DEF expansions. The simple notion of effective time implicitly takes into account the amount of water during time in variable environmental conditions that strongly influence the kinetics of DEF expansions.

From the numerical point of view, we have briefly presented a numerical design for the integration of the chemical strain and the update of the effective time. In particular, this latter must be performed at the integration points level when use is made of the finite element method.

Numerical simulations have shown good agreements with the experimental results issued from an experimental campaign, and others from the literature. However, further studies are ongoing to include this notion within more detailed and complex formulations, i.e. including creep, plasticity and mechanical damage among others.

Conflict of interest

None.

References

- [1] H.F.W. Taylor, C. Famy, K.L. Scrivener, Delayed ettringite formation, *Cem. Concr. Res.* 31 (2001) 683–693.
- [2] M. Al Shamaa, S. Lavaud, L. Divet, G. Nahas, J.-M. Torrenti, Coupling between mechanical and transfer properties and expansion due to DEF in a concrete of a nuclear power plant, *Nucl. Eng. Des.* 266 (2014) 70–77.

- [3] M.M. Karthik, J.B. Mander, S. Hurllebaus, Experimental behavior of large reinforced concrete specimen with ASR and DEF deterioration, *J. Struct. Eng.* 144 (8) (2018) 04018110.
- [4] A. Pavoine, X. Brunetaud, L. Divet, The impact of cement parameters on delayed ettringite formation, *Cem. Concr. Compos.* 34 (2012) 521–528.
- [5] I. Odler, Y. Chen, Effect of cement composition on the expansion of heat-cured cement pastes, *Cem. Concr. Res.* 25 (1995) 853–862.
- [6] S. Kelham, The effect of cement composition and fineness on expansion associated with delayed ettringite formation, *Cem. Concr. Compos.* 18 (1996) 171–179.
- [7] X. Brunetaud, R. Linder, D. Duragrín, D. Damidot, Effect of curing conditions and concrete mix design on the expansion generated by delayed ettringite formation, *Mater. Struct.* 40 (2007) 567–578.
- [8] P.J.M. Monteiro, P.K. Mehta, The transition zone between aggregate and type k expansive cement, *Cem. Concr. Res.* 16 (1986) 111–114.
- [9] P.E. Grattan-Bellew, J.J. Beaudoin, V.G. Vallee, Effect of aggregate particle size and composition on expansion of mortars bars due to delayed ettringite formation, *Cem. Concr. Res.* 28 (8) (1998) 1147–1156.
- [10] X. Brunetaud, Etude de l'influence de différents paramètres et de leurs interactions sur la cinétique et l'amplitude de la réaction sulfatique interne, Ecole Centrale de Paris (2005) (Phd thesis).
- [11] M. Al Shamaa, S. Lavaud, L. Divet, J.B. Colliat, G. Nahas, J.-M. Torrenti, Influence of limestone filler and of the size of the aggregates on def, *Cem. Concr. Compos.* 71 (2016) 175–180.
- [12] C.D. Lawrence, Mortar expansions due to delayed ettringite formation. Effect of curing period and temperature, *Cem. Concr. Res.* 25 (1995) 903–914.
- [13] B. Kchakech, Etude de l'influence de l'échauffement subi par un béton sur le risque d'expansions associées à la réaction sulfatique interne, Université Paris-Est (2015) (Phd thesis).
- [14] A.E. Moore, H.F.W. Taylor, Crystal structure of ettringite, *Acta Crystallogr. A* 26 (4) (1970) 386–393.
- [15] C. Famy, K.L. Scrivener, A. Atkinson, A.R. Brough, Influence of the storage conditions on the dimensional changes of heat-cured mortars, *Cem. Concr. Res.* 31 (2001) 795–803.
- [16] D. Heinz, U. Ludwig, I. Rüdiger, Delayed ettringite formation in heat treated mortars and concretes, *Concr. Precasting Plants Technol.* 11 (1989) 56–61.
- [17] L. Graf, Effect of relative humidity on expansion and microstructure of heat-cured mortars, *Portland Cem. Assoc.* (2007) 50.
- [18] R.-P. Martin, Experimental analysis of the mechanical effects of delayed ettringite formation on concrete structures, Université Paris-Est (2010) (Phd thesis).
- [19] M. Al Shamaa, S. Lavaud, L. Divet, G. Nahas, J.-M. Torrenti, Influence of relative humidity on delayed ettringite formation, *Cem. Concr. Compos.* 58 (2015) 14–22.
- [20] M.M. Karthik, J.B. Mander, S. Hurllebaus, ASR/DEF related expansion in structural concrete: model developments and validation, *Constr. Build. Mater.* 128 (2016) 238–247.
- [21] A. Sellier, S. Multon, Chemical modelling of delayed ettringite formation for assessment of affected concrete structures, *Cem. Concr. Res.* 108 (2018) 72–86.
- [22] M.M. Karthik, J.B. Mander, S. Hurllebaus, Modeling ASR/DEF expansion strains in large reinforced concrete specimens, *J. Struct. Eng.* 144 (7) (2018) 04018085.
- [23] B. Nedjar, A time dependent model for unidirectional fibre-reinforced composites with viscoelastic matrices, *Int. J. Solids Struct.* 48 (2011) 2333–2339.
- [24] B. Nedjar, R. Le Roy, An approach to the modeling of viscoelastic damage. Application to the long-term creep of gypsum rock materials, *Int. J. Numer. Anal. Methods Geomech.* 37 (2014) 1066–1078.
- [25] N. Baghdadi, Modélisation du couplage chimico-mécanique d'un béton atteint d'une réaction sulfatique interne, Université Paris-Est (2008) (Phd thesis).
- [26] C. Larive, Apports combinés de l'expérimentation et de la modélisation à la compréhension de l'alcali-réaction et de ses effets mécaniques, Laboratoire Central des Ponts et Chaussées, OA 28, 1998.
- [27] J.-F. Seignol, N. Baghdadi, F. Toutlemonde, A macroscopic chemo-mechanical model aimed at re-assessment of def-affected concrete structures, in: International Conference on Computational Technologies in Concrete Structures, CTCS'09, Korea, 2009, pp. 422–440.
- [28] S. Poyet, Etude de la dégradation des ouvrages en béton atteints par la réaction alcali-silice: Approche expérimentale et modélisation numérique multi-échelle des dégradations dans un environnement hydro-chemo-mécanique variable, Université de Marne-la-Vallée (2003) (Phd thesis).
- [29] B. Nedjar, On a concept of directional damage gradient in transversely isotropic materials, *Int. J. Solids Struct.* 88–89 (2016) 56–67.

8.2 Conclusions

The work presented in this paper aims to develop a model to predict the deformation of cementitious materials by taking into account several phenomena: plastic deformation of the material, thermal expansion, hydric expansion and expansion due to the delayed formation of ettringite.

For the first three phenomena mentioned above, the literature presents models whose validity has already been demonstrated. Thus, we focus here on the influence of DEF in the deformation, and in particular on the importance of relative humidity in the development of this phenomenon. Chemically, the water supply required for DEF is known and the literature includes kinetic behavioural models for water saturation of the material. The experimental campaigns carried out make it possible to highlight the impact of relative humidity over time on the deformation of the material through the submission of specimens to soaking/drying cycles. It then appears that a relative humidity threshold value is required for the DEF. For a relative humidity below this value, ettringite formation is not possible. It is thus possible using soaking/drying cycles to characterize the DEF for a relative humidity above this threshold, but for a configuration not saturated with water. It was then determined the expression and participation of the intrinsic parameters of the material influencing the kinetics of DEF under fixed water conditions, as well as their contribution to the overall deformation of the material samples.

From a numerical point of view, the simulations made it possible to validate the prediction model developed and to obtain results that were consistent with the experiments. The implementation of these results in the prediction of the deformation of a material sample makes it possible to consider using the model developed in larger-scale simulations with a finite element method.

Further studies are planned to enrich this model, taking into account additional phenomena such as creep, plasticity and damage.

References

- Al Shamaa, M., S. Lavaud, L. Divet, J. B. Colliat, et al. (2016). “Influence of limestone filler and of the size of the aggregates on DEF”. In: *Cement and Concrete Composites* 71, pp. 175–180.
- Al Shamaa, M., S. Lavaud, L. Divet, G. Nahas, et al. (2014). “Coupling between mechanical and transfer properties and expansion due to DEF in a concrete of a nuclear power plant”. In: *Nuclear Engineering and Design* 266, pp. 70–77.
- (2015). “Influence of relative humidity on delayed ettringite formation”. In: *Cement and Concrete Composites* 58, pp. 14–22.
- Al Shamaa, Mohamad (2012). “Etude du risque de développement d’une réaction sulfatique interne et de ses conséquences dans les bétons de structure des ouvrages nucléaires”. PhD thesis. Université Paris-Est.
- Bagdadi, Nizar (2008). “Modélisation du couplage chimico-mécanique d’un béton atteint d’une réaction sulfatique interne”. PhD thesis. Ecole Nationale des Ponts et Chaussées.
- Barbarulo, R. et al. (2005). “Delayed ettringite formation symptoms on mortars induced by high temperature due to cement heat of hydration or late thermal cycle”. In: *Cement and Concrete Research* 35(1), pp. 125–131.
- Barbarulo, Remi (2002). “Comportement des matériaux cimentaires : actions des sulfates et de la température”. PhD thesis. École Normale Supérieure de Cachan.
- Bazant, Z.-P. (1972). “Nonlinear water diffusion in nonsaturated concrete”. In: *Matériaux et constructions* 5(25), pp. 3–20.
- Bouzabata, H et al. (2012). “Swellings due to alkali-silica reaction and delayed ettringite formation: Characterisation of expansion isotropy and effect of moisture conditions”. In: *Cement and Concrete Composites* 34(3), pp. 349–356.
- Brunetaud, X. et al. (2007). “Effect of curing conditions and concrete mix design on the expansion generated by delayed ettringite formation”. In: *Materials and Structures* 40, pp. 567–578.
- Brunetaud, Xavier (2005). “Etude de l’influence de différents paramètres et de leurs interactions sur la cinétique et l’amplitude de la réaction sulfatique interne au béton”. PhD thesis. Ecole Centrale Paris.
- Damidot, D. and F.P. Glasser (1993). “Thermodynamic investigation of the CaO-Al₂O₃-CaSO₄-H₂O system at 25 °C and the influence of Na₂O”. In: *Cement and Concrete Research* 23(1), pp. 221–238.
- Day, R.L. (1992). “The Effect of Secondary Ettringite Formation on the Durability of Concrete: A Literature Analysis”. In: *Tech. rept. Portland Cement Association*.
- Diamond, S. (2004). “Delayed ettringite formation : A current assessment, Internal Sulfate Attack and Delayed Ettringite Formation”. In: *Proceedings of the International RILEM TC 186-ISA Workshop, PRO 35*.

- Divet, L. and R. Randriambololona (1998). “Delayed Ettringite Formation: The Effect of Temperature and Basicity on the Interaction of Sulphate and C-S-H Phase”. In: *Cement and Concrete Research* 28(3), pp. 357–363.
- Divet, Loïc (2001). “Les réactions sulfatiques internes au béton : contribution à contribution à l’étude des mécanismes de la formation différée de l’ettringite”. PhD thesis. Conservatoire National des Arts et Métiers.
- Escadeillas, G. et al. (2007). “Some factors affecting delayed ettringite formation in heat-cured mortars”. In: *Cement and Concrete Research* 37(10), pp. 1445–1452.
- Famy, C. (1999). “Expansion of heat-cured mortars”. PhD thesis. University of London.
- Famy, C. et al. (2001). “Influence of the storage conditions on the dimensional changes of heat-cured mortars”. In: *Cement and Concrete Research* 31, pp. 795–803.
- Fu, Y. (1996). “Delayed Ettringite Formation in Portland Cement Products”. PhD thesis. CNRC, Ottawa, Canada.
- Fu, Y., J. Ding, and J.J. Beaudoin (1997). “Expansion of portland cement mortar due to internal sulfate attack”. In: *Cement and Concrete Research* 27(9), pp. 1299–1306.
- Godart, B. and L. Divet (2013). *Lessons learned from structures damaged by delayed ettringite formation and the French prevention strategy*. Tech. rep. Université Paris-Est, IFSTTAR.
- Graf, L. (2007). “Effect of relative humidity on expansion and microstructure of heat-cured mortars”. In: *Portland Cement Association*, p. 50.
- Grattan-Bellew, P. E., J. J. Beaudoin, and V. G. Vallee (1998). “Effect of aggregate particle size and composition on expansion of mortars bars due to delayed ettringite formation”. In: *Cement and Concrete Research* 28(8), pp. 1147–1156.
- Heinz, D., M. Kalde, et al. (1999). “Present State of Investigation on Damaging Late Ettringite Formation (DLEF) in Mortars and Concretes in Ettringite the Sometimes Host of Destruction”. In: *ACI International SP 177-1*, pp. 1–14.
- Heinz, D. and U. Ludwig (1987). “Mechanism of Secondary Ettringite Formation in Mortars and Concretes Subjected to Heat Treatment”. In: *ACI* 100, pp. 2059–2072.
- Heinz, D., U. Ludwig, and I. Rudiger (1989). “Delayed ettringite formation in heat treated mortars and concretes”. In: *Concrete Precasting Plants and Technology* 11, pp. 56–61.
- Hime, W.G. and S.L. Marusin (1999). “Delayed ettringite formation: many questions and some answers - Ettringite, the sometimes host of destruction”. In: *ACI International SP-177*, pp. 199–206.
- Karthik, M. M., J. B. Mander, and S. Hurlebaus (2016). “ASR/DEF related expansion in structural concrete: model developments and validation”. In: *Construction and Building Materials* 128, pp. 238–247.
- Kelham, S. (1996). “The effect of cement composition and fineness on expansion associated with delayed ettringite formation”. In: *Cement and Concrete Composites* 18, pp. 171–179.
- Larive, C. (1998). *Apports combinés de l’expérimentation et de la modélisation à la compréhension de l’alcali-réaction et de ses effets mécaniques*. Laboratoire Central des Ponts et Chaussées, OA 28.
- Lawrence, C. D. (1995). “Mortar expansions due to delayed ettringite formation. Effect of curing period and temperature”. In: *Cement and Concrete Research* 25, pp. 903–914.
- Lawrence, C.D. (1999). *Long-term expansion of mortars and concretes, volume SP 177, chapter Ettringite the sometimes host of destruction*. American Concrete Institute International, Farmington Hills, MI, USA, B. Erlin edition.
- Leklou, Nordine (2008). “Contribution à la connaissance de la réaction sulfatique interne”. PhD thesis. Université de Toulouse.

- Li, G., P. Le Bescop, and M. Moranville (1996). "Expansion Mechanism Associated with the Secondary Formation of the U Phase in Cement-Based Systems Containing High Amounts of Na_2SO_4 ". In: *Cement and Concrete Research* 26, pp. 195–201.
- M.C., Lewis, Scrivener K.L., and Kelham S. (1995). "Heat Curing and Delayed Ettringite Formation". In: *Materials Research Society Symposium Proceedings, Boston, Massachusetts*, pp. 67–76.
- Magnus, A., N. Lars-Olof, and M. Ben Haha (2015). "A method to determine the critical moisture level for unsaturated transport of ions". In: *Materials and Structures (RILEM)* 48(1-2), pp. 53–65.
- Martin, R.-P. (2010). "Experimental analysis of the mechanical effects of Delayed Ettringite Formation on concrete structures". PhD thesis. Université Paris-Est.
- Martin, R.-P., O. Omikrine Metalsi, and F. Toutlemonde (2013). "Importance of considering the coupling between transfer properties, alkali leaching and expansion in the modelling of concrete beams affected by internal swelling reactions". In: *Construction and Building Materials* 49, pp. 23–30.
- Martin, R.P. et al. (2012). "Experimental evidence for understanding DEF sensitivity to early-age thermal history". In: *RILEM PRO-85, ConCrack 3*, pp. 45–54.
- Mehta, P.K. (1973). "Mechanism of Expansion Associated with Ettringite Formation". In: *Cement and Concrete Research* 3, pp. 1–6.
- Mensi, R., P. Acker, and A. Attolou (1988). "Séchage du béton: analyse et modélisation". In: *Materials and Structures* 21, pp. 3–10.
- Monteiro, P. J. M. and P. K. Mehta (1986). "The transition zone between aggregate and type K expansive cement". In: *Cement and Concrete Research* 16, pp. 111–114.
- Moore, A. E. and H. F. W. Taylor (1970). "Crystal Structure of Ettringite". In: *Acta Crystallographica* 26(4), pp. 386–393.
- Multon, S. (2003). "Evaluation expérimentale et théorique des effets mécaniques de l'Alcali-Réaction sur des structures modèles". PhD thesis. Université de Marne-la-Vallée.
- Nedjar, B. (2016). "On a concept of directional damage gradient in transversely isotropic materials". In: *International Journal of Solids and Structures* 88-89, pp. 56–67.
- Nedjar, B. and R. Le Roy (2014). "An approach to the modeling of viscoelastic damage. Application to the long-term creep of gypsum rock materials". In: *International Journal for Numerical and Analytical Methods in Geomechanics* 37, pp. 1066–1078.
- Odler, I. and Y. Chen (1995). "Effect of cement composition on the expansion of heat-cured cement pastes". In: *Cement and Concrete Research* 25(4), pp. 853–862.
- Pavoine, A., X. Brunetaud, and L. Divet (2012). "The impact of cement parameters on Delayed Ettringite Formation". In: *Cement and Concrete Composites* 34, pp. 521–528.
- Pavoine, Alexandre (2003). "Évaluation du potentiel de réactivité des bétons vis-à-vis de la formation différée de l'ettringite". PhD thesis. Université Pierre et Marie Curie.
- Petrov, N. (2003). "Effets combinés de différents facteurs sur l'expansion des bétons causée par la formation différée de l'ettringite". PhD thesis. Université de Sherbrooke.
- Ramlochan, T. et al. (2003). "The effect of pozzolans and slag on the expansion of mortars cured at elevated temperature: Part I: Expansive behaviour". In: *Cement and Concrete Research* 33(6), pp. 807–814.
- Sahu, S. and N. Thaulow (2004). "Delayed ettringite formation in Swedish concrete railroad ties". In: *Cement and Concrete Research* 34(9), pp. 1675–1681.
- Santos Silva, A. et al. (2006). "The use of fly ash and metakaolin for the prevention of alkali-silica reaction and delayed ettringite formation in concrete". In: *Performance based evaluation and indicators for concrete durability: proceedings of the International Rilem Workshop*.

- Scivner, K.L. and H.F.W. Taylor (1993). "Delayed ettringite formation: a microstructural and microanalytical study". In: *Advances in Cement Research* 20, pp. 139–146.
- Seignol, J.-F., N. Baghdadi, and F. Toutlemonde (2009). "A macroscopic chemo-mechanical model aimed at re-assessment of DEF-affected concrete structures". In: *International Conference on Computational Technologies in Concrete Structures, CTCS'09*. Korea, pp. 422–440.
- Sellier, A. and S. Multon (2018). "Chemical modelling of Delayed Ettringite Formation for assessment of affected concrete structures". In: *Cement and Concrete Research* 108, pp. 72–86.
- Taylor, H. F. W., C. Famy, and K. L. Scrivener (2001). "Delayed ettringite formation". In: *Cement and Concrete Research* 31, pp. 683–693.
- Thomas, M et al. (2008). "Diagnosing delayed ettringite formation in concrete structures". In: *Cement and Concrete Research* 38(6), pp. 841–847.
- Torrenti, J.-M. et al. (1999). "Modeling Concrete Shrinkage under Variable Ambient Conditions". In: *ACI Materials Journal* 96, pp. 35–39.
- Tosun, K. (2006). "Effect of SO₃ content and fineness on the rate of delayed ettringite formation in heat cured Portland cement mortars". In: *Cement and Concrete Composites* 28(9), pp. 761–772.
- Yang, R. et al. (1999). "Delayed ettringite formation in heat-cured Portland cement mortars". In: *Cement and Concrete Research* 29(1), pp. 17–25.
- Zhang, Z., J. Olek, and S. Diamond (2002). "Studies on delayed ettringite formation in heat-cured mortars: II - Characteristics of cement that may be susceptible to DEF". In: *Cement and Concrete Research* 32(11), pp. 1737–1742.

Chapter 9

Conclusions and perspectives

The main objective of this thesis work was to highlight and understand the participation of aggregates in damage mechanisms under hydric and/or chemical stress. First, aggregate parameters were identified in an introductory chapter. Then bibliographic studies on desiccation (Chapter 2) and DEF (Chapter 5) were conducted, focusing on the role of aggregates, which allowed the selection of influential aggregate parameters. On the one hand, it is the size and volume fraction of aggregates for desiccation, and on the other hand, the mineralogical nature for DEF. Parametric experimental campaigns have been set up to highlight the influence of these parameters on the evolution of the material, its transfer and mechanical properties as well as on cracking.

On one hand, the desiccation study is carried out on so-called morphologically controlled materials, i.e. with controlled granular skeleton, in order to decouple the effects of the aggregates. Seven formulations are subjected to an environment where the temperature is set at 25°C and the relative humidity at 30% for 200 days. They are monitored throughout the experimental procedure and different test milestones have been set to evaluate the performance of the materials and their evolution. In addition, observations of cracking patterns were made via optical microscopy and the use of an X-ray microtomograph. These tests revealed a strong influence of the size of the aggregates and the volume fraction of aggregates in the concrete, on the evolution of delayed deformations, as well as on the mechanical properties and cracking. On the other hand, they also show that transfer properties are only slightly influenced by these mechanisms.

On the other hand, delayed ettringite is studied on conventional materials, whose mineralogical nature varies (limestone or silica), and subjected to a heat treatment of 80°C for 3 days. The same experimental methodology has been used: monitoring of delayed deformations and regular evaluations of the material properties. These tests highlighted the important influence of the mineralogical nature of the aggregates on both the kinetics and the rate of progression of the pathology, as well as on the mechanical properties.

In a final chapter, the coupling between the two solicitations was studied. A conventional concrete formulation, based on calcareous aggregates, was subjected to imbibition-drying cycles to evaluate the effect of hydric damage on the progression of DEF. This has shown that the crystallization reaction of the delayed ettringite is completely stopped during the drying times, and if the soaking water is not replaced between each soaking period, the reaction resumes its course according to the initial evolution. No significant change in kinetics or expansion rates was observed once the notion of effective imbibition time was introduced. This confirms the observations of Al Shamaa [AlShamaa12], who showed that the water atmosphere was very decisive on the initialization and progression of the pathology.

Based on the work carried out within the framework of this thesis, several proposals for complementary campaigns and future research axes can be identified:

- Completing the mechanical characterisation campaigns with a complete chemical characterisation of our materials in their different states of evolution. These tests would verify the conclusions proposed in the different studies.
- In the thesis, the hydric stresses are characterised by the environmental relative humidity. However, it would be interesting to assess the sorption curves of the different materials used in our campaigns in order to fully characterise the saturation levels in the materials and conclude more precisely on the mechanisms at stake.
- It would be interesting to take the cracking observations further and work on volume correlation, which shows promising results in our preliminary study. This would allow an assessment of cracking mechanisms, cracks distribution and openings. In addition, a thorough understanding of this cracking phenomena would allow a better appreciation of the contribution of pathology-induced cracking to mechanical failure mechanisms.
- It could be adapted to complete the different campaigns by choosing intermediate parameter values in order to identify potential behavioural laws.
- The different results presented in this thesis can be used to enrich homogenized numerical models; for example, through damage laws depending on aggregate parameters on the model developed by [Hubert 2004]; or mesoscopic models, as used by [Benkemoun, Roubin, and J.-B. Colliat 2017] and [El Sawda et al. 2019], through the use of information on the influence of aggregates on ITZs and the damage induced at its level.

Appendix A

Materials composition

A.1 Composition of cement : CEM II/A-LL 42,5 R

Constituent	Mass fraction (%)
SiO ₂	19.37
Al ₂ O ₃	4.58
Fe ₂ O ₃	3.06
TiO ₂	0.28
MnO	0.07
CaO	63.66
MgO	1.30
SO ₃	2.87
K ₂ O	1.20
Na ₂ O	0.15
P ₂ O ₅	0.50
Na ₂ O _{eq}	0.96
S ²⁻	<0,02
Cl ²⁻	0.03

Table A.1 – Cement chemical composition

Constituent	Mass fraction (%)
Clinker	92
Limestone addition	6
Other	2

Table A.2 – Cement composition

Constituent	Mass fraction (%)
C3S	65.7
C2S	9.8
C3A	7.4
C4AF	11.4

Table A.3 – Clinker mineralogical composition

A.2 Composition of Boulonnais aggregates

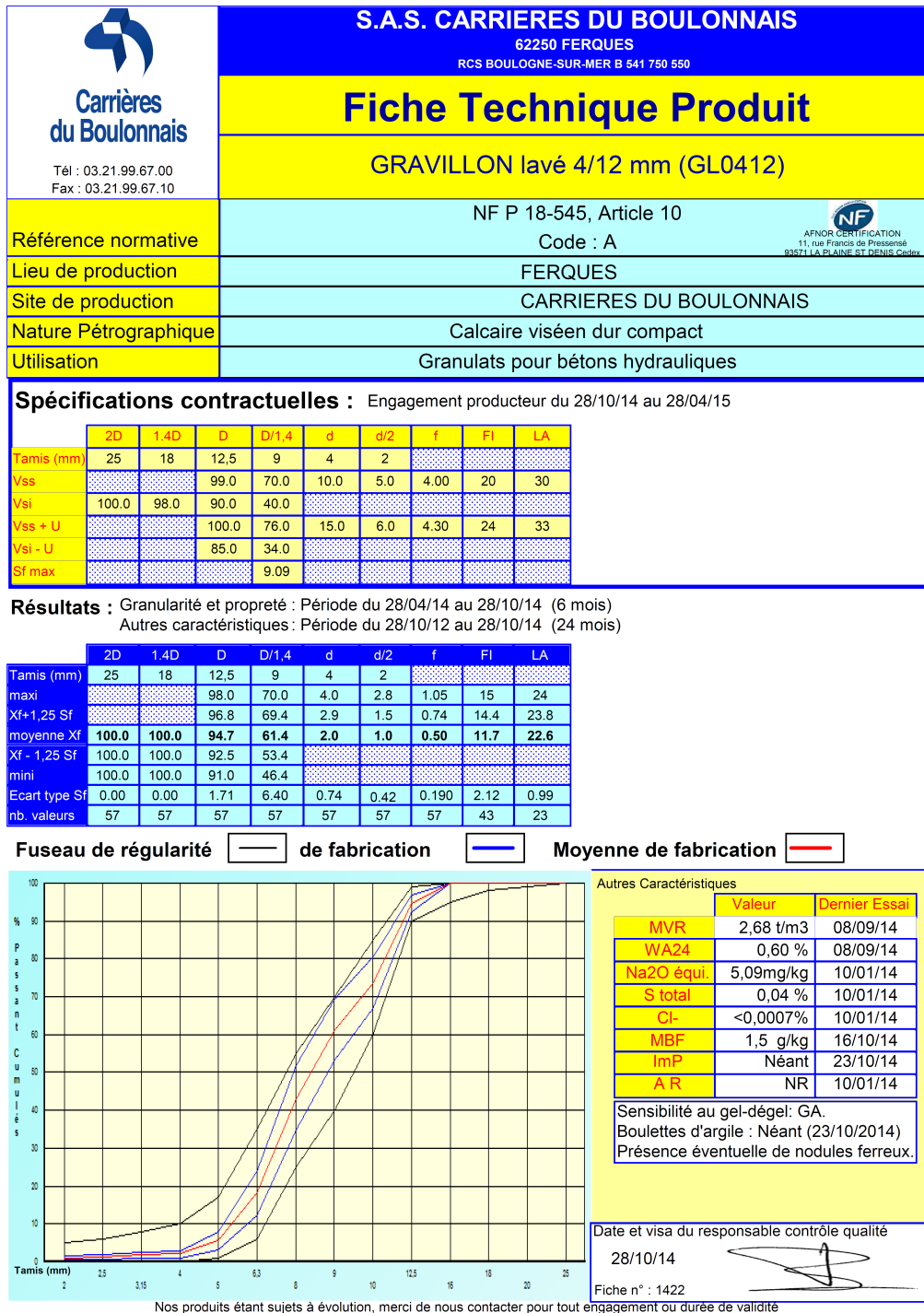
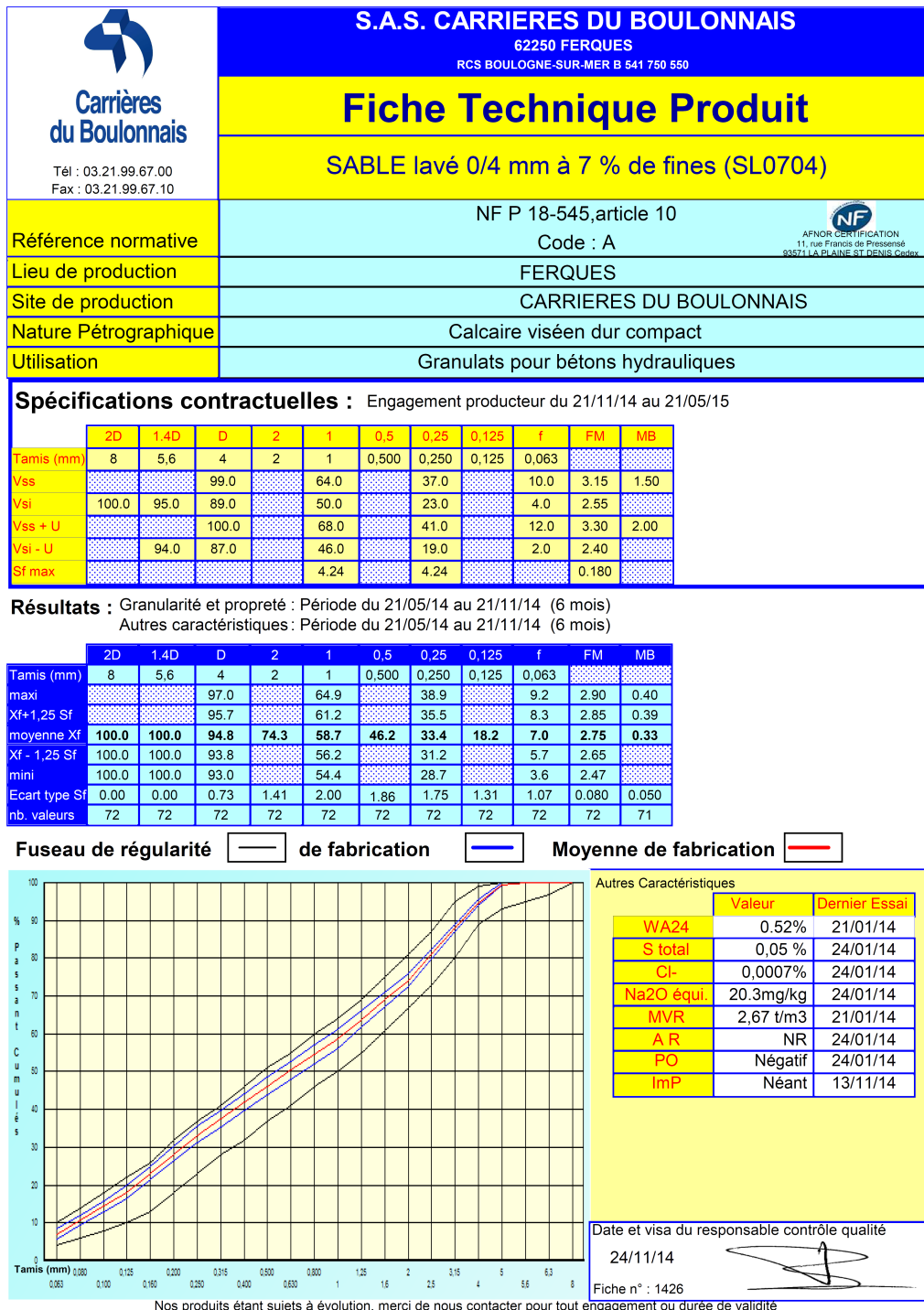


Figure A.1 – Boulonnais aggregates technical sheet



Appendix B

Article de Projet d'Initiation à la Recherche de Matthieu Briat, Élève de Master 1 : *Experimental study on the effect of a viscosity modifying admixture on the delayed deformations and mechanical properties of cement-based materials.*

Experimental study on the effect of a viscosity modifying admixture on the delayed deformations and mechanical properties of cement-based materials

M. Briat^(a) and M. Malbois^(b)

(a) ENS – Paris-Saclay, 61 Avenue du Président Wilson 94230 CACHAN
matthieu.briat@ens-paris-saclay.fr;

(b) LMT, ENS – Paris-Saclay, 61 Avenue du Président Wilson 94230 CACHAN
malbois@lmt.ens-cachan.fr

Abstract

The use of admixtures in cementitious materials makes it possible, in certain cases, to modify their properties in the short term, i.e. in their fluid state. However their introduction in a formulation can have an impact on the long term, more especially on the delayed behaviour. The objective of this article is to present the effect of the viscosity modifying admixture Sika® Stabilizer 400 on the behaviour of cement-based materials. This additive is used to increase the viscosity of the mix and to eliminate the phenomenon of segregation. An experimental campaign is conducted on mortar and cement paste with and without Sika® Stabilizer 400. The delayed deformations, mechanical properties, cracking and geometrical characteristics of these two materials are studied. These tests have shown that the admixture allows the good homogenisation of the material. It reduces the bleeding phenomenon during manufacturing, without preventing it completely. As the cement is better hydrated, the mechanical characteristics of the material are therefore assured. Moreover, this study shows that, if the formulation is adapted, the use of an adjuvant has neither an impact on the drying phenomena, nor the delayed deformations and the mechanical properties. Finally, the admixture tends to reduce the amount of cracking induced by desiccation.

I. Introduction

The viscosity modifying admixture Sika® Stabilizer 400 was used in a previous experimental campaign to prevent segregation in model materials. These materials were then studied under drying conditions. However, this additive was not part of the reference formulation studied, and its possible effects on the behaviours induced by drying were not quantified.

This paper takes an interest in two compositions: cement paste and mortar, and different properties are therefore studied. To begin with, the shrinkage by drying is analysed. It is completed by an analysis of the endogenous shrinkage which will make it possible to characterize the desiccation shrinkage. The shrinkage study is completed by a characterization of the mass loss of the materials.

The mechanical characteristics are determined by three-point bending tests. Finally, a cracking observation is conducted.

II. Materials

The study was carried out on mortar and cement paste with or without admixture. The cement used to manufacture the test pieces was Calcia CEM II/A-LL 42.5. The sand needed to make the mortar is 0/4mm washed sand with 7% fines (Boulonnais). The viscosity builder is Sika® Stabilizer 400.

Several characteristics are settled for the compositions:

- Water cement ratio: $W/C = 0.57$;
- Sand proportion: 32% of the total volume;

- Admixture proportion: 1.6% of the cement weight. This proportion was defined in the previous study in order to optimize the rheological properties.

The compositions are presented in Table 1.

Table 1 : Mortar and cement paste compositions

Materials	Mortar		Cement paste	
	With admixture	Without admixture	With admixture	Without admixture
Sand	854 kg	854 kg	-	-
Cement	750 kg	763 kg	1102 kg	1122 kg
Water	427 kg	435 kg	628 kg	639 kg
Admixture	12 kg	-	17.6 kg	-
Density mass	2043 kg/m³	2052 kg/m³	1746.7 kg/m³	1761 kg/m³

III. Experimental procedure

III. 1. Procedure

Each formulation follows the same experimental procedure presented in Figure 1.

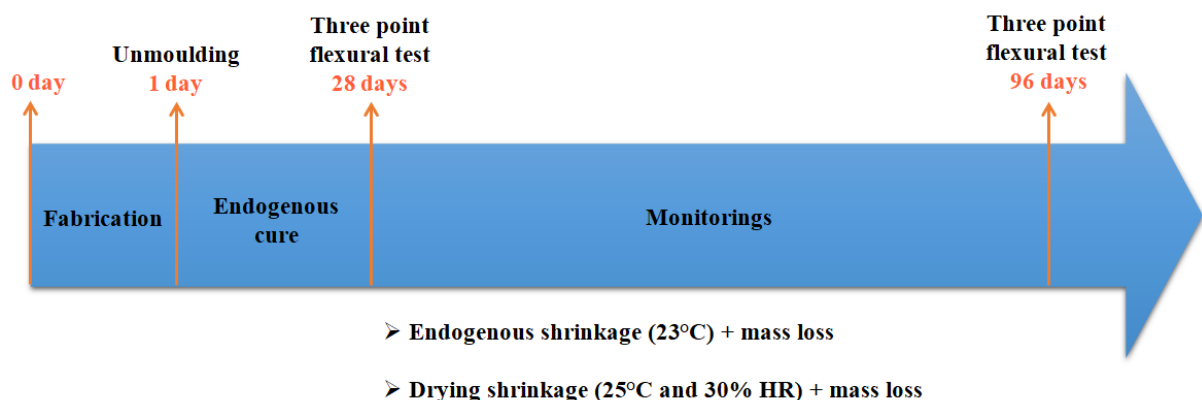


Figure 1 : Experimental procedure for each formulation

After the endogenous cure, a monitoring of the endogenous shrinkage of the drying shrinkage is carried out. At the same time, the drying phenomenon is characterised by the monitoring of the samples mass losses. Finally, mechanical characterisation is performed after the endogenous cure and at the end of the procedure, when the samples have reached the age of 96 days.

III. 2. Protocols

III.2. a. Conditioning of the samples

The study is carried out on 4x4x16 cm prismatic specimens. 24 hours after casting, the samples are unmoulded. They are then packed with 2 layers of aluminium foil to undergo an endogenous cure of 28 days at a temperature of 23°C.

After that period, specimens are separated in three categories:

- Specimens used to assess the material characteristics at the end of the cure;
- Specimens used to study drying;
- Specimens kept in endogenous conditions.

Specimens used to study desiccation are unwrapped and then put in a room controlled in temperature (25°C) and relative humidity (30%HR). Moreover, one layer of aluminium foil is placed on the superior and inferior 4x4cm faces of each specimen.

III.2. b. Monitoring

Mass loss and shrinkage are regularly measured on each formulation.

The device showed in Figure 2 is used to measure the shrinkage. The specimen is placed on the device by apparatus made of brass embedded at the top and to bottom of the sample. The lower embedded apparatus rests on the base while the upper one is locked by a dial gauge to measure shrinkage. The comparator accuracy is $\pm 2\mu\text{m}$. A scale with an accuracy of $\pm 0.1\text{g}$ is used to weigh regularly the specimens.



Figure 2: Device to measure shrinkage.

III.2. c. Three-point flexural test

Three-point flexural tests are performed at different steps of the study on each composition:

- The first series of tests is performed 28 days after the specimen fabrications, at the end of the endogenous cure.
- The second series is performed at the end of the procedure.

Three prismatic specimens (4x4x16 cm) are tested for each test of each formulation.

Figure 3 shows the system for the three-point flexural test. An apparatus is fixed on the specimen, on which a LVDT comparator is fixed ($\pm 0.01\mu\text{m}$) allowing the measure of the displacement in the middle of the specimen. The test is controlled with the loading parameter, at a speed of 0.5 mm/s.



Figure 3: Device for the 3 points flexural test.

From this test, the flexural strength is determined from equation (1).

$$R_f = \frac{3 F L}{2 b h^2} \quad (1)$$

In this equation:

- R_f is the bending strength [MPa] ;
- F is the maximum applied force [N] ;
- L is the distance between supports [mm] ;
- b is the base of the specimen section [mm] ;
- h is the height of the specimen section [mm].

In addition, the evolution of the applied force as a function of deformation can be drawn. The stiffness of the material is deduced from this curve: it is the slope of the curve, between 10% and 30% of the maximal force. Thus, the Young Modulus of material is determined from equation (2).

$$E = \frac{K L^3}{4 b h^3} \quad (2)$$

In this equation:

- E is the Young's Modulus [MPa] ;
- K is the stiffness [N/mm] ;
- L is the distance between supports [mm] ;
- b is the base of the specimen section [mm] ;
- h is the height of the specimen section [mm].

III.2. d. Observation of cracking

For each composition, the impact of the use of the admixture on superficial cracking is observed. The study is performed on an area of one specimen (see Figure 4). Cracks were measured and counted thanks to a numerical microscope KEYENCE (see Figure 4). The crack size is measured with an average of five measures. In this way, for each composition, the average, maximum and minimum crack widths and the cracks linear density (number of cracks/cm) are measured

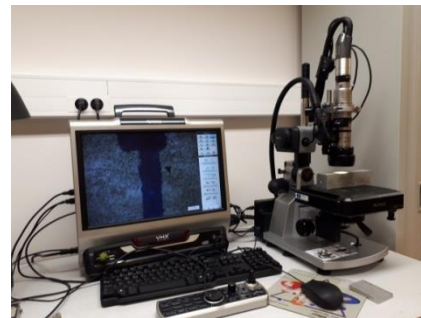
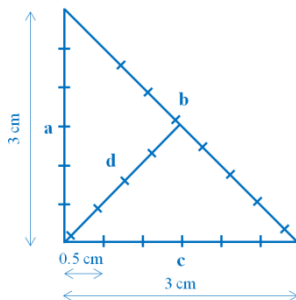


Figure 4 : Crack study area at left and microscope at right

III.2. e. Observation of samples characteristics

After the three-point bending tests, two characteristics can be observed on the cracking surfaces.

The first characteristic is the real geometry of the sample. Indeed, the samples geometries are not 40x40 cm as in theory. This variation in is due to the possible imperfections of the mould, to the

casting process and especially to the bleeding of cementitious material. This bleeding leads to the formation of a layer of water on the top of the sample after its manufacture. This layer of water does not participate to the hydration of the cement, and evaporates. As a consequence, the samples do not have the expected geometry, and water-cement ratio. The real specimen cross-section is measured using a calliper with an accuracy of ± 0.01 mm.

The second characteristic is the distribution of the materials constituting the sample. Thus it can be seen whether a segregation phenomenon has occurred during manufacture.

IV. Results and analysis

IV. 1. Impact on endogenous delayed behaviour

IV.1. a. Endogenous mass

Figure 5 displays the evolution of the mass loss as a function of time root for the four formulations under endogenous conditions.

- The mass loss increases with time for the four formulations;
- Mass loss after 96 days of study is less than 0.2% for all formulations;

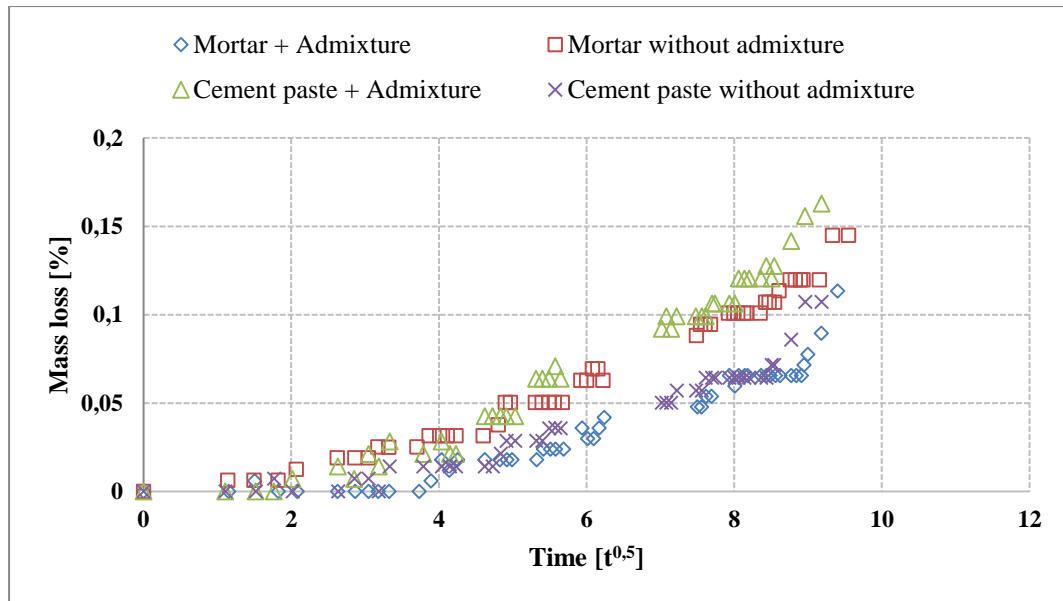


Figure 5 : Evolution of mass loss as a function of the root of time in endogenous conditions

A normalisation of the mass loss thus makes it possible to have a better comparison. This normalisation is obtained by equation (3).

$$M_{normed} = \frac{1}{f_{cp}} \frac{\rho_{specimen}}{\rho_w} M \quad (3)$$

- M_{normed} is the standard mass ;
- f_{cp} is the volume fraction of cement paste, between 0 and 1 ;
- $\rho_{specimen} = \frac{M_i}{V_{th}}$ is the average density of the test pieces studied. Calculated with the mass at each instant M_i and the theoretical volume of the test piece V_{th} ;
- ρ_w is the water density ;
- M is the mass to be standardized.

Figure 6 shows the evolution of the normed mass loss as a function of time root for the four formulations under endogenous conditions.

- The mass loss increases with time for the 4 formulations;
- The evolution of the mortar and the cement paste with admixture is essentially identical;
- Mass loss after 96 days of study is less than 0.5% after normalisation for all formulations;

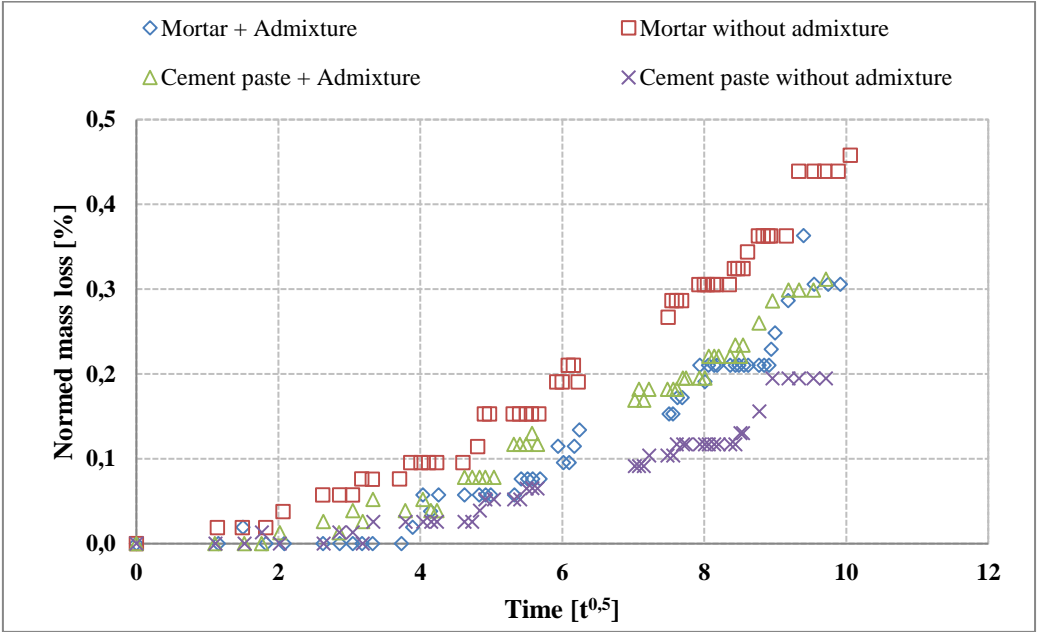


Figure 6 : Evolution of mass loss normed as a function of the root of time in endogenous conditions

IV.1. b. Endogenous shrinkage

Figure 7 and Figure 8 show the evolution of the deformation respectively as a function of the square root of time or of the normed mass loss. The four formulations are represented under endogenous conditions.

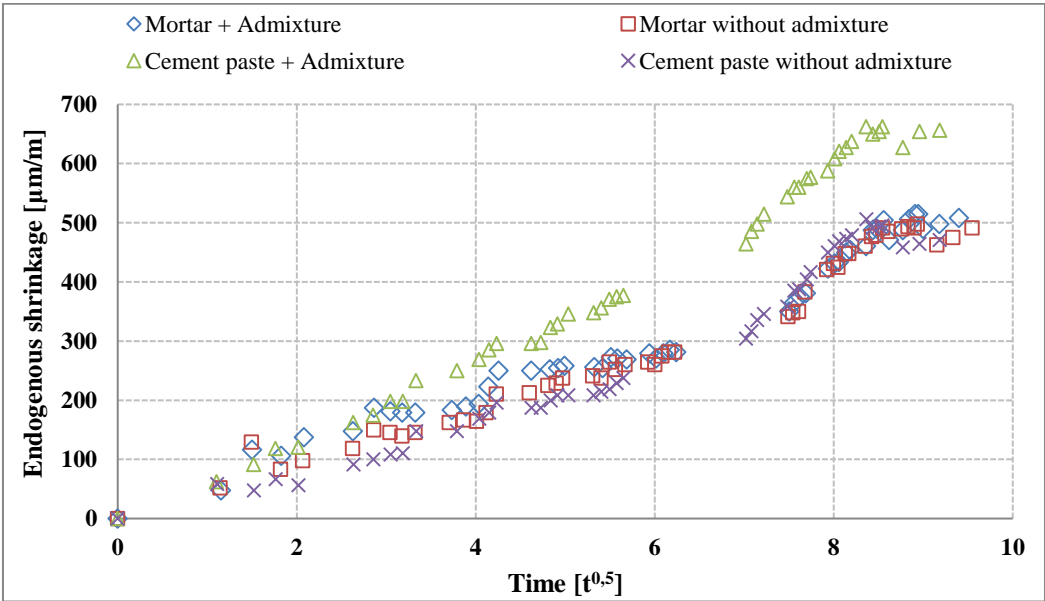


Figure 7 : Evolution of deformation as a function of the root of time in endogenous conditions

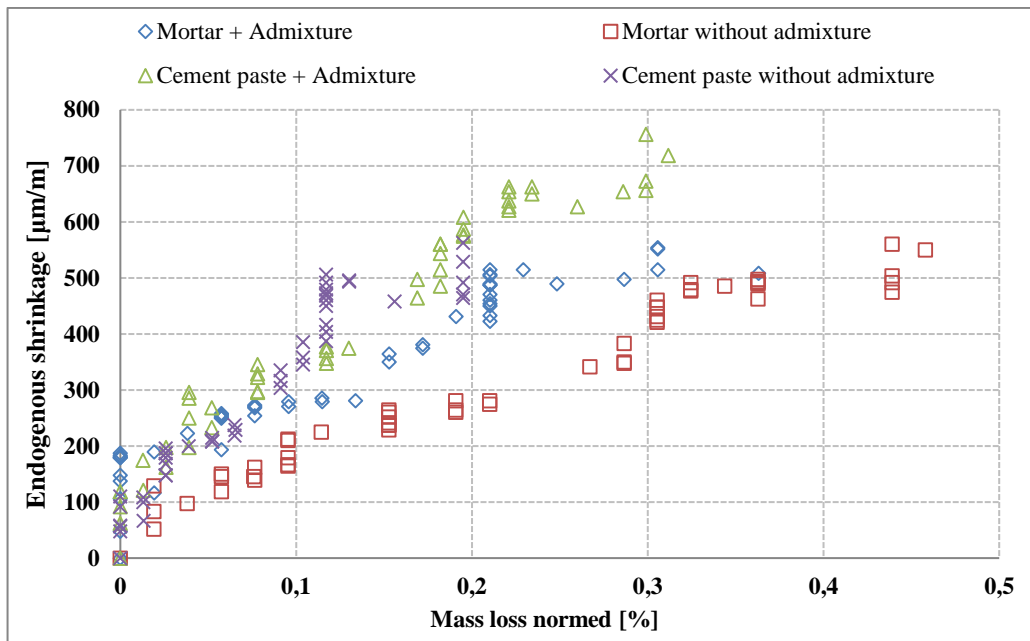


Figure 8 : Evolution of deformation as a function of mass loss normed in endogenous conditions

It can be noticed that:

- Endogenous shrinkage increases with time and with mass loss for all formulations;
- The evolution of the endogenous shrinkages of the cement paste with admixture is superior to the 3 other formulations;
- The deformations of the mortar with admixture, the mortar without admixture and the cement paste without admixture very similar under endogenous conditions;
- The endogenous shrinkage remains inferior to 700 $\mu\text{m}/\text{m}$ throughout the study;
- The evolution of endogenous shrinkage of all formulations is proportional to their mass loss. This reveals that, even if precautions were taken to completely seal the samples, the samples suffered parasite drying.

We have seen here that the cement paste formulations tend to shrink more than the mortar formulations, due to the presence of aggregates and thus difference of cement paste quantities in the samples.

Also, it was noticed that shrinkage is greater for cement paste with admixture than without admixture. This difference is not noticeable in the case of mortar. Two hypotheses could be made regarding this difference of behaviour. In the absence of admixture, either, the homogenisation of the cement paste is not good, and the presence of anhydrous cement leads to restraint in the material; or, the cement paste suffers from an excessive bleeding during the manufacturing of samples, that could induce a difference of cement paste quantities and even of water-cement ratio, and thus a different delayed behaviour.

Finally, the specimens suffer from parasitic drying because the endogenous shrinkage is proportional to the loss in mass. This parasitic drying can be due to losses by the embedded apparatus and by the aluminium which remains a bit permeable, even with two layers.

IV. 2. Impact on delayed behaviour under drying

IV.2. a. Impact on drying: study of mass loss

Figure 9 shows the evolution of mass loss as a function of the square root of time for the four formulations under drying conditions.

Several observations can be made:

- The mass loss increases with time for the four formulations;
- Mortar with and without admixture exhibit exactly the same mass loss;
- The mass losses of cement paste with and without admixture are close;
- The mass loss is greater for cement paste than for mortar. At the end of the study, the mass loss of the cement paste is about 14.5% while that of the mortar is 8%. This observation is logical. Indeed, the mass loss is due to the departure of water from the material via drying, and this water is mostly in the cement paste. However, mortar is only composed of 68% of cement paste. Thus its mass loss is lower than a sample composed entirely of cement paste.
- The cement paste compositions display a change in the mass loss kinetics around when the root of time is equal to 2. A problem with the climatic chamber was encountered: relative humidity reached 50% at the beginning of the study due to a malfunction, the samples were then put back in a 30%HR environment.

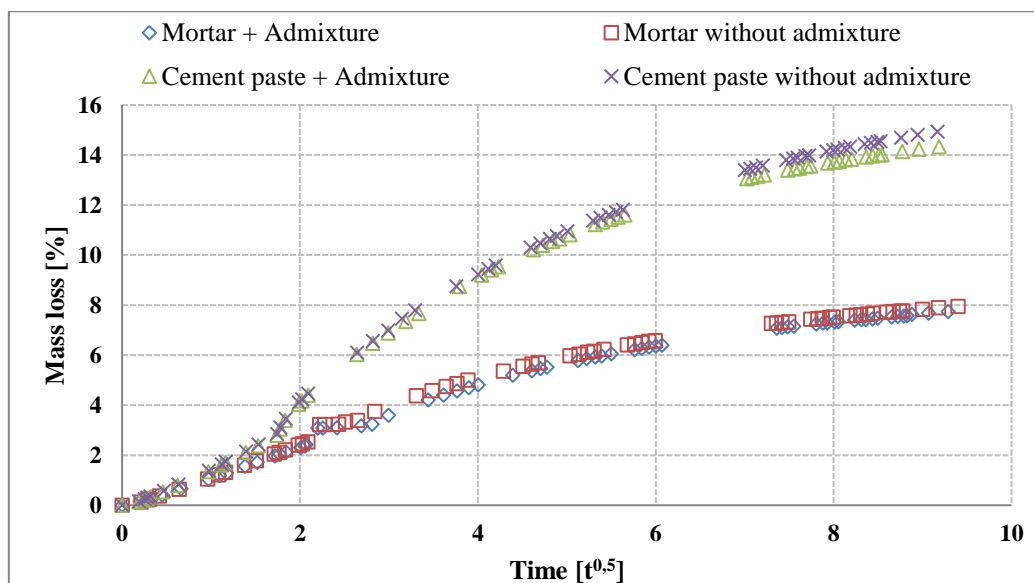


Figure 9 : Evolution of mass loss as a function of the root of time in drying conditions

A normalisation of the mass loss thus makes it possible to have a better comparison. This normalisation is obtained by equation (3) as for the mass loss under endogenous conditions. Figure 10 displays the evolution of the normed mass loss of the four formulations as a function of time root. It can be observed that the evolution is identical for the 4 formulations.

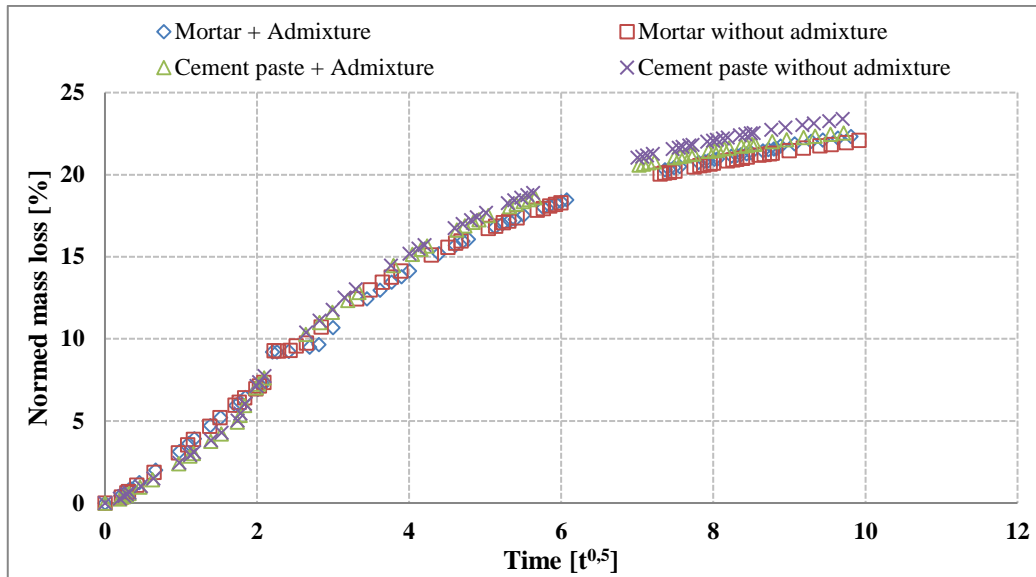


Figure 10 : Evolution of mass loss normed as a function of the root of time in drying conditions

The mass loss is greater for cement paste than for mortar. Indeed, the mass loss depends on the quantity of cement paste, so for mortar there is less cement paste the mass loss is thus lower.

For mortar and cement paste, whether there is admixture or not, it does not seem to vary. Thus it can be deduced that the admixture does not impact on the departure of water of the specimens. This trend is confirmed with the loss in normed mass loss since all formulations have an almost identical normed mass loss.

Finally, the change of the climatic chamber does not seem to have had an impact on drying, the trends are identical.

IV.2. b. Apparent shrinkage under drying conditions

Figure 11 and Figure 12 show the evolution of deformation respectively as a function of the square root of time and of normed mass loss under drying conditions.

- Shrinkage by drying increases over time for all formulations;
- The deformations of the cement paste samples are greater than those of the mortar samples. Mortar compositions are composed of 68% of cement paste, as it is mostly the cement paste that shrinks under drying, it is logical to observe this difference;
- The shrinkage of mortar with and without admixture is approximately identical, and reach about 2200 $\mu\text{m}/\text{m}$ after 96 days of study;
- The shrinkage of the cement paste with admixture is greater than that of the cement paste without admixture;
- Cement paste deformations are greater than 4000 $\mu\text{m}/\text{m}$ after 96 days of study;

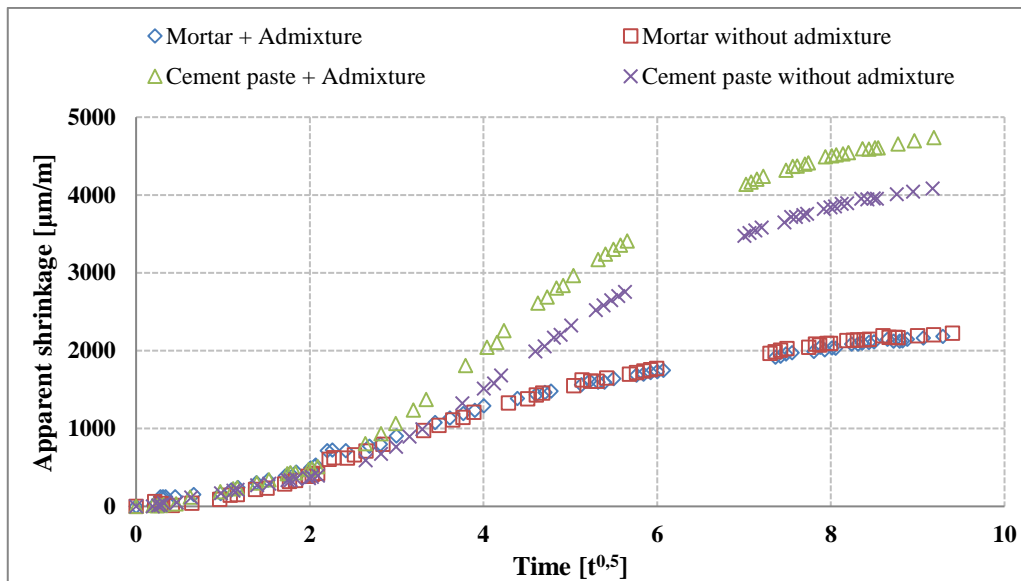


Figure 11 : Evolution of deformation as a function of the root of time in drying conditions

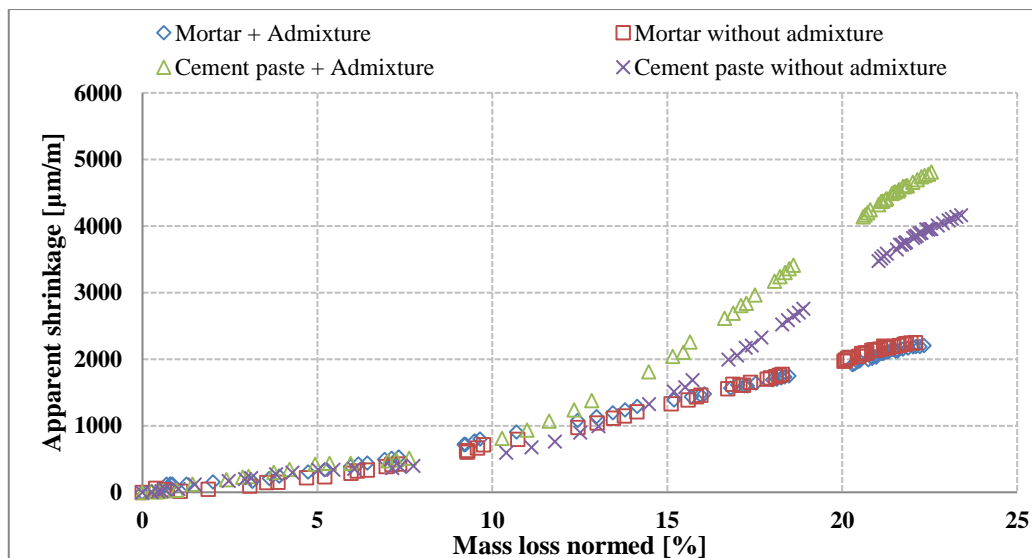


Figure 12 : Evolution of deformation as a function of mass loss normed in drying conditions

Apparent shrinkage is greater for cement paste specimens than for mortar ones. Indeed there is less cement paste in the mortar due to the addition of inert aggregates; therefore there is less water departure in the mortar. As the water movement causes drying shrinkage, the apparent shrinkage observed under drying conditions of the mortar is lower than that of the cement paste.

As it was observed for the study of endogenous shrinkage, the shrinkage is greater for cement paste with admixture than without admixture, and the mortar compositions do not show any differences of deformations. The hypotheses emitted then remain valid.

Usually for high water-cement ratios, endogenous shrinkage is negligible before drying shrinkage. In our case, the maximum endogenous shrinkage is around 700 $\mu\text{m/m}$ after 96 days of study while the maximum drying shrinkage is less than 4000 $\mu\text{m/m}$. Endogenous shrinkage is therefore not negligible compared to drying shrinkage. However, as the endogenous shrinkage was submitted to a parasitic drying, the two phenomena cannot be decoupled.

IV. 3. Impact on mechanical properties

The results of the three-point flexural tests are presented in Table 2 and discussed afterward.

Table 2 : Results of the 3 points flexion test after 28 days and at the end of the study

Composition	Tensile resistance [MPa]			Young Modulus [GPa]		
	At 28 days	At the end of study		At 28 days	At the end of study	
		Endogenous	Drying		Endogenous	Drying
Mortar with admixture	6.6	6.1	7.5	18.7	25.5	17.9
Mortar without admixture	7.4	6.8	7.4	37.3	24.2	16.9
Cement paste with admixture	3.2	2.9	2.0	14.3	19.4	4.3
Cement paste without admixture	6.6	3.3	2.6	28.0	7.0	8.4

Comparisons between the end of endogenous cure and the end of the endogenous study:

- Under endogenous conditions between the end of the endogenous cure and the end of the study, a global decrease of flexural strength and Young's Modulus can be observed. This observation is unusual, as the mechanical properties usually tend to increase with the extension of the endogenous cure. However, these results are in accordance with the monitoring of endogenous shrinkage: the samples underwent a parasite drying that damaged partially the materials;
- Young's Modulus are weaker at the end of the study under drying conditions than after the endogenous cure, showing that the material is clearly damaged by the drying phenomenon;
- When we take an interest in flexural strength, they are lower for cement paste at the end of the study under drying conditions than after the 28 days of endogenous cure, highlighting here again the effect of drying;
- While the mortar resistances are the same or even higher after drying than after the endogenous cure, this phenomenon is probably due to the capillary effect;

Comparisons between mortar and cement paste:

- The flexural strength and Young's Modulus of mortar formulations are higher than those of cement paste. This observation was expected. Indeed, as mortar contains 32% of sand, which has a higher Young's Modulus than cement paste, it is normal to observe an increase of mechanical properties compared to the cement paste samples;

Comparisons between cement pastes:

- Young's Modulus and flexural strength of the cement paste without admixture are generally greater than those of the cement paste with admixture;

- Whereas Young's Modulus and flexural strength of mortar seems unchanged by the use of the admixture.

The drying of the cement paste results in a decrease in flexural strength and Young's Modulus, as expected. Indeed, the drying phenomenon induces a damaging of the material, leading to the decrease of the mechanical properties.

The flexural strength and Young's modulus of mortars are higher than those of cement paste due to the presence of sand with a higher Young's modulus. However the mortar formulations under drying conditions are not following the same behaviour than the cement paste ones. The material is damaged by the desiccation, like the cement paste, and this could lead to the observed decrease of the Young Modulus. However, the introduction of aggregates may make the cracking less localised and less opened. Under these conditions, when the water leaves the rigid skeleton, a suction phenomenon occurs and the material the material would be as pre-stressed. This phenomenon is called the capillary effect. This could explain why an increase of the flexural strength is noticed.

Finally, a global decrease is observed between the end of the endogenous cure and the end of the study under endogenous conditions. In theory, cement hydration would continue and mechanical properties would increase over time, but here it is the opposite. These results confirm the parasitic drying observed previously, that induced a damaging of the samples.

IV. 4. Impact on the material

IV.4. a. Segregation

Table 3 exhibits the sections of the specimens broken after three-point flexural tests for all compositions under drying and endogenous conditions.

Several observations can be made:

- For the mortar the sand grains are distributed evenly when there is admixture. Indeed, when there is no admixture, the coarse grains of sand are in the lower part of the section of the test piece and in the upper part when there is none;
- For the cement paste, it can be seen that with the admixture, the material has a homogeneous grey colour on the section. While without the adjuvant, there are many anhydrous grains. Moreover, the large grains are at the bottom and the smallest at the top;
- There is an obvious grey gradation for cement paste without admixture under endogenous conditions;

IV.4. b. Geometry

Table 3 also presents the dimensions of the sections of each formulation.

- The dimensions of the sections are different from the theoretical 40x40 cm section for all compositions. There is in all cases one side larger than 40 cm and another smaller;
- Sections are larger when there is adjuvant than without adjuvant. On average there is an increase of 4.7% between a section of material with adjuvant compared to a section of material without adjuvant;

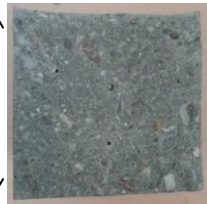



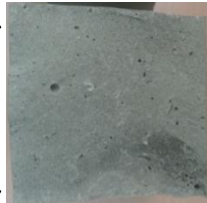
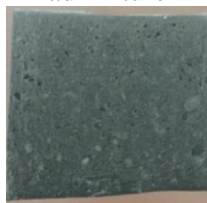
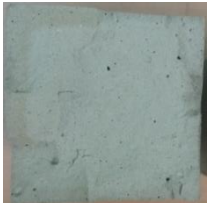

The differences in cross-section obtained may be due to the use of flexible silicone moulds. Indeed, these moulds have a more variable geometry than steel moulds. This choice of silicone mould

is justified by the fact that the water to cement ratio is important, so they limit water loss during manufacture.

In addition, the unformed surface (the top surface in the photos in Table 3) has the same shape as a water meniscus in a tube. This shows the presence of bleeding especially in the case of cement paste.

Materials with admixture have larger cross-sections than materials without admixture. The admixture helps to limit bleeding phenomena. However, it does not eliminate it.

Table 3 : The sections of the specimens for all compositions

Endogenous		Drying	
Mortar with admixture	Mortar without admixture	Mortar with admixture	Mortar without admixture
			
39.95 mm	38.31 mm	39.59 mm	38.63 mm
40.61 mm	40.65 mm	40.58 mm	40.57 mm
Cement paste with admixture	Cement paste without admixture	Cement paste with admixture	Cement paste without admixture
			
39.52 mm	36.77 mm	38.59 mm	36.79 mm
40.51 mm	40.47 mm	40.28 mm	40.48 mm

IV.4. c. Cracking

The results of cracking study are showed in Table 4.

Several observations can be made:

- The crack ratio per centimetre is lower when there is admixture. This observation is valid for mortar and cement paste;
- The order of magnitude of the number of cracks per centimetre is different for the mortar formulation without admixture;
- Overall, crack sizes are larger for cement paste than for mortar with and without admixture;
- For cement paste, cracks are larger when there is no admixture;
- For mortar, cracks are larger when there is admixture;

The number of cracks for materials with admixture is lower than for materials without admixture. Therefore, it can be concluded that the admixture tends to reduce the formation of cracking. Also, the number of cracks per centimetre of the mortar without admixture is high compared to other formulations. To measure the quantity of cracks per centimetre, a quantification of the cracks cutting on the sides a b c and d of the study area (see Figure 4) is carried out. For the mortar without admixture,

numerous crack crossings were present. It was decided to count two cracks in these cases where other people would have counted only one. This may be one of the reasons for the high value.

Table 4 : Results of cracking study

Composition	Crack size			Number of cracks per centimetre
	Average	Minimum	Maximum	
Mortar with admixture	12,85	5,96	33,67	0,40
Mortar without admixture	7,13	0,73	23,73	3,72
Cement paste with admixture	16,66	9,09	25,46	0,32
Cement paste without admixture	26,08	14,02	66,98	0,57

On average the crack sizes in the formulations with aggregates are smaller than in the cement paste. The introduction of aggregates, with a higher Young's Modulus, increases the mechanical characteristics of the mortar and limits the cracking due to the hydric gradient induced by the water departure under drying conditions. Thus the cracks are smaller for the mortar than for the cement paste.

Finally, with admixture in the mortar the cracks are larger than without admixture while for cement paste it is the opposite. The admixture therefore does not seem to have an impact on the crack opening size.

V. Conclusion

In this paper, an experimental study on the effect of the Sika® Stabilizer 400 on the delayed behaviour and on the mechanical properties of cement paste and mortar. Several observations have been made, and thus, several phenomena have been identified and are summarised here:

- The use of this admixture tends to homogenise the material. It allows a better hydration of the cement, and therefore, insuring the materials characteristics - for example, the water-cement ratio and geometry of the samples. It does so by limiting the bleeding phenomenon during the manufacturing of the samples, but it does not prevent it completely. Moreover, it eliminates the phenomenon of segregation in the material, especially with the introduction of aggregates.
- The introduction of admixture does not interfere with the drying phenomenon as the mass losses of the formulations are unchanged with its use.
- It neither affects endogenous shrinkage, nor the desiccation one.
- Use of the admixture decreases flexural strength but does not impact Young's modulus.
- The admixture reduces cracking density, but does impact the size of the cracks.

These tests would gain from a chemical analysis that could not be performed in our study.

Appendix C

Article de Projet d'Initiation à la
Recherche de Pierre Aymeric, Élève
de Master 2 Recherche : *Étude du
fluage du béton suivant les
caractéristiques des granulats.*

Protocole expérimental

Après la phase bibliographique qui a occupé la majorité du travail du PIR, il était prévu une phase expérimentale. Cependant, le manque de temps nous a empêché d'effectuer un essai avant la fin du PIR. Cependant, le PIR se poursuivant sur le stage de fin de Master 2 recherche, la campagne expérimentale sera réalisée pendant le stage.

Nous avons donc pu profiter de la fin du PIR afin de discuter les paramètres de cette campagne. En effet le travail bibliographique a permis d'effectuer un premier tri des caractéristiques des granulats auxquels nous souhaiterions nous intéresser. Nous avons donc discuté des objectifs de la campagne expérimentale du stage ainsi que du protocole qui allait être mis en place.

I/ Objectif de la campagne expérimentale

L'objectif de la campagne expérimentale est de venir caractériser une fonction de fluage afin de venir compléter les résultats de Marie Malbois et permettre une modélisation complète des matériaux cimentaires.

$$\varepsilon_{tot} = \varepsilon_{elast} + \varepsilon_{séchage} + \varepsilon_{fluage}$$

Nous pourrions donc ajouter un modèle pour la déformation de fluage.

Nous allons étudier deux séries d'éprouvettes possédant différentes tailles de granulats (6.3-8 ou 10-12.5mm) avec une proportion de granulat de 50%. Les deux séries d'essais seront réalisées sur des éprouvettes en condition endogène ou condition séchante.

II/ Protocole expérimental

1) Formulations des éprouvettes

Les éprouvettes disponibles pour les essais ont déjà été réalisées. Celles-ci ont été coulées en Décembre 2014 et ont été placées soit en conditions endogènes, soit dans une atmosphère contrôlée et ont été séchées. Nous n'étudierons ici le béton dans un premier temps sur des éprouvettes en conditions endogènes. Ces éprouvettes seront ensuite placées en conditions séchantes afin de mesurer le fluage de dessiccation.

L'ensemble des éprouvettes sont des 70*70*280mm et possèdent une seule fraction de tailles de granulats à raison de 50% de granulats en volume.

Ces proportions ne correspondent pas aux caractéristiques usuelles d'un béton car les ordres de grandeur des proportions de granulats sont usuellement de 75%. Le matériau étudié est donc un matériau modèle, dit morphologiquement contrôlé, du fait de la sélection des proportions de granulats et de leur taille. De plus, de véritables granulats sont utilisés afin d'avoir une condition aux interfaces réelle au contraire d'inclusions de billes de verre par exemple.

2) Matériel d'essai

Nous avons utilisé pour cette campagne expérimentale quatre bâtis de fluage dont deux possèdent une cellule de mesure d'effort. Les bâtis sont montés par deux en parallèle avec un bâti instrumenté afin de connaître avec précision la contrainte dans nos éprouvettes.

Le suivi des déformations est réalisé grâce aux plots qui sont fixés sur les éprouvettes avant de les placer dans les bâtis de fluage. Afin de pouvoir mesurer uniquement les déformations de fluage, il est nécessaire de mesurer sur des éprouvettes non chargées les déformations de retrait.

$$\varepsilon_{fluage} = \varepsilon_{mesuré} - \varepsilon_{retrait}$$

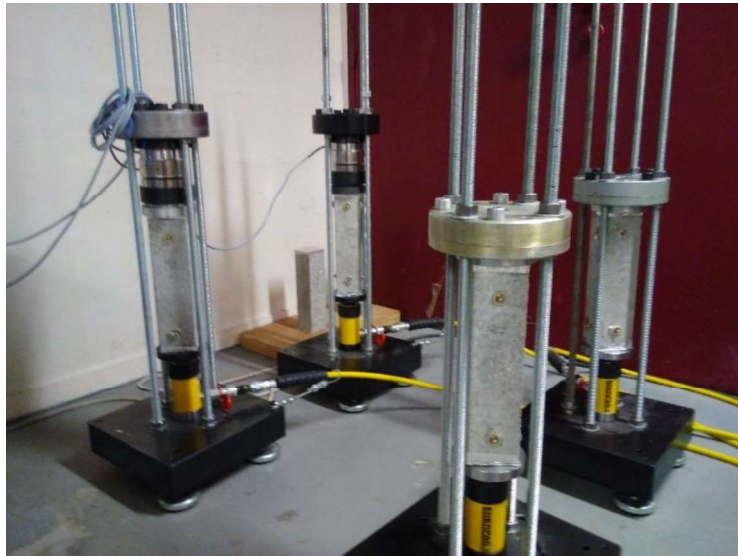


Figure 9 : Bâtis de fluage

On observe ici sur la Figure 9 : Bâtis de fluage un bâti de fluage sur lequel deux éprouvettes sont testées simultanément. Nous aurons donc à notre disposition des bâtis identiques, dont deux instrumentés de capteurs d'effort.



Figure 10 : compresseur asservi en pression

Il est donc nécessaire, après avoir choisi le format expérimental de la campagne, de décider la durée des expériences, ainsi que le protocole de relevé des mesures. Les chargements des éprouvettes auront lieu dans une salle contrôlée en température et hygrométrie ($27\pm 3^{\circ}\text{C}$ et $50\pm 5\% \text{HR}$) afin de maîtriser les conditions d'essai tout au long de la campagne.

Les éprouvettes considérées pour la campagne expérimentale sont les suivantes :

- 6.3-8mm (RE1 et RE2)
- 10-12.5mm (RE1 et RE2)

Ces références d'éprouvettes seront utilisées dans les tableaux et les différentes courbes de ce rapport afin de facilement les identifier.

Bien que les éprouvettes aient été scellées après une cure de 28 jours en décembre 2014, nous avons voulu nous assurer que celles-ci n'avaient pas subi de séchage parasite. Leur masse initiale m'a été fournie et j'ai pu effectuer une pesée afin de connaître la perte de masse éventuelle.

% inclusions	Taille granulats	Ref	m _{initiale, décembre 2014}	M _{avril 2018}	Perte de masse (%)
50%	6mm-8mm	RE1	3191,4	3184,3	0,22
		RE2	3198,2	3189,5	0,27
		RE3	3169,3	3158,7	0,33
	10mm-12mm	RE1	3199,3	3186,4	0,40
		RE2	3211,2	3205,4	0,18
		RE3	3217	3206,2	0,34

La campagne expérimentale se subdivise en 3 phases :

- Mesure du fluage propre sur des éprouvettes en condition endogène (30 jours)
- Déchargement des éprouvettes et mesure des déformations (5 jours)
- Déballage des éprouvette et chargement pour la mesure du fluage (propre + dessiccation) (39 jours)

Nous avons choisi d'effectuer un chargement à 30% de la résistance en compression du béton. Cette valeur en compression a été choisie car jusqu'à 40% de la résistance en compression, le comportement du béton est quasi-linéaire, il n'y a donc pas d'endommagement.

III/ Etude préliminaire

Nous avons choisi de mettre en place une première expérience test afin de :

- Maitriser la mise en place des éprouvettes
- Maitriser le compresseur et la commande en pression
- Maitriser le déformètre à bille et la prise de mesure

Nous avons constaté qu'un grand nombre de paramètres pouvaient influencer la mesure et affecter la précision ainsi que la répétabilité de l'expérience. Parmi ces paramètres nous noterons principalement les variations de température, d'hygrométrie, de chargement dues à l'asservissement en pression, la répétabilité humaine de la mesure...

Nous avons choisi grâce à cette étude préliminaire de quantifier les erreurs et incertitudes introduites lors des mesures afin de quantifier la précision du résultat obtenu. Nous avons listé les paramètres suivants :

- La différence de coefficient de dilatation thermique entre le béton et l'acier
- La précision du déformètre à bille
- La variation de contrainte tout au long de l'essai

1) Variation de température

La variation de température au sein de la pièce climatisée génère une imprécision sur le relevé de déformation. Nous disposons des données suivantes concernant les matériaux :

$$\begin{cases} \alpha_a = 12 * 10^{-6} \\ 4 * 10^{-6} < \alpha_c < 18 * 10^{-6} \end{cases}$$

De plus les mesures que nous avons effectuée au sein de la pièce permet d'estimer la variation de température à $\pm 3^\circ\text{C}$.

Les données concernant le coefficient de dilatation du béton étant trop incertaines, nous avons choisi de mesurer celui-ci. Pour cela, nous avons placé deux éprouvettes ayant subies près de 3 années de dessiccation dans une étuve à 60°C . Nous avons donc obtenu les résultats suivants :

Tableau 4 : mesure du coefficient de dilatation thermique du béton

	Eprouvette 1	Eprouvette 2
T1	26,800	26,800
T2	60,000	60,000
α	4,217	5,873
α_{moyen}	5,045	
m1	3020,000	3081,300
m2	3004,500	3065,700
δ_m	0,513	0,506

$$\delta_T = \pm 4.17 \mu\text{m}/\text{m}$$

2) Imprécision du déformètre à bille

La précision du déformètre à bille est de $\pm 1 \mu\text{m}$. Sachant que la mesure de déformation est effectuée sur un étalon de 20cm, nous obtenons l'incertitude suivante sur la mesure :

$$\delta_{pr} = \pm 5 \mu\text{m}/\text{m}$$

3) Variation de la contrainte sollicitante

L'asservissement du compresseur n'étant pas parfait, la pression dans le système de chargement n'est pas constante. Nous avons pu constater une variation de la pression autour de la pression de consigne de $\pm 1.5\%$. Nous avons donc pu calculer la variation de déformation associée. Pour cela, nous avons utilisé les modules Young mesurés lors des phases de chargement et de déchargement.

$$\delta_\sigma = \pm 3.25 \mu\text{m}/\text{m}$$

4) Incertitude totale sur la mesure

Nous allons maintenant estimer l'incertitude totale de notre mesure

$$\delta_{tot}^2 = \delta_T^2 + \delta_{pr}^2 + \delta_\sigma^2$$

Soit une incertitude totale de :

$$\delta_{tot} = \pm 9.59 \mu\text{m}/\text{m}$$

Nous pourrions donc par la suite indiquer l'incertitude sur les mesures que nous avons obtenu. Afin d'éviter ces biais de mesure importants, nous allons porter une attention particulière à la prise de mesure et aux incohérences pouvant apparaître. De plus, nous effectuerons des relevés locaux complémentaires de température et d'hygrométrie afin de détecter d'éventuelles variations importantes.

Analyse des résultats

Nous allons maintenant présenter les résultats que nous avons obtenus lors de notre campagne expérimentale.

I/ Etude du fluage propre en conditions endogènes

1) Essais et résultats

Comme présenté dans le protocole expérimental, nous avons dans un premier temps effectué les mesures de fluage propre de nos éprouvettes en conditions endogènes. Nous avons pu à l'issue cet essai tracer la courbe du fluage propre.

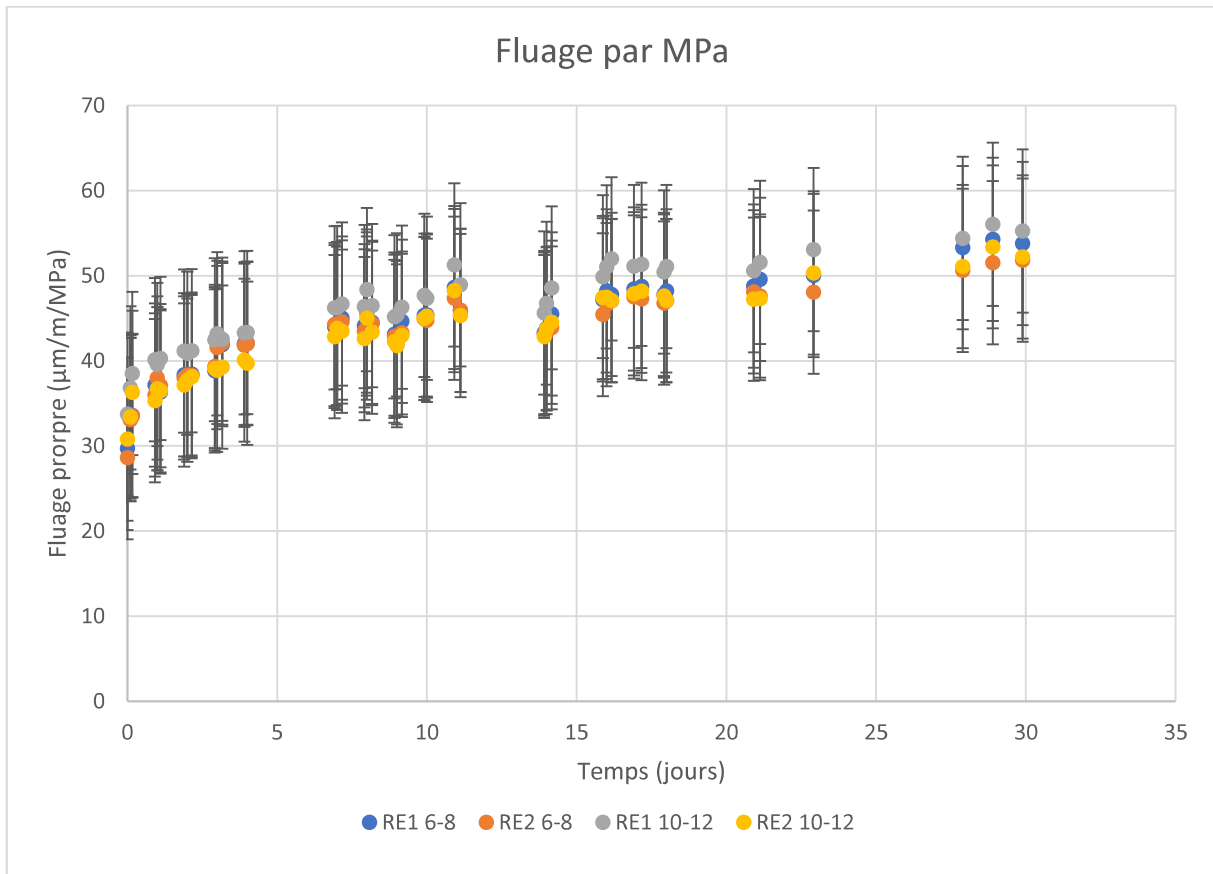


Figure 11 : fluage propre par MPa

Afin de pouvoir exploiter les données obtenues dans ce premier essai, nous avons dû modéliser le fluage afin d'avoir un modèle qui serait exploitable dans la seconde partie de notre étude. Nous avons pour cela utilisé le modèle de Burger qui est classiquement utilisé pour modéliser le fluage.

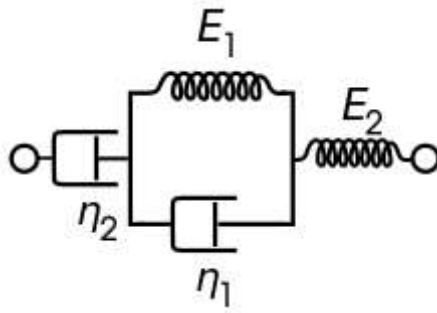


Figure 12 : modèle de Burger

La mise en équation nous a permis d’obtenir le comportement suivant

$$\varepsilon_{Burger} = \frac{F}{A * E_b} + \frac{F}{A * \eta} * \log\left(\frac{t_0 + t}{t_0}\right) + \frac{F}{A * E_2} * \left(1 - \exp\left(-\frac{t}{\tau}\right)\right)$$

Afin de déterminer les 4 paramètres inconnus du modèle, nous avons choisi d’appliquer la méthode des moindres carrés. Nous avons pour cela utilisé le solveur d’Excel qui nous a permis d’obtenir une solution pertinente. Voici donc les paramètres que nous avons pu déterminer pour chaque taille de granulat :

Tableau 5 : modèle de Burger

Paramètres du modèle de Burger			
Paramètres	Eprouvettes 6-8	Eprouvettes 10-12	Unité
E_b	32.04	30.98	GPa
η	0.85	0.62	GPa
E_2	106.19	144.91	GPa
τ	0.20	15.81	s

De plus nous avons pu tracer sur nos courbe le modèle de Burger que nous avons obtenu :

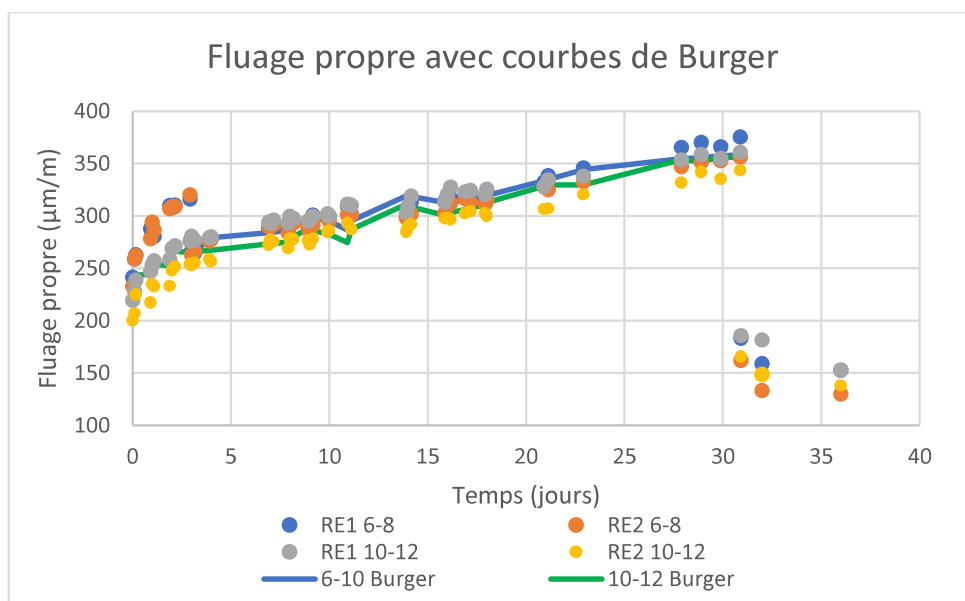


Figure 13 : Comparaison du fluage expérimental et le fluage du modèle de Burger

Nous pouvons ici constater que, au vu des incertitudes sur les résultats, les courbes de toutes nos éprouvettes se trouvent toutes dans un même fuseau. Nous pouvons donc en déduire ici que la différence de taille des granulats n'a pas eu une influence suffisante pour que celle-ci apparaisse clairement.

2) Anomalies

Nous avons choisi initialement de charger chacune des éprouvettes à 30% de sa résistance en compression. Il a cependant été décidé de finalement charger l'ensemble des éprouvettes à 30% de la résistance en compression minimale. C'est pourquoi nous pouvons observer pour le premier jeu d'éprouvettes un déchargement partiel au début du troisième jour.

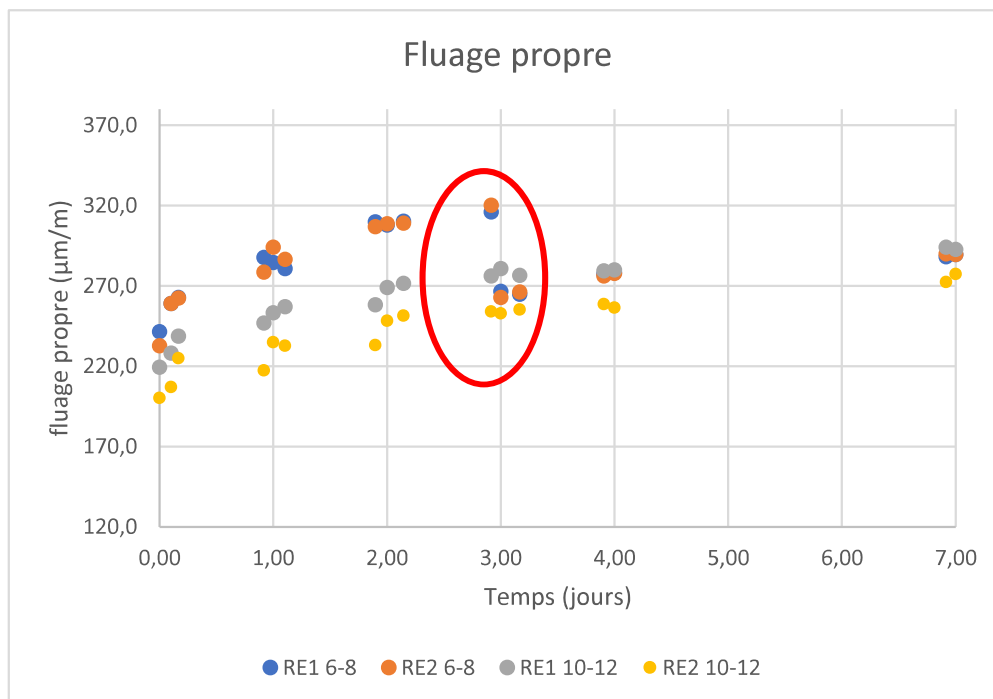


Figure 14 : Déchargement partiel

3) Mesures complémentaires

Nous avons aussi pu exploiter ces courbes afin de déterminer le module d'Young de chaque éprouvette lors du chargement et du déchargement. Nous avons obtenu les résultats suivants que nous avons comparés aux essais en compression réalisés à 28 jours.

J'ai choisi ici de considérer comme référence le module d'Young calculé à 28 jours à partir des essais de flexion réalisés sur des éprouvettes provenant de la même gâchée.

L'important écart que nous avons mesuré entre nos valeurs et celle à 28 jours peut aisément être expliqué par le vieillissement du matériau et donc l'avancement de la réaction d'hydratation du ciment. L'augmentation du module d'Young lors de la décharge peut s'expliquer par une stabilisation après déchargement qui n'est pas instantané. De plus, on observe sur nos éprouvettes une faible variabilité des résultats entre l'éprouvette 1 et 2 en charge comme en décharge. Ces résultats me semblent donc suffisamment pertinents pour pouvoir les utiliser par la suite.

Tableau 6 : mesure des modules d'Young

	Eprouvette 1	Eprouvette 2	Eprouvette 3	Eprouvette 4
$E_{\text{chargement}}$ (GPa)	33,7	34,9	29,6	32,5
$E_{\text{décharg}}$ (GPa)	35,3	34,8	36,3	35,9
$E_{28 \text{ jours}}$ (GPa)	23,5		22,2	
Erreur _{charge} (%)	43,6	49,0	33,3	46,0
Erreur _{décharge} (%)	50,5	48,6	63,2	60,5

Nous avons donc obtenu suffisamment de résultats pour pouvoir effectuer la seconde partie de notre étude expérimentale qui quantifiera le fluage de dessiccation

II/ Etude du fluage de dessiccation en conditions séchantes

Nous allons maintenant pouvoir quantifier le fluage de dessiccation de nos deux séries d'éprouvette. Afin de pouvoir mesurer ce fluage de dessiccation, il est nécessaire de connaître le fluage propre, ce qui est chose faite, et de mesurer le retrait dans notre matériau.

1) Mesure du retrait et de la perte de masse

Nous avons donc effectué en parallèle de nos essais de fluage des mesures quotidiennes de la masse de deux éprouvettes témoins ainsi que des mesures de retrait. Les figures 15 et 16 présentent le retrait mesuré. Les résultats obtenus sont concluants car ils correspondent au comportement de retrait attendu du béton.

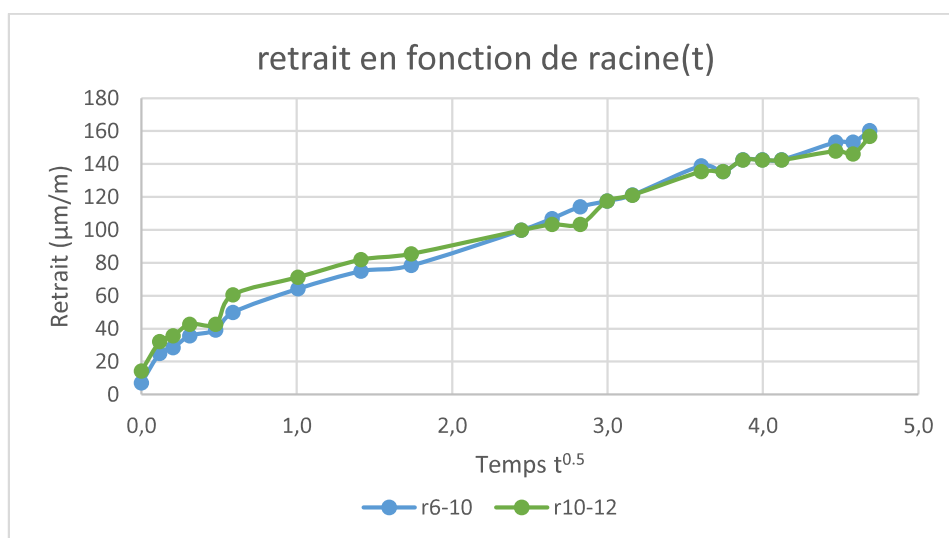


Figure 15 : retrait exprimé en fonction de la racine du temps

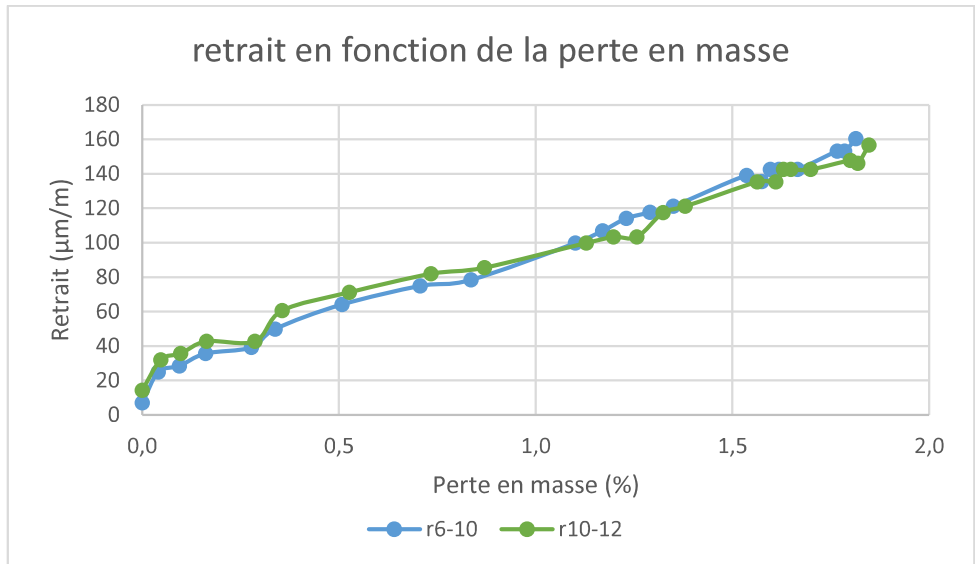


Figure 16 : retrait mesuré exprimé en fonction de la perte en masse

En plus d’avoir un comportement attendu, il apparait ici que le comportement de nos deux compositions est identique. Nous n’observons pas de différences notables de comportement pour les différentes tailles de granulats. La taille de granulats ne semble donc pas avoir d’influence sur le retrait de dessiccation à court terme. Cependant, conclure sur un unique essai ne serait pas raisonnable, il faudrait pour cela réitérer l’expérience sur un plus grand nombre d’éprouvettes.

Nous pouvons constater qu’il apparait une inflexion anormale à la fin du premier jour d’essai sur la courbe de perte en masse. Cette inflexion est due à une augmentation de l’hygrométrie en fin de journée qui a eu un fort impact sur la cinétique de dessiccation du matériau. Voici la courbe de l’hygrométrie que nous avons mesuré dans la salle d’essai :

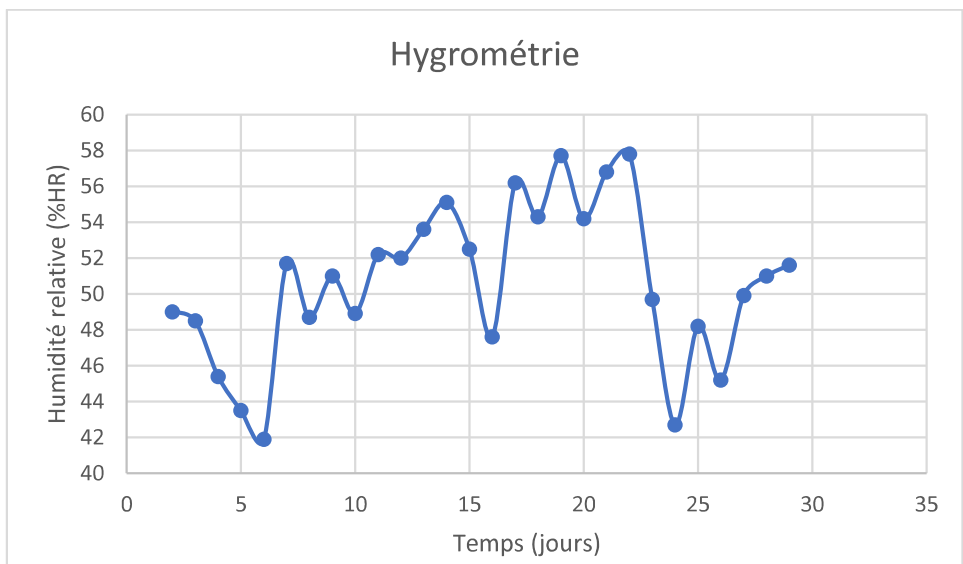


Figure 17 : mesure de l’hygrométrie

2) Mesure du fluage total

Nous avons réalisé, en utilisant le même protocole expérimental, les déformations de nos éprouvettes dans les bâtis de fluage. La courbe suivante est le résultat de ces essais :

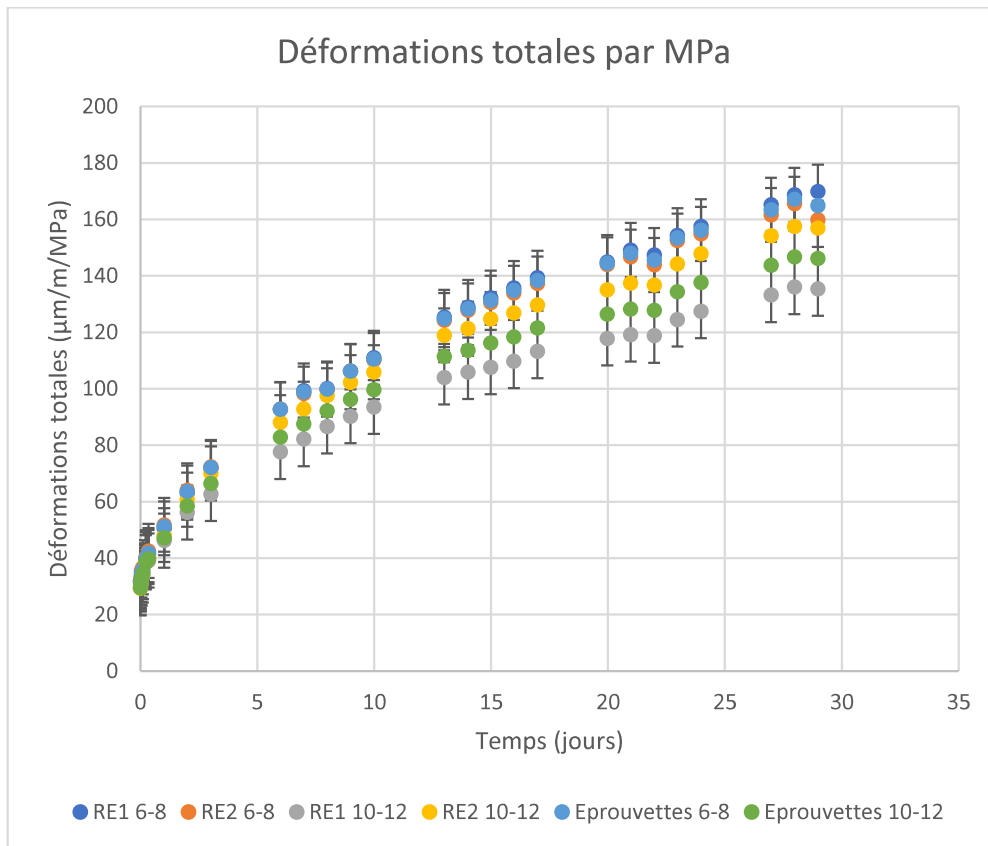


Figure 18 : déformations totales mesurées incluant le retrait et le fluage propre

Nous pouvons constater ici une séparation du comportement entre les éprouvettes à petits granulats et les éprouvettes à gros granulats. Nous observons un fluage plus important dans les éprouvettes à petits granulats. Cette augmentation du fluage est due à une plus faible restriction des déformations de fluage pour de petites inclusions rigides. Il y'a donc moins d'incompatibilité des déformations et donc de réduction de celles-ci.

3) Expression du fluage de dessiccation

Afin de pouvoir exprimer uniquement le fluage de dessiccation, nous avons déduit le retrait que nous avons mesuré ainsi que le fluage propre en utilisant le modèle de Burger avec les paramètres que nous avons obtenus dans un premier temps.

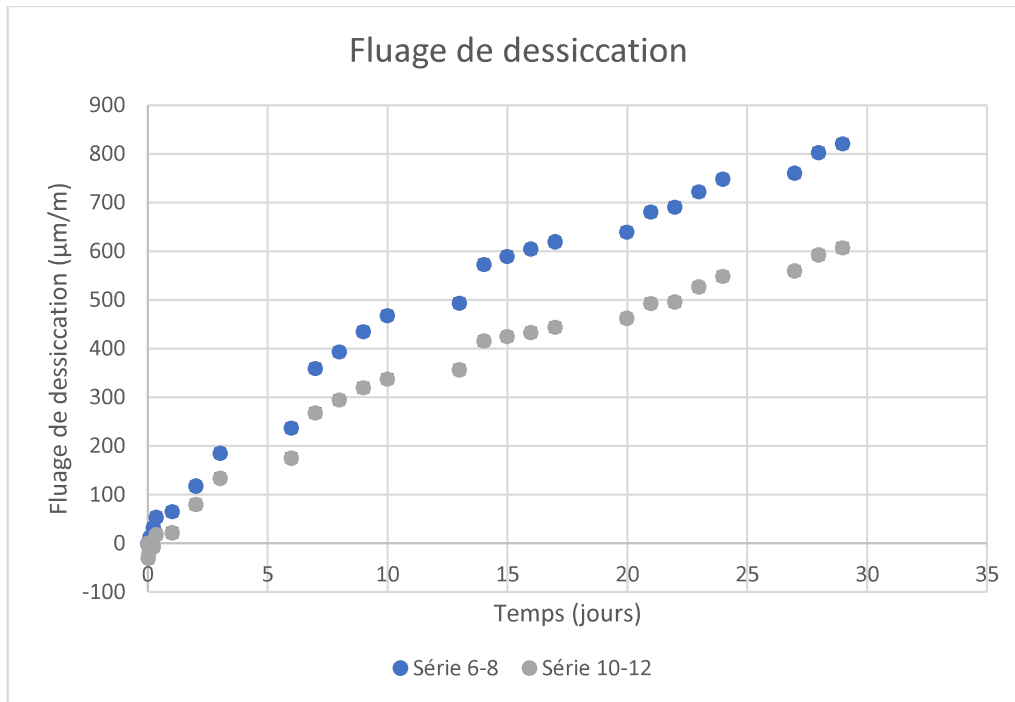


Figure 19 : fluage de dessiccation

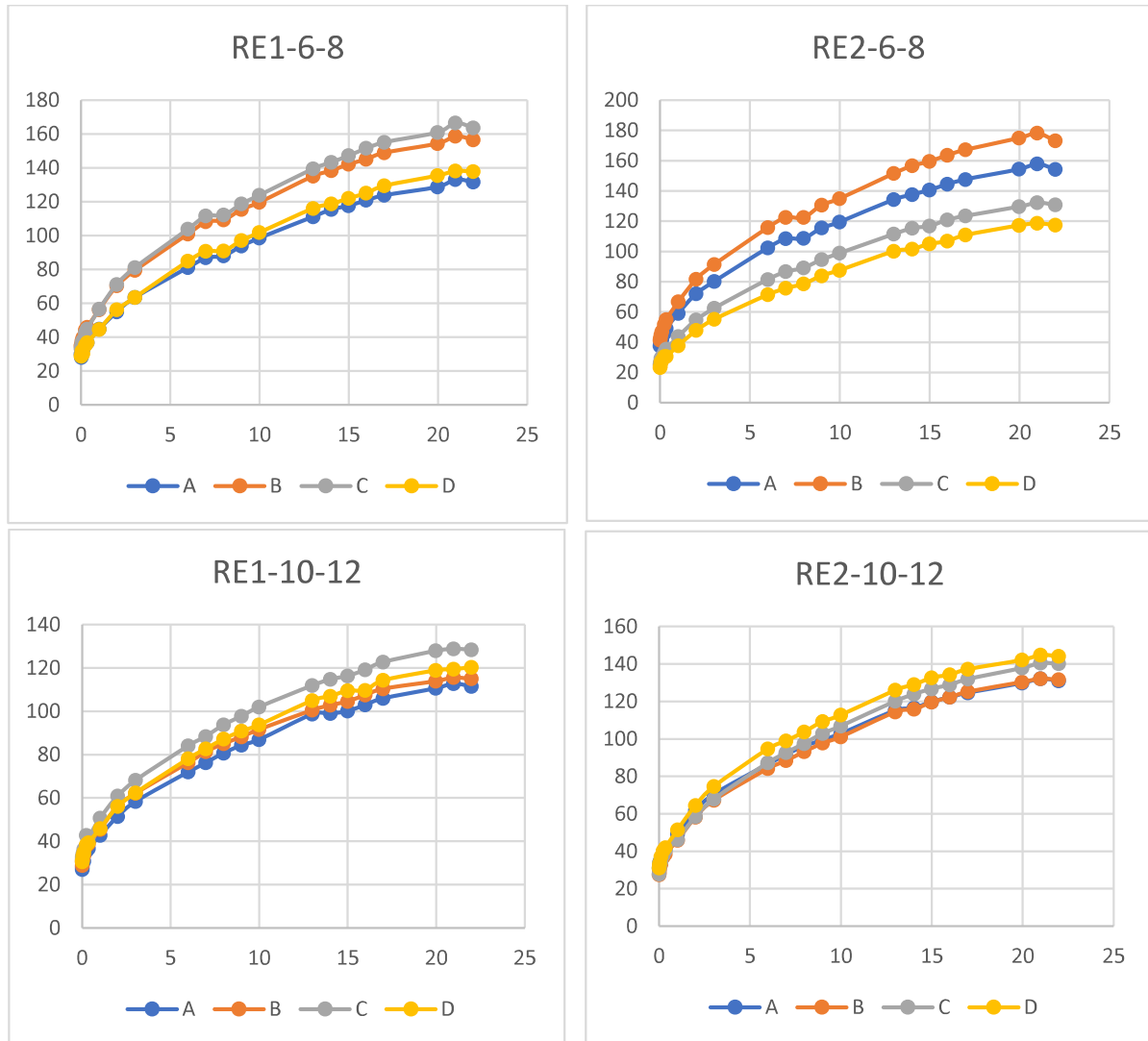
Nous n'avons pas pu exploiter les premiers points de certaines courbes car le modèle de Burger que nous avons utilisé ne nous a pas permis d'obtenir des résultats en accord avec les mesures de fluage du premier jour. En effet, nous obtenons des fluages de dessiccation négatifs le premier jour. Le modèle de Burger ou les paramètres que nous avons définis ne sont donc pas adaptés pour décrire le fluage à très court terme. Contrairement au fluage propre, ici le fluage de dessiccation est fortement influencé par la taille des inclusions. Nous observons au terme de 30 jours d'essais une différence de 26%. Cette différence non négligeable était attendue comme nous l'avons vu dans la bibliographie avec les essais sur des bétons de sable [9]. Notre étude vient donc confirmer le fort impact de la taille des inclusions sur le fluage de dessiccation.

4) Vérification de l'excentrement

La mise en place des éprouvettes étant contrainte par le manque d'espace pour manoeuvrer les éprouvettes dans les bâtis, le centrage des éprouvettes n'est pas parfait. Nous avons donc souhaité quantifier la flexion induite par l'excentrement de nos éprouvettes.

Nous avons dans un premier temps tracé l'évolution des déformations sur chaque face des éprouvettes :

Tableau 7 : déformation sur chaque face de chaque éprouvette



Nous avons ensuite calculé les moments de flexion associés à ces déformations à l'aide de la formule suivante :

$$\varepsilon = \frac{\sigma}{E_b} = \frac{M * y}{E_b * I}$$

Nous avons donc obtenu les moments et excentrements suivants :

Tableau 8 : calcul des moments parasites et des excentrements associés

Mesure de l'excentrement et du moment parasite				
Eprouvette	M_{A-C}	e_{A-C}	M_{B-D}	e_{B-D}
	N.m	mm	N.m	mm
RE1-6-8	19.7	0.7	36.1	1.2
RE2-6-8	73.1	2.5	107.9	3.7
RE1-10-12	28.3	0.9	9.4	0.3
RE2-10-12	19.5	0.7	21.1	0.7

La connaissance de ces excentrements permet d'effectuer un contrôle sur les conditions d'exécution de l'essai. En effet un excentrement important générerait un important moment un une grande variation de la contrainte en fibre tendue et comprimée. Les variations de chargement dans nos fibres sont donc les suivantes :

Tableau 9 : impact de l'excentrement sur le chargement

Variation de contrainte dans les fibres externes			
Eprouvette	Chargement (MPa)	Impact du moment sur le chargement (MPa)	Variation du chargement (%)
RE1-6-8	29.4	0.6	2.1
RE2-6-8	29.4	1.9	6.4
RE1-10-12	30.0	0.5	1.6
RE2-10-12	30.0	0.4	1.2

Nous pouvons donc constater ici que la variation de contrainte dans les fibres extérieures de notre éprouvette est négligeable.

Nous avons donc pu déterminer notre fonction de fluage de dessiccation. L'impact de la taille des granulats à un impact sur le fluage de dessiccation comme nous avons pu le constater lors de nos essais. Il reste cependant difficile de conclure quant à l'influence de ce paramètre sur le fluage propre. En effet, les incertitudes de mesure restent trop importantes vis-à-vis des déformations mesurées pour pouvoir tirer une quelconque conclusion.

Conclusions

Nous avons pu constater dans un premier temps la complexité du comportement du béton à long terme. En effet, celui-ci subit à la fois du retrait et du fluage, tous deux des phénomènes complexes encore étudiés. Nous pouvons distinguer deux grands cas de fluage : le fluage propre du matériau ainsi que le fluage de dessiccation, dont le séchage du matériau est à l'origine.

Nous avons dans un second temps pu constater qu'aucune publication majeure ne venait apporter un éclairage sur l'influence des inclusions sur le fluage du matériau. En effet, de nombreux paramètres aussi bien matériaux, géométriques ou encore minéralogiques viennent influencer le comportement du béton sous chargement à long terme. Il existe donc un verrou scientifique qu'il est nécessaire de lever afin d'améliorer la compréhension du matériau et d'améliorer la prédiction du comportement de celui-ci.

Nous avons donc pu, à l'aide de cette étude bibliographique établir un cahier des charges de la campagne expérimentale que nous allons mener. Nous avons choisi de nous focaliser sur un unique paramètre plutôt que de nous disperser en essayant d'en étudier plusieurs. Le paramètre que nous avons choisi est la taille des inclusions. La campagne expérimentale s'est déroulée en 3 temps : nous avons tout d'abord effectué une expérience préliminaire afin de déterminer les erreurs et incertitudes auxquelles nous pourrions être confronté par la suite. Nous avons ensuite effectué une première série d'essai afin de déterminer la courbe de fluage propre et nous avons pu identifier les paramètres associés au modèle de Burger. Dans un dernier temps, nous avons exposé les éprouvettes à des conditions séchantes et nous avons mesuré une courbe de fluage apparent et de dessiccation ; ainsi qu'une courbe de mesure du retrait et de perte en masse. De ces différentes courbes nous avons pu en déduire la fonction de fluage propre, celle de fluage de dessiccation et celle du retrait de dessiccation.

De plus, ces courbes, ainsi que les paramètres des modèles, serviront dans le travail de Marie Malbois en venant compléter les expériences qu'elle a mené durant son doctorat.

A) Equation de fluage de Nielsen

Équation 1 : Fonction de fluage

$$c(t, \tau) = \frac{1}{E_c(\tau)} \left(1 + \alpha_c \left(1 - \frac{\tau^2}{t} \right) \right) + \frac{1}{K} \left(\log \left(\frac{t}{\tau} \right) + \sqrt{\frac{7}{t_0}} \frac{t_0^2}{\tau} \left(1 - \frac{\tau^2}{t} \right) \right)$$

Avec :

$$\alpha_c = 1 - C_a$$

$$E_c = f(E_{\text{granulat}}, \dots)$$

 $t_0 = \text{date du premier chargement}$

B) Contraintes de fluage selon Hobbs

$$\sigma_m = \frac{(E_m + E_a)\sigma}{(E_a - E_m)D_a + E_m + E_a}$$

$$\sigma_a = \frac{2E_a\sigma}{(E_a - E_m)D_a + E_m + E_a}$$

Avec D_a la concentration volumique.Ces équations peuvent être simplifiées si $E_a \gg E_c$:

$$\sigma_m = \frac{\sigma}{1 + D_a}$$

$$\sigma_a = \frac{2\sigma}{1 + D_a}$$

C) Caractéristiques supplémentaires des granulats des essais de Mario et Gerardo

Tableau 10 : Caractéristiques supplémentaires des granulats

Propriétés Granulat	Masse volumique en vrac (kg/m ³)	Masse volumique moyenne du grain (kg/m ³)	Masse spécifique (kg/m ³)	Porosité (%)	Coefficient d'imbibition à 24 h (%)	Résistance à l'écrasement des grains (MPa)	Module fictif de déformabilité des grains en vrac (MPa)
d'argile expansée (LECA)	370	600	2.580	76,7	16,80	0,45	4,12
de cendre de fuel-oil pulvérisée frittée (LYTAG)	750	1.560	2.660	41,3	12,60	4,88	24,82
courant alluvionnaire (VAILATA)	1.530	2.720	2.810	3,2	0,73	17,89	58,48
lourd (BARYTINE)	2.210	4.200	4.380	4,1	0,11	3,31	16,46

Title: Multi-scale analysis of delayed deformations in cement-based materials submitted to drying or delayed ettringite formation

Keywords: Drying, Delayed ettringite formation, Delayed deformations, Cracking, aggregates, mesoscopic scale

Abstract: Today, the operating life of some concrete structures is likely to be extended, in parallel, structures show early signs of damage due sometimes to poor consideration of environmental conditions. Ensuring the sustainability of structures also means ensuring their safe, economical and ecological operation. Our objective is first to understand the phenomena and mechanisms at play, as well as their potential couplings; then, in a second step, to create reliable predictive models of these behaviours. The work presented is particularly interested in nuclear structures, which, in addition to having a major stake in our societies, present risks with regard to desiccation and thermo-activated pathologies such as the delayed ettringite formation (DEF). More precisely, the objective of this thesis is to understand the participation of aggregates in the degradation mechanisms of the material under these two respective stresses, and then their coupling. To this end, a multi-scale experimental approach is being conducted. It takes interest in the evolution of delayed deformations as well as the mechanical and transfer properties of cementitious materials subjected to either desiccation or DEF. In both cases, the influential parameters of the aggregates in the mechanisms were identified and a parametric study was carried out to clearly identify the influence of these parameters. First, the desiccation study is based on the monitoring and characterization of seven model formulations; i.e. granular skeletons were controlled and selected according to the size and volume fraction of the aggregates in the material; over 200 days. The tests revealed the influence of these parameters in the phenomenon of aggregate restraint. In parallel, the experimental study of DEF aims at characterizing the influence of the mineralogical nature of aggregates on the formation and progression of the pathology. We are interested in the influence of this parameter on the reaction kinetics and rate, but also on the evolution of the material properties, in order to identify all the physico-chemical mechanisms at stake. Finally, a final study is interested in the coupling between RSI and desiccation. Here, the aggregate parameters were set, and samples reactive to DEF were subjected to drying and soaking cycles.

